The analysis of Presenilin processing and activity with a focus on its implications for Alzheimer's disease pathogenesis using *Danio Rerio* as a model organism

Lachlan Wilson

Supervised by Michael Lardelli and Joan Kelly

Submitted for partial fulfilment for the degree of Doctor of Philosophy (PhD)

Discipline of Genetics

School of Molecular and Biomedical Science

The University of Adelaide University SA

AUSTRALIA

July 2013

Declaration

I certify that this work contains no material which has been accepted for the award of any other degree or diploma in my name, in any university or other tertiary institution and, to the best of my knowledge and belief, contains no material previously published or written by another person, except where due reference has been made in the text. In addition, I certify that no part of this work will, in the future, be used in a submission in my name, for any other degree or diploma in any university or other tertiary institution without the prior approval of the University of Adelaide and where applicable, any partner institution responsible for the joint-award of this degree.

I give consent to this copy of my thesis when deposited in the University Library, being made available for loan and photocopying, subject to the provisions of the Copyright Act 1968.

The author acknowledges that copyright of published works contained within this thesis resides with the copyright holder(s) of those works.

I also give permission for the digital version of my thesis to be made available on the web, via the University's digital research repository, the Library Search and also through web search engines, unless permission has been granted by the University to restrict access for a period of time.

Signed

…… ……Date……

Table of Contents

List of Publications contributed to during Ph.D candidature **5**

Acknowledgements **6**

Abstract **8**

CHAPTER I **10**

1.1. Literature Review **10**

1.2 Summary of Chapters II-IV and Links Between Them **53**

CHAPTER II **56**

Research Paper I **56**

CHAPTER III **58**

Research Paper II **58**

Supplemental Data **122**

CHAPTER IV **126**

Research Paper III **126**

Supplemental Data **185**

Discussion **188**

Further Directions **193**

References **197**

APPENDIX I **219**

Research Paper IV **219**

APPENDIX II **220**

Research Paper V **220**

List of Publications contributed to during Ph.D candidature

A zebrafish melanophore model of amyloid beta toxicity.

Morgan Newman, Lachlan Wilson, Giuseppe Verdile, Esther Camp

Ralph Martins and Michael Lardelli

Zebrafish, 2010, Vol7, No2 155-9.

The BACE1-PSEN-AβPP regulatory axis has an ancient role in response to low oxygen/oxidative stress.

Seyyed Hani Moussavi Nik, Lachlan Wilson, Morgan Newman, Kevin Croft, Trevor A Mori, Ian Musgrave and Michael Lardelli

Journal of Alzheimer's Disease, 2011,

The Development of an *in vivo* γ-Secretase Assay using Zebrafish Embryos.

Lachlan Wilson and Michael Lardelli

Journal of Alzheimer's Disease, 2013,

Acknowledgements

I would like to give my thanks and appreciation to:

Michael Lardelli, for providing me with this magnificent opportunity. Your knowledge, wisdom and continual patience with me throughout my studies has been so very appreciated. You have been a continuous inspiration for the scientific process and the virtues of a critical thinking lifestyle.

Morgan Newman, for being a continuous support and always being ready to assist me and my incessant questions. You have been there from the start to finish, from my third year placement in the lab till now. Thank you.

Past and present members of the Genetics discipline for their support and advice over the last few years. Particularly Simon Wells and Jai Denton for the advice, feedback and for reminding me that no matter how long it takes you can get it done. It kept me going in times of serious doubt.

Hani Mousavanik, you made everyday coming into the lab something to look forward to. Always laughing, and seeing the funny side of life. Our conversations, both intellectual and social have been enlightening and a treasure. You are a dear friend of mine, I will miss not coming into the lab everyday to share in your company.

To Mum and Dad thank you for being there through thick and thin. I know I haven't always been the easiest person and I thank you for your constant support. I couldn't have made it in any capacity without the opportunities that you have given me. The education, the love, understanding and continuous support. Thank you for letting me be me.

Garth, I know you hate my sentimentality and romanticism, so I will keep it stark. I would not be here, or the person I am without you. This, and all the things I have done, would not have occurred without you in my life.

Finally, my friends for providing timely distractions and listening to me rabble on about this and that.

Without these people (science related or not), none of this would have been possible.

This thesis is for Garth. My Brother. My Best Friend. My Constant.

Abstract

Aberrant proteolytic processing of AMYLOID BETA PRECURSOR PROTEIN (AβPP) may result in an imbalance between production and clearance of the amyloid-β (Aβ) peptide proteolytic product and promote neuronal dysfunction and death. β-site amyloid-β A4 precursor protein-cleaving enzyme 1 (BACE1) with γ -secretase are responsible for the cleavage of AβPP to produce Aβ peptide. Presenilin proteins form the catalytic core of γ-secretase complexes. *PRESENILIN1* (*PSEN1*) is the major locus for mutations causing familial Alzheimer's disease (FAD) and is also mutated in Pick disease of brain, familial acne inversa and dilated cardiomyopathy. It is a critical facilitator of Notch signalling. The zebrafish, *Danio rerio*, is a versatile vertebrate model for investigating the molecular bases of Alzheimer's disease (AD) pathology. It possesses genes orthologous to human *PSEN1* and *PSEN2*, and the genes *appa* and *appb* that are duplicates of an ancestral *AβPP* orthologue).

This thesis primarily utilizes zebrafish as a system to investigate AD pathogenesis.. **Chapter I** describes an assay in which the level of a γ-secretase substrate (a modified form of Appa protein) is observed in zebrafish embryos by western immunoblotting relative to a co-expressed protein not subject to γ-secretase activity. Prior to the development of this assay there existed no *in vivo* assay appropriate for directly monitoring γ-secretase activity. The assay was subsequently used to analyse the effects on γ-secretase activity of blocking translation of zebrafish *psen1* and/or *psen2*. **Chapter II** explores various truncations of human PSEN1 (or zebrafish Psen1) protein that have differential effects on Notch signalling and cleavage of zebrafish Appa (a paralogue of human AβPP). Different truncations can suppress or stimulate

Notch signalling but not Appa cleavage and vice versa. The results show that the truncated protein potentially translated from these transcripts incorporates into stable Psen1-dependent higher molecular weight complexes and suppresses cleavage of Appa but not Notch signalling. In contrast, the truncated protein potentially produced by the P242LfsX11 acne inversa mutation has no effect on Appa cleavage but, unexpectedly, enhances Notch signalling. The results suggest novel hypotheses for the pathological mechanisms underlying AD. **Chapter III** investigates truncated isoforms of PRESENILIN known to form naturally. In particular a truncated PSEN2 isoform "PS2V" has been previously identified. PS2V is formed by exclusion of exon 5 from *PSEN2* transcripts leading to a frameshift after exon 4 sequence and a premature stop codon. This truncates the ORF/protein after PSEN2's first transmembrane domain. The K115Efx10 mutation in *PSEN2* is the only completely truncating mutation of the *PRESENILIN* genes that is thought to cause AD. K115Efx10 is especially interesting since, if expressed, it would generate a truncated protein very similar to PS2V and would be expected to boost Aβ production. Zebrafish possess an isoform of Psen1 that has a similar role to PS2V and zebrafish Psen1 truncated after exon 4 sequence behaves in a similar manner to PS2V. We have modeled human and zebrafish PS2V and K115Efx10-like mutations in zebrafish to investigate their effect on gene expression profiles, γ-secretase activity and complex constitution.

CHAPTER I

1.1. Literature Review

It is estimated that there are over 35 million people in the world living with some form of dementia [1, 2]. This number is expected to double within 20 years [1, 2]. Of those diagnosed with dementia, Alzheimer's disease (AD) accounts for over 50% of patients [3]. AD is broken into two subtypes: Late onset AD (LOAD) and early onset familial AD (FAD). LOAD occurs beyond the age of 65 and represents 95% of all AD cases [3]. LOAD lacks a clear genetic etiology. However, the remaining 5% of cases are due to the autosomally inherited FAD [4, 5]. Regardless of age of onset both forms of AD share two pathological hallmarks - extracellular deposits of neuritic Aβ plaques and intraneuronal aggregates of hyperphosphorlyated tau.

The fundamental pathology leading to these phenotypes is poorly understood. An early form of what has become known as the 'Amyloid Cascade Hypothesis' was postulated to explain AD neuronal death seen in patients [6-9]. It suggested that the decreased clearance or increased production of Aβ peptides, derived from the amyloid precursor protein (AβPP), resulted in the hydrophobic aggregation of toxic insoluble plaques. This is supported by genetic analysis of FAD patients that has identified causative mutations in AβPP along with mutations in the proteases responsible for its cleavage, PRESENILIN 1 (PSEN1) and PRESENILIN 2 (PSEN2) [10, 11]. Proteolytic processing of AβPP by the PRESENILINs (PSEN) produces the Aβ

peptides. Of the Aβ plaques the longer Aβ42 peptide has been shown to be more prone to aggregation and is toxic *in vitro* [12, 13]. FAD mutations in PSEN1 or AβPP can lead to an increase in Aβ42 or decrease in Aβ40 production [14]. This has led some to conclude that an increase in 42/40 ratio is pathogenic. This has been observed in AD where higher levels of Aβ42 are inversely related to the age of onset of dementia [15]. Furthermore *in vitro* and *in vivo* model systems have demonstrated that higher order soluble aggregates of Aβ (oligomers) may contribute as toxic pathogenic agents [16, 17] with distinct classes identified in both mouse and human AD brains [18, 19]. However little is known about how they form *in vivo* or how they induce toxicity.

With progressive developments and understanding of pathogenic AβPP activity the nature of the original amyloid cascade hypothesis has changed over time for many reasons [7]. Despite the volume of research investigating AβPP since the discovery of Aβ [20] its non-pathological roles still remains largely unknown. Therefore it is not surprising that Aβ's involvement in AD progression has been questioned. This is evident with the observation that disease severity does not correlate well with plaque load [21-23]. Many AD patients with impaired memory have been shown to have no plaques. Mouse studies support this with memory defects occurring prior to any plaques being observed [24]. Likewise, *in vivo* neuroimaging has identified cognitively normal people with severe plaque loads [25, 26]. This may be indicative of people at high AD risk, but displays that the presence of plaques does not necessitate cognitive defects. There is evidence to suggest that Aβ plaques may even be protective [27]. Indeed under normal physiological conditions AβPP's extracellular fragments (released upon proteolytic processing) have roles in cell survival,

proliferation and adhesion [28]. Furthermore the small AβPP intracellular domain (AICD), upon liberation by cleavage, is able to act as a transcriptional regulator [29].

Supported by the failures of Aβ-targeted therapies [30, 31], the idea that Aβ may be a contributing factor, but not exclusively the cause of Alzheimer's disease, appears to be more consistent with the broad spectrum of accumulated data on AD. While the concept of a single factor being the cause to this heterogonous disease seems unlikely, there are candidates, particularly PRESENILIN that are coupled to a plethora of pathological phenomena that have, quite rightly, not lead to this idea being entirely dismissed. In this review I will discuss PRESENILIN and its γ-secretase related activities in depth.

PRESENILIN

Mutations throughout the PRESENILIN genes are associated with four diseases in particular – AD [32-37], Frontal Temporal Dementia (FTD) [38], dilated cardiomyopathy [39-41], and acne inversa (AI) [42, 43]. The contribution of PRESENILINs to disease pathology is not surprising given the crucial role it plays in γ-secretase proteolytic activity (explored in great depth later in this review), in cell signaling [44-48], tau phosphorylation [49-52], oxidative stress [49, 53, 54], calcium homeostasis [55-68] and autophagy [69-72] – factors pivotal in neurodegeneration and specifically AD pathogenesis. Of all known FAD mutations, 90% are within the PRESENILIN genes, with the large majority (over 180, ~ 94%) of them being identified in PSEN1. Of these mutations, all are dominantly inherited, primarily as missense mutations. Given that the bulk of all known FAD gene mutations exist in PRESENILIN genes, and multiple molecular events considered to be critical in AD

pathology can be linked to PRESENILIN function, this implies that PRESENILIN dysfunction may play a critical role in both familial and sporadic AD (Figure 1). However, to date there is no convincing explanation as to how PRESENILIN function may differ in the brains of normal, aged individuals and those who develop sporadic AD.

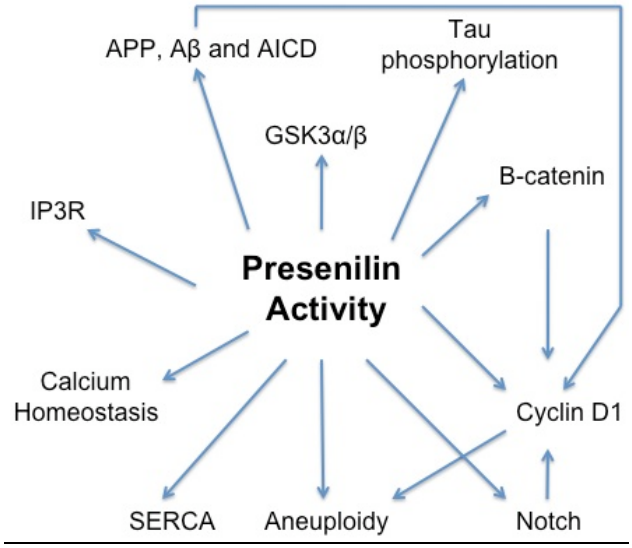

Figure 1: PRESENILIN proteins interact directly with many molecular processes thought to be involved in AD pathology. The PRESENILINs directly interact with AβPP, Tau, GSK3alpha/β, and β-catenin. PRESENILIN also influences calcium ion homeostasis. They regulate proteins controlling the cell cycle and are involved in chromosome segregation during mitosis. They facilitate a great number of cell signalling pathways through γ-secretase activity and also have highly conserved non-γ-scretase functions involving microtubule/cytoskeletion function. Little is known about these functions and so possible, non-γ-secretase effects of the numerous AD mutations in the PRESENILINs are rarely considered.

Expression

Reverse transcription polymerase transcription reaction (RT-PCR) analysis has shown ubiquitous expression of PSEN1 and PSEN2 in most adult human tissues [73-79]. This distribution of PSEN1 and PSEN2 in all brain regions and peripheral tissues has been verified by immunoblot and immunohistochemistry experiments [79-81]. However, evidence in mice suggests that the levels of transcriptional expression of PSEN1 and PSEN2 maybe be different over the course of development, particularly in the developing brain [82-84]. Mouse studies have shown that PSEN1 is expressed earlier than PSEN2, with as much as twice the amount of mRNA until day E12.5 when PSEN2 mRNA levels begin to match PSEN1[75]. Likewise in the cortex of newborn mice there is as much as three times the amount of PSEN1 than PSEN2, followed by mRNA levels equalising in mature mice [75]. As the two PRESENILINs do not share the same pattern of altered expression, they may contribute independently of each other to molecular events and not always share redundancy.

Subcellar localisation

Supporting the idea of multiple mutually exclusive roles of PSEN1 and PSEN2 is the discordance between their individual localisation and abundance in those regions. Recently there has been a dramatic revision regarding the subcellular localisation of the PRESENILINs. This has significant implications on their function and involvement in disease pathogenesis. Previously PSEN1 had been experimentally localised to various compartment of the cell – the ER [85], Golgi [85], the trans Golgi network [86], the ER-Golgi intermediate compartment [85], the nuclear envelope [87], endosomes [88], lysosomes [89], mitochondria [90], kinetochores and centrosomes [91], and plasma membrane. However it has been shown that PSEN1 and PSEN2 are all predominately found within a specialised part of the ER that closely associates with mitochondria, known as the mitochondrial associated membranes

(MAM) [92]. Indeed, in subcellular fractionation experiments PSEN2 appears to be exclusively localised to the MAM. The same group further showed that the MAM is the main site of γ-secretase activity within the cell as identified by a fluorescence based energy transfer-based assay and the production of AICD.

Protein Structure, Functional Domains and Turnover

Currently there is no crystal structure for PRESENILIN. However we do know that both PRESENILINs initially exist as a holoprotein of approximately 50kDa with nine transmembrane domains [93, 94]. After endoproteolysis [95] [96] PRESENILIN forms a 30kDa N-terminal fragment (NTF) (with a large intracellular loop between transmembrane (TMD) 6 and TMD7) and a 20kDa C-terminal fragment (CTF) that exist together as a heterodimer [97].

Despite numerous studies only the structure of the CTF has been elucidated [98]. The CTF consists of soluble helix in the unstructured amino-terminal loop, a half-membrane spanning helix and a severally kinked helical structure towards the carboxyl terminus [98]. Though there is no NMR structure of the NTF the consensus is that it has a classical transmembrane topology with six α-helices [98].

Full length PRESENILIN is degraded via the proteasomal pathway [99]. Both full length PRESENILINs have a rapid turn over and a short half-life (approximately 1.5hrs) in contrast to their more stable endoproteolytic fragments that have half-lives of up to 24 hours [100]. It is worth noting that upon the over expression of full length PRESENILIN, it is able to accumulate when the amino terminal fragment (NTF) and carboxyl terminal fragment (CTF) levels reach a saturation threshold [101].

PS2V and Hypoxia

A novel splice variant of *PSEN2*, PS2V, has been shown to exist in the brains of patients with sporadic AD [102]. PS2V mRNA encodes the N-terminal portion of PSEN2 from Met1- Leu119 and an additional 5 amino acids at its C-terminal [103]. The alternative splicing of *PSEN2* is induced under hypoxic conditions [102]. Hypoxic conditions induce the expression of *HMGA1a* that causes the alternative splicing of *PSEN2* transcripts to create PS2V [104]. *HMGA1a* binds to a specific binding site adjacent to the 5′splice site of exon 5 and interferes with the U_1SNRP splicing factor. This results in exclusion of exon 5 from *PSEN2* pre-mRNA [105, 106]. PS2V proteins aggregate in intracellular inclusion bodies (PS2V bodies) that exist in pyramidal cells of the cerebral cortex and the hippocampus at the early stages of disease development [107]. PS2V is seen at raised levels in the brains of sporadic Alzhimers disease (SAD) patients. PS2V is reported to increase Aβ levels and influence tau protein conformation [104, 107]. *In vitro* studies showed that PS2V diminishes the signaling pathway of the unfolded protein response (UPR) making cells susceptible to various endoplasmic reticulum (ER) stresses, and also increases Aβ production. PS2V is also known to change the conformation of tau protein, the major component of neurofibillary tangles [104, 106-109]

γ-*secretase independent activity*

The vast majority of research on PRESENILIN has been focused on its role as the catalytic core of the aspartyl protease γ-secretase. Although the mechanisms are poorly defined, multiple studies have associated PRESENILIN with γ-secretase independent functions [110-113].

There is a significant amount of data supporting an independent role of PRESENILIN in Ca^{2+} homeostasis. AD mutations in PRESENILINs, as well as knockouts, have

resulted in an increase of Ca^{2+} concentration into the ER [58, 65, 114, 115]. Clinical mutations in PRESENILINs have also been shown to affect capacitate calcium entry (CCE) [58, 59], ryanodine-sensitive Ca^{2+} pools [116], and inositol 1,4,5-triphosphate (InsP3)-mediated intracellular Ca^{2+} release [114, 117]. The fashion in which PRESENILIN affects Ca^{2+} homesostasis is unknown, however it has been shown that PRESENILINs can act as Ca2+ leak channels that allow passive movement of Ca^{2+} across the ER membranes [65, 115].

PRESENILIN is also known to interact with β-Catenin [118]. PRESENILIN 1 is able to act as a scaffold to allow β-catenin to be phosphorylated by GSK-3β and PKA, followed by rapid proteasomal degradation [119]. This mechanism works alongside the Wnt-regulated axin-mediated pathway to regulate β-catenin turnover and phosphorylation [120]. Alternatively PRESENILIN and β-catenin may interact at the cell surface via E-cadherin interacting with β-catenin. However, this is γ-secretase dependent where the cleavage of E-cadherin breaks down the complex and redistributes β-catenin in the cell [121, 122].

γ-secretase

PRESENILIN is at the catalytic core of the γ-secretase complex, a proteolytic complex critical in processing AβPP to Aβ peptides, as well as cleaving more than 90 different substrates [123-125]. The complex consists of four essential proteins, PSEN1 or PSEN2, Nicastrin (NCT), anterior pharynx defective 1 (APH-1), and PRESENILIN enhancer 2 (PSENEN or Pen-2). These four proteins are critical to the

catalysis, specificity and stability of the complex. A series of different studies have shown that the stoichiometry of these respective proteins in the complex to be at a ratio of 1:1:1:1[126, 127]. Given that in humans there are two homologues of *PSEN*, and dual *APH-1* genes such as *APH-1a* and *APH-1b*, there can be at least four different forms of γ-secretase complex [128]. Confounding this is the existence of alternately spliced forms of PRESENILIN and *APH-1a*, contributing to the myriad of possible complex formations [129, 130].

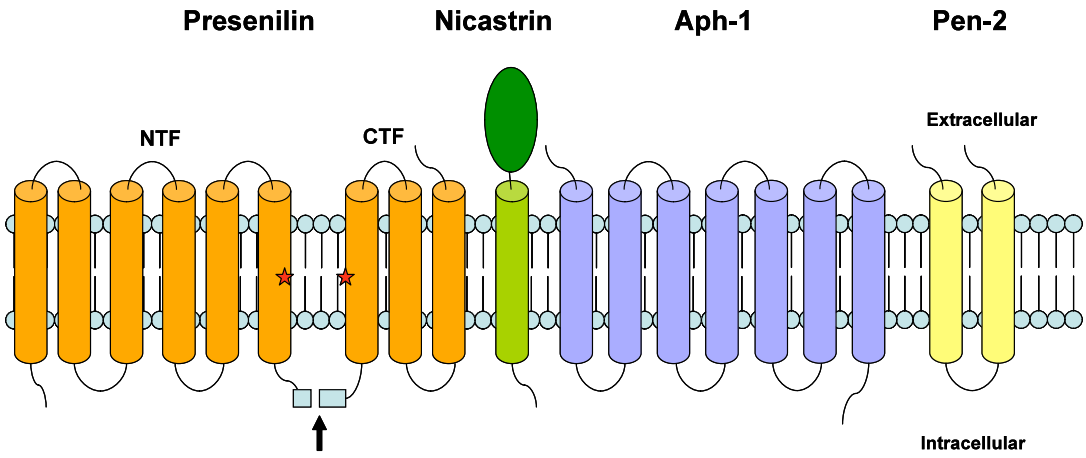

Figure 2: The four members of the γ-secretase complex within the cellular membrane. PRESENILIN has nine transmembrane domains which are cleaved into NTF and CTF fragments, with two intramembrane aspartates (asterisks) which are the active sites of the complex. The arrow indicates the site of endoprotelysis of PSEN. The remaining proteins, NCT with its ectodomain in dark green, APH-1 and PSENEN (Pen-2) make up the rest of the γ-secretase complex.

Members of the γ-secretase complex

In order to elucidate the activity of the complex a substantial amount of literature has been published attempting to understand the structure and assembly that underpins the complex's proteolytic activity.

APH-1

In *Homo sapiens* there are two homologues of APH-1, APH-1a and APH-1b. Aph-1a has two C-terminal splice variants known as long (APH-1aL) and short (APH-1aS). APH-1a (being either splice variant APH-1aL or APH-1aS) and APH-1b appear to be functionally redundant in their ability to form active γ-secretase complexes with the other complex subunits [131], consistent with the fact that they are differentially expressed in several tissues [132]. There also exists an additional variant in mice, Aph-1c [133]. APH-1 has 7 transmembrane domains with the N-terminal in the ER/lumen and the C-terminal in the cytosol [134]. Given the possibility for there to be alternatively spliced forms of APH-1a and the existence of two APH-1 homologues, it has been suggested that the inclusion of these different isoforms may induce different catalytic activities and substrate specificity for γ-secretase [131, 135]. This is supported by mouse knock out studies where the knock-out of Aph-1a leads to severe embryonic phenotypes where as Aph-1b ablation does not cause any defects, indicating that Aph-1a (and not Aph-1b) is critical for embryonic development [132, 136]. However Aph-1b knock-out mice exhibit acute behavioural phenotypes [137]. Although the exact role of APH-1 in γ-secretase is poorly defined APH-1 isoforms have been shown to contribute to Aβ production [132]. Mutational analysis has shown that the GXXG motif in transmembrane (TMD) 4 is critical for the assembly and maturation of γ-secretase [138, 139]. Multiple polar residues in TMD5 and TMD6

of APH1 are known to influence the activity and assembly of γ-secretase complexes. These residues may work to present the substrate to the protease [140, 141].

Nicastrin

NCT is a large type I transmembrane glycoprotein with a heavily glycosylated ectodomain (ECD). It was discovered through co-immunoprecipitation studies with PSEN that affected Notch and AβPP processing [142]. Early experiments showed the interaction of NCT with membrane-tethered substrates that lead to the suggestion that NCT could act as a receptor [143]. This suspicion was supported by the ectodomain of NCT showing similarities to both aminopeptidases and the transferring receptor super family [144]. Mutational analysis of the ectodomain has shown that the region from residues 312-369 is able to modulate AβPP cleavage by γ-secretase while Notch S3-cleavage is unaltered[145]. The appropriate processing of AβPP is dependent on the availability of mature NCT, with studies showing that processing can be modulated by directing NCT to various subcellular compartments [146]. Furthermore the glutamate 333 (E333) residue within the DAP domain of NCT is thought to be vital for substrate delivery and binding for processing [143, 147]. This has been disputed however, with other studies suggesting that E333 may instead have a significant role in the maturation of NCT via the secretory pathway, and the overall assembly and maturation of the γ-secretase complex [148]. The role of NCT in complex stability is supported indirectly by an analysis of γ-secretase containing PSEN that has both missense mutations F411Y and S438P, which is able to stabilise the complex whilst dispensing of NCT [149]. Indeed, it has been shown that in NCT deficient fibroblasts the Notch substrate can be processed, suggesting that it is not exclusively required for γ-secretase processing [150]. In contrast γ-secretase has been inhibited by monoclonal

antibodies directed against the NCT ectodomain, masking the substrate-binding region [151]. As is evident the exact role of NCT, be it substrate recruitment or stabilisation of the γ-secretase complex, is poorly defined regardless of the verified NCT-dependant difference in substrate processing [152].

PSENEN

In humans, PSENEN is a 101-amino acid protein with two putative transmembrane domains with amino and carboxyl terminals that both face the lumen of the ER [153]. PSENEN is critical in stabilising the γ-secretase complex as well as promoting the endoproteolytic cleavage of PRESENILIN into NTF and CTF fragments [154, 155].

The assembly of the γ-secretase complex

The formation of the γ-secretase complex is initiated when a sub-complex containing the highly hydrophobic APH1 [134] and immature glycosylated forms of NCT directly interact to form an intermediate scaffold for the assembling complex [130, 156-159]. The formation of this intermediate is governed by the ER retention factor, retrieval to endoplasmic reticulum 1 protein (RER1p), which can inhibit APH1 binding to NCT [160, 161]. It has been suggested that PSEN (1 or 2) may directly bind to the APH1-NCT scaffold followed by PSENEN [162]. It has also been postulated that a sub-complex of PSEN-PSENEN may bind to the APH1-NCT complex to form a stable γ-secretase complex [157, 163]. Experiments utilising chimaeric PSEN1 have shown that the 'NFGVVGM' motif within TMD4 of PSEN1 is necessary for binding to PSENEN [164], while the proximal two-thirds of TMD1, as well as the full sequence of PSENEN C-terminal domain [154, 165], is needed to

bind to PSEN1 [166]. Upon the binding of PSENEN, the PSEN TM6-TM7 loop domain is positioned into the transmembrane channel to allow endoproteoylsis to occur thereby activating the complex for cleavage of other substrates [167].

Transient and non-constitutive components of γ-secretase

Affiliated with the four key components of γ-secretase are several other transiently associated factors known to regulate its activity [168]. The glycosylated type I transmembrane protein CD147 has been identified as a subunit of the γ-secretase complex in HeLa cell membrane studies [169]. Depletion of CD147 by RNA interference results in increased Aβ production but does not alter the expression level of γ-secretase components or AβPP substrates [169]. CD147 over-expression, on the other hand, has no significant effect on Aβ production, γ-secretase components or AβPP substrates. This suggests that the CD147 subunit within the γ-secretase complex down-modulates the production of Aβ-peptides [169]. How CD147 interacts with the other members of the γ-secretase complex, and the molecular mechanisms by which it does, are unknown.

Glycogen synthase kinase-3 (GSK-3), involved in tau phosphorylation and associated with neurofibrillary tangles, binds to PSEN1 [170]. It has been suggested that GSK-3β aids PSEN endoproteolysis. Data also implies that PSEN1 may regulate the interaction between tau and GSK-3 [170, 171].

Linked to γ-secretase regulation is phospholipase PLD1, a protein integral to a series of diverse functions including signal transduction, membrane trafficking, cellular pathways, mitosis regulation and the regulation of perinuclear intravesicular

membrane traffic [168, 172]. PSEN1 has been shown to interact and recruit PLD1 to the golgi/trans-golgi network (TGN) via its hydrophilic loop region [173]. Interestingly over expression of PLD1 has been shown to decrease Aβ production while down regulation of PLD1 increases Aβ production [173]. PLD1 has not been shown to interact with any of the other γ-secretase components, and its regulative activity is independent of it phospolipase catalytic activity [173].

Type I membrane protein TMP21 has been shown to be involved in regulating γ-cleavage of AβPP, without disrupting ε-cleavage [174]. The protein is a member of the p24 cargo protein family, involved in vesicular protein trafficking between the ER and the Golgi complex [174]. Studies suggest that TMP21 acts to modulate γ-secretase activity in a fashion that does not affect γ-secretase component expression levels [174].

γ-secretase activity has also been shown to be stimulated by inflammatory cytokines. Several studies have shown that INF-γ, IL-1 β, and TNF-α can stimulate γ-secretase activity and its production of Aβ peptides [175-178].

The structure and function relationship of γ-secretase

Critical in analysing the function of γ-secretase has been the elucidation of the membrane topology of its members. PSEN1 and PSEN2 have been shown via N-linked glycoslation scanning to cross the membrane at least nine times with the carboxyl and amino termini being located at the luminal and cytoplamsic sides, respectively [93]. As stated earlier APH-1 is a 7 TMD protein with its carboxyl and amino terminal on the cytoplasmic and luminal sides respectively [134]. NCT is a

type single-spaning membrane protein with a large extracellular domain that is tightly folded and heavily glycolyslated upon maturation [179]. Finally, PSENEN spans the membrane twice with the carboxyl and amino termini facing the ER lumen [153] (Figure 2).

Cumulatively this 19 TMD complex is unstable making crystal purification exceptionally difficult. However, a wide variety of different indirect approaches have been utilised to elucidate its structure (See De Strooper *et. al.* for a review on these studies) [97]. Rather than reflecting a similar type of γ -secretase structure, these studies have yielded significant differences in shape and size of the catalytic complex that reflects the monomeric or possible oligomeric states that can exist for the complex. The discrepancy may also be due to the distinct experimental conditions between the studies to extract, purify and reconstruct the complex, not to mention resolution limitations at the atomic level when trying to divine the γ-secretase internal structure.

One of the unique properties of γ-secretase is its ability to cleave membrane-spanning substrates within a hydrophobic lipid bilayer. This is achieved by the section bordering the two opposed catalytic aspartate residues in TMD6 and TMD7 of the PSENs forming a catalytic pore structure by partly turning towards a hydrophilic environment that allows for the intramembrane proteolysis [167, 180]. The formation of a hydrophilic cavity within the membrane is supported by the GxGD catalytic motif in TMD7 being water accessible, while the lumial section of TMD6 may provide a site for substrate or inhibitor binding on the α-helix facing a hydrophilic environment. The luminal end of TMD9 that extends to the carboxyl terminus may function as a possible catalytic site. It also influences the recruitment of substrates due to it being

able to form an amphipathic α-helix-like structure that spreads out over the region between the membrane and the extracellular environment. Likewise situated near the catalytic center, are the residues around the proline-alanine-leucine (PAL) motif and luminal side of the TMD9.

Cleavage specificity and efficiency of PSEN1 vs PSEN2 in γ-secretase

The γ-secretase complex is made up of four components of which two, PRESENILIN and APH1, have multiple forms in humans. The PRESENILIN proteins, PSEN1 and PSEN2, share ~67% identity. The two APH1 isoforms, APH1a (which has two C-terminal splice variants, Aph-1aL and Aph-1aS) and APH-1b, also share a similar degree of identity (~58% homology)[131]. These multiple PSEN and APH1 isoforms are indicative of the heterogeneity of γ-secretase complexes and the potential for the existence of different subtypes with variable specificities [131, 133, 135].

Several lines of evidence have specifically implicated both PSEN1 and PSEN2 in AβPP and Notch processing [181-184]. Studies have shown that while both proteins have overlapping substrate preferences [185], their selective affinity and catalytic efficiencies differ [186]. This has been highlighted by the differential responses of PSEN1- and PSEN2-mediated activities to γ-secretase inhibitors [187, 188]. Knockout of *PSEN1* and *PSEN2* in mice produces differing phenotypes that have been attributed to the differential actions of these ubiquitously-expressed proteins [189, 190]. Experiments using murine embryonic fibroblast and neuronal cells have also shown that the depletion of PSEN2 has a minor affect on cleavage of AβPP, Notch and ephrinB substrates in comparison to PSEN1 [182, 191, 192]. This is supported by an *in-vitro* analysis using a flag tagged AβPP substrate and γ-secretase complexes

containing PSEN1 that showed that these are more active cleaving the AβPP substrate than complexes containing PSEN2 [193]. However, a different study comparing Aβ production from reconstituted human γ-secretase complexes containing either PSEN1 or PSEN2 suggested that those containing PSEN1 do not show significantly higher activity that those containing PSEN2 [194]. Indeed it has been shown that γ-secretase containing PSEN2 cleaves more AβPP than that containing PSEN1 in murine microglia cells [195]. The discordance between these studies may be due to differences in the affinity of PSEN1 and PSEN2 for other secretase components and/or their localization and relative abundance within cells [92] rather than actual differences in their catalytic activity.

Complex localisation and the location of γ-secretase cleavage

γ-secretase components (such as PRESENILINs) localization and substrate abundance has the potential to have a significant impact on γ-secretase mediated cleavage. Prior to γ-secretase cleavage the substrates require an N-terminal ectodomain stub for catalytic processing. This predominately occurs either by α or β-secretase protease cleavage. Lipoprotein-related protein (LRP)[196] and voltage-gated sodium channel β-2 subunit (Navbeta2) [197] are also known to effectively cleave N-terminal stubs for γ-secretase processing. α-secretase meditated ectodomain shedding is thought to take place primarily at the cell surface [198-201]. It is worth noting that there is evidence of AβPP being processed in the trans-golgi network by α-secretase. α-secretase is able to constituently shed the ectodomain though it can potentially be induced by an influx of Ca^{2+} or protein kinase C (PKC) activation by phorbol esters.

β-secretase cleavage occurs at the plasma membrane, in the endocytic compartments, and in the trans-Golgi network or Golgi apparatus [202-206].

γ-secretase components localise to a variety of different cellular compartments, leading to the possibility of a variety of different locations for substrate processing. These include the plasma membrane, early and late endosomes, autophagic vacuoles, lysosomes, mitochondria, Golgi, and the ER [88, 89, 207-211].

The location of the γ-secretase mediated cleavage of its substrates is poorly understood. Most α-cleavage occurs at the cell surface, given that most of the substrates ectodomain cleavage shedding is performed by the A Disintegrin And Metalloproteinase (ADAM) family metalloproteases. The rest of the substrate stubs can then be cleaved by γ-secretase at the plasma membrane or conversely after endocytosis [212-214]. Endocytosis is thought to precede cleavage due to the deposition of the CTF in the intracellular compartments and an overall decrease in surface expression of the proteins. Furthermore AβPP endocytosis appears to be critical for processing to Aβ, as the endocytic compartments are likely to provide the optimal pH for β-site amyloid precursor protein cleavage enzyme (BACE) activity [202, 203, 207, 215]. The AβPP C-terminal stub is then either processed in the endocytic compartments by γ-secretase or recycled back to the plasma membrane [210, 212, 216]. As AβPP traffics through the secretory and endocytic pathways it is can be processed in the TGN, plasma membrane, and endocytic compartments. However AβPP reaching the plasma membrane is preferentially cleaved by α-secretase activity and undergoes non-amyloidogenic processing.

As yet an overall study to investigate the role of sub-cellular compartments in γ-secretase cleavage has not been undertaken. The need for this has become even more

apparent given the recent discovery that PSEN1 protein appears to be primarily localized to the MAM and that PSEN2 resides exclusively in this structure [92, 217].

Substrate requirements for γ-secretase cleavage

γ-secretase is known to cleave up to as many as 90 different substrates [123-125]. With varied function, localisation and structure these substrates nonetheless share many common attributes [218-220]. Primarily the substrates consist of type-I transmembrane proteins. They often feature an expansive ectodomain, likely retaining cell adhesion molecule-like domains, a single spanning TMD, as well as a cytoplamic C-terminal that is able to mediate and initiate intracellular signalling events. It is worth noting that the breakdown of these cellular signalling events (such as cell fate determination, neurite outgrowth and axon guidance) is often critical in the pathology of AD [221, 222]. γ-secretase preferentially cleaves membrane-bound protein stubs after ectodomain shedding of the full-length substrate [219]. Common to most substrates is the γ-like cleavage at or close to the periphery of the cytoplasmic and transmembrane domains. This ε-like cleavage site borders a region rich in lysine and/or arginine resides. However it is important to note that evidence suggests that γ-secretase cleavage is reliant on the conformation state of the transmembrane domain rather than a recognition sequence at or adjoining the cleavage site [223].

The mechanism of γ-secretase cleavage on substrates: A case of progressive proteolysis

As discussed previously the method and action of γ-secretase cleavage requires specific conditions. γ-secretase initially undertakes an endopeptidase-like cleavage succeeded by progressive carboxypeptidase-like catalysis (Figure 3) [224]. The first cleavage events of the transmembrane substrate occur at what is called the ε-site, which exist between the border of the membrane and cytosol [225, 226]. It has been shown that to allow access to the catalytic site of γ-secretase the structure surrounding the ε-site must be malleable in the membrane [227, 228]. Upon ε-cleavage the substrates intracellular domain is then liberated from the membrane. γ-secretase then proceeds to progressively shave off the rest of the hydrophobic substrate by every 3-4 residues from the cytosolic side [229]. This form of progressive proteolysis has been clearly demonstrated with AβPP, where it is initially cleaved at the ε-site to produce Aβ48 and Aβ49, which are then both progressively trimmed the variety of Aβ peptides from 46 to 38 amino acids long [230, 231].

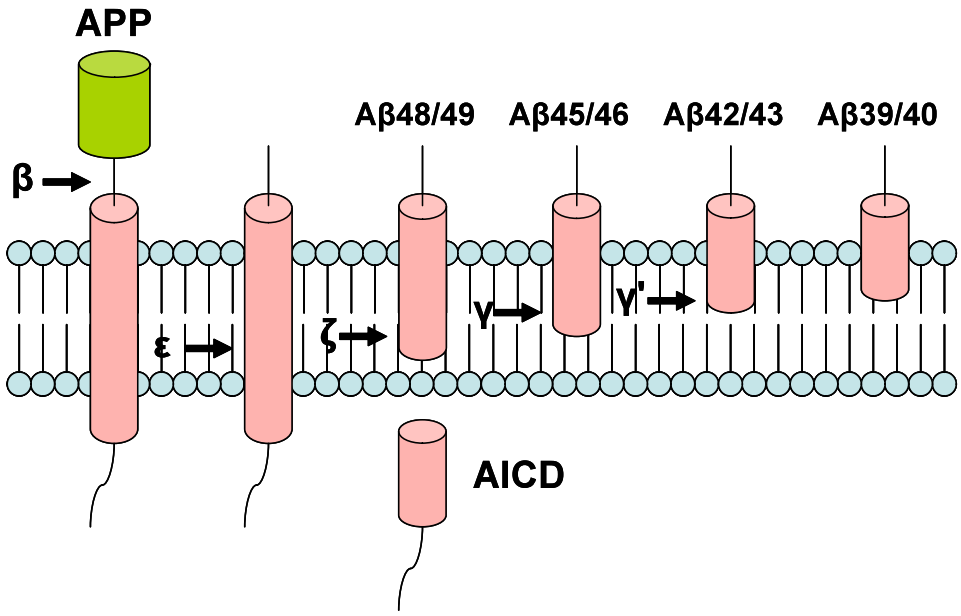

Figure 3: The model of processive proteolysis of the amyloid precursor protein transmembrane domain by γ-secretase. PRESENILIN mutations may decrease cleavage activity by lowering Aβ production while increasing the Aβ42 to Aβ40 ratio. Longer Aβ, with a more hydrophobic transmembrane domain is more likely to be retained in the plasma membrane, while the shorter peptides are more likely to be released. Less catalytically efficient γ-secretase complexes would allow for more time for the release of longer Aβ peptides. While FAD PRESENILIN mutations shift the initial ε-cleavage site to produce more Aβ48 which leads to Aβ42 production.

γ-secretase assays

It is evident that many factors in AD pathogenesis are poorly understood. In order to define AD pathogenesis, attempts to mimic *in vivo* activities by *in vitro* expression in cell culture or abiotic assays have been undertaken. In particular *in vitro* γ-secretase assays have proven vital in determining the mechanism of cleavage inhibitors [232-235], the composition of the complex [236, 237] and action of its regulatory factors [236, 238].

Aβ peptide production has been viewed as indicative of γ-secretase activity. Previously enzyme-linked immunosorbent assays (ELISA) have been used to analyse conditioned cell media for Aβ40 and Aβ42 levels [12, 239, 240]. However, low aggregate concentration and complex heterogeneous cell lysate have made assaying intracellular levels of Aβ difficult. It has been shown that Aβ40 and Aβ42 polypeptides non-covalently interact with proteins to form complexes that reduce recovery efficiencies and shield antibody epitopes [241, 242]. A lack of specific antibodies for other Aβ variants has also limited the analysis of earlier cleavage events. However, in Aβ pathogenesis many of the factors that exert an effect on Aβ accumulation have no direct affect on γ-secretase activity [243]. These factors impact observations on Aβ and inappropriately influence γ-secretase analysis. This is evident with the inherently high interassay variation of the Aβ-antibody assays [244]. In contrast, cell based reporter assays have a definitive advantage over traditional Aβ-antibody based assays by being able to directly measure γ-secretase activity.

Cell based in vitro assays

Many cell-based reporter gene assays have been implemented to monitor γ-secretase cleavage of AβPP and Notch. Predominately these assays have utilised a synthetic version of AβPP (often the post-BACE cleaved C-terminal domain stub of AβPP - C100 or C99) or Notch (described in greater depth below). Transfection of cell lines with these constructs either hybridised or attached to a reporter system provides direct indicators of

γ-secretase activity. As many of these assays utilise transfected cells, they are suitable for large scale, high throughput, studies of γ-secretase inhibition.

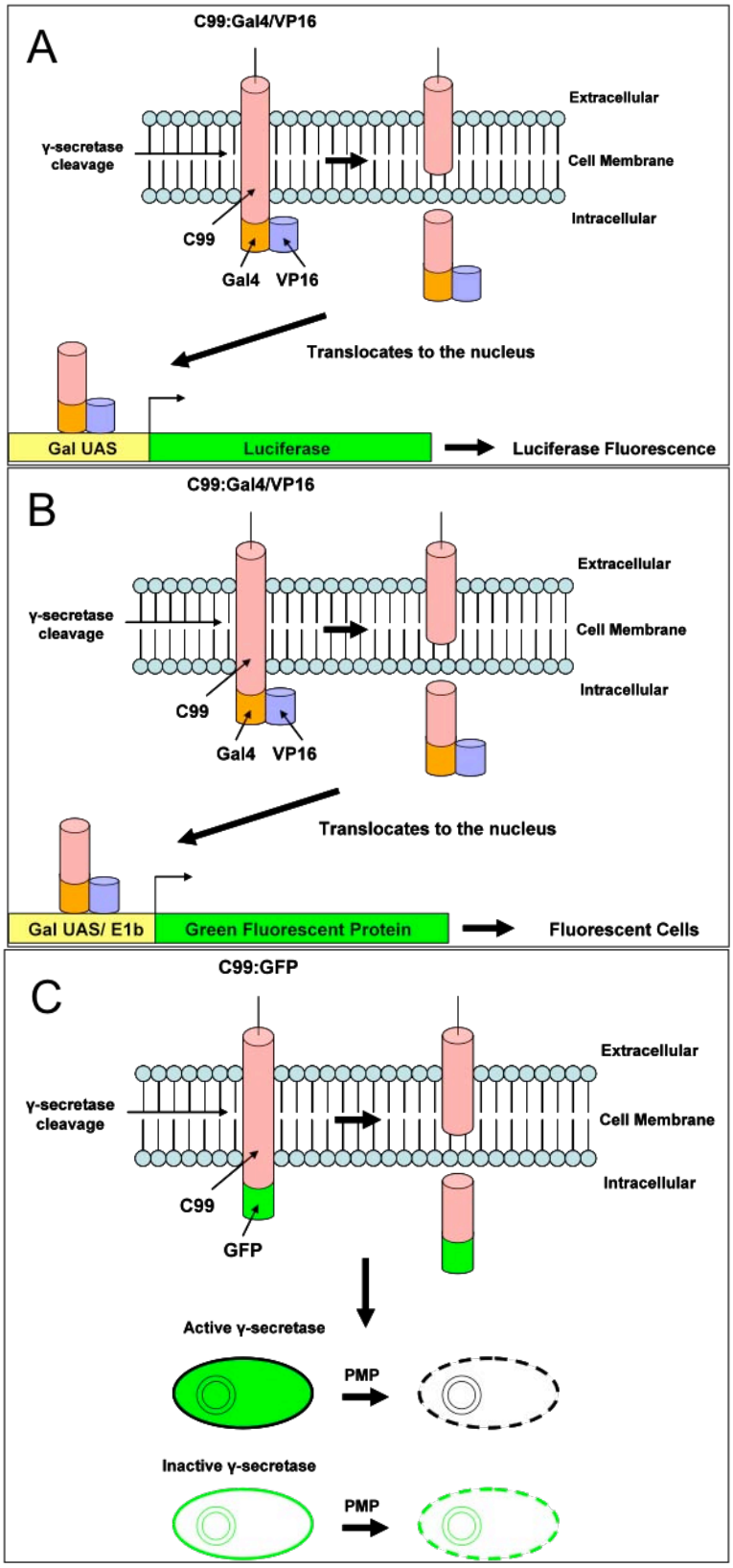
A
C99:Gal4/VP16
γ-secretase cleavage
Extracellular
Cell Membrane
Intracellular
C99
Gal4
VP16
Translocates to the nucleus
Gal UAS
Luciferase
Luciferase Fluorescence
B
C99:Gal4/VP16
γ-secretase cleavage
Extracellular
Cell Membrane
Intracellular
C99
Gal4
VP16
Translocates to the nucleus
Gal UAS/ E1b
Green Fluorescent Protein
Fluorescent Cells
C
C99:GFP
γ-secretase cleavage
Extracellular
Cell Membrane
Intracellular
C99
GFP
Active γ-secretase
PMP
Inactive γ-secretase
PMP

Figure 4: A schematic representation of the γ-secretase cell-based assays.

A. Gal4 based luciferase reporter based assays. The membrane-tethered C-terminal fragment of AβPP (C99) fused with a C-terminal Gal4/VP16 acts as the immediate substrate for γ-secretase. The cleavage of C99-GVP by γ-secretase releases the activator domain to the cytosol where it then traffics to the nucleus to activate the expression of the luciferase reporter gene from the UAS promoter.
B. The γ-secretase-dependent GFP reporter assay by Sernee *et al* [243]. The cleavage of C99-GVP by γ-secretase releases the activator domain to the cytosol where it initiates the transcription of the green fluorescnence protein (GFP) gene by binding to the UAS/ 5Gal-E1b domain of the GFP reporter construct.
C. The γ-secretase-dependent AβPP-GFP fusion assay developed by Florean *et al* [250]. After γ-secretase cleavage of the C99-GFP fusion, the AICD-GFP is then release to the cytosol. This enables the analysis of the fluorescence before and after plasma membrane permeabilisation (PMP) in cells with functional or inhibited γ-secretase. Only membranous fluorescence is conserved upon PMP; by comparing residual membrane-bound fluorescence with the initial total fluorescence measured before permeabilisation, the fluorescence retention ratio is determined and γ-secretase activity can be calculated.

An early example of a γ-secretase cell based reporter assay, by Karlstrom *et al* [245], utilises a C99 form of APP incorporated into a Gal4/VP16 transactivitation (GVP) domain system (Figure 4A). These are transfected into carcinoma cells [245]. Upon cleavage of the intermediate substrate by γ-secretase, the liberated C-terminal (which

includes the GVP moiety), translocates to the nuclease via localisation signals. The GVP signals through a UAS-luciferase reporter gene via the transactiviation domain binding specifically to a UAS promoter. With the direct correlation between AICD production and γ -secretase activity having been previously established, the degree of luciferase fluoresce correlates directly to the extent of γ-secretase activity [246]. Many γ-secretase assays use similar reporter-based systems due to their relative ease and simplicity [247, 248]. The C99::GVP fusion protein is often only a few residues from the C-terminal of the γ-secretase cleavage sites, minimising non-specific cleavage. The sensitive interaction between the bait and prey of the reporter system also enables small changes in γ-secretase activity to be observed. These assays exclusively measure the cleavage of the C99-GVP protein, being insensitive to cellular endogenous γ-secretase substrates which could otherwise confound results. Importantly, all γ-secretase activity can be recorded regardless of the size of its cleavage product, either it be Aβ42, β 40, or another Aβ fragment. This however highlights the assays limitations. Only overall cleavage activity is measured, preventing the analysis of specific cleavage events when γ -secretase is subjected to inhibitors and other treatments.

In order to optimise the responsiveness of the reporter system Liao *et al* [175] produced an assay using a Gal4-luciferase reporter gene and C99-GVP [175]. In contrast to Karlstrom *et al* [245], Liao *et al* [175] utilised tetracycline-regulated mammalian expression to induce the expression of C99-GVP only when detection of γ-secretase was required. This decreased the background luminescence from constitutive C99-GVP expression. However, residual luminescence was still evident regardless of γ-secretase activity being inhibited. It was found that some uncleaved chimeric C99-GVP was able to

localize to the nucleus, having escaped cleavage, to cause the residual luciferase expression independent of γ-secretase activity.

Unlike the luciferase assays, Sernee *et al* [243] developed a cell-based γ-secretase assay that utilised a modified AβPP substrate that would promote the expression of an enhanced green fluorescent protein (EGFP) reporter (Figure 4B) [243]. The substrate consisted of an AβPP signal peptide and an AβPP fragment with a Gal4-VP16 transcription factor. After AβPP cleavage the released AICD binds to the Gal4 binding sites to promote the expression of EGFP. They successfully showed that γ-secretase activity correlated with EGFP expression, with the degree of fluorescence parallel to the extent of Aβ production. Unlike previous cell based systems this assay could isolate cells with a stable difference in γ-secretase activity via a fluorescent activated cell sorter (FACS). Additionally, the Sernee *et al* 2003 assay is unaffected by luciferase reporter complications. Proteasome inhibitors have been shown to directly interfere with luciferase reporter enzymes, like those used by Karlsstrom *et al* [245] and Liao *et al* [175], by a post-transcriptional mechanism, disrupting reporter integrity [249]. It is thought that they either inhibit the translation of the proteins, or by blocking proteasome activity they enhance the proteolysis of the luciferase and β -galactosidase via an independent pathway [249].

With the limitations of a reporter based system evident, Florean *et al* [250] expanded the use of a GFP fragment to investigate γ-secretase by fusing the cleavage substrate to GFP (Figure 4C) [250]. Upon transfection into carcinoma cells γ-secretase cleavage would release the ICD-GFP fragment to the cytosol. By utilising plasma membrane

permeablisation (PMP), where only membrane florescence is conserved, they were able to compare the total florescence, which is measured prior to PMP, to the residual membrane-bound fluorescence. γ-secretase activity could be determined as the inverse index of the fluorescence retention ratio. Furthermore, the construct's stability, indicative of the reduced protease degrading compared to unmodified AICD, enabled γ-secretase cleavage to be evaluated by using antibodies against GFP and visualised on a western blot. The Florean *et al* [250] GFP assay, unlike Sernee *et al* [243], provides a method that allows comprehensive analysis of γ-secretase activity directly in cells without the need for image acquisition or analysis. In contrast to cell-based reporter assays utilising the Gal4/VP16, the Florean *et al* [250] assay does not depend upon the responsiveness of a reporter.

These cell based assays provide a method that identifies cellular factors and inhibitors that interact directly with γ-secretase as well as compounds that impact upstream of enzyme activation. However, these assays cannot avoid indirect, whole cell-related effects on substrate processing. Similarly the existence of possible confounding factors, such as background reporter activity from uncleaved substrate and the aberrant gene/protein expression patterns of carcinoma cell lines, still affect the integrity of these assays.

Cell-free assays

Unlike cell based assays, cell-free assays enable the γ-secretase complex to be solubilised with the intent that this will closely reflect the native enzymatic activity of the complex in

its normal environment, without being affected by background confounding factors. γ-secretase cell-free assays often utilise the same reporter based systems. However, in cell-free assays the AICD is not broken down as rapidly, unlike the rapid degradation seen under cellular conditions. It has been demonstrated that AICD is degraded by cytoplasmic metalloproteases, which are not present in cell-free assays, lending itself to a more definitive correlation between AICD and γ-secretase over cell-based assays [251]. This is not unexpected since AICD has rapid turnover and a half-life that is potentially as short as 5 min [252]. Indeed, one difficulty in determining a physiological role for AICD has been its instability. The extreme instability of AICD has been linked to its rapid degradation by a cytoplasmic thiol-dependent metalloprotease, the insulin-degrading enzyme (IDE), which also works to clear extracellular Aβ and functions as an Aβ-degrading enzyme [253-255]. The AICD may also be broken down by the proteasome [256]. This however is controversial [257].

Cell-free assays are easy to manipulate as the solution conditions can be altered and readily subjected to various treatments. Previous cell assays have utilised radiolabelled CTF or *in vitro* translated radiolabelled AβPP CTF [95, 258, 259]. Unfortunately, detection of cleavage by immunoprecipation against amyloid was limited due to a lack of soluble γ-secretase to produce cleaved AβPP fragments.

To maintain its structural integrity it is essential to solubilise γ-secretase with a detergent that is able to replicate the physical properties of its native bilayer. Cell free assays, especially in regard to γ-secretase, require a stable complex in the detergent-solubilised state. Hence the necessity to elucidate conditions where the physical environment of the protein is least agitated by the annulment of its original membrane. At the same time a

detergent that stabilizes the protein, but is also compatible with the experimental techniques, is required.

An early attempt at providing a specific lipid environment that could retain a stable solubilised active γ-secretase was by Mclendon *et al* [260]. After isolating the membranes from chinese hamster ovary CHO cells transfected with AβPP, Mclendon *et al* [260] attempted to evaluate the effect of various detergents on γ-secretase activity by measuring Aβ production. It was found that Tween® 80 and BRIJ™ 35 were able to enhance Aβ production by up to five times [260]. Since then several other studies investigated the ability to recuperate catalytically adequate γ-secretase and have acknowledged the critical nature of detergent choice. Li *et al* [261] were the first to use CHAPSO to yield an active enzyme [261]. Pinnix *et al* [262] would go on to elucidate that Triton™ X-100, methyl β-cyclodextrin, digitonin, Nonidet™ P-40, CHAPS, and octyl β-glucoside detergent are ineffective in recovering an active γ-secretase [262].

The majority of these studies used artificial systems with an overexpressed APP or exogenous substrate, while neglecting to investigate the effect of detergent concentration on endogenous AβPP processing. Franberg *et al* [263] decided to investigate the effect of different detergents at a range of concentrations on γ-secretase processing of endogenous AβPP CTFs in membranes from rat brain [263]. They aimed to determine the appropriate detergent concentration in a sample that would not interfere with the membrane proteins stability and crystallisation. At 0.25% they found that CHAPSO had a positive effect on activity and determined the optimal CHAPSO concentration to be 0.4%, just below the critical micelle concentration (CMC) of 0.5% [263]. The positive effect of CHAPSO on

γ-secretase activity could be a result of its ability to form mixed micelles with membrane lipids below the CMC [264]. Indeed, γ-secretase is dependent on the lipid environment for its activity, as shown by the favourable effects of sphingolipids and cholesterols on γ-secretase activity [265-267]. The structure of CHAPSO resembles cholesterol and is known to be effective at preserving interactions between cholesterol, sphingolipids, and other proteins [268], and hence provide a suitable environment for γ-secretase.

Cellular conditions and lipid environment are known to have a dramatic effect on γ-secretase activity [168]. Cellular cholesterol levels are able to regulate γ-secretase activity [269]. This was shown when γ-secretase cleavage was inhibited by a decrease in cholesterol levels [269]. A prevalent problem with cell free assays and the study of membrane proteins is obtaining sufficient protein from a medium which typically has membrane proteins in low abundance. Indeed Franburg *et al* [263] found that not only is detergent concentration of importance but also protein concentration, and determined that a 4:1 protein to detergent ratio is required for optimal γ-secretase activity [263].

pH has been show to have a pivotal role in analysing γ-secretase activity. This was evident in a study by Yagishita *et al* [270] that investigated Aβ46 processing to Aβ40 and Aβ43 in low density membrane domains (LDM) [270]. Their results suggested that Aβ40 and Aβ42 processing is functionally different, arising from different precursors, Aβ46 and Aβ45 respectively. However Zhao *et al* [271] reported that Aβ46 is a precursor to both Aβ40 and Aβ42 [271]. A difference in the pH has been linked to the inconsistencies between the two studies. Zhao *et al* [271] used a total membrane fraction at a pH of 6.5, while Yagishita *et al* [270] utilised LDM extracts at a pH of 7.0. Yagishita *et al* [270] determined that Aβ processing at a lower pH of 6.5 occurs in a γ-secretase-independent

manner by another protease, possibly involving cathepsin D. This highlights the importance of a correct pH environment and brings into question many of the observations on γ-secretase cleavage performed under alternate pH conditions.

The elucidation of the MAM as the main subcellular location of the PRESENILIN proteins, γ-secretase activity and γ-secretase cleavage of AβPP in neural tissue [272] has significant implications for assaying γ-secretase activity. The sub-cellular distribution of the PRESENILINs was unknown until recently due to the MAM's tight physical association with mitochondria and its lipid raft-like characteristics that prevented its permeabilisation by most immunohistochemistry detergents [272, 273]. Furthermore it was recently shown that the site of γ-secretase cleavage within AβPP is affected by the thickness of the lipid bilayer within which AβPP resides [274]. This raises the question of how solubilisation of γ-secretase with detergents in cell-free assays affects observations of AβPP cleavage and the different forms of Aβ formed by different PRESENILIN mutants. Likewise changes in PRESENILIN activity have been shown to affect the movement of cholesterol into and out of MAM membranes [275]. This raises the possibility that changes in the profile of Aβ lengths observed in FAD PRESENILIN mutants may be the secondary effect of changes in the lipid constitution of MAM membranes rather than a direct effect of the mutations on the cleavage interaction between a PRESENILIN molecule and an AβPP molecule within the γ-secretase complex itself.

Regardless of the difficulties associated with working with membrane proteins, in particular γ -secretase, their importance in the regulation of fundamental cellular

processes has lead, after much perseverance, to the development of effective assays that provide useful information to their activity and control of fundamental biochemical processes.

Animal models analysing γ-secretase and AβPP processing

Though *in vitro* analyses have proven effective, their ability to replicate the complexities of an *in vivo* cellular system are limited. In order to thoroughly and properly investigate cellular biology an *in vivo* system must be used. There is, and has been, a need to develop appropriate *in vivo* systems to investigate the γ-secretase complex, and AD in general. Importantly *in vivo* animal models provide readily available techniques and experimental methods that are denied to human studies.

Mouse

Mouse models have been vital in broadening our knowledge of PSEN physiological role in neurodegenerative disease. During the early stages of development PSEN proteins are critical for the regulation of cell division. *Psen1* and *Psen2* mRNA is ubiquitous in the neuro-epithelial cells during early development. In mature mice the expression of *PSEN* is lowered but is found predominately in the neurons of the cortex, hippocampus and cerebellum [276].

PRESENILIN 1 (PSEN1) knockout mice develop neurodegeneration of the cerebral cortex and deterioration of memory and synaptic functions with increasing age [190].

These observed complications can be rescued by crossing these mice to a transgenic line expressing human *PSEN1*. A similar phenotype is also seen in Notch1 knockout mice, which show skeletal and somite defects [190]. The expression in transgenic mice of human PSEN1 rescues the developmental phenotype of *Psen1*$^{-/-}$ mice [276, 277]. While *Psen1*$^{-/-}$mice show embryonic lethality, *Psen2*$^{-/-}$ mice are viable and fertile with only a mild pulmonary phenotype and no central nervous system (CNS) abnormalities. Abnormal expression of Notch ligand and downregulation of Notch target genes shows that knockdown of both *Psen1* and *Psen2* results in the loss of Notch signaling [278].

To generate AD animal models exhibiting senile plaques and Aβ associated neuropathology different types of transgenic mice that express human AβPP and other genes involved in AD have been designed [279]. Games *et al* 1995 produced a line of transgenic mice overexpressing FAD mutant human amyloid precursor protein V717F, the PDAPP mouse [280]. These mice produce characteristic AD plaques with a loss of synaptic density. The progressive nature of the plaque formation followed the regional specificity of human AD, from the hippocampus to cortical and limbic areas. However no apparent cell loss and no NFT pathology was observed [280]. Subsequently, more than 20 mouse models exist that replicate amyloid pathology via over-expressing AβPP mutants [281-285].

In order to investigate the interaction between PRESENILIN and AβPP, FAD-associated PRESENILIN mutations have been introduced into transgenic mice models. It was shown that the over expression of M146L and M146V *PSEN1* mutations selectively increased brain Aβ42 while wildtype *PSEN1* does not [286]. Similarly *PSEN1* mutant mice crossed

with AβPP mutant mice have accelerated plaque deposition, suggesting *PSEN* mutants increase Aβ plaque pathology [287, 288].

Transgenic mouse models that overexpress mutated human AβPP, with or without mutated PRESENILIN, develop a diverse spectrum of vascular and parenchymal amyloid deposits, cerebral amyloid angiopathy, dystrophic neurites and synapses, and amyloid-associated neuroinflammation. However other characteristics of AD, such as neurofibrillary tangles and nerve cell loss, are not effectively replicated in these models. Though these lesions are similar to those in human AD brains, differences in posttranslational modifications and other biochemical properties exist. Some models predominantly develop neuritic plaques, while others exhibit diffuse plaques to a greater extent [258, 283]. Transgenic mouse models lack widespread neuronal loss [289, 290] in the hippocampus and neocortical regions commonly seen in AD brains [291, 292]. Only region specific neuron loss that is coupled with amyloid accumulation has been observed in mice [284].

A well-rounded, comprehensive AD mouse model has yet to be developed. Interestingly Aβ disposition in transgenic AβPP and PSEN mice does not lead directly to neuronal cell death. Rather this is provoked by a secondary factor, such as reactive oxygen species (ROS) [289, 293]. Even though this is inconsistent with the amyloid cascade hypotheses, it is consistent with human neuropathological studies that have observed no correlation between the total amyloid accumulation and memory loss in AD [294].

Caenorhabditis elegans

In contrast to mouse models, the self-fertilizing nematode *C.elegans* is the preferred model for investigating geronotology [295]. With a short lifespan, completely sequenced genome, inexpensive maintenance and complete cell fate map, it provides an informative investigative tool for human senile diseases [295].

C.elegans has been vital in identifying the components of γ -secretase. *C.elegans* possesses an AβPP homolog, *apl-1* [296]. APL-1 is expressed in neurons, hypodermal cells and muscles [297]. The NTF of APL-1 has been shown to be critical for its function as it is able to effectively rescue the loss of APL-1 [297]. *C.elegans* contains three PRESENILIN orthologs; *sel-12*[298], *hop-1*[299], and *spe-4*[300]. Human PSEN1 and PSEN2 activity is reminiscent of SEL-12 protein function, and this was utilised to determine the transmembrane domains of human PSEN1[282]. *C.elegans* has been an effective tool for investigating PRESENILIN function, as exemplified by the elucidation of *sel-12*'s role in the conserved Notch pathway.

C.elegans provided the first invertebrate model for AD, involving the transgenic expression of a human Aβ42 minigene from a constitutive muscle-specific promoter [301, 302]. Human AβPP was utilised in preference to the invertebrate AβPP due the absence of a native region encoding the neurotoxic Aβ42 [296, 303]. The lack of this coding sequence meant that *C.elegans* was not initially thought to be an effective model of AD, as mutated endogenous expression of AβPP would be irrelevant. However, the human transgene model successfully produced a progressive paralysis phenotype, with the deposition of intracellular Aβ deposits [301]. Though these models did not reflect AD pathology, they successfully demonstrated that Aβ could form deposits *in vivo*, and could

be used effectively to investigate the correlation between Aβ sequence, amyloid formation and oxidative damage [301, 302].

Transgenic nematodes have subsequently been used together with DNA microarrays to derive global gene expression changes in Aβ-expressing strains [304]. It has provided a method that allows gene expression profiles to be easily analysed after expression of Aβ *in vivo*. Temperature-dependent induction of Aβ transgenic *C.elegans* has been produced [304]. Inducible Aβ expression has enabled the identification of specific candidate Aβ responsive genes, rather than a global description of responsive gene expression to Aβ accumulation. It is hoped that these models will allow the recognition of core cellular responses to Aβ accumulation.

The *C.elegans* system has also been used to give insight into initial Aβ metabolism and chaperone association in early AD development [305]. Studies have previously indicated that HSP-70 and alphaB-crystallin-related protein expression may be involved in AD plaque formation [306, 307]. In *C.elegans* AβPP transgenic models, the chaperone protein HSP-16 was found to co-localise with intracellular Aβ, suggesting it interacts with monomeric Aβ or prefibrillar Aβ oligomers. Similarly they found that F26D10.3, a cytoplasmic HSP70 chaperone, could specifically interact with Aβ42 [305]. The role of these interactions is unknown.

The investigation of neurological damage from free-radical induced oxidative damage in AD has utilised nematode transgenic models [303, 308]. Aβ expressing models have shown higher levels of ROS when compared to wildtype [309, 310]. In an attempt to associate Aβ expression and toxicity, Aβ expression in *C.elegans* induced oxidative stress

that produced a paralytic phenotype, supporting the idea that an Aβ soluble oligomer is involved in mediating AD toxicity [310].

Drosophila melangaster

Drosophila, like *C.elegans*, has been used in human disease research, ranging from investigating cell proliferation and differentiation, neuronal connectivity, cell cycle control, and tissue patterning to apoptosis.

Drosophila homologs of AβPP and PSEN, *Appl* and *Psen* respectively, have been found. Mutations in *Drosophila Psen* have been shown to give rise to Notch-like mutant phenotypes. This has been invaluable in discerning the involvement of PRESENILIN in Notch signalling. In conjunction with *Psen*, homologs of the three other constituents of the γ-secretase complex have been found and are active within *Drosophila* [311, 312]. *Appl* expression is restricted to neurons, with APPL knock out still being viable [313]. *Appl*, shares approximately 30% amino identity with human AβPP but does not contain the AβPP cleaved segment for producing pathogenic peptides [314]. However, deletions of *Appl* result in a defective locomotor behaviour, which can be rescued by a human AβPP [315]. Many groups have generated AβPP mediated AD-like pathologies in flies by expressing transgenic wild type or FAD human AβPP. For example the co-expression of human wild-type AβPP and BACE with *Drosophila* Psen leads to Aβ generation and age dependent AD-like pathogenesis, and neurodegeneration and accumulation of Aβ. The phenotype can be inhibited by loss of function mutations in *Psen*, whilst co-expression with FAD-associated *Psen* transgenes enhances neurodegeneration.

Expression of FAD human AβPP with *Drosophila* FAD Psen in flies shows an increase in Aβ42 production and enhanced amyloid deposition. Interestingly, when FAD AβPP was expressed the flies showed axonal transport defects and neuronal apoptosis was observed. The expression of Aβ42 and not Aβ40 in the fly brain is able to produce clear amyloid deposits, age-dependent locomotor defects and neurodegeneration. Notably, expression of Aβ42 and high levels of Aβ40 caused deficits in short-term memory, indicating that excessive Aβ40 may also be toxic to synaptic plasticity. Unlike most mouse models of Aβ, transgenic flies expressing Aβ42 exhibit extensive cell loss, a difference that may be due to the fact that Aβ accumulates intracellularly within neurons in flies, whereas they are extracellular in most mouse models. While the traditional clinical pathology of AD is that of extracellular amyloid plaques, human AD brains show significant accumulation of intraneuronal Aβ42.

Flies co-expressing AβPP and either β -secretase or a dominant–negative human PRESENILIN have displayed neuronal-degeneration and amyloid plaque formation. Particularly, AβPP involvement in the impairment of axonal transport in *Drosophila* has been extensively studied [316, 317].

Though neurodegeneration is observed in fly models, the ability to recapitulate all of the pathological features of AD is not possible with the limited complexity of flies. However this does not dismiss them as an effective model for AD. They provide a sensitive genetic system that enables easy, effective screening, and isolation of genes, which are not as accessible in more complex models.

Danio rerio

Danio rerio (zebrafish) provide an effective vertebrate animal model for investigating human cell and developmental biology. Zebrafish are easy to maintain, small, and are sexually reproductive after 3 months, enabling the quick establishment of a transgenic line. Their embryos develop rapidly, with gastrulation complete after 10 hours post fertilization (hpf), while the organs are formed and functional within the first 5 days. This rapid, external development of a predominantly transparent embryo highlights their potential as a cell biology investigative model. Many non-invasive experiments can be conducted, allowing dynamic cellular processes and early embryo development to be observed. The injection of morpholino antisense oligonucleotides (MOs) into zebrafish embryos has enabled the quick and easy assessment of gene function. These are typically 25 bases in length and designed to bind to a complementary sequence of RNA. Morpholinos hybridized with mRNA can interfere with progression of the ribosomal initiation complex from the 5' cap to the start codon. This prevents translation of the coding region of the targeted transcript [318]. MOs efficiently block translation initiation or mRNA splicing. Embryos injected with an MO at the one-cell stage effectively show a loss of gene function [319]. Several hundred embryos can be injected per hour, providing an effective method for genetic screens.

The zebrafish genes *appa* and *appb* are duplicates of an ancestral orthologue of human *AβPP [320]*. Alignment of the sequence of the human APP695 protein isoform with the sequences of the zebrafish Appa and Appb proteins reveal that Appa is 74% identical to human AβPP, while Appb is 71% identical to human AβPP. The two zebrafish App protein sequences share 77% identity with each other. The Appa protein sequence is

highly conserved, sharing 94% identity with human AβPP in the cytoplamsic region, 95% identity in the transmembrane domain and 80% identity in the Aβ42 region. Appb shares 100% identity with human AβPP in the transmembrane domain, 94% in the cytoplasmic region and is 71% identical to human Aβ. Appa is more similar than Appb to the human App770 isoform of AβPP which is ubiquitously expressed and has the Kunitz Protease Inhibitor (KPI) domain, whereas Appb has a greater similarity to human APP695 which is expressed exclusively in the mammalian brain. Both *appa* and *appb* have diffuse expression through the early stages of development. During segmentation their expression patterns diverge, but by 25 hpf they share expression in the posterior lateral line ganglia, the ventral diencepholon, in the telencephalon and the trigeminal ganglia [321]. Indicative of conserved AβPP gene function in vertebrate evolution, the expression pattern of *appa* and *appb* is similar to the mouse AβPP-695 isoform [322].

The injection of MOs blocking the translation of Appa and Appb proteins in zebrafish has been used to analyze endogenous AβPP function in zebrafish [321]. Inhibition of Appa during development does not appear to have a signficiant effect on viability in contrast to Appb abolition, which has been showed to be critical in the correct convergent extension cellular movements. The embryonic defects of blocked Appb can be rescued by the coinjection of human AβPP, indicative of the conserved function between human and zebrafish. It is worth noting that mRNA injection of the human AβPP extracellular domain is able to effectively rescue the convergent extension defects, while a larger protein containing the transmembrane domain (but lacking the EYNPTY motif, which functions as a docking site for multiple adapter proteins) or AβPP with the Swedish mutation (K595N/M596L) is not able to rescue the phenotype. The loss of Appb has also

been shown to cause defective neuronal development particularly axon outgrowth defects that can be rescued only by full length human APP [323].

Zebrafish contain orthologues of human *PSEN1* and *PSEN2*, identified as psen*1* and *psen2* in *Danio rerio* respectively [324, 325]. The maternally inherited Psen1 shares 74% identity to PSEN1 requiring the two critical aspartate residues for catalytic function [325]. It has been shown that a decrease in *psen1* expression results in a disruption of somite formation indicative of disrupted Notch signaling in the presomitic mesoderm and disruption of *myoD* expression [326, 327]. Similarly the inhibition of *psen1* involvement in reducing Notch signaling is supported by the loss of Notch target gene *her6* (orthologue of human HES1) expression and increased expression of neural progenitor cell marker *neurogenin 1* (*ngn1*) [328]. *In vitro,* studies showed that zebrafish Psen1 is able to replace human PSEN1 and is efficient in producing Aβ42 from AβPP containing the Swedish FAD mutation (K670N/M671L) [325].

PSEN1 splice variants have been studied extensively utilizing MOs targeting splice acceptor sites in zebrafish [329]. Experiments were initially aimed at producing the human PSEN1 L271V [330] and mutations after PSEN1 exon 9 [331, 332], whereby the MOs binding would exclude exons 8 and 9 respectively. However this failed, but rather led to the splicing out of introns 7 and 8 that lead to truncated sequences after exon 6 and 7. These aberrant zebrafish *psen1* transcripts resulted in dominant negative effects on Psen1 activity [329]. The translation of such protein products is believed to be due to the simultaneous inhibition of nonsense-mediated decay by MOs. Furthermore it was observed that these dominant negative effects also suppressed Psen2 activity [329].

Zebrafish Psen2 shares 74% homology to human PSEN2, and 70% identity to Psen1 [333]. Sharing a highly conserved primary structure with human PSEN2, the two proteins vary considerable in the amino and carboxyl terminal fragments of the cytoplasmic loop domain [324]. Though expressed uniquely at the early stages of development the expression of *psen2* becomes more specific by 24 hours post fertilization (hpf). Psen2 protein expression begins from 6 hpf to 12 hpf, indicative of a tight translational regulation of *psen2*. By 24 hpf *psen2* transcript can be detected at high levels in cells derived from the neural crest, in the anterior developing CNS and eye, and in the midline of the developing spinal cord [334]. It has been shown in zebrafish that blocking of *psen2* expression by MOs produces a reduction of pigmentation and hydrocephalus in similar phenotypic fashion to the loss of *psen1* [329, 334]. Reduced Psen*2* translation causes an expansion of brain ventricles at 48hpf and reduced trunk neural crest formation with a greater amount of Dorsal Longitudinal Ascending (DoLA) neurons at 24 hpf [334].

Other components of γ-secretase, PSENEN (encoded by *psenen*) and APH-1 (encoded by *aph1b*) have been identified in zebrafish. *Aph1b* share 62% identity to both of the human *APH-1* (*APH-1a* and *APH-1b*), while zebrafish *psenen* has 74% identity with human PSENEN [335]. Like *PSEN1*, both genes encoding these proteins are maternally expressed and are at their highest level of expression at 12hpf of development. Injection of embryos with MOs blocking *aph1b* or *psenen* expression decreases PSEN1 CTF levels, indicating that, as in mammals, Aph1b and Psenen are essential for stabilization of PSEN1 fragments. Psenen knockdown results in a severe phenotype, including opaque regions throughout the embryo indicating cell death. Being part of the γ -secretase complex, Aph1b and Psenen are involved in Notch signaling. Injection of MOs blocking

aph1b and *psenen* translation decreases Notch target gene *her6* expression and increases *neurog1* expression indicating a decrease in Notch signaling and γ-secretase activity [336]. The orthologue of human NCT has been identified in zebrafish and shares 56% identity [337]. The inhibition of γ-secretase complex activity by N-[N-(3,5-Difluorophenacetyl-l-analyl)]-5-phenylglycine t-butyl ester (DAPT), has been shown to reduce Aβ peptide levels in the brain [338] and impairs somitogenesis and neurogenesis in developing embryos [339]. DAPT impairs Notch processing by disrupting Presenilin activity to prevent Notch dependent cell fate decisions [339].

1.2 Summary of Chapters II-IV and Links Between Them

Zebrafish embryos have a unique combination of characteristics that allows genetic manipulation and analysis. The embryos are numerous, macroscopic, external to the mother and transparent making them easy to inject and observe. Changes in different aspects of their rapid development can be used as bioassays to assess gene activity. Currently there is no *in vivo* assay appropriate for directly monitoring γ-secretase activity. **Chapter II** describes an assay in which the level of a γ-secretase substrate (a modified form of Appa protein) is observed in zebrafish embryos by western immunoblotting relative to a co-expressed protein not subject to γ-secretase activity. The assay was used to analyze the effects on γ-secretase activity of blocking translation of zebrafish *psen1* and/or *psen2*.

More than 180 *PSEN1* and 23 *PSEN2* mis-sense mutations have been isolated in families with early onset Alzheimer's disease (EOAD). No non-sense mutations have been found in EOAD pedigrees which has led to the idea that truncated PRESENILIN proteins are not functional in AD. One of the Lardelli labs most significant discoveries using zebrafish has been to show that truncated PRESENILIN proteins can actually have potent dominant negative effects on Notch signalling [340]. This may explain why mutations causing truncation of PRESENILIN proteins are rarely ever found. The Lardelli lab has continued to pioneer the use of zebrafish embryos to study AD, particularly *PRESENILIN* gene and protein function ([340], [341], [282], [342], [343]). **Chapter III** furthers this work to show that various truncations of human PSEN1 and zebrafish Psen1 protein have clear differential effects on Notch signalling and cleavage of zebrafish Appa. Different truncations can suppress or stimulate Notch signalling but not Appa cleavage and *vice versa*. The G183V Picks disease mutation causes production of aberrant transcripts where the open reading frame is truncated after exon 5 sequence. Paper IV shows that the truncated protein potentially translated from these transcripts avidly incorporates into stable Psen1-dependent higher molecular weight complexes and suppresses cleavage of Appa but not Notch signalling. In contrast, the truncated protein potentially produced by the P242LfsX11 acne inversa mutation has no effect on Appa cleavage but, unexpectedly, enhances Notch signalling. The results suggest a novel hypothesis for the pathological mechanisms underlying these diseases and illustrate the importance of investigating the function of dominant mutations at physiologically-relevant expression levels and in the normally heterozygous state in which they cause human disease rather than in isolation from healthy alleles.

Two truncated isoforms of PRESENILIN are known to form naturally. Both are isoforms of mammalian Psen2. “PS2β” is formed in brain tissue by the use of an alternative splice donor site at the end of *Psen2* exon 10. This causes a frameshift that terminates the ORF/protein within the cytosolic loop domain. PS2β decreases γ-secretase activity by inhibiting complex assembly [344]. A second, normal truncated PSEN2 isoform “PS2V” has been identified [102]. PS2V is formed by exclusion of exon 5 from *PSEN2* transcripts leading to a frameshift after exon 4 sequence and a premature stop codon. This truncates the ORF/protein after the first transmembrane domain of PSEN2. The K115Efx10 mutation in *PSEN2* is the only completely truncating mutation of the *PRESENILIN* genes that is thought to cause AD. K115Efx10 is especially interesting since, if expressed, it would generate a truncated protein highly similar to PS2V and would be expected to boost Aβ production. Zebrafish possess an isoform of Psen1 that has a similar role to PS2V and zebrafish Psen1 truncated after exon 4 sequence behaves in a similar manner to PS2V. **Chapter III** examines the evolutionary conservation of PS2V and models the K115Efx10 mutation in zebrafish to investigate its effect on gene expression profiles, γ-secretase activity and complex constitution.

CHAPTER II

Research Paper I

The Development of an *in vivo* γ-Secretase Assay using Zebrafish Embryos.

Lachlan Wilson and Michael Lardelli

Discipline of Genetics, School of Molecular and Biomedical Science, The University of Adelaide, SA 5005, Australia

Journal of Alzheimer's Disease, 2013 May 10

STATEMENT OF AUTHORSHIP

The Development of an *in vivo* γ-Secretase Assay using Zebrafish Embryos.

Journal of Alzheimer's Disease, 2013 May 10

Lachlan Wilson (Candidate/Author)

Performed all experiments and wrote manuscript.

Certification that the statement of contribution is accurate

Signed

…… …….Date……

Michael Lardelli (co-author)

Planned the research and supervised development of work.

Certification that the statement of contribution is accurate

Signed

…… …….Date……

Journal of Alzheimer's Disease 36 (2013) 521–534
DOI 10.3233/JAD-130332
IOS Press

The Development of an *in vivo* γ-Secretase Assay using Zebrafish Embryos

Lachlan Wilson* and Michael Lardelli
Discipline of Genetics, School of Molecular and Biomedical Sciences, The University of Adelaide, SA, Australia

Accepted 4 April 2013

Abstract. Aberrant proteolytic processing of amyloid-β protein precursor by γ-secretase complexes may result in an imbalance between production and clearance of the Aβ proteolytic product and promote neuronal dysfunction and death. Presenilin proteins form the catalytic core of γ-secretase complexes. The zebrafish, *Danio rerio*, is a versatile vertebrate model for investigating the molecular basis of Alzheimer's disease pathology. It possesses genes orthologous to human *PSEN1* and *PSEN2* (*psen1* and *psen2* respectively), and *AβPP* (*appa* and *appb* that are duplicates of an ancestral *AβPP* orthologue). Currently there is no *in vivo* assay appropriate for directly monitoring γ-secretase activity. Here, we describe such an assay in which the level of a γ-secretase substrate (a modified form of Appa protein) is observed in zebrafish embryos by western immunoblotting relative to a co-expressed protein not subject to γ-secretase activity. We have used the assay to analyze the effects on γ-secretase activity of blocking translation of transcripts of zebrafish *psen1* and/or *psen2*.

Keywords: Alzheimer's disease, amyloid-β protein precursor, assay, γ-secretase, morpholinos, presenilin, truncated protein, zebrafish

INTRODUCTION

A detailed understanding of the molecular and cellular basis of Alzheimer's disease (AD) remains elusive. The most widely accepted possible mechanism for development of AD pathology is the 'amyloid cascade hypothesis' [1, 2]. This proposes that aberrant proteolytic processing of amyloid-β (Aβ) results in an imbalance between Aβ production and Aβ clearance [2, 3]. This results in intraneuronal accumulation of Aβ that promotes cell death.

Aβ is a cleavage fragment of the Amyloid-β A4 Precursor Protein (AβPP). Full-length AβPP is composed of a large extracellular domain, a single transmembrane region, and a short cytoplasmic tail. Aβ is generated at the plasma membrane from AβPP via a series of endoproteolytic cleavages by three membrane-bound aspartyl proteases: α-, β-, and γ-secretase [4, 5]. Sequential cleavage of AβPP to form Aβ begins with β-secretase cleavage to produce a large N-terminal fragment (sAβPPβ) and a lipid-membrane spanning C-terminal fragment of 99 amino acid (aa) residues in length (C99) [6–8]. C99 is then cleaved sequentially by γ-secretase in the transmembrane domain ([9–11] see below). γ-secretase activity is attributed to a protein complex comprised of nicastrin, anterior pharynax defective (APH), presenilin enhancer 2, and presenilin 1 (PSEN1) or presenilin 2 (PSEN2) [12–19]. The γ-secretase complex initially cleaves C99 at the ε-site near the cytosolic surface of the lipid bilayer to release the cytosolic AβPP intracellular domain (AICD) that translocates to the nucleus and acts as a transcription factor. The N-terminus of AICD is either the Leu 645 or Val 646 residue of the original AβPP protein (residue identities given are based on the 695 aa isoform of AβPP), giving AICD lengths of 57–59 aa due to the heterogeneous γ-secretase cleavage by γ-secretase [20, 21]). AICDs of 48, 50, 51, and 53 aa

*Correspondence to: Lachlan Wilson, Discipline of Genetics, School of Molecular and Biomedical Sciences, The University of Adelaide, SA 5005, Australia. Tel.: +61 8 8313 4863; Fax: +61 8 8313 7534; E-mail: lachlan.wilson@adelaide.edu.au.

ISSN 1387-2877/13/$27.50

can also be generated by the ζ and ε-cleavage activities of the γ-secretase complex [21–24]. γ-secretase cleavage then mediates the release of Aβ peptides of variable lengths. The most abundant cleavage product is $A\beta_{40}$, but the longer $A\beta_{42}$ peptide is more evident in AD senile plaques [25]. $A\beta_{42}$ is more hydrophobic and prone to aggregation than the $A\beta_{40}$ fragment [26–29]. Evidence suggests that $A\beta_{42}$ accelerates amyloid plaque formation [26]. It is thought that the change in the ratio of $A\beta_{40}$ to $A\beta_{42}$ in the cell (increased $A\beta_{42}$ relative to $A\beta_{40}$ present) affects neuron viability [26]. The size of the Aβ peptide liberated by γ-secretase is dependent on the exact cleavage site in the AβPP substrate remaining after β-secretase cleavage. The mechanism by which γ-secretase produces cleavage products of different length is not fully understood, although several hypotheses exist [30–35]. Furthermore the substrate specificity of the γ-secretase complex and its catalytic core, presenilin, is poorly defined [36].

γ-secretase plays an important role in development and neurogenesis as highlighted by the diversity of its substrates [37]. γ-secretase comes from a class of intramembrane cleaving proteases (I-CliPs) that cleave peptide bonds within lipid bilayers. Of all the I-CliPs, γ-secretase has the greatest number of known substrates, cleaving more than 90 type-I transmembrane proteins [36–38]. The activities of these substrates range from cell fate determination to neurite outgrowth and synapse formation. The catalytic core proteins of γ-secretase complexes, the presenilins, also have other crucial roles in cell signaling [39–43], tau phosphorylation [44–47], oxidative stress [44, 48, 49], calcium homeostasis [50–63], and autophagy [64–67]—factors pivotal in AD pathogenesis. The majority of familial AD cases are due to mutations in the presenilin genes with over 180 mutations known in *PSEN1* alone [68] (http://www.molgen.ua.ac.be/ADMutations). These mutations may cause neuronal dysfunction by pathways independent of AβPP and Aβ [69–75]. Indeed, connections can be found between presenilin dysfunction and almost all aspects of AD pathology.

In order to investigate the role of presenilin/γ-secretase in AD pathogenesis, many attempts to assess γ-secretase activity by *in vitro* expression in cell culture or cell-free assays have been undertaken. *In vitro* γ-secretase assays have proven vital in elucidating the mechanisms of action of cleavage inhibitors, the composition of the complex, and the action of factors regulating it [76–79]. These have mainly consisted of ELISA assays against Aβ peptide production, or cell-based or cell-free reporter assays utilizing AβPP [78, 80–83] or Notch [81–83] γ-secretase substrates. In many of these studies, γ-secretase activity has proven to be very sensitive to changes in lipids, pH, and temperature. It has been shown that, in a cell-free assay, Aβ processing at pH lower than 6.5 occurs in a γ-secretase-independent manner via another protease, possibly involving cathepsin D [84]. This highlights the sensitivity of apparent γ-secretase to correct cellular conditions and calls into question the validity of some observations on cleavage from *in vitro* systems. Previously our laboratory has examined γ-secretase activity by observing relative transcript levels from genes controlled by Notch signaling. However, there is currently no *in vivo* assay that has been used to directly investigate the action of γ-secretase activity at the molecular level.

In all non-human vertebrates investigated, single orthologues of the two human presenilin genes have been found. The zebrafish orthologues of human *PSEN1* and *PSEN2* are denoted *psen1* and *psen2*, respectively [85, 86]. The paralogous zebrafish genes *appa* and *appb* (encoding proteins Appa and Appb) both show a high degree of identity to human *AβPP* and arose by duplication of an ancestral *AβPP* orthologue [86–90]. This paper describes the development of an *in vivo* γ-secretase assay utilizing a modified form of the protein product of zebrafish *appa* to measure relative rates of γ-secretase cleavage. Differences in levels of the γ-secretase substrate between zebrafish embryos subjected to different treatments are quantified after normalization against a co-expressed protein that is not cleaved by γ-secretase. We show that the protein products of both the *psen1* and *psen2* genes contribute to the γ-secretase activity required for cleavage of our Appa-derived substrate.

MATERIALS AND METHODS

Ethics

This work was conducted under the auspices of The Animal Ethics Committee of The University of Adelaide and in accordance with EC Directive 86/609/EEC for animal experiments and the Uniform Requirements for manuscripts submitted to Biomedical journals.

Isolation of appa cDNA and generation of C100

A positive cDNA clone of zebrafish *appa695* was obtained by RT-PCR and cloned using the Zero Blunt TOPO PCR cloning Kit (Invitrogen, Carlsbad,

CA, USA). The AppaC100 was amplified by polymerase chain reaction (PCR) using the following primers C100F 5′-GCATGAATTCATGGAAGCTG AAGAGAGAC-3′ and C100R 5′-GCATGAATTCT CATTTGTCGTCGTCGTCTTTGTA GTCGTTGTG CATCTGCTCAAAG-3′. The amplified AppaC100 was then cloned into the *Bam*HI sites of the pEAP vector.

PCR amplification of intermediate fragments

Amplification of AppaC100 and dGFP were performed using primers listed in Table 1. A 50 μl PCR reaction with 1 unit of DyNAzyme DNA polymerase (Finnzymes, Espoo, Finland) and 400 ng of plasmid DNA template was performed. The thermal cycling parameters were as follows: 94°C for 2 min, followed by cycles of 94°C for 30 s, 45°C for 30 s, ramp up at 0.5°C/s to 72°C, and 72°C for 2 min. AppaC100 and dGFP were amplified through 20 and 10 PCR cycles, respectively.

PCR-mediated recombination and cloning into expression vectors

PCR-mediated recombination was modified from Fang et al. [91]. The thermal cycling parameters were: 94°C for 8 min followed by 10 cycles of 94°C for 3 min, ramp up at 0.5°C/s to 72°C and 72°C for 2 min. The PCR reaction was performed in 50 μl total volume with 1 unit of DyNAzyme and *Pfu* turbo polymerase (Stratagene, La Jolla, CA, USA) mix (8 : 2 ratio) and 100 ng of AppaC100 and dGFP intermediate fragments as the DNA template and megaprimers.

Included 5′ to the C100 is a secretory signal sequence (ss) [92] (5-ATGTGGTGGCGCCTGTGG TGGCTGCTGCTGCTGCTGCTGCTGTGGCC CATGGTGTGGGCC-3′) which serves to direct the protein substrate to the membrane and a consensus Kozak sequence (5′-GCCACCATG-3′). The AppaC100::dGFP, including the Kozak and ss sequences, were ligated into the vector pXT7 between the Xho*I* and Spe*I* sites. Using primers (5′-CGGGAT CCACCATGTGGTGGCGCCTG-3′ and 5′-CCA TGGATCTACACCATTGATCCTAGCAGA-3′), the AppaC100::dGFP, including SS and Kozak sequences, were amplified and cloned into pT2AL200R150G between *Bam*HI and *Cla*I sites.

Removal of AICD

To remove the AICD, the ssAppaC100 fragment was amplified by PCR using the following primers: 5′-ATGGTGAGCAAGGGCGAGGAGCTG-3′ and 5′-GCCGTTCTGCTGCA TCTTAGATAG-3′. The PCR fragment was then purified using the Quagen PCR-purification kit, and transformed into DH5α electrocompetent cells.

Mutagenesis

Two separate primer extension reactions were conducted, one containing the forward primer and one containing the reverse primer: 5 μl of 10X *Pfu* Buffer, 1 μl of 10 mM primer, 0.1–0.2 mg plasmid template, 1 μl of 10 mM dNTP mix, and H_2O to a final volume of 50 μl. 1 μl of Pfu turbo polymerase (Stratagene, La Jolla, CA, USA) was then added. The reactions were then subjected to PCR, with the following cycling parameters: 94°C for 30 s, 95°C for 30 s, 55°C for 1 min, ramp up at 0.5°C/s to 68°C and then 68°C for 2 min. Steps 2–4 were repeated for 4 cycles. It was then held at 4°C while 25 μl from each extension reaction was combined. 1 μl *Pfu* polymerase was then added. The thermal cycling as above was repeated for a total of 18 cycles. 25 μl was then removed of the reaction. 10 units of *Dpn*I enzyme was added. The reaction was incubated at 37°C for 1 h. 5 μl of the reaction was then transformed into electrocompetent cells.

Automated sequencing of expression vectors

Automated sequencing of plasmid DNA was prepared for Cycle Sequencing using the Tol2 primer 5′-GGCCCCTCTGCTAACCAT-3′ and Big Dye Terminator Mix (Applied Biosystems, Foster City, CA, USA) according to manufacturer's instructions. The products were analyzed on an ABI DNA sequencer (Applied Biosystems Foster City, CA, USA).

Table 1
Primers utilized for the amplification of C100 and dGFP

Primer	Primer Sequence (5′ – 3′)
F Xho-C100	CCGCTCGAGCCACCATGTGGTGGCGC
R C100::dGFP	CTCGCCCTTGCTCACCATGTTGTGCATCGCTCAAA
F dGFP-C100	TTTGAGCAGATGCACAACATGGTGAGCAAGGGCGAG
R dGFP-Spe	CCTGATCACTACACATTGTCCTAGCAGAAGC

Table 2
Morpholino sequences

Morpholino	Morpholino Sequences (5′ - 3′)
MoCont	CCTCTTACCTCAGTTACAATTTATA
MoPS1Tln	ACTAAATCAGCCATCGGAACTGTGA
MoPS2Tln	GTGACTGAATTTACATGAAGGATGA

Morpholino, plasmid, and mRNA microinjection of zebrafish embryos

Morpholinos were synthesized by Gene Tools LLC (Corvallis, OR, USA) and are listed in Table 2.

Fertilized zebrafish eggs were rinsed in embryo medium and injected before cleavage. Tol2 transposase (pCS-TP) mRNA was synthesized *in vitro* using the mMESSAGE mMACHINE SP6 Kit (Ambion Inc., Austin, TX, USA). All mRNA was precipitated in 5.3 M LiCl, 35 mM EDTA and then redissolved in water for injection. Approximately 1 μl of a DNA/RNA solution containing 50 ng/μl circular DNA of pT2AL200R150G (as an expression standard) and pT2ssAppaC100::dGFP/ssAPPaC86::dGFP*/AppaC86::dGFP* were combined with 25 ng/μl transposase mRNA, and injected into fertilized eggs at the one cell stage. When an embryo was injected with a combination of morpholino(s), DNA and mRNA, the DNA/mRNA mix was injected first followed by morpholino injection before the first cleavage. To ensure consistency of morpholino injection, eggs were always injected with solutions at 1 mM total concentration. Dilutions of experimental morpholinos were carried out by mixing these with standard negative control morpholino, MoCont. This ensured that assay variation observed was not due to change in the total injection concentration. The maximum concentration of experimental morpholino injected was always 0.5 mM. Titration of morpholinos to find effective concentrations has been shown previously [93].

Treatment of zebrafish embryos with DAPT

Zebrafish embryos were collected at fertilization and groups of 20–25 embryos were placed in individual wells of a microtitre tray with 1 ml per group of E3 medium (5 mM NaCl, 0.17 mM KCl, 0.33 mM $CaCl_2$, 0.33 mM $MgSO_4$). At 3 hpf, one group was left untreated, one group was treated with 1% DMSO in E3 medium, and a third group was treated with 100 μM DAPT (γ-secretase inhibitor IX, Calbiochem, San Diego, CA, USA) in 1% DMSO in E3 medium. Embryos were harvested for western blotting at 12 hpf. The embryos were maintained in standard temperature conditions in a humid incubator.

Western immunoblot analyses

Dechorionated and deyolked embryos were placed in sample buffer (2% sodium dodecyl sulfate (SDS), 5% β-mercaptoethanol, 25% v/v glycerol, 0.0625 M Tris–HCl (pH 6.8), and bromphenol blue), heated immediately at 100°C for 5 min, and then stored at –20°C prior to protein separation on 10% SDS–polyacrylamide gels. Proteins were transferred to nitrocellulose membranes using a semidry electrotransfer system. When immunoblotting with anti-GFP antibodies, the membranes were blocked with 5% w/v skim milk powder in TBST, incubated with a 1/5,000 dilution of primary antibodies in TBST containing 1% w/v skim milk, washed in TBST, and incubated with a 1/20,000 dilution of donkey anti-Goat IgG (Rockland Immunochemicals Inc., Gilbertsville, PA, USA). For incubation with anti-β-tubulin antibodies (Antibody E7, Developmental Studies Hybridoma Bank, The University of Iowa, IA, USA), the conditions were the same as for western blotting with anti-GFP antibodies except that the primary antibodies were diluted 1/200 and donkey antimouse IgG secondary antibodies (Jackson ImmunoResearch Laboratories Inc., West Grove, PA, USA) were diluted 1/3,000. After incubation with secondary antibodies, all the membranes were washed four times for 10 min in TBST and visualized with luminol reagents (Amresco, Ohio, USA) by exposure to X-ray films (GE Healthcare LTD, Amersham Hyperfilm^{TM} ECL, UK) and the ChemiDoc™ MP imaging system (Bio-Rad, Hercules, CA, USA).

RESULTS AND DISCUSSION

Construction of γ-secretase assay constructs

The zebrafish genes *appa* and *appb* are duplicates of an ancestral orthologue of human *AβPP*. Alignment of the sequence of the human AβPP695 protein isoform with the sequences of the zebrafish Appa and Appb proteins reveals that Appa is 74% identical to human AβPP, while Appb is 71% identical to human AβPP. The two zebrafish App protein sequences share 77% identity (Fig. 1). The Appa protein sequence is highly conserved in its C-terminal region that is subject to γ-secretase-dependent cleavage (Fig. 1), whereas regions known to be subject to α- and β-secretase-dependent proteolysis are less conserved. To become a cleavage substrate for γ-secretase, human AβPP must first be

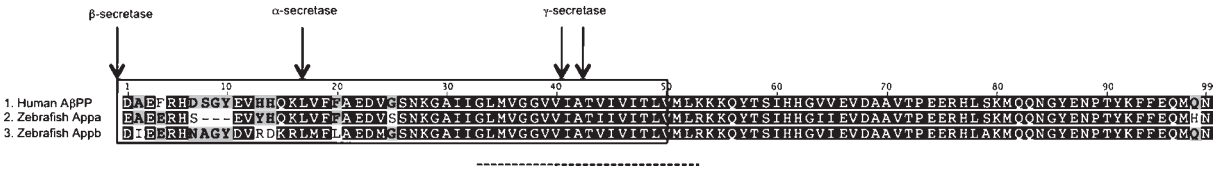

Fig. 1. Sequence alignment of AβPP proteins from human and zebrafish. Identical amino acids are shaded black. Dashes indicate gaps introduced for optical alignment. Arrows indicate the cleavage sites of α-, β-, and γ-secretase. The 40–42 aa Aβ peptide is boxed. Amino acid residue numbering starts from the β-secretase cleavage site. The transmembrane domain is indicated by a dashed line.

proteolytically cleaved to remove most of its extracellular/luminal domain. This is performed by either α- or β-secretase [9, 94–97] to form the C-terminal fragments denoted C83 or C99 respectively. When examining cleavage of AβPP in cells, the steady state levels of these C-terminal products or the levels of Aβ have been regarded as indicating γ-secretase activity. However, this is problematic, since cleavage of AβPP by α- or β-secretase might be rate-limiting and there is evidence that β-secretase expression may be dependent on γ-secretase action in certain circumstances [98]. Therefore, in order to study γ-secretase activity independent of any rate limits imposed by α- or β-secretase, many groups have directly expressed AβPP's C99 fragment itself in cells so that it is immediately available to γ-secretase for cleavage [94, 99].

Several groups have previously utilized truncated and tagged substrates such as C99 or NotchΔE (lacking most of its extracellular domain) to monitor γ-secretase catalysis [78, 80–83, 100]. To construct a zebrafish assay for γ-secretase cleavage of AβPP, we proposed to use a form of zebrafish Appa truncated to resemble the putative C-terminal fragment produced by β-secretase cleavage of Appa and fused to a highly active secretory signal sequence (ss, [92]) to ensure its insertion into lipid bilayers. We describe this as ssAppaC100 (see Fig. 2). The ssAppaC100 substrate was fused to a destabilized green fluorescent protein (dGFP) at its C-terminus to form ssAppaC100::dGFP. This construct was generated as described in Materials and Methods.

To examine γ-secretase cleavage of ssAppaC100::dGFP, a set ratio of Tol2-based expression constructs producing either the ssAppaC100::dGFP substrate or free GFP (to act as an expression standard) was injected into embryos at the one-cell stage. At 12 hpf, yolks are removed from the embryos and the embryos were then lysed and subjected to SDS polyacrylamide gel electrophoresis and western immunoblotting with anti-GFP antibody for detection of GFP. The uncleaved ssAppaC100::dGFP substrate is weakly visible on western immunoblots as a band of ∼43kDa. Its identity is confirmed by treatment

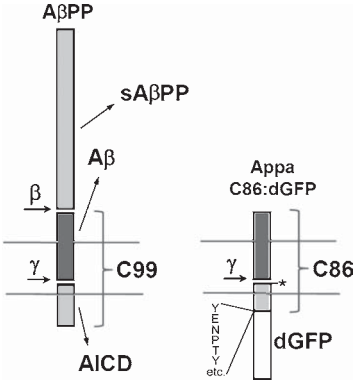

Fig. 2. The AppaC86:dGFP substate used to assay γ-secretase cleavage of Appa in zebrafish embryos. A secretory signal peptide (not shown) is fused at the N-terminus to the part of Appa predicted to be downstream of the site of β-secretase cleavage. In the transmembrane domain we have engineered the "Austrian mutation" (T714I) of human AβPP (*) to reduce γ-secretase cleavage [143] and the cytosolic YENPTY motif and downstream aa residues of Appa have been deleted to reduce interference with normal Appa function and so increase embryo viability [144]. The resultant Appa fragment is named "C86". A destabilized form of green fluorescent protein (dGFP) is fused at the C-terminus of Appa to assist in detection in living injected embryos and on western immunoblots. The structure of human AβPP and its cleavage products—secreted AβPP (sAβPP), Aβ and the AβPP Intracellular Domain (AICD)—are shown for comparison (not to scale).

of the embryos with DAPT from 3 hpf until 12 hpf after injection. This inhibits γ-secretase cleavage of ssAppaC100::dGFP and increases the intensity of the band on the immunoblot (e.g., see Fig. 4). The smaller, cytosolic (dGFP-containing) product of γ-secretase cleavage of ssAppaC100::dGFP proved highly unstable and difficult to observe (data not shown, see discussion below). However, as described later in this paper, variations in the levels of the uncleaved derivatives of ssAppaC100::dGFP relative to free GFP (that is not subject to γ-secretase cleavage) can be used to measure relative differences in γ-secretase activity.

Several missense mutations in AβPP have been identified in familial AD patients causing amino acid residue (aa) changes that decrease the rate of AβPP cleavage by γ-secretase. Of these, the Austrian

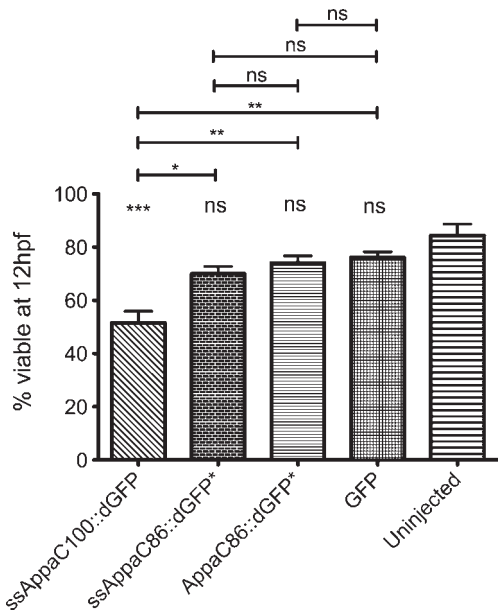

Fig. 3. The number of embryos surviving post injection of the series of Appa::dGFP constructs. Embryos were separately injected at the one cell stage with pCS-TP transposase mRNA with ssAppaC100::dGFP, ssAppaC86::dGFP* or AppaC86::dGFP* respectively. At 12 hpf, the percentage of embryos surviving was calculated. Error bars show standard errors of the means. The denoted statistical significance is with regard to uninjected embryos. *$p < 0.05$, **$p < 0.01$, ***$p < 0.001$. ns, not significant. (Raw data and statistical analysis is given in Supplementary Table 1; available here: http://dx.doi.org/10.3233/JAD-130332).

mutation (T639I) reduces cleavage efficiency due to its close proximity to the γ-secretase cleavage sites [101]. To increase the observable level of the γ-secretase substrate in our assay, this mutation was introduced into the subsequent derivatives of the ssAppaC100::dGFP construct. The mutated substrates are denoted by an asterisk (e.g., see ssAppaC86::dGFP* below).

Modification of the γ-secretase substrate to increase embryo viability

Approximately 10% of AβPP processing occurs via the amyloidogenic pathway in which the extracellular domain is cleaved by β-secretase [102–104]. This releases an extracellular soluble form of AβPP, sAβPPβ, and leaves C99 embedded in the lipid bilayer. Subsequent variable cleavage by γ-secretase releases a variety of possible Aβ peptides into lumenal/extracellular space with two possible AICD peptides released into the cytosol. Although there are extensive studies on AβPP and the Aβ peptide, their *in vivo* biological function and subcellular localizations are not completely defined and their contributions to the neural and vascular pathogenesis of AD are not completely understood [105–109].

To evaluate the viability of embryos expressing our modified Appa substrate in zebrafish, we recorded the number of embryos surviving to 12 hpf after injection of a Tol2-based expression construct encoding AppaC100::dGFP (co-injected with mRNA coding for the Tol2 transposase). Significantly fewer embryos survive to 12 hpf after injection with AppaC100::dGFP relative to embryos injected with the Tol2 vector expressing free GFP ($p < 0.01$) or relative to uninjected embryos ($p < 0.001$) (Fig. 3). Thus, expression of the AppaC100::dGFP substrate appears to be somewhat toxic to embryos.

Forced expression of ssAppaC100::dGFP may be toxic due to either increased and inappropriate pro-

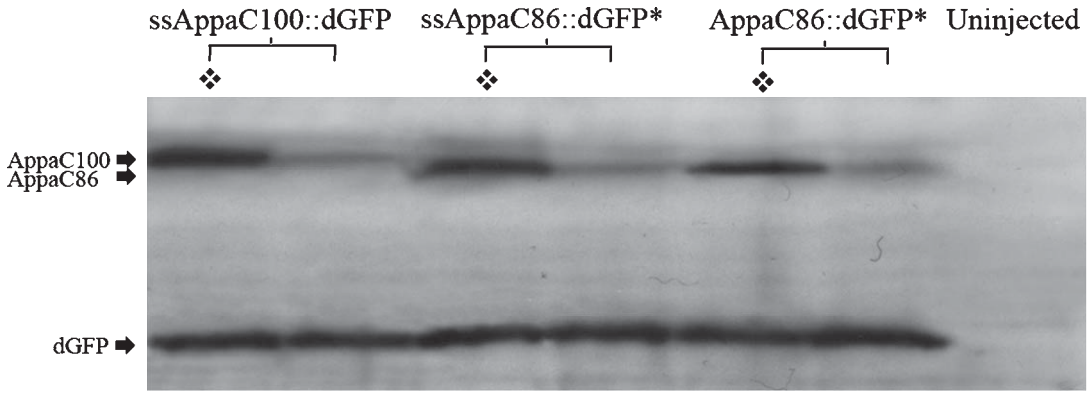

Fig. 4. Western blot analysis of substrate expression from embryos at 12 hpf injected with constructs for ssAppaC100::dGFP or ssAPPaC86::dGFP* or AppaC86::dGFP*. The Western blot was probed with anti-GFP antibody. Labeled arrows indicate protein bands. Embryos were injected at the one cell with the respective constructs. ssAppaC100::dGFP runs at ∼43kDa, while ssAppaC86::dGFP* and AppaC86::dGFP* run at ∼42kDa. ❖ Denotes treatment with DAPT. At 3 hpf half of each injected batch of embryos was treated with 100 μM of DAPT until 12 hpf.

duction of zebrafish Aβ (presumably produced when our Appa-derived substrate construct is cleaved by γ-secretase) and/or due to e.g. AICD acting as a positive regulator of apoptosis [110]. Indeed, elevated levels of AICD-like peptides have been identified in the brains of both normal control and sporadic AD patients [111]. AICD contains at least three functionally important motifs able to interact with different intracellular adaptor proteins [112]. Of particular interest is the YENPTY motif that acts as an internalization signal via clathrin-coated pits for membrane–associated receptor proteins [113–115]. Proteins containing phosphotyrosine interaction domains (PTB domains) recognize this motif. Mutation studies have suggested that YENPTY is the most important motif in AICD for inducing neurotoxicity [116, 117]. However, it has previously been shown that the cytosolic sequences of AβPP can be removed without affecting γ-secretase cleavage of the remaining protein [94]. Therefore, in an attempt to diminish the detrimental effects of constitutive C100::dGFP expression, the YENPTY motif and the remaining eight C-terminal amino acids residues downstream of it were deleted from ssAppaC100::dGFP to generate ssAppaC86::dGFP*.

The proportion of embryos surviving to 12 hpf after injection of a Tol2-based construct driving ssAppaC86::dGFP* expression is significantly greater than for those injected with the construct expressing the ssAppaC100::dGFP substrate that retains the YENPTY domain (18%, $p < 0.05$, Fig. 3). This supports that overexpression of AICD contributes to increased lethality.

Removal of the secretory signal sequence from AppaC86::dGFP still permits γ-secretase cleavage*

A number of studies have suggested that AβPP's C99 fragment can spontaneously insert into lipid bilayers. Indeed, the membrane insertion of an artificially expressed AβPP C99 derivative (C100) lacking a signal peptide was previously confirmed suggesting that the transmembrane domain could act as an internal signal peptide [6, 118, 119]. To investigate the dependence of γ-secretase cleavage of our Appa-derived assay construct on secretory signal sequence insertion into the lipid bilayer, we deleted the secretory signal sequence from ssAppaC86::dGFP* to generate AppaC86::dGFP* (see below).

The stability of the ssAppaC100::dGFP, ssAppaC86::dGFP*, and AppaC86::dGFP* fusion proteins and their ability to be cleaved by γ-secretase activity was then examined. To do this, a set ratio of a Tol2-based vector expressing an assay construct and a similar vector expressing free GFP (plus mRNA encoding the Tol2 transposase) was injected into embryos at the one-cell stage of development. A subset of each injected batch of embryos was incubated from 3 hpf onwards in the presence of the γ-secretase inhibitor DAPT (see Materials and Methods). Western immunoblotting to detect GFP in embryos lysed at 12 hpf was performed and revealed that, as expected, the uncleaved protein product of ssAppaC100::dGFP appears (qualitatively) to be less stable (more readily cleaved) than that of ssAppaC86::dGFP* and AppaC86::dGFP* (Fig. 4). The fact that all these modified substrates are subject to γ-secretase cleavage is confirmed by their increased levels in the presence of the γ-secretase inhibitor DAPT (Fig. 4). Also, the removal of the YENPTY motif and downstream amino acid residues evidently still permits γ-secretase cleavage.

Intriguingly there was little difference in expression level or γ-secretase cleavage between ssAppaC86::dGFP* and the AppaC86::dGFP* substrate lacking the secretory signal sequence. The latter substrate is still available for cleavage by γ-secretase. This supports that expression of AβPP C99-like fragments lacking signal sequences is a reasonable way to assess γ-secretase cleavage of AβPP.

The products of γ-secretase cleavage of all of our substrates (i.e., in effect, derivatives of AICD fused to dGFP) proved too unstable to detect by our western blotting procedure. However, this is not unexpected since AICD has very rapid turnover and a half-life that is potentially as short as 5 min [120]. Indeed, one difficulty in determining a physiological role for AICD has been its instability. The extreme instability of AICD has been linked to its rapid degradation by a cytoplasmic thiol-dependent metalloprotease, the insulin degrading enzyme (IDE), that also works to clear extracellular Aβ and functions as an Aβ-degrading enzyme [121–123]. The AICD may also be broken down by the proteasome [124]; however, this is debated [112].

γ-secretase cleavage of ssAppaC86::dGFP is dependent upon both Psen1 and Psen2 proteins in zebrafish*

The γ-secretase complex is made up of four components of which two, presenilin and APH1, have multiple forms in humans. The presenilin proteins, PSEN1 and PSEN2, share ∼67% identity. The two

APH1 isoforms, APH1a (which has two C-terminal splice variants, Aph-1aL and Aph-1aS) and APH-1b, also share a similar degree of identity (∼58% homology) [125]. These multiple PSEN and APH1 isoforms are indicative of the heterogeneity of γ-secretase complexes and the potential for the existence of different subtypes with variable specificities [125–127].

Several lines of evidence have specifically implicated both PSEN1 and PSEN2 in AβPP and Notch processing [128–131]. Studies have shown that while both proteins have overlapping substrate preferences [132], their selective affinity and catalytic efficiencies differ [133]. This has been highlighted by the differential responses of PSEN1- and PSEN2-mediated activities to γ-secretase inhibitors [134, 135]. Knockout of *Psen1* and *Psen2* in mice produces differing phenotypes that have been attributed to the differential actions of these ubiquitously-expressed proteins [136, 137]. Experiments using murine embryonic fibroblast and neuronal cells have also shown that the depletion of PSEN2 has a minor effect on cleavage of AβPP, Notch, and ephrinB substrates in comparison to PSEN1 [9, 129, 138]. This is supported by an *in vitro* analysis using flag tagged C100 substrates and γ-secretase complexes containing PSEN1 that showed that these are more active in cleavage of C100 than complexes containing PSEN2 [139]. However, a different study comparing Aβ production from reconstituted human γ-secretase complexes containing either PSEN1 or PSEN2 suggested that those containing PSEN1 do not show significantly higher activity that those containing PSEN2 [140]. Indeed it has been shown that γ-secretase containing PSEN2 cleaves more AβPP than that containing PSEN1 in murine microglia cells [141]. The discordance between these studies may be due to differences in the affinity of PSEN1 and PSEN2 for other secretase components and/or their localization and relative abundance within cells [142] rather than actual differences in their catalytic activity.

To examine the dependence of the γ-secretase activity detected by our Appa-based assay on complexes containing either zebrafish Psen1 or Psen2, we injected embryos with the vectors expressing ssAppaC86::dGFP* and free GFP, transposase mRNA as well as morpholinos inhibiting translation of Psen1, Psen2, or both proteins simultaneously. All these treatments significantly increased the relative level of uncleaved ssAppaC86::dGFP* relative to embryos injected with a negative control (inactive) morpholino (Fig. 5). This indicates that both Psen1 and Psen2 proteins contribute to γ-secretase cleavage of the Appa-based substrate. Inhibition of Psen1 translation

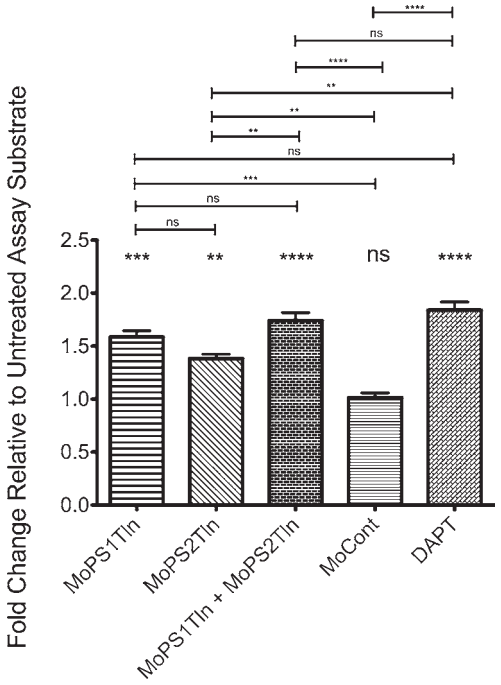

Fig. 5. Assays of zebrafish ssAppaC86::dGFP* cleavage at 12 hpf after injection of Mo's blocking endogenous expression of zebrafish Psen1 and Psen2. The denoted statistical significance is with regard to untreated embryos. Blocking Psen1 (MoPS1Tln) and Psen2 (MoPS2Tln) separately inhibits Appa Cleavage. Blocking both Psen1 and Psen2 translation simultaneously (MoTln+MoPS2Tln) decreases Appa cleavage comparably to treatment with the γ-secretase inhibitor DAPT. Injection of a control Mo (MoCont) has no significant effect. Error bars show standard errors of the means. $^{**}p < 0.01$, $^{***}p < 0.001$, ns, not significant. (Raw data and statistical analysis is given in Supplementary Table 2).

was not significantly different from inhibition of Psen2 in reducing this γ-secretase cleavage. This is consistent with the observations of Yonemura et al. on the roles of human PSEN1 and PSEN2 in the cleavage of AβPP [140]. However, simultaneous inhibition of translation of both zebrafish Psen1 and Psen2 apparently caused a significantly greater inhibition of γ-secretase activity than inhibition of Psen2 alone ($p \leq 0.01$) but not inhibition of Psen1 alone suggesting that Psen1 may actually play a slightly greater role that Psen2 in cleavage of Appa in zebrafish. The simultaneous reduction of Psen1 and Psen2 translation inhibited γ-secretase activity to a degree similar to exposure to DAPT, a direct chemical inhibitor of γ-secretase (Fig. 5).

CONCLUSION

We have created a novel substrate, ssAppaC86::dGFP*, for direct molecular analysis of

γ-secretase activity *in vivo* using zebrafish embryos. We have exploited the assay to analyze the effect on γ-secretase activity of inhibiting translation of the endogenous zebrafish Psen1 and Psen2 proteins. We note that ectopic expression of the AICD of Appa appears to be deleterious to embryo survival, that a secretory signal sequence is not required for access of a C100 fragment of Appa to γ-secretase activity, and that the YENPTY motif and downstream amino acid residues are not required to permit γ-secretase cleavage of Appa.

ACKNOWLEDGMENTS

The authors would like to thank Yanny Handoko for her initial work of the fusion of the AppaC100::dGFP construct and Svanhild Nornes for her contribution in the removal of the YENPTY motif. The Antibody E7 was obtained from the Developmental Studies Hybridoma bank developed under the auspices of the NICHD and maintained by The University of Iowa, Department of Biology, Iowa City, IA 52242.

This work was supported by a project grant from the National Health and Medical Research Council of Australia (453622), the ARC Special Research Centre for the Molecular Genetics of Development (S00001541), and the School of Molecular and Biomedical Sciences of The University of Adelaide.

Authors' disclosures available online (http://www.j-alz.com/disclosures/view.php?id=1740).

SUPPLEMENTARY MATERIAL

Supplementary material can be found here: http://dx.doi.org/10.3233/JAD-130332

REFERENCES

[1] Tanzi RE, Bertram L (2005) Twenty years of the Alzheimer's disease amyloid hypothesis: A genetic perspective. *Cell* **120**, 545-555.

[2] Hardy JA, Higgins GA (1992) Alzheimer's disease: The amyloid cascade hypothesis. *Science* **256**, 184-185.

[3] Hardy J, Selkoe DJ (2002) The amyloid hypothesis of Alzheimer's disease: Progress and problems on the road to therapeutics. *Science* **297**, 353-356.

[4] Haass C, Selkoe DJ (1993) Cellular processing of beta-amyloid precursor protein and the genesis of amyloid beta-peptide. *Cell* **75**, 1039-1042.

[5] Kamenetz F, Tomita T, Hsieh H, Seabrook G, Borchelt D, Iwatsubo T, Sisodia S, Malinow R (2003) APP processing and synaptic function. *Neuron* **37**, 925-937.

[6] Dyrks T, Weidemann A, Multhaup G, Salbaum JM, Lemaire HG, Kang J, Muller-Hill B, Masters CL, Beyreuther K (1988) Identification, transmembrane orientation and biogenesis of the amyloid A4 precursor of Alzheimer's disease. *EMBO J* **7**, 949-957.

[7] Busciglio J, Gabuzda DH, Matsudaira P, Yankner BA (1993) Generation of beta-amyloid in the secretory pathway in neuronal and nonneuronal cells. *Proc Natl Acad Sci U S A* **90**, 2092-2096.

[8] Higaki J, Quon D, Zhong Z, Cordell B (1995) Inhibition of beta-amyloid formation identifies proteolytic precursors and subcellular site of catabolism. *Neuron* **14**, 651-659.

[9] De Strooper B, Saftig P, Craessaerts K, Vanderstichele H, Guhde G, Annaert W, Von Figura K, Van Leuven F (1998) Deficiency of presenilin-1 inhibits the normal cleavage of amyloid precursor protein. *Nature* **391**, 387-390.

[10] Tarassishin L, Yin YI, Bassit B, Li YM (2004) Processing of Notch and amyloid precursor protein by gamma-secretase is spatially distinct. *Proc Natl Acad Sci U S A* **101**, 17050-17055.

[11] Chyung JH, Raper DM, Selkoe DJ (2005) Gamma-secretase exists on the plasma membrane as an intact complex that accepts substrates and effects intramembrane cleavage. *J Biol Chem* **280**, 4383-4392.

[12] Wolfe MS, De Los Angeles J, Miller DD, Xia W, Selkoe DJ (1999) Are presenilins intramembrane-cleaving proteases? Implications for the molecular mechanism of Alzheimer's disease. *Biochemistry* **38**, 11223-11230.

[13] Yu G, Nishimura M, Arawaka S, Levitan D, Zhang L, Tandon A, Song YQ, Rogaeva E, Chen F, Kawarai T, Supala A, Levesque L, Yu H, Yang DS, Holmes E, Milman P, Liang Y, Zhang DM, Xu DH, Sato C, Rogaev E, Smith M, Janus C, Zhang Y, Aebersold R, Farrer LS, Sorbi S, Bruni A, Fraser P, St George-Hyslop P (2000) Nicastrin modulates presenilin-mediated notch/glp-1 signal transduction and betaAPP processing. *Nature* **407**, 48-54.

[14] Goutte C, Tsunozaki M, Hale VA, Priess JR (2002) APH-1 is a multipass membrane protein essential for the Notch signaling pathway in Caenorhabditis elegans embryos. *Proc Natl Acad Sci U S A* **99**, 775-779.

[15] Lee SF, Shah S, Li H, Yu C, Han W, Yu G (2002) Mammalian APH-1 interacts with presenilin and nicastrin and is required for intramembrane proteolysis of amyloid-beta precursor protein and Notch. *J Biol Chem* **277**, 45013-45019.

[16] Francis R, McGrath G, Zhang J, Ruddy DA, Sym M, Apfeld J, Nicoll M, Maxwell M, Hai B, Ellis MC, Parks AL, Xu W, Li J, Gurney M, Myers RL, Himes CS, Hiebsch R, Ruble C, Nye JS, Curtis D (2002) aph-1 and pen-2 are required for Notch pathway signaling, gamma-secretase cleavage of betaAPP, and presenilin protein accumulation. *Dev Cell* **3**, 85-97.

[17] Steiner H, Winkler E, Edbauer D, Prokop S, Basset G, Yamasaki A, Kostka M, Haass C (2002) PEN-2 is an integral component of the gamma-secretase complex required for coordinated expression of presenilin and nicastrin. *J Biol Chem* **277**, 39062-39065.

[18] Haass C, Steiner H (2002) Alzheimer disease gamma-secretase: A complex story of GxGD-type presenilin proteases. *Trends Cell Biol* **12**, 556-562.

[19] De Strooper B (2003) Aph-1, Pen-2, and Nicastrin with Presenilin generate an active gamma-Secretase complex. *Neuron* **38**, 9-12.

[20] Gu Y, Misonou H, Sato T, Dohmae N, Takio K, Ihara Y (2001) Distinct intramembrane cleavage of the beta-amyloid

precursor protein family resembling gamma-secretase-like cleavage of Notch. *J Biol Chem* **276**, 35235-35238.

[21] Yu C, Kim SH, Ikeuchi T, Xu H, Gasparini L, Wang R, Sisodia SS (2001) Characterization of a presenilin-mediated amyloid precursor protein carboxyl-terminal fragment gamma. Evidence for distinct mechanisms involved in gamma -secretase processing of the APP and Notch1 transmembrane domains. *J Biol Chem* **276**, 43756-43760.

[22] Zhao G, Mao G, Tan J, Dong Y, Cui MZ, Kim SH, Xu X (2004) Identification of a new presenilin-dependent zeta-cleavage site within the transmembrane domain of amyloid precursor protein. *J Biol Chem* **279**, 50647-50650.

[23] Sastre M, Steiner H, Fuchs K, Capell A, Multhaup G, Condron MM, Teplow DB, Haass C (2001) Presenilin-dependent gamma-secretase processing of beta-amyloid precursor protein at a site corresponding to the S3 cleavage of Notch. *EMBO Reports* **2**, 835-841.

[24] Weidemann A, Eggert S, Reinhard FB, Vogel M, Paliga K, Baier G, Masters CL, Beyreuther K, Evin G (2002) A novel epsilon-cleavage within the transmembrane domain of the Alzheimer amyloid precursor protein demonstrates homology with Notch processing. *Biochemistry* **41**, 2825-2835.

[25] Iwatsubo T, Odaka A, Suzuki N, Mizusawa H, Nukina N, Ihara Y (1994) Visualization of A beta 42(43) and A beta 40 in senile plaques with end-specific A beta monoclonals: Evidence that an initially deposited species is A beta 42(43). *Neuron* **13**, 45-53.

[26] Jarrett JT, Berger EP, Lansbury PT, Jr (1993) The carboxy terminus of the beta amyloid protein is critical for the seeding of amyloid formation: Implications for the pathogenesis of Alzheimer's disease. *Biochemistry* **32**, 4693-4697.

[27] Jarrett JT, Lansbury PT, Jr (1993) Seeding "one-dimensional crystallization" of amyloid: A pathogenic mechanism in Alzheimer's disease and scrapie? *Cell* **73**, 1055-1058.

[28] Fraser PE, Nguyen JT, Inouye H, Surewicz WK, Selkoe DJ, Podlisny MB, Kirschner DA (1992) Fibril formation by primate, rodent, and Dutch-hemorrhagic analogues of Alzheimer amyloid beta-protein. *Biochemistry* **31**, 10716-10723.

[29] Pike CJ, Burdick D, Walencewicz AJ, Glabe CG, Cotman CW (1993) Neurodegeneration induced by beta-amyloid peptides *in vitro*: The role of peptide assembly state. *J Neurosci* **13**, 1676-1687.

[30] Qi-Takahara Y, Morishima-Kawashima M, Tanimura Y, Dolios G, Hirotani N, Horikoshi Y, Kametani F, Maeda M, Saido TC, Wang R, Ihara Y (2005) Longer forms of amyloid beta protein: Implications for the mechanism of intramembrane cleavage by gamma-secretase. *J Neurosci* **25**, 436-445.

[31] Rodriguez-Manotas M, Amorin-Diaz M, Cabezas-Herrera J, Acedo-Martinez A, Llorca-Escuin I (2012) Are gamma-secretase and its associated Alzheimer's disease gamma problems? *Med Hypotheses* **78**, 299-304.

[32] Xu X (2009) Gamma-secretase catalyzes sequential cleavages of the AbetaPP transmembrane domain. *J Alzheimers Dis* **16**, 211-224.

[33] Klafki H, Abramowski D, Swoboda R, Paganetti PA, Staufenbiel M (1996) The carboxyl termini of beta-amyloid peptides 1-40 and 1-42 are generated by distinct gamma-secretase activities. *J Biol Chem* **271**, 28655-28659.

[34] Citron M, Diehl TS, Gordon G, Biere AL, Seubert P, Selkoe DJ (1996) Evidence that the 42- and 40-amino acid forms of amyloid beta protein are generated from the beta-amyloid precursor protein by different protease activities. *Proc Natl Acad Sci U S A* **93**, 13170-13175.

[35] Zhao G, Tan J, Mao G, Cui MZ, Xu X (2007) The same gamma-secretase accounts for the multiple intramembrane cleavages of APP. *J Neurochem* **100**, 1234-1246.

[36] McCarthy JV, Twomey C, Wujek P (2009) Presenilin-dependent regulated intramembrane proteolysis and gamma-secretase activity. *Cell Mol Life Sci* **66**, 1534-1555.

[37] Haapasalo A, Kovacs DM (2011) The many substrates of presenilin/gamma-secretase. *J Alzheimers Dis* **25**, 3-28.

[38] Hemming ML, Elias JE, Gygi SP, Selkoe DJ (2008) Proteomic profiling of gamma-secretase substrates and mapping of substrate requirements. *PLoS Biol* **6**, e257.

[39] Cowburn RF, Popescu BO, Ankarcrona M, Dehvari N, Cedazo-Minguez A (2007) Presenilin-mediated signal transduction. *Physiol Behav* **92**, 93-97.

[40] McCarthy JV (2005) Involvement of presenilins in cell-survival signalling pathways. *Biochem Soc Trans* **33**, 568-572.

[41] Annaert W, De Strooper B (1999) Presenilins: Molecular switches between proteolysis and signal transduction. *Trends Neurosci* **22**, 439-443.

[42] Koo EH, Kopan R (2004) Potential role of presenilin-regulated signaling pathways in sporadic neurodegeneration. *Nat Med* **10 Suppl**, S26-33.

[43] Raurell I, Castano J, Franci C, Garcia de Herreros A, Dunach M (2006) Presenilin-1 interacts with plakoglobin and enhances plakoglobin-Tcf-4 association. Implications for the regulation of beta-catenin/Tcf-4-dependent transcription. *J Biol Chem* **281**, 1401-1411.

[44] Baki L, Shioi J, Wen P, Shao Z, Schwarzman A, Gama-Sosa M, Neve R, Robakis NK (2004) PS1 activates PI3K thus inhibiting GSK-3 activity and tau overphosphorylation: Effects of FAD mutations. *EMBO J* **23**, 2586-2596.

[45] Dewachter I, Ris L, Croes S, Borghgraef P, Devijver H, Voets T, Nilius B, Godaux E, Van Leuven F (2008) Modulation of synaptic plasticity and Tau phosphorylation by wild-type and mutant presenilin1. *Neurobiol Aging* **29**, 639-652.

[46] Feng R, Wang H, Wang J, Shrom D, Zeng X, Tsien JZ (2004) Forebrain degeneration and ventricle enlargement caused by double knockout of Alzheimer's presenilin-1 and presenilin-2. *Proc Natl Acad Sci U S A* **101**, 8162-8167.

[47] Saura CA, Choi SY, Beglopoulos V, Malkani S, Zhang D, Shankaranarayana Rao BS, Chattarji S, Kelleher RJ, 3rd, Kandel ER, Duff K, Kirkwood A, Shen J (2004) Loss of presenilin function causes impairments of memory and synaptic plasticity followed by age-dependent neurodegeneration. *Neuron* **42**, 23-36.

[48] Zhu M, Gu F, Shi J, Hu J, Hu Y, Zhao Z (2008) Increased oxidative stress and astrogliosis responses in conditional double-knockout mice of Alzheimer-like presenilin-1 and presenilin-2. *Free Radic Biol Med* **45**, 1493-1499.

[49] Takahashi N, Kariya S, Hirano M, Ueno S (2003) Two novel spliced presenilin 2 transcripts in human lymphocyte with oxidant stress and brain. *Mol Cell Biochem* **252**, 279-283.

[50] LaFerla FM (2002) Calcium dyshomeostasis and intracellular signalling in Alzheimer's disease. *Nat Rev Neurosci* **3**, 862-872.

[51] Mattson MP (2010) ER calcium and Alzheimer's disease: In a state of flux. *Sci Signal* **3**, pe10.

[52] Cook DG, Li X, Cherry SD, Cantrell AR (2005) Presenilin 1 deficiency alters the activity of voltage-gated Ca2+channels in cultured cortical neurons. *J Neurophysiol* **94**, 4421-4429.

[53] Leissring MA, Akbari Y, Fanger CM, Cahalan MD, Mattson MP, LaFerla FM (2000) Capacitative calcium entry deficits and elevated luminal calcium content in mutant presenilin-1 knockin mice. *J Cell Biol* **149**, 793-798.

[54] Yoo AS, Cheng I, Chung S, Grenfell TZ, Lee H, Pack-Chung E, Handler M, Shen J, Xia W, Tesco G, Saunders AJ, Ding K, Frosch MP, Tanzi RE, Kim TW (2000) Presenilin-mediated modulation of capacitative calcium entry. *Neuron* **27**, 561-572.

[55] Green KN, Demuro A, Akbari Y, Hitt BD, Smith IF, Parker I, LaFerla FM (2008) SERCA pump activity is physiologically regulated by presenilin and regulates amyloid beta production. *J Cell Biol* **181**, 1107-1116.

[56] Cheung KH, Shineman D, Muller M, Cardenas C, Mei L, Yang J, Tomita T, Iwatsubo T, Lee VM, Foskett JK (2008) Mechanism of Ca2+ disruption in Alzheimer's disease by presenilin regulation of InsP3 receptor channel gating. *Neuron* **58**, 871-883.

[57] Stutzmann GE, Smith I, Caccamo A, Oddo S, Laferla FM, Parker I (2006) Enhanced ryanodine receptor recruitment contributes to Ca2+ disruptions in young, adult, and aged Alzheimer's disease mice. *J Neurosci* **26**, 5180-5189.

[58] Cheung KH, Mei L, Mak DO, Hayashi I, Iwatsubo T, Kang DE, Foskett JK (2010) Gain-of-function enhancement of IP3 receptor modal gating by familial Alzheimer's disease-linked presenilin mutants in human cells and mouse neurons. *Sci Signal* **3**, ra22.

[59] Zatti G, Burgo A, Giacomello M, Barbiero L, Ghidoni R, Sinigaglia G, Florean C, Bagnoli S, Binetti G, Sorbi S, Pizzo P, Fasolato C (2006) Presenilin mutations linked to familial Alzheimer's disease reduce endoplasmic reticulum and Golgi apparatus calcium levels. *Cell Calcium* **39**, 539-550.

[60] Nelson O, Tu H, Lei T, Bentahir M, de Strooper B, Bezprozvanny I (2007) Familial Alzheimer disease-linked mutations specifically disrupt Ca2+ leak function of presenilin 1. *J Clin Investig* **117**, 1230-1239.

[61] Shen J, Kelleher RJ, 3rd (2007) The presenilin hypothesis of Alzheimer's disease: Evidence for a loss-of-function pathogenic mechanism. *Proc Natl Acad Sci U S A* **104**, 403-409.

[62] Michno K, Knight D, Campusano JM, van de Hoef D, Boulianne GL (2009) Intracellular calcium deficits in Drosophila cholinergic neurons expressing wild type or FAD-mutant presenilin. *PLoS One* **4**, e6904.

[63] Herms J, Schneider I, Dewachter I, Caluwaerts N, Kretzschmar H, Van Leuven F (2003) Capacitive calcium entry is directly attenuated by mutant presenilin-1, independent of the expression of the amyloid precursor protein. *J Biol Chem* **278**, 2484-2489.

[64] Lee JH, Yu WH, Kumar A, Lee S, Mohan PS, Peterhoff CM, Wolfe DM, Martinez-Vicente M, Massey AC, Sovak G, Uchiyama Y, Westaway D, Cuervo AM, Nixon RA (2010) Lysosomal proteolysis and autophagy require presenilin 1 and are disrupted by Alzheimer-related PS1 mutations. *Cell* **141**, 1146-1158.

[65] Williamson WR, Hiesinger PR (2010) On the role of v-ATPase V0a1-dependent degradation in Alzheimer disease. *Commun Integr Biol* **3**, 604-607.

[66] Neely KM, Green KN, LaFerla FM (2011) Presenilin is necessary for efficient proteolysis through the autophagy-lysosome system in a gamma-secretase-independent manner. *J Neurosci* **31**, 2781-2791.

[67] Neely KM, Green KN (2011) Presenilins mediate efficient proteolysis via the autophagosome-lysosome system. *Autophagy* **7**, 664-665.

[68] Sherrington R, Rogaev EI, Liang Y, Rogaeva EA, Levesque G, Ikeda M, Chi H, Lin C, Li G, Holman K, Tsuda T, Mar L, Foncin JF, Bruni AC, Montesi MP, Sorbi S, Rainero I, Pinessi L, Nee L, Chumakov I, Pollen D, Brookes A, Sanseau P, Polinsky RJ, Wasco W, Da Silva HA, Haines JL, Perkicak-Vance MA, Tanzi RE, Roses AD, Fraser PE, Rommens JM, St George-Hyslop PH (1995) Cloning of a gene bearing missense mutations in early-onset familial Alzheimer's disease. *Nature* **375**, 754-760.

[69] Saura CA, Servian-Morilla E, Scholl FG (2011) Presenilin/gamma-secretase regulates neurexin processing at synapses. *PLoS One* **6**, e19430.

[70] Kunimoto S, Nakamura S, Wada K, Inoue T (2010) Chronic stress-mutated presenilin 1 gene interaction perturbs neurogenesis and accelerates neurodegeneration. *Exp Neurol* **221**, 175-185.

[71] Barthet G, Dunys J, Shao Z, Xuan Z, Ren Y, Xu J, Arbez N, Mauger G, Bruban J, Georgakopoulos A, Shioi J, Robakis NK (2013) Presenilin mediates neuroprotective functions of ephrinB and brain-derived neurotrophic factor and regulates ligand-induced internalization and metabolism of EphB2 and TrkB receptors. *Neurobiol Aging* **34**, 499-510.

[72] Shvartsman AL, Sarantseva SV, Vitek MP (2011) [Potential role of presenilin 1 in regulation of synaptic function]. *Tsitologiia* **53**, 959-967.

[73] Ho A, Shen J (2011) Presenilins in synaptic function and disease. *Trends Mol Med* **17**, 617-624.

[74] Supnet C, Bezprozvanny I (2011) Presenilins function in ER calcium leak and Alzheimer's disease pathogenesis. *Cell Calcium* **50**, 303-309.

[75] Chan SL, Culmsee C, Haughey N, Klapper W, Mattson MP (2002) Presenilin-1 mutations sensitize neurons to DNA damage-induced death by a mechanism involving perturbed calcium homeostasis and activation of calpains and caspase-12. *Neurobiol Dis* **11**, 2-19.

[76] McLendon C, Xin T, Ziani-Cherif C, Murphy MP, Findlay KA, Lewis PA, Pinnix I, Sambamurti K, Wang R, Fauq A, Golde TE (2000) Cell-free assays for gamma-secretase activity. *FASEB J* **14**, 2383-2386.

[77] Czech C, Burns MP, Vardanian L, Augustin A, Jacobsen H, Baumann K, Rebeck GW (2007) Cholesterol independent effect of LXR agonist TO-901317 on gamma-secretase. *J Neurochem* **101**, 929-936.

[78] Hoke DE, Tan JL, Ilaya NT, Culvenor JG, Smith SJ, White AR, Masters CL, Evin GM (2005) In vitro gamma-secretase cleavage of the Alzheimer's amyloid precursor protein correlates to a subset of presenilin complexes and is inhibited by zinc. *FEBS J* **272**, 5544-5557.

[79] Kim SK, Park HJ, Hong HS, Baik EJ, Jung MW, Mook-Jung I (2006) ERK1/2 is an endogenous negative regulator of the gamma-secretase activity. *FASEB J* **20**, 157-159.

[80] Li YM, Lai MT, Xu M, Huang Q, DiMuzio-Mower J, Sardana MK, Shi XP, Yin KC, Shafer JA, Gardell SJ (2000) Presenilin 1 is linked with gamma-secretase activity in the detergent solubilized state. *Proc Natl Acad Sci U S A* **97**, 6138-6143.

[81] Sernee MF, Evin G, Culvenor JG, Villadangos JA, Beyreuther K, Masters CL, Cappai R (2003) Selecting cells with different Alzheimer's disease gamma-secretase activity using FACS. Differential effect on presenilin exon 9 gamma- and epsilon-cleavage. *Eur J Biochem* **270**, 495-506.

[82] Karlstrom H, Bergman A, Lendahl U, Naslund J, Lundkvist J (2002) A sensitive and quantitative assay for measuring cleavage of presenilin substrates. *J Biol Chem* **277**, 6763-6766.

[83] Liao YF, Wang BJ, Cheng HT, Kuo LH, Wolfe MS (2004) Tumor necrosis factor-alpha, interleukin-1beta, and interferon-gamma stimulate gamma-secretase-mediated cleavage of amyloid precursor protein through a JNK-dependent MAPK pathway. *J Biol Chem* **279**, 49523-49532.

[84] Yagishita S, Futai E, Ishiura S (2008) In vitro reconstitution of gamma-secretase activity using yeast microsomes. *Biochem Biophys Res Commun* **377**, 141-145.

[85] Leimer U, Lun K, Romig H, Walter J, Grunberg J, Brand M, Haass C (1999) Zebrafish (Danio rerio) presenilin promotes aberrant amyloid beta-peptide production and requires a critical aspartate residue for its function in amyloidogenesis. *Biochemistry* **38**, 13602-13609.

[86] Groth C, Nornes S, McCarty R, Tamme R, Lardelli M (2002) Identification of a second presenilin gene in zebrafish with similarity to the human Alzheimer's disease gene presenilin2. *Dev Genes Evol* **212**, 486-490.

[87] Newman M, Musgrave IF, Lardelli M (2007) Alzheimer disease: Amyloidogenesis, the presenilins and animal models. *Biochim Biophys Acta* **1772**, 285-297.

[88] Nornes S, Groth C, Camp E, Ey P, Lardelli M (2003) Developmental control of Presenilin1 expression, endoproteolysis, and interaction in zebrafish embryos. *Exp Cell Res* **289**, 124-132.

[89] Musa A, Lehrach H, Russo VA (2001) Distinct expression patterns of two zebrafish homologues of the human APP gene during embryonic development. *Dev Genes Evol* **211**, 563-567.

[90] Joshi P, Liang JO, DiMonte K, Sullivan J, Pimplikar SW (2009) Amyloid precursor protein is required for convergent-extension movements during Zebrafish development. *Dev Biol* **335**, 1-11.

[91] Fang G, Weiser B, Visosky A, Moran T, Burger H (1999) PCR-mediated recombination: A general method applied to construct chimeric infectious molecular clones of plasma-derived HIV-1 RNA. *Nat Med* **5**, 239-242.

[92] Barash S, Wang W, Shi Y (2002) Human secretory signal peptide description by hidden Markov model and generation of a strong artificial signal peptide for secreted protein expression. *Biochem Biophys Res Commun* **294**, 835-842.

[93] Nornes S, Newman M, Verdile G, Wells S, Stoick-Cooper CL, Tucker B, Frederich-Sleptsova I, Martins R, Lardelli M (2008) Interference with splicing of Presenilin transcripts has potent dominant negative effects on Presenilin activity. *Hum Mol Genet* **17**, 402-412.

[94] Cupers P, Bentahir M, Craessaerts K, Orlans I, Vanderstichele H, Saftig P, De Strooper B, Annaert W (2001) The discrepancy between presenilin subcellular localization and gamma-secretase processing of amyloid precursor protein. *J Cell Biol* **154**, 731-740.

[95] Brou C, Logeat F, Gupta N, Bessia C, LeBail O, Doedens JR, Cumano A, Roux P, Black RA, Israel A (2000) A novel proteolytic cleavage involved in Notch signaling: The role of the disintegrin-metalloprotease TACE. *Mol Cell* **5**, 207-216.

[96] Mumm JS, Schroeter EH, Saxena MT, Griesemer A, Tian X, Pan DJ, Ray WJ, Kopan R (2000) A ligand-induced extracellular cleavage regulates gamma-secretase-like proteolytic activation of Notch1. *Mol Cell* **5**, 197-206.

[97] Struhl G, Adachi A (2000) Requirements for presenilin-dependent cleavage of notch and other transmembrane proteins. *Mol Cell* **6**, 625-636.

[98] Tamagno E, Guglielmotto M, Aragno M, Borghi R, Autelli R, Giliberto L, Muraca G, Danni O, Zhu X, Smith MA, Perry G, Jo DG, Mattson MP, Tabaton M (2008) Oxidative stress activates a positive feedback between the gamma- and beta-secretase cleavages of the beta-amyloid precursor protein. *J Neurochem* **104**, 683-695.

[99] Lichtenthaler SF, Multhaup G, Masters CL, Beyreuther K (1999) A novel substrate for analyzing Alzheimer's disease gamma-secretase. *FEBS Lett* **453**, 288-292.

[100] Zhang C, Khandelwal PJ, Chakraborty R, Cuellar TL, Sarangi S, Patel SA, Cosentino CP, O'Connor M, Lee JC, Tanzi RE, Saunders AJ (2007) An AICD-based functional screen to identify APP metabolism regulators. *Mol Neurodegener* **2**, 15.

[101] Wiley JC, Hudson M, Kanning KC, Schecterson LC, Bothwell M (2005) Familial Alzheimer's disease mutations inhibit gamma-secretase-mediated liberation of beta-amyloid precursor protein carboxy-terminal fragment. *J Neurochem* **94**, 1189-1201.

[102] Marlow L, Cain M, Pappolla MA, Sambamurti K (2003) Beta-secretase processing of the Alzheimer's amyloid protein precursor (APP). *J Mol Neurosci* **20**, 233-239.

[103] Almkvist O, Basun H, Wagner SL, Rowe BA, Wahlund LO, Lannfelt L (1997) Cerebrospinal fluid levels of alpha-secretase-cleaved soluble amyloid precursor protein mirror cognition in a Swedish family with Alzheimer disease and a gene mutation. *Arch Neurol* **54**, 641-644.

[104] Kobayashi DT, Chen KS (2005) Behavioral phenotypes of amyloid-based genetically modified mouse models of Alzheimer's disease. *Genes Brain Behav* **4**, 173-196.

[105] Puig KL, Combs CK (2012) Expression and function of APP and its metabolites outside the central nervous system. *Exp Gerontol*, doi: 10.1016/j.exger.2012.07.009.

[106] Marchesi VT (2012) Alzheimer's disease 2012: The great amyloid gamble. *Am J Pathol* **180**, 1762-1767.

[107] Reitz C (2012) Alzheimer's disease and the amyloid cascade hypothesis: A critical review. *Int J Alzheimers Dis* **2012**, 369808.

[108] Castellani RJ, Lee HG, Siedlak SL, Nunomura A, Hayashi T, Nakamura M, Zhu X, Perry G, Smith MA (2009) Reexamining Alzheimer's disease: Evidence for a protective role for amyloid-beta protein precursor and amyloid-beta. *J Alzheimers Dis* **18**, 447-452.

[109] Hunter S, Brayne C (2012) Relationships between the amyloid precursor protein and its various proteolytic fragments and neuronal systems. *Alzheimers Res Therap* **4**, 10.

[110] Kogel D, Concannon CG, Muller T, Konig H, Bonner C, Poeschel S, Chang S, Egensperger R, Prehn JH (2012) The APP intracellular domain (AICD) potentiates ER stress-induced apoptosis. *Neurobiol Aging* **33**, 2200-2209.

[111] Passer B, Pellegrini L, Russo C, Siegel RM, Lenardo MJ, Schettini G, Bachmann M, Tabaton M, D'Adamio L (2000) Generation of an apoptotic intracellular peptide by gamma-secretase cleavage of Alzheimer's amyloid beta protein precursor. *J Alzheimers Dis* **2**, 289-301.

[112] Buoso E, Lanni C, Schettini G, Govoni S, Racchi M (2010) beta-Amyloid precursor protein metabolism: Focus on the functions and degradation of its intracellular domain. *Pharmacol Res* **62**, 308-317.

[113] Chen WJ, Goldstein JL, Brown MS (1990) NPXY, a sequence often found in cytoplasmic tails, is required

for coated pit-mediated internalization of the low density lipoprotein receptor. *J Biol Chem* **265**, 3116-3123.

[114] Koo EH, Squazzo SL (1994) Evidence that production and release of amyloid beta-protein involves the endocytic pathway. *J Biol Chem* **269**, 17386-17389.

[115] Lai A, Sisodia SS, Trowbridge IS (1995) Characterization of sorting signals in the beta-amyloid precursor protein cytoplasmic domain. *J Biol Chem* **270**, 3565-3573.

[116] Kim HS, Kim EM, Lee JP, Park CH, Kim S, Seo JH, Chang KA, Yu E, Jeong SJ, Chong YH, Suh YH (2003) C-terminal fragments of amyloid precursor protein exert neurotoxicity by inducing glycogen synthase kinase-3beta expression. *FASEB J* **17**, 1951-1953.

[117] Shaked GM, Kummer MP, Lu DC, Galvan V, Bredesen DE, Koo EH (2006) Abeta induces cell death by direct interaction with its cognate extracellular domain on APP (APP 597-624). *FASEB J* **20**, 1254-1256.

[118] McPhie DL, Golde T, Eckman CB, Yager D, Brant JB, Neve RL (2001) Beta-Secretase cleavage of the amyloid precursor protein mediates neuronal apoptosis caused by familial Alzheimer's disease mutations. *Brain Res Mol Brain Res* **97**, 103-113.

[119] Dyrks T, Dyrks E, Monning U, Urmoneit B, Turner J, Beyreuther K (1993) Generation of beta A4 from the amyloid protein precursor and fragments thereof. *FEBS Lett* **335**, 89-93.

[120] Cupers P, Orlans I, Craessaerts K, Annaert W, De Strooper B (2001) The amyloid precursor protein (APP)-cytoplasmic fragment generated by gamma-secretase is rapidly degraded but distributes partially in a nuclear fraction of neurones in culture. *J Neurochem* **78**, 1168-1178.

[121] Edbauer D, Willem M, Lammich S, Steiner H, Haass C (2002) Insulin-degrading enzyme rapidly removes the beta-amyloid precursor protein intracellular domain (AICD). *J Biol Chem* **277**, 13389-13393.

[122] Venugopal C, Pappolla MA, Sambamurti K (2007) Insulysin cleaves the APP cytoplasmic fragment at multiple sites. *Neurochem Res* **32**, 2225-2234.

[123] Farris W, Mansourian S, Chang Y, Lindsley L, Eckman EA, Frosch MP, Eckman CB, Tanzi RE, Selkoe DJ, Guenette S (2003) Insulin-degrading enzyme regulates the levels of insulin, amyloid beta-protein, and the beta-amyloid precursor protein intracellular domain *in vivo*. *Proc Natl Acad Sci U S A* **100**, 4162-4167.

[124] Nunan J, Shearman MS, Checler F, Cappai R, Evin G, Beyreuther K, Masters CL, Small DH (2001) The C-terminal fragment of the Alzheimer's disease amyloid protein precursor is degraded by a proteasome-dependent mechanism distinct from gamma-secretase. *Eur J Biochem* **268**, 5329-5336.

[125] Shirotani K, Edbauer D, Prokop S, Haass C, Steiner H (2004) Identification of distinct gamma-secretase complexes with different APH-1 variants. *J Biol Chem* **279**, 41340-41345.

[126] Serneels L, Van Biervliet J, Craessaerts K, Dejaegere T, Horre K, Van Houtvin T, Esselmann H, Paul S, Schafer MK, Berezovska O, Hyman BT, Sprangers B, Sciot R, Moons L, Jucker M, Yang Z, May PC, Karran E, Wiltfang J, D'Hooge R, De Strooper B (2009) Gamma-Secretase heterogeneity in the Aph1 subunit: Relevance for Alzheimer's disease. *Science* **324**, 639-642.

[127] Hebert SS, Serneels L, Dejaegere T, Horre K, Dabrowski M, Baert V, Annaert W, Hartmann D, De Strooper B (2004) Coordinated and widespread expression of gamma-secretase *in vivo*: Evidence for size and molecular heterogeneity. *Neurobiol Dis* **17**, 260-272.

[128] Herreman A, Serneels L, Annaert W, Collen D, Schoonjans L, De Strooper B (2000) Total inactivation of gamma-secretase activity in presenilin-deficient embryonic stem cells. *Nat Cell Biol* **2**, 461-462.

[129] Herreman A, Hartmann D, Annaert W, Saftig P, Craessaerts K, Serneels L, Umans L, Schrijvers V, Checler F, Vanderstichele H, Baekelandt V, Dressel R, Cupers P, Huylebroeck D, Zwijsen A, Van Leuven F, De Strooper B (1999) Presenilin 2 deficiency causes a mild pulmonary phenotype and no changes in amyloid precursor protein processing but enhances the embryonic lethal phenotype of presenilin 1 deficiency. *Proc Natl Acad Sci U S A* **96**, 11872-11877.

[130] Zhang Z, Nadeau P, Song W, Donoviel D, Yuan M, Bernstein A, Yankner BA (2000) Presenilins are required for gamma-secretase cleavage of beta-APP and transmembrane cleavage of Notch-1. *Nat Cell Biol* **2**, 463-465.

[131] Donoviel DB, Hadjantonakis AK, Ikeda M, Zheng H, Hyslop PS, Bernstein A (1999) Mice lacking both presenilin genes exhibit early embryonic patterning defects. *Genes Dev* **13**, 2801-2810.

[132] Li YM, Xu M, Lai MT, Huang Q, Castro JL, DiMuzio-Mower J, Harrison T, Lellis C, Nadin A, Neduvelil JG, Register RB, Sardana MK, Shearman MS, Smith AL, Shi XP, Yin KC, Shafer JA, Gardell SJ (2000) Photoactivated gamma-secretase inhibitors directed to the active site covalently label presenilin 1. *Nature* **405**, 689-694.

[133] Jayadev S, Leverenz JB, Steinbart E, Stahl J, Klunk W, Yu CE, Bird TD (2010) Alzheimer's disease phenotypes and genotypes associated with mutations in presenilin 2. *Brain* **133**, 1143-1154.

[134] Zhao B, Yu M, Neitzel M, Marugg J, Jagodzinski J, Lee M, Hu K, Schenk D, Yednock T, Basi G (2008) Identification of gamma-secretase inhibitor potency determinants on presenilin. *J Biol Chem* **283**, 2927-2938.

[135] Lee J, Song L, Terracina G, Bara T, Josien H, Asberom T, Sasikumar TK, Burnett DA, Clader J, Parker EM, Zhang L (2011) Identification of presenilin 1-selective gamma-secretase inhibitors with reconstituted gamma-secretase complexes. *Biochemistry* **50**, 4973-4980.

[136] Shen J, Bronson RT, Chen DF, Xia W, Selkoe DJ, Tonegawa S (1997) Skeletal and CNS defects in Presenilin-1-deficient mice. *Cell* **89**, 629-639.

[137] Wong PC, Zheng H, Chen H, Becher MW, Sirinathsinghji DJ, Trumbauer ME, Chen HY, Price DL, Van der Ploeg LH, Sisodia SS (1997) Presenilin 1 is required for Notch1 and DII1 expression in the paraxial mesoderm. *Nature* **387**, 288-292.

[138] Franberg J, Svensson AI, Winblad B, Karlstrom H, Frykman S (2011) Minor contribution of presenilin 2 for gamma-secretase activity in mouse embryonic fibroblasts and adult mouse brain. *Biochem Biophys Res Commun* **404**, 564-568.

[139] Lai MT, Chen E, Crouthamel MC, DiMuzio-Mower J, Xu M, Huang Q, Price E, Register RB, Shi XP, Donoviel DB, Bernstein A, Hazuda D, Gardell SJ, Li YM (2003) Presenilin-1 and presenilin-2 exhibit distinct yet overlapping gamma-secretase activities. *J Biol Chem* **278**, 22475-22481.

[140] Yonemura Y, Futai E, Yagishita S, Suo S, Tomita T, Iwatsubo T, Ishiura S (2011) Comparison of presenilin 1 and presenilin 2 gamma-secretase activities using a yeast reconstitution system. *J Biol Chem* **286**, 44569-44575.

[141] Jayadev S, Case A, Eastman AJ, Nguyen H, Pollak J, Wiley JC, Moller T, Morrison RS, Garden GA (2010) Presenilin 2 is the predominant gamma-secretase in microglia and modulates cytokine release. *PLoS One* **5**, e15743.

[142] Area-Gomez E, de Groof AJ, Boldogh I, Bird TD, Gibson GE, Koehler CM, Yu WH, Duff KE, Yaffe MP, Pon LA, Schon EA (2009) Presenilins are enriched in endoplasmic reticulum membranes associated with mitochondria. *Am J Pathol* **175**, 1810-1816.

[143] Wiley JC, Hudson M, Kanning KC, Schecterson LC, Bothwell M (2005) Familial Alzheimer's disease mutations inhibit gamma-secretase-mediated liberation of beta-amyloid precursor protein carboxy-terminal fragment. *J Neurochem* **94**, 1189-1201.

[144] Barbagallo AP, Wang Z, Zheng H, D'Adamio L (2011) A single tyrosine residue in the amyloid precursor protein intracellular domain is essential for developmental function. *J Biol Chem* **286**, 8717-8721.

Journal of Alzheimer's Disease xx (20xx) x–xx
DOI 10.3233/JAD-130332
IOS Press

Supplementary Data

The Development of an *in vivo* γ-Secretase Assay using Zebrafish Embryos

Lachlan Wilson and Michael Lardelli*
Discipline of Genetics, School of Molecular and Biomedical Sciences, The University of Adelaide, SA, Australia

Accepted 4 April 2013

*Correspondence to: Michael Lardelli, Discipline of Genetics, School of Molecular and Biomedical Sciences, The University of Adelaide, SA 5005, Australia. Tel.: +61 8 8313 3212; Fax: +61 8 8313 7534; E-mail: michael.lardelli@adelaide.edu.au.

ISSN 1387-2877/13/$27.50

Supplementary Table 1

Analysis of Appa lethality at 12 hpf after injection of DNA vectors encoding Appa zebrafish variants. To analyze the number of embryos surviving the overexpression of Appa, embryos were separately injected at the one cell stage with pCS-TP transposase mRNA and ssAppaC100::dGFP, ssAppaC86::dGFP*, AppaC86::dGFP* respectively. At 12 hpf, the percentage of embryos surviving was then calculated

	Injected	Viable at 12 hpf	% Viable
Replicate 1			
C86			
ssAppaC100::dGFP	127	56	44.09
ssAppaC86::dGFP*	84	59	70.23
AppaC86::dGFP*	126	87	69.04
GFP	75	54	72
Uninjected	100	76	76
Replicate 2			
C86			
ssAppaC100::dGFP	140	72	51.43
ssAppaC86::dGFP*	103	67	65.04
AppaC86::dGFP*	95	72	75.79
GFP	95	74	77.89
Uninjected	125	112	89.6
Replicate 3			
C86			
ssAppaC100::dGFP	115	68	59.13
ssAppaC86::dGFP*	87	65	74.71
AppaC86::dGFP*	89	69	77.53
GFP	112	88	78.57
Uninjected	130	114	87.69

One-way analysis of variance

The statistical significance of changes in relative intensity was assessed by one-way ANOVA with the Bonferroni Post Hoc test.

Bonferroni's Multiple Comparison Test	Mean Diff.	t	Significant? $p < 0.05$?	Summary	95% CI of diff.
ssAppaC100::dGFP versus ssAppaC86::dGFP*	−18.44	3.904	Yes	*	−35.36 to −1.526
ssAppaC100::dGFP versus AppaC86::dGFP*	−22.57	4.778	Yes	**	−39.49 to −5.652
ssAppaC100::dGFP versus Uninjected	−32.88	6.961	Yes	***	−49.80 to −15.96
ssAppaC100::dGFP versus GFP	−24.6	5.208	Yes	**	−41.52 to −7.686
ssAppaC86::dGFP* versus AppaC86::dGFP*	−4.127	0.8736	No	ns	−21.04 to 12.79
ssAppaC86::dGFP* versus Uninjected	−14.44	3.056	No	ns	−31.35 to 2.481
ssAppaC86::dGFP* versus GFP	−6.16	1.304	No	ns	−23.08 to 10.76
AppaC86::dGFP* versus Uninjected	−10.31	2.183	No	ns	−27.23 to 6.608
AppaC86::dGFP* versus GFP	−2.033	0.4304	No	ns	−18.95 to 14.88
Uninjected versus GFP	8.277	1.752	No	ns	−8.641 to 25.19

Supplementary Table 2

Assays of zebrafish Appa cleavage at 12 hpf after injection of MO's blocking zebrafish Psen1 and Psen2 expression. To assay γ-secretase activity, we injected a mixture of DNA encoding AppaC86::GFP and free GFP (that is not subject to γ-secretase cleavage). We then measured the relative amounts* of the two proteins on western immunoblots. (Greater γ-secretase activity results in a lower ratio of AppaC86::GFP to free GFP.) *The intensity of each western immunoblot band, either C86 or GFP, was quantified on a Typhoon trio imaging device (Amersham Bioscience Corp., Piscataway, NJ, USA). Variations in relative Appa cleavage due to various treatments are observed by comparing the AppaC86:dGFP bands on blots after normalization. To normalize the data, the intensities of the free GFP standards in each replicate set were normalized to the mean of these intensities and then the C86 intensity values were adjusted accordingly. Fold changes for the C86 values were then calculated against the "Untreated" sample and these values from the replicate sets were included in the statistical analysis. Appa assay cleavage at 12 hpf after injection of Mo's blocking endogenous expression of zebrafish Psen1 and Psen2

	Intensity of C86	Intensity of GFP standard	Normalized	Fold change relative to untreated C86
Replicate 1				
MoPS1Tln	16.84	12.78	15.7553581	1.5822977
MoPS2Tln	12.37	11.34	13.0568406	1.3112878
MoTln+MoPS2Tln	15.07	11.22	16.0573737	1.61262887
MoCont	11.02	13.36	9.77787896	0.98198437
Untreated	9.11	10.89	9.95726541	1
DAPT	18.65	12.45	17.9613687	1.80384553
Mean		12.0066667		
Replicate 2				
MoPS1Tln	28.4	18.67	30.765892	1.49377378
MoPS2Tln	27.31	19.34	28.6866743	1.3928217
MoTln+MoPS2Tln	37.43	19.87	38.3427774	1.86165367
MoCont	21.92	22.09	20.0652308	0.97422547
Untreated	20.64	20.41	20.5960851	1
DAPT	38.46	21.82	35.7155548	1.73409435
Mean		20.3666667		
Replicate 3				
MoPS1Tln	7.32	28.55	7.58045716	1.6925981
MoPS2Tln	6.19	28.19	6.48552528	1.44811685
MoTln+MoPS2Tln	7.16	26.53	7.90333071	1.76469074
MoCont	5.15	30.82	4.93834028	1.10265452
Untreated	4.78	31.47	4.4785925	1
DAPT	9.73	32.06	8.92254476	1.99226537
Mean		29.6033333		

One-way analysis of variance

The statistical significance of changes in relative intensity were assessed by one-way ANOVA with the Bonferroni Post Hoc test.

Bonferroni's Multiple Comparison Test	Mean Diff.	t	Significant? $p < 0.01$?	Summary	99% CI of diff
MoTln versus MoPS2Tln	0.2033	2.622	No	ns	−0.1495 to 0.5562
MoTln versus MoTln + MoPS2Tln	−0.1567	2.02	No	ns	−0.5095 to 0.1962
MoTln versus MoCont	0.57	7.35	Yes	***	0.2172 to 0.9228
MoTln versus C86	0.5867	7.565	Yes	****	0.2338 to 0.9395
MoTln versus DAPT	−0.2533	3.266	No	ns	−0.6062 to 0.09951
MoPS2Tln versus MoTln + MoPS2Tln	−0.36	4.642	Yes	**	−0.7128 to −0.007155
MoPS2Tln versus MoCont	0.3667	4.728	Yes	**	0.01382 to 0.7195
MoPS2Tln versus C86	0.3833	4.943	Yes	**	0.03049 to 0.7362
MoPS2Tln versus DAPT	−0.4567	5.888	Yes	**	−0.8095 to −0.1038
MoTln + MoPS2Tln versus MoCont	0.7267	9.37	Yes	****	0.3738 to 1.080
MoTln + MoPS2Tln versus C86	0.7433	9.585	Yes	****	0.3905 to 1.096
MoTln + MoPS2Tln versus DAPT	−0.09667	1.246	No	ns	−0.4495 to 0.2562
MoCont versus C86	0.01667	0.2149	No	ns	−0.3362 to 0.3695
MoCont versus DAPT	−0.8233	10.62	Yes	****	−1.176 to −0.4705
C86 versus DAPT	−0.84	10.83	Yes	****	−1.193 to −0.4872

Further Statistical Analysis

Paired *t*-test	*p*-value
MoPS1Tln	0.0096
MoPS2Tln	0.011
MoTln + MoPS2Tln	0.0094
MoCont	0.7284
DAPT	0.0084

ns, not significant, i.e., $p \geq 0.01$; **$p < 0.01$, ***$p < 0.001$, **** $p < 0.0001$.

CHAPTER III

Research Paper II

Differential, dominant activation and inhibition of Notch signalling and APP cleavage by truncations of PSEN1 in human disease.

Morgan Newman[1], Lachlan Wilson[1], Giuseppe Verdile[2,3,4], Anne Lim[1], Imran Khan[2,3,4], Sharon Pursglove[5,6], Gavin Chapman[5,6], Ralph Martins [2,3,4] and Michael Lardelli[1]

[1]Discipline of Genetics, School of Molecular and Biomedical Science, The University of Adelaide, SA 5005, Australia, [2]Centre of Excellence for Alzheimer's Disease Research and Care, School of Exercise, Biomedical and Health, [3]SirJames McCusker Alzheimer's Disease Sciences, Edith Cowan University, Joondalup, WA 6027, Australia, [4]Neurosciences, University of Western Australia, Crawley, WA 6009, Australia, Department of Pharmacology, Howard, [5] Development Biology Program, Victor Chang Cardiac Research Institute, Sydney, NSW, Australia, [6]St. Vincent's Clinical School, University of New South Wales, Sydney, NSW, Australia.

STATEMENT OF AUTHORSHIP

Differential, dominant activation and inhibition of Notch signalling and APP cleavage by truncations of PSEN1 in human disease.

Morgan Newman (Co-author)

- Editing of paper
- Performed injections into zebrafish embryos for Notch assays.
- Performed zebrafish Notch assays (all except where noted)
- Immunoprecipitation experiments (expect where noted)
- Injection of zebrafish embryos for QPCR analysis

Certification that the statement of contribution is accurate and permission is given for the inclusion of the paper in the thesis

Signed…… …….Date

Lachlan Wilson (Co-author)

- Performed all Appa assay experiments, statistical analysis and injections
- Performed all HMW western blot analysis and corresponding injections
- Performed all preliminary IP experiments, injections and preparations of IP samples.
- Performed zebrafish Notch assay on Acne inversa mutations.

Certification that the statement of contribution is accurate and permission is given for the inclusion of the paper in the thesis

Signed

…… ……Date……

Seyyed Hani Moussavi Nik (Co-author)

Performed all QPCR experiments.

Certification that the statement of contribution is accurate

Signed

…… ……Date……

Giuseppe Verdile (co-author)

- Human cell culture experiments on Notch and APP (preliminary and not in the paper).
- Supervised development of work for Khan and intellectual contributions.

Certification that the statement of contribution is accurate and permission is given for the inclusion of the paper in the thesis

Signed

…… ……Date……

Anne Lim (co-author)

All experiments on the MAM and subcellular fractionation (except where noted).

Certification that the statement of contribution is accurate and permission is given for the inclusion of the paper in the thesis

Signed

…… ……Date……

Imran Khan (co-author)

- Human cell culture experiments on Notch and APP (preliminary and not in the final paper).
- Probing of MAM subcellular fraction blots.

Certification that the statement of contribution is accurate and permission is given for the inclusion of the paper in the thesis

Signed

…… ……Date……

Sharon Pursglove (co-author)

Performed mouse cell culture analysis of Notch (preliminary and not in the final paper).

Certification that the statement of contribution is accurate and permission is given for the inclusion of the paper in the thesis

Signed on behalf by Gavin Chapman

…… ….Date……

Gavin Chapman (co-author)

- Performed Human cell culture analysis of Notch (preliminary and not in the final paper).

- Supervised development of work for Pursglove.

Certification that the statement of contribution is accurate and permission is given for the inclusion of the paper in the thesis

Signed

…… …….Date……

Ralph Martins (co-author)

Supervised development of work for Khan and Verdile.

Certification that the statement of contribution is accurate and permission is given for the inclusion of the paper in the thesis

Signed

…… …….Date……

Michael Lardelli (co-author)

Planned the research, wrote the manuscript, acted as corresponding author and supervised development of work for Newman, Wilson, Moussavi Nik and Lim.

Certification that the statement of contribution is accurate and permission is given for the inclusion of the paper in the thesis

Signed

…… …….Date……

Differential, dominant activation and inhibition of Notch signalling and APP cleavage by truncations of PSEN1 in human disease

Morgan Newman*[1], Lachlan Wilson*[1], Giuseppe Verdile[2,3,4], Anne Lim[1], Imran Khan[2,3], Seyyed Hani Moussavi Nik[1], Sharon Pursglove[5], Gavin Chapman[5], Ralph Martins[2,3], Michael Lardelli†[1].

*Contributed equally to this work

† Author for correspondence

Affiliations:

1. Discipline of Genetics, School of Molecular and Biomedical Science, University of Adelaide, SA 5005, Australia

2. Centre of Excellence for Alzheimer's Disease Research and Care, School of Medical Sciences, Edith Cowan University, Joondalup, WA 6027, Australia

3. School of Psychiatry and Clinical Neurosciences, University of Western Australia, Crawley, WA, 6009, Australia.

4. School of Public Health, Curtin University, Bentley, WA 6102, Australia

5. Developmental Biology Division, Victor Chang Cardiac Research Institute, NSW 2010, Australia

Full contact details for corresponding author:

Michael Lardelli

Discipline of Genetics, School of Molecular and Biomedical Sciences, The University of Adelaide, SA 5005, Australia.

Tel. (+61 8) 83133212, Fax (+61 8) 83134362

email: michael.lardelli@adelaide.edu.au

Abstract

PRESENILIN1 (*PSEN1*) is the major locus for mutations causing familial Alzheimer's disease (FAD) and is also mutated in Pick's disease of brain, familial acne inversa and dilated cardiomyopathy. It is a critical facilitator of Notch signalling and many other signalling pathways and protein cleavage events including production of the Amyloidβ (Aβ) peptide from the AMYLOID BETA A4 PRECURSOR PROTEIN (AβPP). We previously reported that interference with splicing of the zebrafish orthologue of *PSEN1* creates dominant negative effects on Notch signalling. Here we extend this work to show that various truncations of human PSEN1 (or zebrafish Psen1) protein have starkly differential effects on Notch signalling and cleavage of zebrafish Appa (a paralogue of human AβPP). Different truncations can suppress or stimulate Notch signalling but not Appa cleavage and vice versa. The G183V Picks disease mutation causes production of aberrant transcripts where the open reading frame is truncated after exon 5 sequence. We show that the truncated protein potentially translated from these transcripts avidly incorporates into very stable Psen1-dependent higher molecular weight complexes and suppresses cleavage of Appa but not Notch signalling. In contrast, the truncated protein potentially produced by the P242LfsX11 acne inversa mutation has no effect on Appa cleavage but, unexpectedly, enhances Notch signalling. Our results suggest novel hypotheses for the pathological mechanisms underlying these diseases and illustrate the importance of investigating the function of dominant mutations at physiologically-relevant expression levels and in the normally heterozygous state in which they cause human disease rather than in isolation from healthy alleles.

Introduction

The human PRESENILIN proteins, PSEN1 and PSEN2, form the central components of γ-secretase complexes that are required for the intra-membrane cleavage of over 70 different substrates including the AβPP protein from which the Aβ peptide is derived (1). Aggregates of Aβ peptide are the major component of the neuritic plaques that are diagnostic of Alzheimer's disease (AD). Activation of γ-secretase activity appears to require the autoproteolytic cleavage of PRESENILIN proteins followed by association of the resulting N- and C-terminal fragments within γ-secretase complexes (2). These complexes consist additionally of the proteins NICASTRIN, PSENEN and APH1A or APH1B (reviewed by (3)). Alternatively, a variety of evidence supports that PSEN1 plays an important role in macroautophagy (4). Lee and colleagues have shown data supporting that an effect of PSEN1 on autophagy is via a γ-secretase-independent role of the PSEN1 holoprotein in acidification of lysosomes (4). However, other published data conflict with this (5, 6). It is currently debated whether PSEN1's primary role in inherited (familial) AD (FAD) occurs via its function in γ-secretase activity or in autophagy (see (7) and resulting correspondence).

Over a decade of research has focussed on the role of mutations in the PRESENILINS in altering the γ-secretase cleavage of AβPP to support varieties of Aβ peptide. Much of this work has been conducted in cultured cells such as HEK293 cells and using cell-free assays where γ-secretase is solublised using the non-denaturing detergent CHAPS (3-[(3-cholamidopropyl)dimethylammonio]-1-propanesulfonate, (8)). Currently, the dominant idea is that FAD mutations promote the formation of more aggregation-prone forms of

Aβ such as the 42 amino acid residue (aa) form relative to the more common (and possibly protective (9)) 40 aa form. This supposedly occurs in endosomes and at the plasma membrane (10, 11). However, recent discoveries raise caveats over these ideas. Winkler et al. (12) have shown that the thickness of the lipid bilayer (affected by its lipid makeup) can influence the site of γ-secretase cleavage of AβPP and so alter Aβ size. Since cell-free assays involve solubilisation of the γ-secretase complex, this must change the lipid environment of γ-secretase and so probably affects Aβ product size. Also, Area-Gomez et al (13) showed in an elegant paper in 2009 that, in mouse brain, the majority of Psen1 protein, all detectable Psen2 protein, and most γ-secretase activity resides in a detergent-impermeable lipid-raft like region of the endoplasmic reticulum named the mitochondrial associated membranes (MAM). The implications of this revision of our understanding of the subcellular distribution of PRESENILIN protein and γ-secretase activity have not yet been examined.

The gene *PSEN1* is the major locus for mutations causing FAD. Interestingly, all of the more than 180 different mutations in PSEN1 known to cause FAD allow retention of the C-terminal sequence of the protein. This – and the absence of FAD mutations in other components of γ-secretase complexes – is consistent with an important role for an autophagy function of the PSEN1 holoprotein in AD pathology. The only disease-causing mutation of PSEN1 involving simple truncation of the open reading frame (rather than partial interference with splicing resulting in multiple transcript isoforms) is the P242LfsX11 mutation causing the inherited skin disease familial acne inversa (FAI) (14). P242LfsX11 causes a frameshift in exon 7 resulting in a premature termination codon. This mutation causes decreased PSEN1 transcript levels in lymphocytes (14) probably

due to nonsense mediated decay (NMD) of transcripts of the mutant allele. Nevertheless, the mutant transcript can still be detected implying that low levels of truncated PSEN1 protein may be produced. Similarly, the G183V mutation causing Pick disease of brain affects the splice donor site of exon 6 producing a transcript encoding a full-length protein with a missense mutation (G183V, (15)) and also transcripts lacking either sequence from exon 6 or exons 6 and 7 (16). These transcripts would have frameshifted open reading frames putatively encoding proteins prematurely truncated after exon 5 sequence. Interestingly, in a mouse knock-in model of this mutation, Watanabe et al. (17) observed aberrantly splicing of PSEN1 only in brain. The aberrant transcripts are subject to NMD but can, nevertheless, be detected. When transfected into cultured HEK293 cells or into MEF cells lacking endogenous PRESENILINS, the G183V full length transcript itself gave only mild effects on Aβ production (15) or no effects on Notch cleavage (17) respectively. This is consistent with the lack of AD pathology seen for G183V. Watanabe et al. suggest that the Picks disease resulting from G183V may be due to decreased overall γ-secretase activity but this contrasts with the observations of Wang et al. (14) where the P242LfsX11 FAI mutation also reduced PSEN1 levels but was not reported to produce Picks disease (and did not appear to cause FAD).

Another change in *PRESENILIN* gene splicing associated with human disease is exclusion of exon 5 sequence from transcripts of *PSEN2* in the brains of people with sporadic, late onset AD (18, 19). This produces a truncated isoform of the PSEN2 protein, PS2V. Interestingly, this isoform can stimulate AβPP cleavage and Aβ production when expressed in mouse Neuro 2a cells (20). We have also recently shown the PS2V transcript to be up-regulated in guinea pig brain under conditions of hypoxia

and cholesterol loading (21). Up-regulation of this transcript was associated with cholesterol-enhanced amyloidogenic processing of AβPP.

In mammals, PSEN1 protein is essential for Notch signalling since it is required for cleavage of Notch receptors within their single transmembrane domains after their extracellular domains are removed as a consequence of binding extracellular ligands. PSEN1-controlled γ-secretase activity releases the Notch intracellular domain (NICD) that subsequently enters the nucleus to regulate gene activity. Notch signalling is essential for maintaining stem cells in an undifferentiated state (22), for controlling cell fate decisions (reviewed by e.g. (23-26)) and is commonly dysregulated in cancer (27). Changes in Notch signalling have been suggested to underlie FAI pathology (14) and this is supported by the discovery of additional mutations causing FAI in other components of γ-secretase complexes (in contrast to FAD) (14).

Rates of aberrant splicing have been seen to increase in ageing and cancerous cells (reviewed in (28, 29)). Aberrant splicing of PSEN1 in particular was observed in sporadic frontotemporal dementia ((30), of which Pick's disease of brain is one type). While NMD plays an essential role in the elimination of transcripts encoding aberrantly truncated proteins it can be incompletely effective under certain circumstances, e.g. when a premature termination codon occurs within 55 bp of a downstream exon-exon junction (31). The modular nature of many proteins where separate domains have separate activities means that it is common for truncated proteins to possess a subset of their normal activities. This allows them to interfere dominantly with the function of normal full-length proteins. Thus it is important to consider the activities of the potential protein

products of aberrant transcripts whenever detection of such transcripts suggests that truncated proteins may exist.

Zebrafish embryos are an excellent system in which to analyse cellular responses to changes in gene expression. Unlike cells grown in culture, the cells of zebrafish embryos exist in an environment of normal substrates and cell-cell interactions. Simultaneous and subtle up-regulation and down-regulation of gene expression is possible at levels consistent with normal cell physiology. In previous work we attempted to use the unique advantages of the zebrafish system to model particular rare FAD mutations in *PSEN1* where protein coding exons are excluded but the reading frame is maintained. We did this by blocking splice acceptor sites in the zebrafish orthologue of *PSEN1* (named *psen1*) using morpholino antisense oligonucleotides ("morpholinos"). Unexpectedly we generated low levels of intron inclusion rather than exon exclusion but some of the aberrant transcripts nevertheless had potently dominant negative effects on the activity of both *psen1* and the zebrafish orthologue of *PSEN2* (named *psen2*) (32).

In the work described in this paper we confirm the predominant MAM-localisation of PSEN1 protein in mammalian (mouse) brain. We then use our zebrafish embryo-based *in vivo* assays of Notch signalling and AβPP cleavage to expand our previous study of the γ-secretase activity of PSEN1 truncations including PSEN1 truncations relevant to human diseases other than AD. We show that, at physiologically relevant levels, different truncations of PSEN1 can have starkly contrasting effects on zebrafish Notch signalling and Appa cleavage. Truncations resembling PS2V boost both Notch and Appa cleavage in a manner dependent on the presence of endogenous zebrafish Psen1 protein but not Psen2 protein. Truncations equivalent to some of the products of the G183V Pick disease

mutation reduce Appa cleavage but do not affect Notch. They also bind full-length endogenous Psen1 and Psen2 and integrate into higher molecular weight complexes. In contrast, the truncation produced by the P242LfsX11 acne inversa mutation unexpectedly increases Notch signalling with no affect on Appa cleavage. Our discoveries imply that *in vivo* analysis of γ-secretase activity may give more realistic insights into the role of γ-secretase activity in human disease. Our observations also suggest transgenic approaches to allow manipulation of Notch signalling without affecting AβPP cleavage and vice versa.

Results

PSEN1 protein is concentrated in the MAM in brain

The majority of FAD is due to mutations in the genes encoding the human proteins PSEN1 and PSEN2. In 2009 Area-Gomez et al. demonstrated that, in the mammalian (mouse) brain, the greatest concentration of PSEN1 protein, γ-secretase activity and γ-secretase cleavage of AβPP is localised to the MAM (13). They also showed that the MAM is difficult to permeabilise for immunohistochemistry using standard detergents since it has a lipid constitution similar to that of lipid rafts (13, 33). Also, Winkler et al (12) recently showed that changes in the thickness of lipid bilayers can affect the cleavage of AβPP proteins by γ-secretase to produce different forms of Aβ. However, much of the debate on the role of γ-secretase activity in AD is based on data obtained from cell-free assays where γ-secretase activity is solubilised using detergents. Such cell-free assays may not entirely reflect the γ-secretase activity found *in vivo*. To confirm independently the controversial MAM-localisation of PSEN1 protein we replicated the sub-cellular fractionation of mouse brain by Area-Gomez et al. (13). As expected, this showed that PSEN1 is predominantly localised to the MAM with lower concentrations in the rest of the endoplasmic reticulum and in mitochondria (Supplemental Data Figure 1).

Delimiting the region of Psen1 in which truncation produces dominant negative effects on Notch signalling

In addition to their role in γ-secretase, PRESENILIN proteins are thought to have multiple cellular activities in e.g. phosphorylation of β-catenin (34, 35), Ca^{2+} transport (36, 37) and macroautophagy (4). The involvement of the PRESENILINs in these other

activities has not been studied in depth and it is unclear to what extent these activities interact with γ-secretase activity. Also, cell-free assays of γ-secretase activity have been shown to be very sensitive to preparation and assay conditions (discussed in (38)). Therefore, analysis of PRESENILIN activity *in vivo* may give a more realistic understanding of their roles in cell biology and disease than analysis in cell-free systems. γ-Secretase activity can be studied using cultured cells (such as HEK293 cells) transfected with assay or other constructs (e.g. (39)). However, due to their unusual environments, cultured cells commonly have unusual patterns of gene and protein expression (40, 41) while high-level expression of genes/proteins through transfection can produce physiologically irrelevant results such as the complete abolition of endogenous Psen protein by exogenous Psen (42). Fertilized zebrafish eggs represent an interesting alternative *in vivo* system in which to analyse gene activity since their large size allows easy, subtle and multifactorial manipulation of gene activity at the 1-cell stage. Also, their subsequent development through the various stages of embryogenesis allows changes in phenotype to be used as bioassays of changes in gene activity.

γ-Secretase activity is required for the intra-membraneous cleavage of Notch receptors that facilitates transcriptional regulation of genes by Notch intracellular domains (reviewed by (43)). We (32, 44) and others (45-48) have previously observed changes in Notch signalling in zebrafish embryos by examining changes in the expression of the *neurogenin1* gene that is a under transcriptional regulation by Notch (45). In previously published work examining PRESENILIN's γ-secretase activity we monitored spinal cord *neurogenin1* transcript levels in zebrafish embryos at 24 hours post fertilisation (hpf @28.5 °C) to assess changes in Notch signalling. This led to discovery of dominant

negative effects on Notch signalling caused by interference with splicing of zebrafish *psen1* gene transcripts (32). These dominant negative effects occur upon interference with splicing to zebrafish *psen1* exons cognate with human *PSEN1* exons 7 and 8 but not 6 or 9. (Hereafter the zebrafish exons are referred to by their human cognate numbers, see Figure 1.) Injection into embryos of mRNA encoding zebrafish Psen1 protein truncated after exon 6 (equivalent to the putative product of the aberrant transcript produced by interference with splicing to exon 7 (32)) produced a similar dominant negative phenotype supporting that this effect is due to the formation of truncated Psen1 protein molecules. We have subsequently shown that our injection of synthetic mRNA into zebrafish embryos gives total mRNA levels less than threefold higher than normal (see Supplemental Data Figure 2). Thus, interference with the splicing of endogenous genes and injection of synthetic mRNAs causes changes in gene activity in zebrafish embryos at physiologically relevant levels.

Notch signalling is an important component of embryo development, stem cell maintenance and human diseases including some cancers. Truncations of the N-terminal fragment (NTF) of human PSEN1 feature in a number of human disease states (see the Introduction and below). Therefore, we sought to use our zebrafish model to analyse how truncations of the NTF in zebrafish Psen1 affect Notch signalling. Since the effects of interference with splicing are not entirely predictable we focussed instead on injection of synthetic mRNAs. We synthesised mRNAs encoding the entire NTF or forms of Psen1 truncated downstream of sequence encoded in exons 3, 4, 5, 6, 7, or 8 (Figure 1). These were injected into zebrafish embryos and their effects on *neurogenin1* expression in the

spinal cord (negatively regulated by Notch signalling) were analysed at 24 hpf. Interestingly, we observed both enhancement and suppression of Notch signalling.

Injection of mRNA encoding a truncation of Psen1 after exon 3 sequence (Psen1Δ>3) proved quite toxic to embryo survival unlike the other, longer truncations. Therefore, we did not analyse this truncation further. Injection of mRNA coding for Psen1 truncated after exon 4 sequence (Psen1Δ>4) caused significant change in *neurogenin1* transcription compared to embryos injected with a negative control mRNA (Figure 2A). Surprisingly, Psen1Δ>4 acts in a "dominant positive" manner to decrease *neurogenin1* transcription, presumably by increasing Notch signalling. In contrast, mRNAs encoding Psen1 proteins truncated after exon 5, 6, 7, or 8 sequence behaved as expected from our previously published analysis using morpholinos (44). Truncation of Psen1 after exons 5 or 8 (Psen1Δ>5 and Psen1Δ>8) or the entire NTF caused no significant change in *neurogenin1* transcription relative to embryos injected with a negative control mRNA. However, mRNAs encoding Psen1 truncated after exons 6 and 7 (Psen1Δ>6 and Psen1Δ>7) caused an increase in *neurogenin1* expression indicative of decreased Notch signalling (Figure 2A).

Our results, and those of our previous study using morpholinos ((32)) initially led us to believe that the region of *psen1* flanked by exons 6 and 8 (i.e. exon 7) encoded a section of the Psen1 protein within which any truncation would produce dominant negative effects on Notch signalling. However, additional analysis showed this interpretation to be incorrect (see later).

Truncations of Psen1 produce distinct and overlapping effects on Notch signalling and cleavage of zebrafish Appa

γ-Secretase cleaves over 70 protein substrates in addition to Notch receptors (reviewed by (1)). Among the most important of these for human disease is the AMYLOID PRECURSOR PROTEIN, AβPP. AβPP is cleaved by γ-secretase after initial cleavage by α–secretase or β–secretase in its N-terminal, luminal/extracellular domain close to the lipid bilayer (49-52). Zebrafish possess two paralogous genes, *appa* and *appb*, derived from an ancestral orthologue of human *AβPP* (53). We recently developed a zebrafish assay for γ-secretase cleavage of Appa that monitors cleavage of an Appa substrate truncated to resemble the putative 86 aa C-terminal product of β-secretase cleavage ("AppaC86::GFP", (38)).

Mutations (54) and drugs (55) affecting Presenilin activity have been reported to have differential effects on Notch and AβPP cleavage. Therefore we exploited our Appa-based assay to investigate whether our truncations of Psen1 had similar or different effects on APP cleavage compared to Notch signalling.

Injection of mRNA encoding Psen1Δ>4 caused increased cleavage of Appa similar to the effect of this truncation on Notch signalling. However, whereas Psen1Δ>5 had no effect on Notch signalling, we found that it acted to inhibit γ-secretase cleavage of Appa (Figure 3A). Futhermore, in contrast to their dominant negative effect on Notch signalling, Psen1Δ>6 and Psen1Δ>7 did not affect Appa cleavage. Psen1Δ>8 and the entire NTF did not affect either Appa cleavage or Notch signalling in our zebrafish embryo system (Figure 3A).

To support that our observations were the result of expression of truncated forms of Psen1 at physiologically relevant levels we attempted to reproduce the above effects on AppaC86::GFP substrate cleavage through directed interference with endogenous *psen1* transcript splicing. Morpholinos that bind over the acceptor sites of exons 5, 7, 8, and 9 exist and can interfere with splicing of endogenous *psen1* transcripts. These cause retention of the respective upstream introns (see Supplemental Data Figure 3) and, presumably, expression of transcripts with open reading frames prematurely terminated after exons 4, 6, 7 and 8 respectively. The assay results from morpholino injection are consistent with those seen for mRNA injection (Figure 3C).

The different effects of particular Psen1 truncations on Notch and Appa are consistent with the idea that differently composed γ-secretase complexes are responsible for Notch and AβPP cleavage (56, 57). Our observations also show that it should be possible to construct transgenes that specifically inhibit Notch cleavage but not AβPP cleavage and vice versa. Alternatively Psen1Δ>4 can be used to boost both Notch signalling and AβPP cleavage in cells, tissues and transgenic animals.

Psen1Δ>4 requires endogenous, normal Psen1, but not Psen2 to increase γ-secretase activity

Psen1Δ>4 is structurally equivalent to the “PS2V” isoform of human PSEN2 that is induced in neurons by hypoxia and is found at increased levels in the brains of people with sporadic, late onset AD. Consistent with our results, PS2V has been shown to increase γ-secretase activity and Aβ levels when its expression is forced in the mouse neuro2a neuroblastoma cell line (20). However, Psen1Δ>4 and PS2V do not possess the

NTF portion of the putative proteolytic site of γ-secretase that includes a conserved, essential Asparagine residue (Asp 257 in human PSEN1 or Asp 263 in human PSEN2). Truncations Psen1Δ>4, Δ>5, Δ>6, and Δ>7 also lack this residue and so would be incapable themselves of contributing directly to γ-secretase cleavage. An explanation for the ability of Psen1Δ>4 and PS2V to boost γ-secretase activity is that they are dependent on endogenous, normal Presenilin proteins to do so.

Zebrafish embryos are a very versatile cellular system in which to dissect molecular interactions since it is possible to block and force expression of multiple gene activities simultaneously. To test the dependence of Psen1Δ>4 on endogenous Presenilin proteins we injected mRNA encoding Psen1Δ>4 while simultaneously blocking translation of either endogenous Psen1 or Psen2 using morpholinos ("MoPsen1Tln" and "MoPsen2Tln" respectively). Analysis of Notch signalling using the *neurogenin1* expression assay was then performed by comparing trunk spinal cord *neurogenin1* expression in these embryos to that in control embryos that had been injected either with negative control (inactive) morpholino "MoCont" or with the MoPsen1Tln or MoPsen2Tln morpholinos as appropriate to block endogenous Psen1 or Psen2 translation respectively (see Figure 4A). Psen1Δ>4 was unable to increase Notch signalling (*neurogenin1* expression) significantly in embryos lacking endogenous full-length Psen1 (Figure 4A). In contrast, blockage of Psen2 translation could not block the ability of Psen1Δ>4 to boost Notch signalling (Figure 4A). This supports that Psen1Δ>4 acts through normal Psen1 in order to boost γ-secretase activity while acting to a lesser extent (if at all) through endogenous Psen2.

Psen1Δ>4 expression also boosts cleavage of Appa (see above). To support that Psen1Δ>4's dependence on endogenous Psen1 also applies for substrates other than Notch we tested its ability to cleave AppaC86::GFP in the absence of Psen1 or Psen2 translation. Consistent with the results for Notch above, Psen1Δ>4 could only increase AppaC86::GFP cleavage when Psen1 was present while blockage of Psen2 translation had no effect on the ability of Psen1Δ>4 to increase AppaC86::GFP cleavage (Figure 4B).

Psen1 truncations incorporate into higher molecular weight complexes

It is commonly observed that Presenilin proteins are incorporated into higher molecular weight (HMW) complexes that are sufficiently stable to withstand the highly denaturing conditions involved in protein resolution by SDS-polyacrylamide gel electrophoresis (PAGE, e.g. see (58-60)). Kim et al (59) previously showed that forced expression of the NTF of human PSEN1 in mouse embryonic fibroblasts (MEFs) resulted in the formation of such stable complexes. A simple model for the dominant effects of truncated Psen1 on Notch signalling and Appa cleavage is that this occurs by interference with formation of γ-secretase complexes. Our various truncated forms of zebrafish Psen1 have been tagged at their N-termini using the FLAG antibody tag. To observe whether the Psen1 truncations could incorporate into HMW complexes we expressed them in zebrafish embryos and then subjected embryo lysates to SDS-PAGE followed by western blotting against the FLAG tag (Figure 5A). This revealed apparent complexes in the range of 50-250 kDa while monomers of the Psen1 truncations in the range of ~15-30 kDa were detected only weakly or not at all. In particular, truncations Psen1Δ>5, Δ>7, Δ>8 and NTF avidly incorporated into SDS-resistant complexes of approximately 200 kDa or

greater (Figure 5A). However, it is known that forced over-expression of proteins in cells can lead to the formation of non-specific SDS-resistant aggregates (e.g. (61)). Since our analysis of Psen1Δ>4 has shown that its activity is dependent on the presence of endogenous Psen1 (see above) we sought to demonstrate that the Psen1 truncations were being incorporated into HMW complexes relevant to endogenous Psen1 activity. We analysed the incorporation of the truncations into SDS-resistant complexes with and without blockage of translation of endogenous Psen1 (Figure 5A). Distinct differences in complex formation were observed for truncations Psen1Δ>5, Δ>7, Δ>8 and NTF when these were expressed with or without endogenous Psen1. Apparently, the loss of endogenous Psen1 enhances the incorporation of the truncated Psen1 molecules into HMW complexes. This supports that the complex formation observed is specific and related, in some way, to Psen1 activity (although not necessarily γ-secretase activity).

As an additional test that our truncated Psen1 proteins can interact with endogenous, normal Psen1 protein we performed immuno-precipitation analysis under non-denaturing conditions using ANTI-FLAG M2 Affinity Gel on embryos injected with mRNA coding for either the most avid apparent interactor Psen1Δ>5 or (as a negative control) a form of GFP tagged at its N-terminal with FLAG. Immunoblotting of the lysates and precipitates clearly demonstrated a specific interaction of Psen1Δ>5 with Psen1 and, interestingly, also with endogenous Psen2 while GFP failed to interact with either endogenous protein (Figure 5B). This suggests that immuno-precipitation of our FLAG-tagged Psen1 truncations under non-denaturing conditions should co-precipitate interacting proteins and permit their identification by proteomics methods.

Remarkably, loss of endogenous Psen1 apparently causes increased incorporation of Psen1Δ>5 into the very largest HMW complexes but a dramatic decrease in the incorporation of this truncation into an ~50 kDa complex with a concomitant increase in levels of the monomeric form. A similar behaviour is shown by Psen1Δ>8 and these are the two truncations that do not appear to influence Notch activity. The behaviour of Psen1Δ>5 is particularly interesting since this is the only truncation that inhibited Appa cleavage. This supports that Notch and AβPP are cleaved by γ-secretase activities in distinct complexes. Also, Psen1Δ>5 resembles the putative protein products of the abnormal transcripts caused by the G183V mutation of human PSEN1 that affects the splice donor site of exon 6. This is the only PSEN1 mutation thought to cause FTD without associated AD pathology. Our analysis suggests that the transcript putatively encoding human PSEN1 truncated after exon 5 sequence may suppress APP cleavage and Aβ peptide formation consistent with the lack of AD histopathology (Aβ plaques).

The ~50 kDa complex seen for all the injected truncations (but not Psen1NTF or the negative control) does not appear to represent dimer formation since the Psen1Δ>5 truncation and larger truncated peptides have monomeric masses of 30 kDa or greater. Also, the mass of the ~50 kDa complex does not appear to change with the size of the truncation injected. Therefore, we suspect that the ~50 kDa complex represents the protease-resistant core of a larger unstable entity that includes part or all of our FLAG-tagged Psen1 truncations.

Truncations of human PSEN1 produce similar effects to their zebrafish equivalents when expressed in zebrafish embryos

To confirm that our observations using zebrafish embryos are relevant to the human system we sought to express truncations of human PSEN1 in the human kidney-derived cell line HEK293. Truncations of human PSEN1 after exon 4, 5, 6, 7 and 8 sequence and with N-terminal HA antibody tags were synthesised in the pcGlobin2 vector that can be used for mRNA synthesis or to express genes downstream of a CMV promoter (62). The truncations of human PSEN1 were named hPSEN1Δ>4, 5, 6, 7 or 8 to correspond to the zebrafish Psen1 truncations. Unfortunately, repeated attempts to generate stably transformed cell lines expressing the human PSEN1 truncations failed. Apparently, the human PSEN1 truncations are too toxic to allow survival and growth of HEK293 cells, possibly because transfection gives excessive, non-physiologically relevant levels of expression. Therefore, we generated mRNAs encoding each of the human PSEN1 truncations and expressed these in zebrafish embryos by mRNA injection. Our assays for Notch signalling (Figure 2B) and Appa cleavage (Figure 3B) showed that the human PSEN1 truncations produce effects on these activities identical to their zebrafish Psen1 equivalents. This supports that our analysis of Presenilin activity in zebrafish is relevant to our understanding of this activity in the human system.

The P242LfsX11 mutation of human *PSEN1* causing acne inversa dominantly increases Notch signalling but not Appa cleavage.

Recently Wang et al (2010) identified that mutations in three of the four protein components of the γ-secretase complex, PSEN1, NICASTRIN and PSENEN, can cause an inherited disease of hair follicles named acne inversa (AI). These researchers discovered only one AI mutation in PSEN1 - a single base deletion, c.725delC, causing a frameshift that results in the premature termination of the open reading frame. The

mutant protein structure is denoted as P242LfsX11. This is the first known inherited mutation in *PSEN1* exclusively causing truncation of the open reading frame. (The FAD mutations of *PSEN1* all still allow synthesis of mRNAs encoding entire open reading frames.) Unexpectedly, none of the families with inherited AI show familial Alzheimer's disease and Wang et al. 2010 (14) suggested that AI may be caused by changes in Notch signalling affecting follicle biology (14). *PSEN1* transcript levels are reduced by varying amounts in heterozygotes suggesting that nonsense mediated decay is destroying transcripts possessing the premature termination codon generated by this mutation. However, supplemental data published with the Wang et al. paper shows that low levels of transcript containing the P242LfsX11 mutation are still observable in lymphocytes from affected individuals. However, the P242LfsX11 mutation places a premature stop codon within 20 bp upstream of the next downstream exon junction (Figure 6A). Thus, the mutation potentially lies too close to the exon-exon junction for nonsense mediated decay to be completely effective (according to the "50-55 bp rule" (31)).

We were surprised to see that P242LfsX11 lies in exon 7 since we believed that truncating mutations in this region would have potently dominant negative effects on Notch signalling and that even minor levels of the mutant transcript might interfere fatally in embryo development – i.e. they would be dominant lethal (32). Therefore, we tested the activity of the putative protein product of the P242LfsX11 mutation in our zebrafish system. Construct hPSEN1-P242LfsX11 incorporating the P242LfsX11 mutation was generated in the pcGlobin2 vector using the human PSEN1 gene and then mRNA was synthesised for injection into zebrafish embryos. No effect was observed on Appa cleavage consistent with the fact that individuals with this AI mutation do not show

early onset FAD (Figure 6B). Also, Notch signalling was observed to increase rather than decrease implying that Notch signalling in individuals heterozygous for P242LfsX11 may be greater than that expected if P242LfsX11 was a simple, loss-of-function mutation (Figure 6C). This discovery also means that it should be possible to construct transgenes that boost Notch signalling without increasing AβPP cleavage.

Discussion

The PRESENILIN proteins are essential to facilitate many signalling pathways and protein cleavage events. They modulate intracellular Ca^{2+} ion levels (36, 37), regulate β-catenin turnover (34, 35) and influence autophagy (4). Therefore, changes in PRESENILIN activity can have widespread effects on cell function and are associated with numerous human diseases. In earlier work we showed that low levels of truncated zebrafish Presenilin molecules can exert potent dominant negative effects on Notch signalling (32). Truncated PRESENILIN proteins (or at least aberrantly spliced transcripts) occur either as natural isoforms (e.g. PS2V (18)), result from mutation (e.g. FAD (63), acne inversa (14)) or exist in particular disease states such as FTD (30). Thus it is important to understand their effects on cell biology.

The discovery of the MAM as the primary subcellular location of the PRESENILIN proteins, γ-secretase activity and γ-secretase cleavage of AβPP in neural tissue (13) is revolutionising our understanding of the role of *PRESENILIN* mutations in FAD (33). We have now independently confirmed the predominant localisation to the MAM of mammalian Psen1 protein. The true sub-cellular distribution of the PRESENILINs remained unknown until recently due to the MAM's tight physical association with mitochondria and its peculiar lipid raft-like characteristics that prevented its permeabilisation by common immunohistochemistry detergents (13, 64). Also, Winkler et al. recently observed that the site of γ-secretase cleavage within AβPP is affected by the thickness of the lipid bilayer within which AβPP resides (12). This raises the question of how solubilisation of γ-secretase with detergents in cell-free assays affects observations of AβPP cleavage and the different forms of Aβ formed by different

PRESENILIN mutants. Interestingly, Area-Gomez et al recently showed that changes in PRESENILIN activity affect movement of cholesterol into and out of MAM membranes (33). This raises the possibility that changes in the profile of Aβ lengths observed in FAD PRESENILIN mutants may be the secondary effect of changes in the lipid constitution of MAM membranes rather than a direct effect of the mutations on the cleavage interaction between a PRESENILIN molecule and an AβPP molecule within the γ-secretase complex itself. Of course, many of the experimental caveats regarding cell-free and cell culture approaches to analysis of γ-secretase would be obviated by the use of *in vivo* assays. Indeed, our *in vivo* assay for γ-secretase cleavage of AβPP (Appa) is unique in this regard.

In disease states, mutant genes encoding truncated *PRESENILIN* open reading frames are always found concomitantly with wild-type *PRESENILIN* genes. However, previous analyses of truncated PRESENILINs have examined their biochemical activities in backgrounds lacking full-length proteins. Thus Laudon et al. 2004 (65) transfected constructs expressing NTF truncations together with the C-terminal fragment (CTF) of PSEN1 into mouse BD8 cells lacking endogenous Psen1 and Psen2 and saw Notch and AβPP cleavage activity only for truncations with at least 288 amino acid residues (aa) which is nearly the complete NTF. Similarly, Kim et al. 2005 (59) saw similar results for Notch cleavage when examining truncations of the PSEN1 NTF together with full-length CTF in mouse embryonic fibroblast cells (MEFs) lacking Psen1 and Psen2. The different results we obtained for the activity of Presenilin truncations in APP cleavage and Notch signalling compared to those above are likely because our analysis has examined the expression of truncated PRESENILINs in the presence of endogenous gene expression.

This illustrates the importance of examining dominant mutations in their real, heterozygous state - in the presence of a normal allele – rather than in isolation since the activity of the dominant mutation can be dependent on the function of the normal allele. Indeed, in our experimental system, when we blocked endogenous Psen1 expression in the presence of Psen1Δ>4 we saw that this truncation could no longer affect γ-secretase activity. This is expected since all the truncations except Psen1Δ>8 (which includes almost the entire NTF) lack the Asp 257 residue that is thought to be essential to the γ-secretase catalytic site (66). Thus, truncations Psen1Δ>4 and P242LfsX11 that both boost Notch signalling must do this by stimulating, (by an unknown mechanism/s), the activity of γ-secretase complexes comprised of normal Presenilin NTFs and CTFs. Interaction of truncated Presenilin NTFs with functional γ-secretase complexes is also supported by the data of Kim et al (59) who saw that incorporation of truncated NTFs into higher molecular weight complexes was greatest in cells possessing both PSEN1 and PSEN2 and was decreased in cells lacking one or both of these genes. For incorporation of our truncated forms of Psen1 into higher molecular weight complexes we also observed evidence for interactions with endogenous (non-mutant) Presenilin proteins. Future work will aim to exploit the FLAG-tagged N-termini of our truncated Psen1 proteins to identify interacting proteins by co-immunoprecipitation and proteomics analyses.

The stimulation of Appa cleavage and Notch signalling by Psen1Δ>4 is consistent with the activity of the PS2V isoform that is an equivalent truncation of PSEN2. Forced expression of PS2V in mouse neuro 2a cells was seen to increase the production of Aβ peptide consistent with an increase in γ-secretase activity (20). Our observations suggest

that PS2V will be found to require full-length Presenilin expression for its ability to increase γ-secretase activity. Since Psen1Δ>4 requires endogenous Psen1 but not Psen2 for its activity, it would be interesting to know whether, by analogy, PS2V requires PSEN2 but not PSEN1 (or vice versa) to increase Aβ production.

The G183V mutation of human *PSEN1* is remarkable as the only known mutation of this gene thought to produce an exclusively Pick disease FTD phenotype rather than FTD associated with AD. Dermaut et al. 2004 (15) showed that the full-length PSEN1 protein incorporating the G183V missense mutation did not cause a greatly increased level of $A\beta_{42}$ to $A\beta_{40}$ production when transfected into HEK293 cells although total levels of Aβ production were not reported. This was consistent with brain histopathology showing Pick bodies and western analysis showing no detectable Aβ. In a comment on unpublished research regarding putative truncated PSEN1 from the aberrant transcript splicing caused by G193V, Dermaut et al. 2005 (16) noted that, "cellular gamma-secretase assays show that the truncated proteins behave as complete null alleles". However, no information was given on the cellular system used or whether endogenous full-length PSEN1 was present. Watanabe et al. (17) engineered the G183V mutation of human *PSEN1* into the mouse *Psen1* gene and observed aberrant splicing of *Psen1* transcripts. However, the aberrant splicing was only observed in the brain and not other tissues. In the mouse brain, homozygosity for the G183V mutation reduced the levels of the normally spliced transcript by approximately half. (In humans, heterozygosity for G183V rather than homozygosity presumably means that the reduction in transcript levels would be less.) These researchers suggested that reduced γ-secretase activity in the brain may be responsible for the Pick's disease phenotype and noted that levels of Aβ are,

unexpectedly, reduced by *more* than half in cell-free assays conducted using mouse brain. Their results supported that the reduction was due to the lower level of PSEN1 protein rather than the G183V mis-sense mutation of the coding sequence since G183V mutant PSEN1 protein had similar activity to wild type PSEN1 in transfected murine embryonic fibroblasts (MEFs) lacking endogenous Presenilin activity. When the same cells were transfected with a truncation after exon 5 sequence of the Psen1 open reading frame, Watanabe et al. saw no γ-secretase activity. However, if we assume that our observations of Psen1Δ>5 activity in the presence of endogenous, normal Presenilin are valid this explains some apparently anomalous observations (below).

In our 2008 paper (32) we showed that a low levels of aberrantly splicing could, nevertheless, have potent dominant phenotypes. Thus, we should not assume that the low levels of Psen1Δ>5-like transcripts generated by aberrant splicing in the G183V mutant carriers have no effect. Indeed, the analyses described in this paper show that Psen1Δ>5 truncated protein is notable for its avid incorporation into very stable higher molecular weight complexes and its ability to bind full-length forms of Psen1 and Psen2. This may explain why Watanabe et al. saw ~50% reductions in both Psen1 transcript levels and Notch cleavage in their homozygous mutant mice but considerably more than a 50% reduction in $A\beta_{40}$ production (for Notch and Aβ synthesis measured by cell-free assays on mouse cortex). Also, the idea that FTD might be due to a reduction of human *PSEN1* transcript levels is not consistent with the absence of any reports of FAD in the FAI mutant family bearing the P242LfsX11 mutation. These individuals show ~50% reduction in wild type *PSEN1* transcript levels. This reduction presumably occurs in all cells of these individuals since it appears to be due to a frameshift mutation affecting all

the transcript products of the mutant allele. Also, aberrant *PSEN1* transcript splicing has been observed in sporadic FTD brains (30) and, apparently, for the L113P FAD mutation of PSEN1 with features of FTD (67). Therefore, we suggest that truncated PSEN1 proteins, and in particular truncations similar to Psen1Δ>5, may play a decisive role in the development of FTD pathology where PSEN1 gene activity is involved. Whether Psen1Δ>5-like truncations perform this role via their effect on AβPP cleavage or by effects on other PRESENILIN activities (such as autophagy, Ca^{2+} transport or β-catenin phosphorylation) or via yet unknown activities not dependent on full-length PRESENILINs remains to be seen. We can begin to investigate this by analysing the higher molecular weight complexes into which Psen1Δ>5 becomes incorporated.

In zebrafish embryos, suppression of Appa cleavage by Psen1Δ>5 was accompanied by an apparent dependence on endogenous Psen1 for complex formation but Psen1Δ>5 had no effect on Notch signalling. This would be consistent with Notch and AβPP cleavage being performed by different forms of γ-secretase complex and/or in different locations within the cell. There is experimental data to support both of these ideas since γ-secretase complexes comprised of different isoforms of Aph1 appear to show different proclivities to cleave Notch and AβPP (57) and Notch is thought to be cleaved by γ-secretase in a process involving endocytosis (reviewed by (68)) while cleavage of AβPP by γ-secretase has been observed to be predominantly in the mitochondrial associated membranes (MAM, (13)). Once again, it will be interesting to pursue the identity of the proteins observed to bind so strongly to Psen1Δ>5 since these may reveal more about the differential cleavage of γ-secretase substrates.

The Psen1Δ>6 and Psen1Δ>7 mutations both inhibited Notch signalling but did not affect cleavage of Appa. However, the idea that these truncations might delimit a region of the PSEN1 NTF within which any truncation could dominantly inhibit Notch signalling was refuted by analysis of the truncation produced by the P242LfsX11 FAI mutation. We observed that this mutation actually boosted Notch signalling rather than inhibiting it. The discoverers of P242LfsX11 noted that levels of *PSEN1* transcript are reduced in lymphocytes taken from people bearing this mutation (14)). However, the mutant transcript can still be detected at low levels (see the supplementary data published with (14)). This is not unexpected since the P242LfsX11 mutation generates a frameshift leading to a premature termination codon that lies within 20 nucleotides upstream of an exon-exon junction that is well within the range defined by the "50-55-bp rule" for inefficient nonsense mediated decay (31). Wang et al (14) suggest that the FAI phenotype is due to haploinsufficiency for genes encoding components of the γ-secretase complex – i.e. a loss of function phenotype. Our result suggests that the effects of these mutations, or at least those of the P242LfsX11 mutation of PSEN1, may be more complex. The putative loss of Notch signalling caused by P242LfsX11 may be less than expected or (depending on the strength of the stimulation) the overall level of Notch signalling might possibly be increased. Any other cleavage events/pathways mediated by γ-secretase may be differentially affected compared to Notch. It will be informative to investigate the differential effects (if they exist) on γ-secretase activity of FAI mutations in the other components of the γ-secretase complex.

Despite the fact that γ-secretase activity is known to cleave over 70 different substrates (1) it is common to study the effects of Notch signalling using chemical inhibitors of γ-

secretase (e.g. (69-71)). One justification for this simplistic approach is that the phenotypes from loss of Notch1 or Psen1 in mouse embryos are similar (72, 73) and so facilitation of Notch signalling may be the major role of γ-secretase during embryogenesis. Of course, it would be preferable to modulate γ-secretase activity in a more substrate-specific manner in order to dissect its role in development and disease. Our discovery that particular truncations of Psen1 differentially affects the functions of various γ-secretase substrates opens the door to a greater degree of substrate-specific manipulation of γ-secretase activity in transgenic animals. It will be valuable to investigate the differential effects of our truncations on γ-secretase substrates such as p75, E-cadherin and others.

Materials and Methods

Zebrafish husbandry and animal ethics

Wild type zebrafish were maintained in a recirculated water system. All work with zebrafish was conducted under the auspices of the Animal Ethics Committee of the University of Adelaide.

Construction of DNAs for expression of truncated zebrafish Psen1 and human PSEN1

cDNAs encoding Presenilin truncations (including truncations equivalent to the NTF) were synthesised by PCR from zebrafish *psen1* cDNA or human *PSEN1* cDNA. All PCR oligonucleotide primer combinations used for constructing cDNAs encoding Presenilin truncations are described in Table 1. The zebrafish Psen1 truncations are fused at their N-termini to a FLAG™ antibody tag, DYKDDDDK (74) that follows a start codon within a consensus Kozak sequence (75). The human PSEN1 truncations are fused at their N-termini to an HA tag (YPYDVPDYA (76)) that follows a start codon within a consensus Kozak sequence. The cDNA encoding the putative protein product of the P242LfsX11 mutation is the human hPSEN1Δ>7 construct into which the P242LfsX11 mutation has been introduced by QuikChange™ Site-Directed Mutagenesis (Stratagene Cloning Systems, La Jolla, CA, USA). As such, it includes the novel codons found downstream of this frameshift mutation before the premature termination codon. The cDNA constructs for synthesis of the negative control zebrafish and human mRNAs denoted as “stop” are full length cDNAs including N-terminal FLAG or HA tag fusions respectively but with codon 4 of the Presenilin coding sequences mutated to the stop codon TAA. All

sequences were cloned into the pcGlobin2 vector (62) between the *Bam H*I and *Eco R*I restriction sites (for zebrafish cDNAs) and *Bam H*I and *Xho* I restriction sites (for human cDNAs) and their sequences confirmed by sequencing before their use for synthesis of mRNA as previously described (32).

Injection of zebrafish embryos

mRNAs were injected as previously described (32). The morpholino antisense oligonucleotides (morpholinos) used in this study and their method of use have been described previously (32). In that paper, Morpholino MoPsen1Tln is named MoTln and MoPsen2Tln is named MoPS2Tln in (32). The inactive, morpholino, MoCont, was used as a negative control in embryo injections and to dilute the experimental morpholinos above as described in (32).

Western immunoblot analyses of HMW complexes

At 6 hpf embryos were dechorionated, deyolked and placed in sample buffer (2% sodium dodecyl sulfate [SDS], 5% β-mercaptoethanol, 25% v/v glycerol, 0.0625 M Tris–HCl [pH 6.8], and bromphenol blue), heated immediately at 100°C for 5 min, and then stored at −20°C prior to separation on 10% SDS–polyacrylamide gels. Proteins were transferred to nitrocellulose membranes using a semidry electrotransfer system. When probed with the anti-FLAG M2 monoclonal antibody (Sigma, Missouri, USA), the membranes were blocked with 5% w/v skim milk powder in TBST and then incubated with a 1 in 5,000 dilution of the antibody in TBST containing 1% w/v skim milk powder. The membranes were then washed four times in TBST and visualized with luminol reagents (Amresco, Ohio, USA) by exposure to X-ray films (GE Healthcare LTD, Amersham Hyperfilm^{TM}

ECL, UK) and the ChemiDoc™ MP imaging system (Bio-Rad, Hercules, CA, USA). For incubation with anti-β-tubulin antibodies (Antibody E7, Developmental Studies Hybridoma Bank, The University of Iowa, IA, USA), primary antibodies were diluted to 1 in 200 in TBST containing 1% w/v skim milk. The membranes were then washed in TBST and incubated with a donkey antimouse IgG secondary antibody (Jackson ImmunoResearch Laboratories, Inc.) diluted to 1 in 3,000 in TBST containing 2% w/v skim milk. After incubation with the secondary antibody the membranes were washed and visualised in the same fashion as for immunoblotting with the anti-FLAG antibody.

Co-immunoprecipitation analyses

Embryos at the one-cell stage were injected with mRNA encoding Psen1Δ>5 or an N-terminally FLAG-tagged GFP molecule. At 6 hpf embryos were dechorionated, deyolked and lysed in cell lysis buffer (Sigma, Missouri, USA). For each FLAG-fusion protein sample a 40µl suspension of ANTI-FLAG M2 affinity gel (Sigma, Missouri, USA) was prepared and washed with TBS twice. The samples were incubated with the affinity gel overnight at 4°C with gentle mixing. After incubation the affinity gel protein sample mix was washed three times with TBS and was left in 10µl of sample buffer (2% sodium dodecyl sulfate [SDS], 25% v/v glycerol, 0.0625 M Tris–HCl [pH 6.8], and bromphenol blue) prior to separation on 12% SDS–polyacrylamide gels. Proteins were transferred to nitrocellulose membranes using a semi-dry electrotransfer system. The membrane was probed with the anti-FLAG M2 monoclonal antibody (Sigma, Missouri, USA) and the polyclonal antibodies raised against Psen1 CTF and Psen2 NTF (previously described in (77)).

qPCR

Embryos at the one-cell stage were injected with mRNAs encoding FLAG-tagged Psen1Δ >6 or zebrafish Psen1 “stop” negative control. Total RNA was extracted from whole embryos at 24 hpf using the QAIGEN RNeasy mini kit (QAIGEN, GmbH, Hilden, Germany). Total RNA was used to synthesise first-strand cDNA by reverse transcription (Superscript III kit; Invitrogen, Camarillo, USA).

qPCR for *psen1* and *ef-1a* expression was performed as described previously in Moussavi Nik *et al.* 2012.

Assays of Notch signalling and Appa cleavage

Our assay for Notch signalling has previously been described (32) and involves comparison of the relative transcription of the Notch target gene *neurogenin1* in the trunk region of negative control and treated embryos at 24 hpf embryos using *in situ* transcript hybridisation followed by chi-square contingency tests. Increases or decreases in Notch signalling are expressed values of p. Smaller values of p may indicate a stronger effect on Notch signalling but cannot be interpreted as directly correlated with the magnitude of the loss or gain of the signal. Raw data and statistical analysis is given in Supplemental Data Table 1.

Our assay for γ-secretase cleavage of AβPP exploits a modified form of zebrafish Appa (see Figure 2A) and will be described in detail elsewhere (Wilson et al. manuscript in preparation). Briefly, mRNAs encoding a set ratio of “C86” fragment of zebrafish Appa fused to destabilised green fluorescent protein (dGFP, see Figure 2A), and free GFP are injected into embryos at the one-cell stage. At 12 hpf yolks are removed from embryos.

These are then lysed and subjected to SDS polyacrylamide gel electrophoresis and western immunoblotting with anti-GFP antibody (Rockland Immunochemicals Inc. Gilbertsville, PA, USA) for detection of GFP. Variations in relative APP cleavage due to various treatments are observed by comparing the C86:dGFP bands on blots after normalising against the free GFP bands. The C86:dGFP band intensity was quantified on a Typhoon trio (Amersham Bioscience Corp., Piscataway, NJ, USA). Note that the γ-secretase cleavage products of C86:dGFP are too unstable to be detected. Assays were completely replicated three times and the statistical significance of changes in relative intensity were assessed by one-way ANOVA with the Bonferroni Post Hoc test. Raw data and statistical analysis is given in Supplemental Data Table 2.

Acknowledgements

The β-tubulin (E7) monoclonal antibody was obtained from the Developmental Studies Hybridoma Bank developed under the auspices of the NICHD and maintained by The University of Iowa, Department of Biology, Iowa City, IA, USA.

Funding

This work was supported by the Australian National Health and Medical Research Council (NHMRC, Project Grant 453622 to ML and RM and Project Grant 1003209 to GC), the Cancer Council of South Australia (research grant to ML), The Australian Research Council (ARC) Centre for the Molecular Genetics of Development (research funds to ML), the School of Molecular and Biomedical Sciences of the University of Adelaide (support of ML and MN), the late Douglas Anders (funds to ML), grants from the McCusker Alzheimer's Disease Research Foundation, the Department of Veterans Affairs, and Hollywood Private Hospital (to RM), funds from McCusker Alzheimer's Disease Research Foundation, particularly the generous support from Helen Sewell (to GV), Edith Cowan University's Strategic Research Grant (to GV) and the Australian Research Council (Discovery Project Grant DP1094119 to GC). We are indebted to Lindsay Carthew for his generous support of MN.

Conflict of Interest Statement

The authors declare no conflict of interest.

Figures

Figure 1

Structure of Presenilin1 protein and truncations. The upper part of the figure shows the relationship of *psen1* exons to protein structure. Alternating thick and thin areas on the protein strand indicate the sequence coded by successive exons (numbered after their cognate human exons). Horizontal grey lines indicate the region of the lipid bilayer. “D” indicates the position of aspartate residues critical for the catalytic site (shown by a star). The arrowhead indicates the site of endoproteolysis that creates the N-terminal fragment (NTF) and C-terminal fragment (CTF) and the N- and C-termini are indicated. The cytoplasmic loop domain and the approximate locations of the G183 Pick disease mutation and P242LfsX11 acne inversa mutation are indicated. Zebrafish Psen1 and human PSEN1 truncations were fused at their N-termini to FLAG or HA antibody tags respectively. The lower part of the figure shows the putative structure of each truncation of Psen1 and summarises their observed effects on Notch signalling and Appa cleavage. ↑indicates increase, ↓indicates decrease, 0 indicates no significant change.

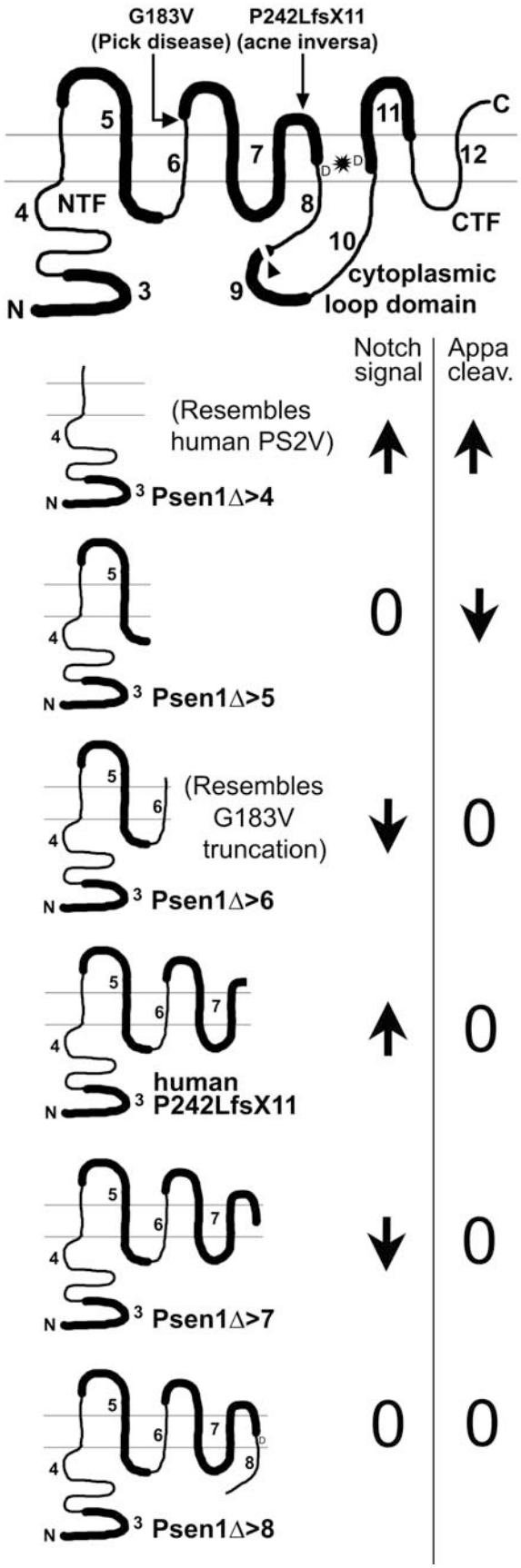
G183V
(Pick disease)
P242LfsX11
(acne inversa)
5
6
7
8
9
10
11
12
C
NTF
CTF
4
N
3
D
D
cytoplasmic
loop domain
Notch
signal
Appa
cleav.
(Resembles
human PS2V)
Psen1Δ>4
Psen1Δ>5
(Resembles
G183V
truncation)
Psen1Δ>6
human
P242LfsX11
Psen1Δ>7
Psen1Δ>8
0
0
0
0

Figure 2

Assays of relative Notch signalling activity in the presence of truncations of the NTF of Psen1. For the Notch assay, comparisons of *neurogenin1* expression in the trunk region of the developing spinal cord at 24 hpf were made between embryos injected with non-translatable Psen1 mRNA (i.e. as the negative control) and embryos injected with mRNAs encoding truncations of the NTF of (**A**) zebrafish Psen1 and (**B**) human PSEN1 (see Materials and Methods and (32)). In A, Psen1Δ>4 stimulates Notch signalling while Psen1Δ>6 and Δ>7 decrease it. Psen1Δ>5, Δ>8 and non-truncated NTF show no significant effect (ns). In **B**, the same effects are observed for the human PSEN1 truncations.

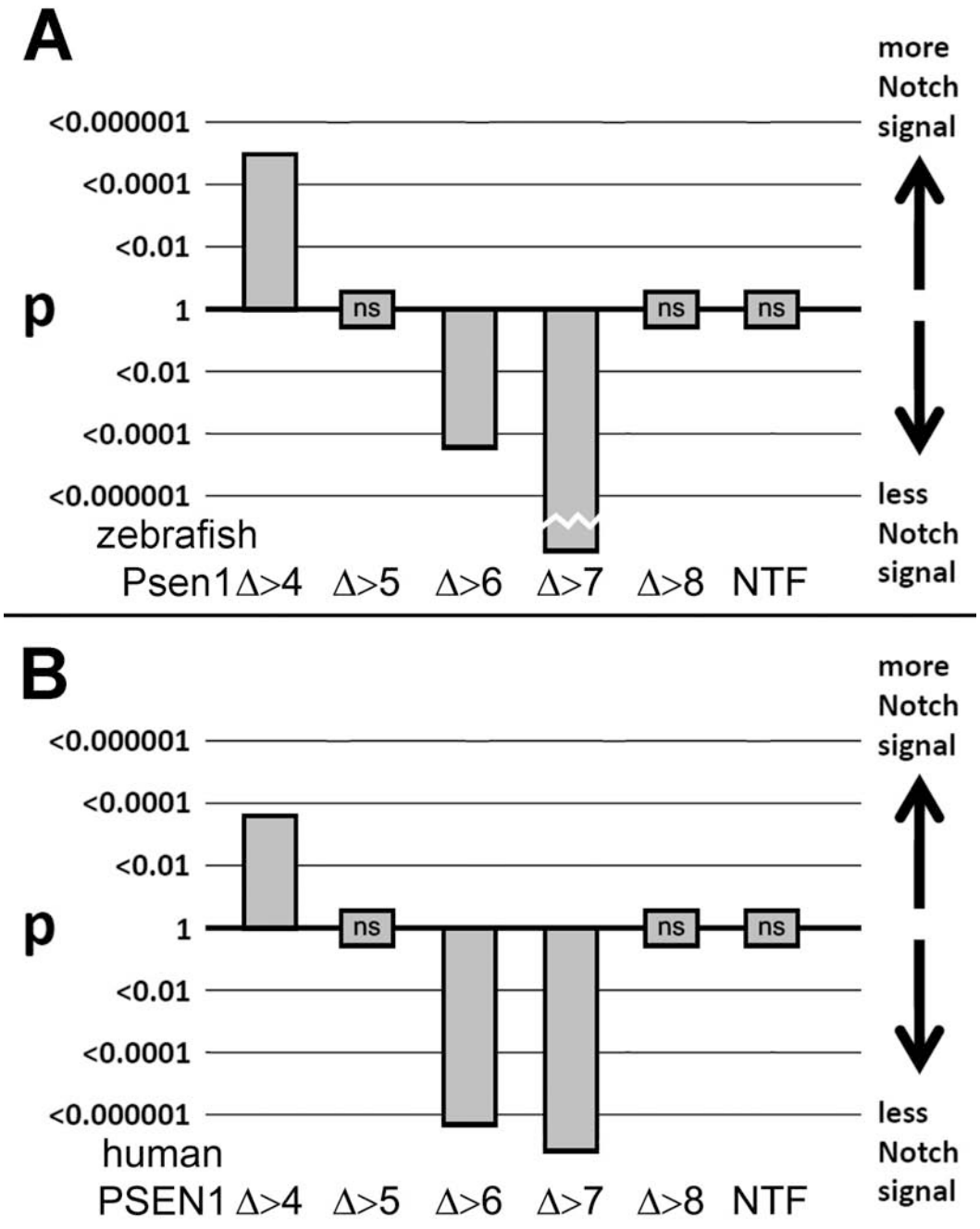
A
more
Notch
signal
<0.000001
<0.0001
<0.01
p
1
<0.01
<0.0001
<0.000001
less
Notch
signal
ns
ns
ns
zebrafish
Psen1Δ>4 Δ>5 Δ>6 Δ>7 Δ>8 NTF
B
more
Notch
signal
<0.000001
<0.0001
<0.01
p
1
<0.01
<0.0001
<0.000001
less
Notch
signal
ns
ns
ns
human
PSEN1 Δ>4 Δ>5 Δ>6 Δ>7 Δ>8 NTF

Figure 3

Assays of zebrafish Appa cleavage at 12 hpf after injection of mRNAs encoding truncations of the NTF of (**A**) zebrafish Psen1, (**B**) human PSEN1 or with morpholinos putatively generating similar truncations by interference with splicing of endogenous zebrafish *psen1* transcripts (**C**). The assay measures levels of the Appa C86 fragment that is a substrate for γ-secretase (see Materials and Methods). In **A**, Psen1Δ>4 increases Appa cleavage while Psen1Δ>5 and the γ-secretase inhibitor DAPT decrease it. Other truncations, the entire NTF (NTF) and a negative control mRNA in which codon 4 of the full-length *psen1* coding sequence is mutated to a stop codon ("stop") have no significant effect. Similar effects are observed using human PSEN1 truncations in **B**. In **C**, morpholino antisense oligonucleotides blocking splice acceptor sites are used to interfere with zebrafish *psen1* transcript splicing as described in (32) putatively resulting in truncated peptides similar to those indicated below within parentheses. Not all Psen1 truncations can be created in this way. "5Ac" hybridises to the acceptor site of exon 5 etc.. Error bars show standard errors of the means. "-ve*" represents embryos injected with the inactive, control morpholino MoCont. **, $p < 0.01$; ***, $p < 0.001$; ****, $p<0.0001$; ns, not significant (i.e. $p \geq 0.01$).

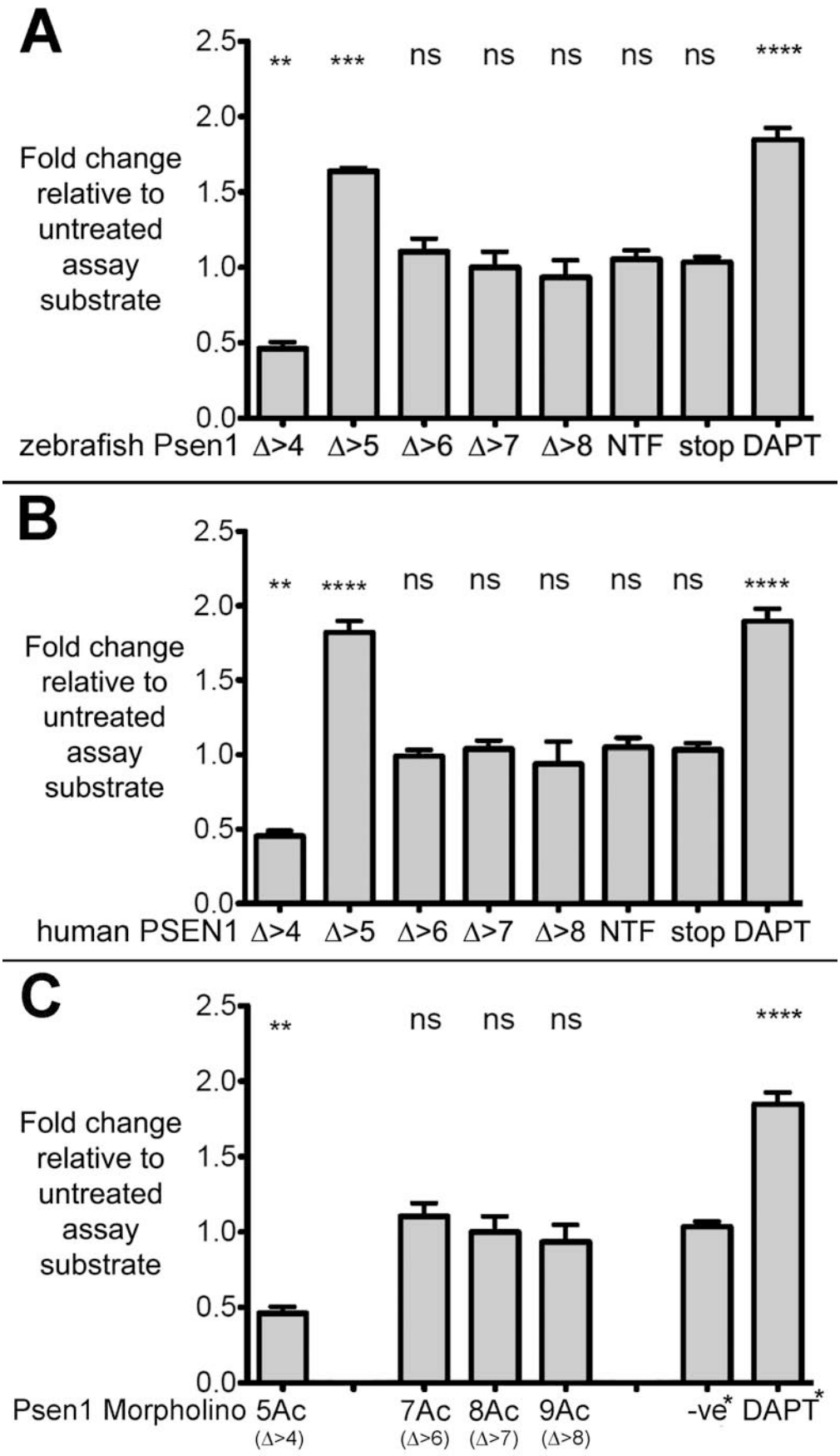
A
Fold change relative to untreated assay substrate
2.5
2.0
1.5
1.0
0.5
0.0
** *** ns ns ns ns ns ****
zebrafish Psen1 Δ>4 Δ>5 Δ>6 Δ>7 Δ>8 NTF stop DAPT
B
Fold change relative to untreated assay substrate
2.5
2.0
1.5
1.0
0.5
0.0
** **** ns ns ns ns ns ****
human PSEN1 Δ>4 Δ>5 Δ>6 Δ>7 Δ>8 NTF stop DAPT
C
Fold change relative to untreated assay substrate
2.5
2.0
1.5
1.0
0.5
0.0
** ns ns ns ****
Psen1 Morpholino 5Ac (Δ>4) 7Ac (Δ>6) 8Ac (Δ>7) 9Ac (Δ>8) -ve* DAPT*

Figure 4

Zebrafish Psen1Δ>4 acts through endogenous Psen1 to increase Notch signalling and Appa cleavage. **A**, Assays of Notch signalling activity in zebrafish embryos at 24 hpf after injection of mRNA encoding either zebrafish Psen1Δ>4 alone (Δ>4), Psen1Δ>4 mRNA with the MoPsen1Tln morpholino blocking endogenous Psen1 translation (Δ>4 – Psen1), or Psen1Δ>4 mRNA with the MoPsen2Tln morpholino blocking endogenous Psen2 translation (Δ>4 – Psen2). For the assay, comparisons of *neurogenin1* expression in the trunk region of the developing spinal cord at 24 hpf were made against control embryos injected with either the MoPsen1Tln or MoPsen2Tln morpholino to block translation of mRNA from the relevant endogenous *presenilin* gene (as indicated) or with an inactive, negative control morpholino (all other results). All control embryos were also injected with zebrafish "stop" negative control mRNA (see Materials and Methods). **B**, Assays of Appa cleavage in embryos injected with the mRNA encoding the assay substrate and with either zebrafish Psen1Δ>4 mRNA alone, Psen1Δ>4 mRNA with the MoPsen1Tln morpholino blocking endogenous Psen1 translation, Psen1Δ>4 mRNA with the MoPsen2Tln morpholino blocking endogenous Psen2 translation (Δ>4 – Psen2), with inactive morpholino MoCont only (-ve cont.), or incubated in γ-secretase inhibitor DAPT. All assays are conducted relative to embryos injected only with the substrate mRNA.

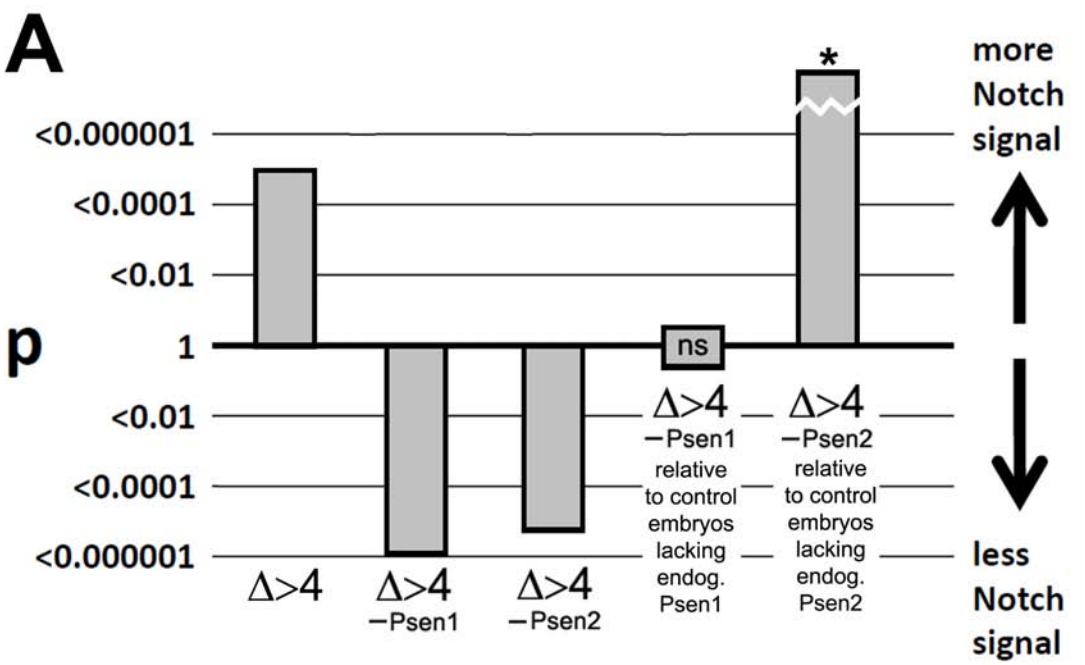
A
<0.000001
<0.0001
<0.01
p
1
<0.01
<0.0001
<0.000001
*
ns
more Notch signal
less Notch signal
Δ>4
Δ>4 −Psen1
Δ>4 −Psen2
Δ>4 −Psen1 relative to control embryos lacking endog. Psen1
Δ>4 −Psen2 relative to control embryos lacking endog. Psen2

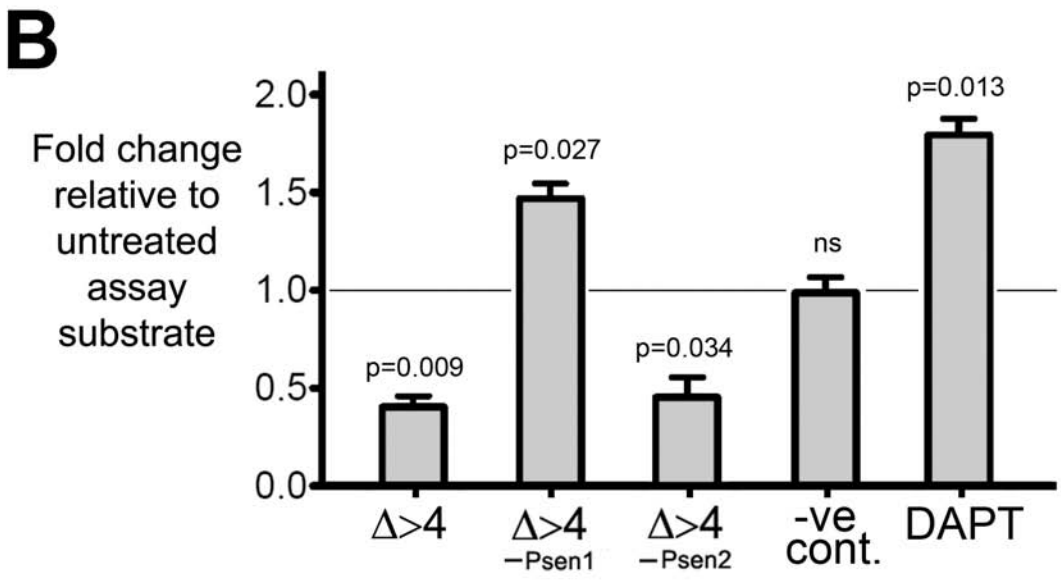
B
Fold change relative to untreated assay substrate
2.0
1.5
1.0
0.5
0.0
p=0.009
p=0.027
p=0.034
ns
p=0.013
Δ>4
Δ>4 −Psen1
Δ>4 −Psen2
-ve cont.
DAPT

Figure 5

Truncations of the Psen1 NTF are incorporated into higher molecular weight complexes. **A**, Embryos were injected with mRNAs encoding the NTF truncations and with either negative control morpholino MoCont or with a morpholino suppressing Psen1 translation MoPsen1Tln (see lanes marked with *). Embryos were then lysed at 6 hpf and their proteins separated by SDS PAGE before immunoblotting with anti-FLAG antibody. Psen1Δ>5 ("Δ>5") and Psen1Δ>8 ("Δ>8") particularly show decreased formation of two bands/complexes at ~50kDa (arrowheads) and increased apparent formation of monomers (arrows) and higher molecular weight complexes when endogenous Psen1 is reduced. The ~50 kDa complexes may include breakdown products of the truncations since their size does not vary with the differences in truncation size. However, the specificity of the anti-FLAG antibody detection of these complexes is illustrated by their absence when endogenous Psen1 expression is blocked in embryos with Psen1Δ>5 or Psen1Δ>8 and by the lack of detectable staining for injection of the zebrafish negative control mRNA "stop" in which codon 4 of the full-length *psen1* coding sequence is mutated to a stop codon ("stop", see Materials and Methods). Ponceau S staining of the blots before antibody exposure confirmed similar amounts of total embryo proteins present in each lane (not shown) and this is also illustrated by staining for β-Tubulin (β-Tub). **B**, The constructs coding for zebrafish Psen1 truncations include N-terminal FLAG antibody tags allowing co-immunoprecipitation of associated proteins. mRNA coding for Psen1Δ>5 (FLAG- Psen1Δ>5) or for N-terminally FLAG-tagged GFP (FLAG-GFP) was injected into zebrafish embryos before lysis under non-denaturing conditions at 6 hpf and

immunoprecipitation using ANTI-FLAG M2 Affinity Gel. Western blotting of the immunoprecipitate revealed binding of endogenous Psen1 and Psen2 proteins only to FLAG- Psen1Δ>5 and not to FLAG-GFP. As expected, this procedure conducted on uninjected embryos as a negative control showed no co-immunoprecipitated proteins.

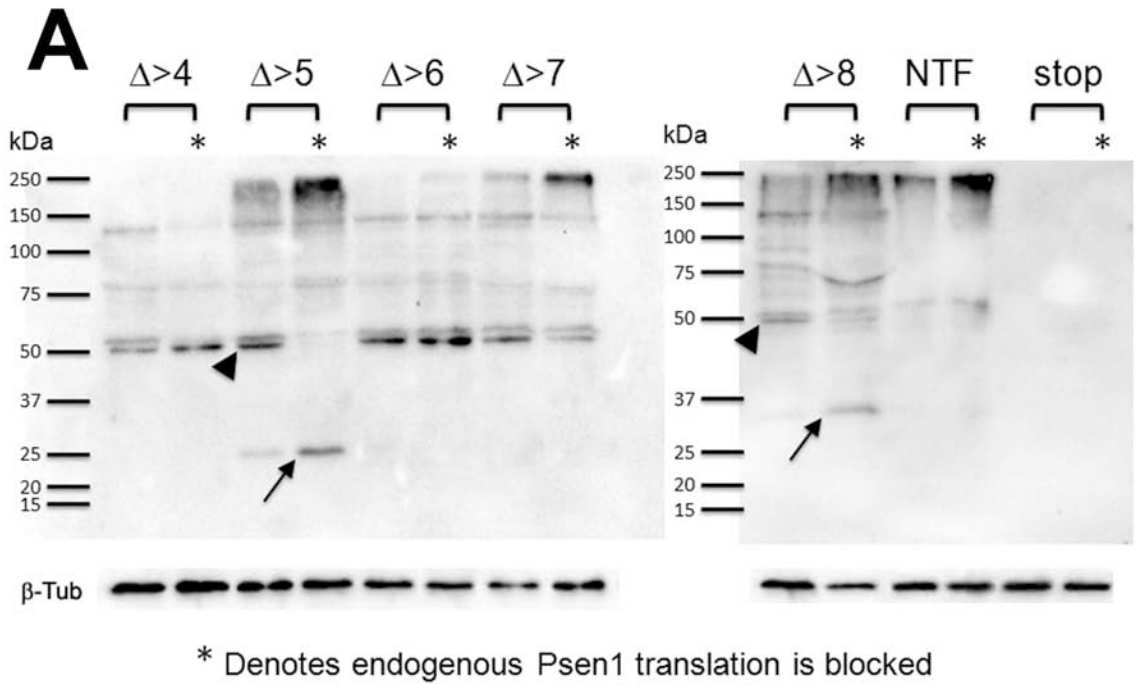

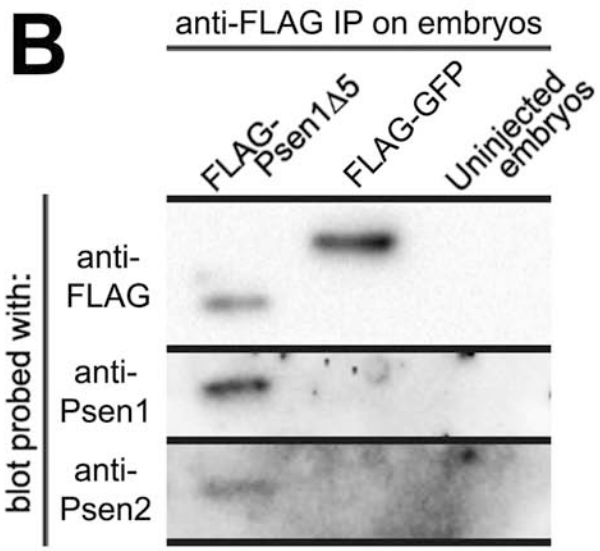

Figure 6

A, Diagram showing the single nucleotide change in exon 7 of human *PSEN1* (light grey shading) that causes the P242LfsX11 mutation and generates a premature stop codon (dark grey shading) within 15 nucleotides of the downstream exon 7 / exon 8 boundary. The novel theoretical C terminal of the truncated protein caused by P242LfsX11 is shown in bold text. Nucleotide sequence in alternating exons is shown in alternating bold and regular text. Codons are indicated using the single amino acid code. Nucleotide and codon numbers are derived from ENSEMBL transcript PSEN1-001. **B**, Assay of zebrafish Appa cleavage at 12 hpf after injection of mRNA encoding the truncated protein putatively formed by the P242LfsX11 mutation. This showed no significant change (ns) relative to a negative control in which embryos were injected with mRNA in which codon 4 of the full-length *PSEN1* coding sequence is mutated to a stop codon ("stop", see Materials and Methods). In contrast, the positive control, DAPT treatment, decreased γ-secretase cleavage of Appa (see legend to Figure 3 for an explanation). The stop control showed no significant change (ns) relative to untreated embryos. Bars show standard errors of the means. **C**, Assay of relative Notch signalling activity (*neurogenin1* expression) in the trunk region of the developing spinal cord of zebrafish embryos at 24 hpf after injection of mRNA encoding the truncated protein putatively formed by the P242LfsX11 mutation. The mutant boosts Notch signalling relative to embryos injected with the stop control ($p = 0.0002$).

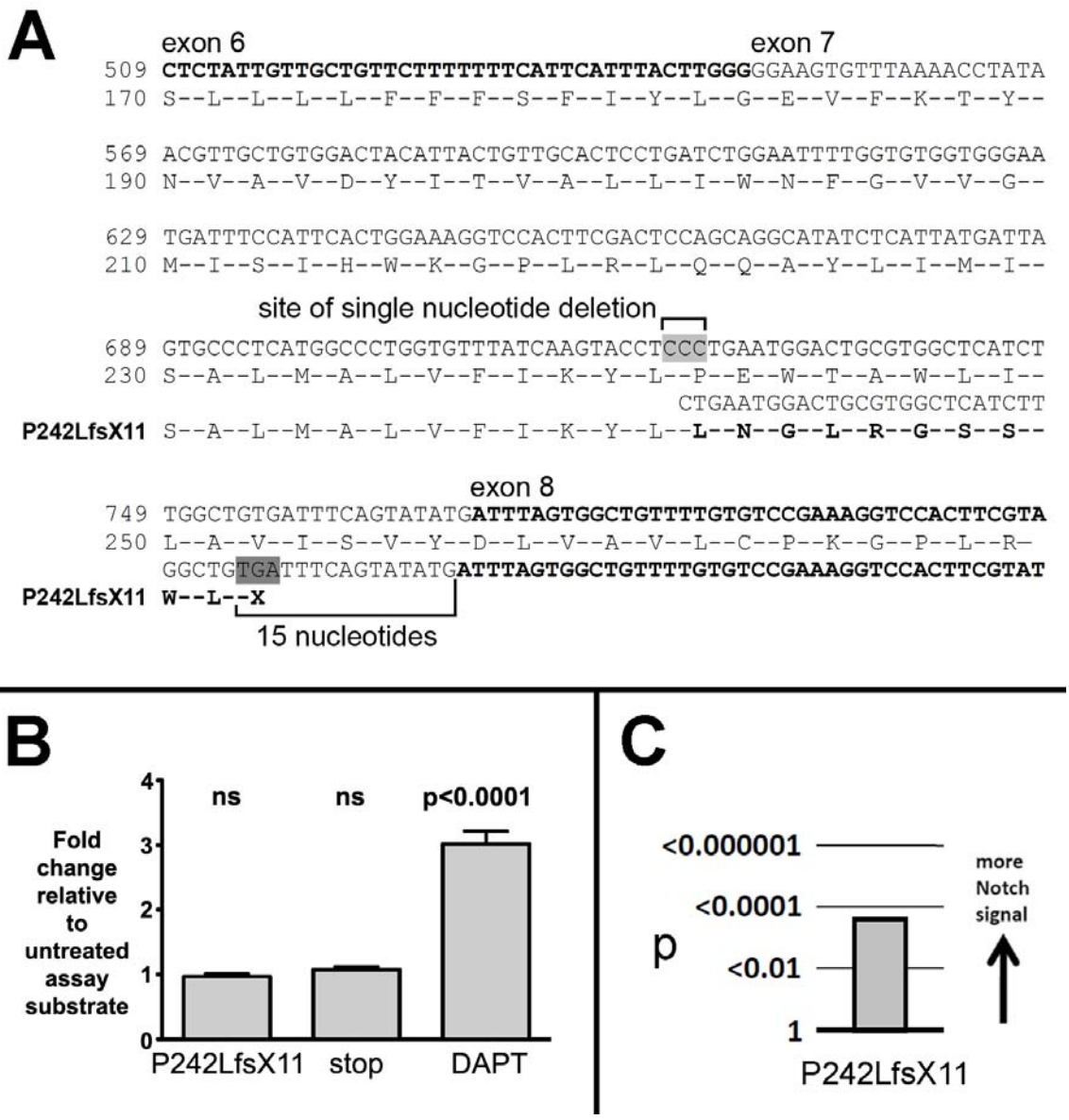
A
exon 6
exon 7
509 CTCTATTGTTGCTGTTCTTTTTTTCATTCATTTACTTGGGGGAAGTGTTTAAAACCTATA
170 S--L--L--L--L--F--F--F--S--F--I--Y--L--G--E--V--F--K--T--Y--
569 ACGTTGCTGTGGACTACATTACTGTTGCACTCCTGATCTGGAATTTTGGTGTGGTGGGAA
190 N--V--A--V--D--Y--I--T--V--A--L--L--I--W--N--F--G--V--V--G--
629 TGATTTCCATTCACTGGAAAGGTCCACTTCGACTCCAGCAGGCATATCTCATTATGATTA
210 M--I--S--I--H--W--K--G--P--L--R--L--Q--Q--A--Y--L--I--M--I--
site of single nucleotide deletion
689 GTGCCCTCATGGCCCTGGTGTTTATCAAGTACCTCCCTGAATGGACTGCGTGGCTCATCT
230 S--A--L--M--A--L--V--F--I--K--Y--L--P--E--W--T--A--W--L--I--
CTGAATGGACTGCGTGGCTCATCTT
P242LfsX11 S--A--L--M--A--L--V--F--I--K--Y--L--L--N--G--L--R--G--S--S--
exon 8
749 TGGCTGTGATTTCAGTATATGATTTAGTGGCTGTTTTGTGTCCGAAAGGTCCACTTCGTA
250 L--A--V--I--S--V--Y--D--L--V--A--V--L--C--P--K--G--P--L--R—
GGCTGTGATTTCAGTATATGATTTAGTGGCTGTTTTGTGTCCGAAAGGTCCACTTCGTAT
P242LfsX11 W--L--X
15 nucleotides
B
Fold change relative to untreated assay substrate
4
3
2
1
0
ns
ns
p<0.0001
P242LfsX11
stop
DAPT
C
p
<0.000001
<0.0001
<0.01
1
more Notch signal
P242LfsX11

Tables

Table 1

PCR primer and morpholino sequences

PCR primers	Sequence (5′–3′)	Amplifies with	To form
zfEx4	GGAATTCTTACTGCTGTCCGTCCTTCTG	zfForwardtag	zebrafish Psen1Δ>4
zfEx5	GGAATTCTTACTTGTAGCATCTGTACTT	zfForwardtag	zebrafish Psen1Δ>5
zfEx6	GGAATTCTTACAAATAAATTAAGGAG	zfForwardtag	zebrafish Psen1Δ>6
zfEx7	GGAATTCTTAGTAGACTGAAATAGCAGCGAGGA	zfForwardtag	zebrafish Psen1Δ>7
zfEx8	GGAATTCTTAGGAGTAGATGAGCGCTGGGA	zfForwardtag	zebrafish Psen1Δ>8
zfNTF	GGAATTCTTACATATTGAAGAGCCACACCAT	zfForwardtag	zebrafish Psen1NTF
zfTAA	CGGGATCCACCATGGACTACAAAGACGACGACGACAAAATGGCTGATTAAGTGCAG	zfFullLengthRev	zebrafish “stop” negative control
zfForwardtag	CGGGATCCACCATGGACTACAAAGACGACGACGACAAAATGGCTGATTTAGTGCAG	zfEx4, zfEx5, zfEx6, zfEx7, zfEx8, zfNTF	zebrafish Psen1Δ>4, Δ>5, Δ>6, Δ>7, Δ>8, NTF
zfFullLengthRev	GGAATTCTTATATGTAGAACTGATGGACG	zfTAA	zebrafish “stop” negative control
huEx4	CCGCTCGAGCTATAGCTGCCCATCCTTC	huForwardtag	human hPSEN1Δ>4
huEx5	CCGCTCGAGCTACTTATAGCACCTGTATTTATACA	huForwardtag	human hPSEN1Δ>5
huEx6	CCGCTCGAGCTACACTTCCCCCAAGTAAATGAATG	huForwardtag	human hPSEN1Δ>6
huEx7	CCGCTCGAGCTAATCATATACTGAAATCACAGCCAA	huForwardtag	human hPSEN1Δ>7
huEx8	CCGCTCGAGCTATGAGGAGTAAATGAGAGCTGG	huForwardtag	human hPSEN1Δ>8
huNTF	GGGAGCTCTTACATATTCACCAACCACACCAT	huForwardtag	human

			hPSEN1NTF
huTAA	CGGGATCCACCATGTACCCATACGATGTTCCAGATTACGCTATGACAGAGTAACCTGCACCG	huFullLengthRev	human “stop” negative control
huForwardtag	CGGGATCCACCATGTACCCATACGATGTTCCAGATTACGCTATGACAGAGTTACCTGCACCG	huEx4, huEx5, huEx6, huEx7, huEx8, huNTF.	human hPSEN1Δ>4, Δ>5, Δ>6, Δ>7, Δ>8, NTF
huFullLengthRev	CCGCTCGAGCTAGATATAAAATTGATGGAATGC	huTAA	human “stop” negative control
QuikChange™ Site-Directed Mutagenesis primers	**Sequence (5′–3′)**	**Used with primer**	**Produces**
c725delcforward	CAAGTACCTCCTGAATGGACTGCGTGGCTC	c725delcreverse	P242LfsX11 acne inversa mutation
c725delcreverse	GAGCCACGCAGTCCATTCAGGAGGTACTTG	c725delcforward	P242LfsX11 acne inversa mutation
Morpholinos	**Sequence (5′–3′)**	**Function**	
MoCont	CCTCTTACCTCAGTTACAATTTATA	Negative control morpholino	
MoPsen1Tln	ACTAAATCAGCCATCGGAACTGTGA	Inhibits endogenous Psen1 translation	
MoPsen2Tln	GTGACTGAATTTACATGAAGGATGA	Inhibits endogenous Psen2 translation	
MoPsen15Ac	GGTGTAGATCCTGCAGAAAAGAAGA	Inhibits transcript splicing to the acceptor site of exon5	
MoPsen16Ac	GCTTGAATCACCTGCAAAAAACAAA	Inhibits transcript splicing to the acceptor site of exon6	

Abbreviations

AD	Alzheimer's disease
APH1A	ANTERIOR PHARYNX DEFECTIVE 1, C. ELEGANS, HOMOLOG OF, A
AβPP	AMYLOID BETA A4 PRECURSOR PROTEIN
ARC	Australian Research Council
CMV	cytomegalovirus
CTF	C-terminal fragment (of a Presenilin protein)
ER	endoplasmic reticulum
FAD	familial Alzheimer's disease
FAI	familial acne inversa
FTD	frontotemporal dementia
GFP	Green Fluorescent Protein
HA	Haemagglutinin
HMW	high molecular weight
hpf	hours post fertilisation
kDa	kiloDaltons
MAM	mitochondrial associated membranes
morpholino	morpholino antisense oligonucleotide
NHMRC	National Health and Medical Research Council (of Australia)
NTF	N-terminal fragment (of a Presenilin protein)
PAGE	polyacrylamide gel electrophoresis
PSEN1,*2* / PSEN1,2	human *PRESENILIN1*,*2* gene / PRESENILIN1, 2 protein
psen1,*2* / Psen1,2	zebrafish *presenilin1*,*2* gene / Presenilin1,2 protein
PSENEN	PRESENILIN ENHANCER 2, C. ELEGANS, HOMOLOG OF
TBST	Tris Buffered Saline with Tween buffer

References

1 Lleo, A. and Saura, C.A. (2011) gamma-secretase substrates and their implications for drug development in Alzheimer's disease. *Curr Top Med Chem*, **11**, 1513-1527.

2 Fukumori, A., Fluhrer, R., Steiner, H. and Haass, C. (2010) Three-amino acid spacing of presenilin endoproteolysis suggests a general stepwise cleavage of gamma-secretase-mediated intramembrane proteolysis. *J Neurosci*, **30**, 7853-7862.

3 St George-Hyslop, P. and Fraser, P.E. (2012) Assembly of the presenilin gamma-/epsilon-secretase complex. *J Neurochem*, **120 Suppl 1**, 84-88.

4 Lee, J.H., Yu, W.H., Kumar, A., Lee, S., Mohan, P.S., Peterhoff, C.M., Wolfe, D.M., Martinez-Vicente, M., Massey, A.C., Sovak, G. *et al.* (2010) Lysosomal proteolysis and autophagy require presenilin 1 and are disrupted by Alzheimer-related PS1 mutations. *Cell*, **141**, 1146-1158.

5 Zhang, X., Garbett, K., Veeraraghavalu, K., Wilburn, B., Gilmore, R., Mirnics, K. and Sisodia, S.S. (2012) A role for presenilins in autophagy revisited: normal acidification of lysosomes in cells lacking PSEN1 and PSEN2. *J Neurosci*, **32**, 8633-8648.

6 Coen, K., Flannagan, R.S., Baron, S., Carraro-Lacroix, L.R., Wang, D., Vermeire, W., Michiels, C., Munck, S., Baert, V., Sugita, S. *et al.* (2012) Lysosomal calcium homeostasis defects, not proton pump defects, cause endo-lysosomal dysfunction in PSEN-deficient cells. *J Cell Biol*, **198**, 23-35.

7 Kelleher, R.J., 3rd and Shen, J. (2010) Genetics. Gamma-secretase and human disease. *Science*, **330**, 1055-1056.

8 Li, Y.M., Lai, M.T., Xu, M., Huang, Q., DiMuzio-Mower, J., Sardana, M.K., Shi, X.P., Yin, K.C., Shafer, J.A. and Gardell, S.J. (2000) Presenilin 1 is linked with gamma-secretase activity in the detergent solubilized state. *Proc Natl Acad Sci U S A*, **97**, 6138-6143.

9 Giuffrida, M.L., Caraci, F., De Bona, P., Pappalardo, G., Nicoletti, F., Rizzarelli, E. and Copani, A. (2010) The monomer state of beta-amyloid: where the Alzheimer's disease protein meets physiology. *Reviews in the neurosciences*, **21**, 83-93.

10 Koo, E.H., Squazzo, S.L., Selkoe, D.J. and Koo, C.H. (1996) Trafficking of cell-surface amyloid beta-protein precursor. I. Secretion, endocytosis and recycling as detected by labeled monoclonal antibody. *Journal of cell science*, **109 (Pt 5)**, 991-998.

11 Yamazaki, T., Koo, E.H. and Selkoe, D.J. (1996) Trafficking of cell-surface amyloid beta-protein precursor. II. Endocytosis, recycling and lysosomal targeting detected by immunolocalization. *Journal of cell science*, **109 (Pt 5)**, 999-1008.

12 Winkler, E., Kamp, F., Scheuring, J., Ebke, A., Fukumori, A. and Steiner, H. (2012) Generation of Alzheimer disease-associated amyloid beta42/43 peptide by gamma-secretase can be inhibited directly by modulation of membrane thickness. *J Biol Chem*, **287**, 21326-21334.

13 Area-Gomez, E., de Groof, A.J., Boldogh, I., Bird, T.D., Gibson, G.E., Koehler, C.M., Yu, W.H., Duff, K.E., Yaffe, M.P., Pon, L.A. *et al.* (2009) Presenilins are enriched in endoplasmic reticulum membranes associated with mitochondria. *Am J Pathol*, **175**, 1810-1816.

14 Wang, B., Yang, W., Wen, W., Sun, J., Su, B., Liu, B., Ma, D., Lv, D., Wen, Y., Qu, T. *et al.* (2010) Gamma-secretase gene mutations in familial acne inversa. *Science*, **330**, 1065.
15 Dermaut, B., Kumar-Singh, S., Engelborghs, S., Theuns, J., Rademakers, R., Saerens, J., Pickut, B.A., Peeters, K., van den Broeck, M., Vennekens, K. *et al.* (2004) A novel presenilin 1 mutation associated with Pick's disease but not beta-amyloid plaques. *Ann Neurol*, **55**, 617-626.
16 Dermaut, B., Kumar-Singh, S., Rademakers, R., Theuns, J., Cruts, M. and Van Broeckhoven, C. (2005) Tau is central in the genetic Alzheimer-frontotemporal dementia spectrum. *Trends Genet*, **21**, 664-672.
17 Watanabe, H., Xia, D., Kanekiyo, T., Kelleher, R.J., 3rd and Shen, J. (2012) Familial frontotemporal dementia-associated presenilin-1 c.548G>T mutation causes decreased mRNA expression and reduced presenilin function in knock-in mice. *J Neurosci*, **32**, 5085-5096.
18 Sato, N., Hori, O., Yamaguchi, A., Lambert, J.C., Chartier-Harlin, M.C., Robinson, P.A., Delacourte, A., Schmidt, A.M., Furuyama, T., Imaizumi, K. *et al.* (1999) A novel presenilin-2 splice variant in human Alzheimer's disease brain tissue. *J Neurochem*, **72**, 2498-2505.
19 Smith, M.J., Sharples, R.A., Evin, G., McLean, C.A., Dean, B., Pavey, G., Fantino, E., Cotton, R.G., Imaizumi, K., Masters, C.L. *et al.* (2004) Expression of truncated presenilin 2 splice variant in Alzheimer's disease, bipolar disorder, and schizophrenia brain cortex. *Brain Res Mol Brain Res*, **127**, 128-135.
20 Sato, N., Imaizumi, K., Manabe, T., Taniguchi, M., Hitomi, J., Katayama, T., Yoneda, T., Morihara, T., Yasuda, Y., Takagi, T. *et al.* (2001) Increased production of beta-amyloid and vulnerability to endoplasmic reticulum stress by an aberrant spliced form of presenilin 2. *J Biol Chem*, **276**, 2108-2114.
21 Sharman, M., Moussavi Nik, S.H., Chen, M., Ong, D., Wijaya, L., Laws, S.M., Taddei, K., Newman, M., Lardelli, M., Martins, R.N., Verdile, G. (2013) The Guinea Pig as a Model for Sporadic Alzheimer's Disease (AD): The Impact of Cholesterol Intake on Expression of AD-Related Genes. *PLoS One*, **(in press)**.
22 Gustafsson, M.V., Zheng, X., Pereira, T., Gradin, K., Jin, S., Lundkvist, J., Ruas, J.L., Poellinger, L., Lendahl, U. and Bondesson, M. (2005) Hypoxia requires notch signaling to maintain the undifferentiated cell state. *Dev Cell*, **9**, 617-628.
23 Tung, J.J., Tattersall, I.W. and Kitajewski, J. (2012) Tips, Stalks, Tubes: Notch-Mediated Cell Fate Determination and Mechanisms of Tubulogenesis during Angiogenesis. *Cold Spring Harb Perspect Med*, **2**, a006601.
24 Thompson, P.K. and Zuniga-Pflucker, J.C. (2011) On becoming a T cell, a convergence of factors kick it up a Notch along the way. *Semin Immunol*, **23**, 350-359.
25 Sato, C., Zhao, G. and Ilagan, M.X. (2011) An Overview of Notch Signaling in Adult Tissue Renewal and Maintenance. *Curr Alzheimer Res*.
26 Hester, S.D., Belmonte, J.M., Gens, J.S., Clendenon, S.G. and Glazier, J.A. (2011) A multi-cell, multi-scale model of vertebrate segmentation and somite formation. *PLoS Comput Biol*, **7**, e1002155.
27 South, A.P., Cho, R.J. and Aster, J.C. (2012) The double-edged sword of Notch signaling in cancer. *Semin Cell Dev Biol*.

28 Meshorer, E. and Soreq, H. (2002) Pre-mRNA splicing modulations in senescence. *Aging Cell*, **1**, 10-16.
29 Fackenthal, J.D. and Godley, L.A. (2008) Aberrant RNA splicing and its functional consequences in cancer cells. *Dis Model Mech*, **1**, 37-42.
30 Evin, G., Smith, M.J., Tziotis, A., McLean, C., Canterford, L., Sharples, R.A., Cappai, R., Weidemann, A., Beyreuther, K., Cotton, R.G. *et al.* (2002) Alternative transcripts of presenilin-1 associated with frontotemporal dementia. *Neuroreport*, **13**, 917-921.
31 Nagy, E. and Maquat, L.E. (1998) A rule for termination-codon position within intron-containing genes: when nonsense affects RNA abundance. *Trends Biochem Sci*, **23**, 198-199.
32 Nornes, S., Newman, M., Verdile, G., Wells, S., Stoick-Cooper, C.L., Tucker, B., Frederich-Sleptsova, I., Martins, R. and Lardelli, M. (2008) Interference with splicing of Presenilin transcripts has potent dominant negative effects on Presenilin activity. *Hum Mol Genet*, **17**, 402-412.
33 Area-Gomez, E., Del Carmen Lara Castillo, M., Tambini, M.D., Guardia-Laguarta, C., de Groof, A.J., Madra, M., Ikenouchi, J., Umeda, M., Bird, T.D., Sturley, S.L. *et al.* (2012) Upregulated function of mitochondria-associated ER membranes in Alzheimer disease. *EMBO J*, **31**, 4106-4123.
34 Kang, D.E., Soriano, S., Xia, X., Eberhart, C.G., De Strooper, B., Zheng, H. and Koo, E.H. (2002) Presenilin couples the paired phosphorylation of beta-catenin independent of axin: implications for beta-catenin activation in tumorigenesis. *Cell*, **110**, 751-762.
35 Soriano, S., Kang, D.E., Fu, M., Pestell, R., Chevallier, N., Zheng, H. and Koo, E.H. (2001) Presenilin 1 negatively regulates beta-catenin/T cell factor/lymphoid enhancer factor-1 signaling independently of beta-amyloid precursor protein and notch processing. *J Cell Biol*, **152**, 785-794.
36 Nelson, O., Tu, H., Lei, T., Bentahir, M., de Strooper, B. and Bezprozvanny, I. (2007) Familial Alzheimer disease-linked mutations specifically disrupt Ca2+ leak function of presenilin 1. *J Clin Invest*, **117**, 1230-1239.
37 Tu, H., Nelson, O., Bezprozvanny, A., Wang, Z., Lee, S.F., Hao, Y.H., Serneels, L., De Strooper, B., Yu, G. and Bezprozvanny, I. (2006) Presenilins form ER Ca2+ leak channels, a function disrupted by familial Alzheimer's disease-linked mutations. *Cell*, **126**, 981-993.
38 Wilson, L. and Lardelli, M. (2013) The Development of an in vivo gamma-Secretase Assay using Zebrafish Embryos. *Journal of Alzheimer's disease : JAD*.
39 King, G.D., Cherian, K. and Turner, R.S. (2004) X11alpha impairs gamma- but not beta-cleavage of amyloid precursor protein. *J Neurochem*, **88**, 971-982.
40 Montzka, K., Lassonczyk, N., Tschoke, B., Neuss, S., Fuhrmann, T., Franzen, R., Smeets, R., Brook, G.A. and Woltje, M. (2009) Neural differentiation potential of human bone marrow-derived mesenchymal stromal cells: misleading marker gene expression. *BMC neuroscience*, **10**, 16.
41 Neumann, E., Riepl, B., Knedla, A., Lefevre, S., Tarner, I.H., Grifka, J., Steinmeyer, J., Scholmerich, J., Gay, S. and Muller-Ladner, U. (2010) Cell culture and passaging alters gene expression pattern and proliferation rate in rheumatoid arthritis synovial fibroblasts. *Arthritis research & therapy*, **12**, R83.
42 Thinakaran, G., Harris, C.L., Ratovitski, T., Davenport, F., Slunt, H.H., Price, D.L., Borchelt, D.R. and Sisodia, S.S. (1997) Evidence that levels of presenilins (PS1 and

PS2) are coordinately regulated by competition for limiting cellular factors. *J Biol Chem*, **272**, 28415-28422.
43 Fortini, M.E. (2009) Notch signaling: the core pathway and its posttranslational regulation. *Dev Cell*, **16**, 633-647.
44 Nornes, S., Newman, M., Wells, S., Verdile, G., Martins, R.N. and Lardelli, M. (2009) Independent and cooperative action of Psen2 with Psen1 in zebrafish embryos. *Exp Cell Res*, **315**, 2791-2801.
45 Geling, A., Steiner, H., Willem, M., Bally-Cuif, L. and Haass, C. (2002) A gamma-secretase inhibitor blocks Notch signaling in vivo and causes a severe neurogenic phenotype in zebrafish. *EMBO Rep*, **3**, 688-694.
46 Cornell, R.A. and Eisen, J.S. (2002) Delta/Notch signaling promotes formation of zebrafish neural crest by repressing Neurogenin 1 function. *Development*, **129**, 2639-2648.
47 Campbell, W.A., Yang, H., Zetterberg, H., Baulac, S., Sears, J.A., Liu, T., Wong, S.T., Zhong, T.P. and Xia, W. (2006) Zebrafish lacking Alzheimer presenilin enhancer 2 (Pen-2) demonstrate excessive p53-dependent apoptosis and neuronal loss. *J Neurochem*, **96**, 1423-1440.
48 Itoh, M., Kim, C.H., Palardy, G., Oda, T., Jiang, Y.J., Maust, D., Yeo, S.Y., Lorick, K., Wright, G.J., Ariza-McNaughton, L. *et al.* (2003) Mind bomb is a ubiquitin ligase that is essential for efficient activation of Notch signaling by Delta. *Dev Cell*, **4**, 67-82.
49 Lemere, C.A., Lopera, F., Kosik, K.S., Lendon, C.L., Ossa, J., Saido, T.C., Yamaguchi, H., Ruiz, A., Martinez, A., Madrigal, L. *et al.* (1996) The E280A presenilin 1 Alzheimer mutation produces increased A beta 42 deposition and severe cerebellar pathology. *Nat Med*, **2**, 1146-1150.
50 Duff, K., Eckman, C., Zehr, C., Yu, X., Prada, C.M., Perez-tur, J., Hutton, M., Buee, L., Harigaya, Y., Yager, D. *et al.* (1996) Increased amyloid-beta42(43) in brains of mice expressing mutant presenilin 1. *Nature*, **383**, 710-713.
51 Borchelt, D.R., Thinakaran, G., Eckman, C.B., Lee, M.K., Davenport, F., Ratovitsky, T., Prada, C.M., Kim, G., Seekins, S., Yager, D. *et al.* (1996) Familial Alzheimer's disease-linked presenilin 1 variants elevate Abeta1-42/1-40 ratio in vitro and in vivo. *Neuron*, **17**, 1005-1013.
52 De Strooper, B., Saftig, P., Craessaerts, K., Vanderstichele, H., Guhde, G., Annaert, W., Von Figura, K. and Van Leuven, F. (1998) Deficiency of presenilin-1 inhibits the normal cleavage of amyloid precursor protein. *Nature*, **391**, 387-390.
53 Musa, A., Lehrach, H. and Russo, V.A. (2001) Distinct expression patterns of two zebrafish homologues of the human APP gene during embryonic development. *Dev Genes Evol*, **211**, 563-567.
54 Gong, P., Vetrivel, K.S., Nguyen, P.D., Meckler, X., Cheng, H., Kounnas, M.Z., Wagner, S.L., Parent, A.T. and Thinakaran, G. (2010) Mutation analysis of the presenilin 1 N-terminal domain reveals a broad spectrum of gamma-secretase activity toward amyloid precursor protein and other substrates. *J Biol Chem*, **285**, 38042-38052.
55 Fraering, P.C., Ye, W., LaVoie, M.J., Ostaszewski, B.L., Selkoe, D.J. and Wolfe, M.S. (2005) gamma-Secretase substrate selectivity can be modulated directly via interaction with a nucleotide-binding site. *J Biol Chem*, **280**, 41987-41996.

56 Mastrangelo, P., Mathews, P.M., Chishti, M.A., Schmidt, S.D., Gu, Y., Yang, J., Mazzella, M.J., Coomaraswamy, J., Horne, P., Strome, B. *et al.* (2005) Dissociated phenotypes in presenilin transgenic mice define functionally distinct gamma-secretases. *Proc Natl Acad Sci U S A*, **102**, 8972-8977.
57 Serneels, L., Van Biervliet, J., Craessaerts, K., Dejaegere, T., Horre, K., Van Houtvin, T., Esselmann, H., Paul, S., Schafer, M.K., Berezovska, O. *et al.* (2009) gamma-Secretase heterogeneity in the Aph1 subunit: relevance for Alzheimer's disease. *Science*, **324**, 639-642.
58 Podlisny, M.B., Citron, M., Amarante, P., Sherrington, R., Xia, W., Zhang, J., Diehl, T., Levesque, G., Fraser, P., Haass, C. *et al.* (1997) Presenilin proteins undergo heterogeneous endoproteolysis between Thr291 and Ala299 and occur as stable N- and C-terminal fragments in normal and Alzheimer brain tissue. *Neurobiol Dis*, **3**, 325-337.
59 Kim, H., Ki, H., Park, H.S. and Kim, K. (2005) Presenilin-1 D257A and D385A mutants fail to cleave Notch in their endoproteolyzed forms, but only presenilin-1 D385A mutant can restore its gamma-secretase activity with the compensatory overexpression of normal C-terminal fragment. *J Biol Chem*, **280**, 22462-22472.
60 Capell, A., Grunberg, J., Pesold, B., Diehlmann, A., Citron, M., Nixon, R., Beyreuther, K., Selkoe, D.J. and Haass, C. (1998) The proteolytic fragments of the Alzheimer's disease-associated presenilin-1 form heterodimers and occur as a 100-150-kDa molecular mass complex. *J Biol Chem*, **273**, 3205-3211.
61 Zhang, Y.B., Howitt, J., McCorkle, S., Lawrence, P., Springer, K. and Freimuth, P. (2004) Protein aggregation during overexpression limited by peptide extensions with large net negative charge. *Protein Expr Purif*, **36**, 207-216.
62 Ro, H., Soun, K., Kim, E.J. and Rhee, M. (2004) Novel vector systems optimized for injecting in vitro-synthesized mRNA into zebrafish embryos. *Mol Cells*, **17**, 373-376.
63 De Jonghe, C., Cruts, M., Rogaeva, E.A., Tysoe, C., Singleton, A., Vanderstichele, H., Meschino, W., Dermaut, B., Vanderhoeven, I., Backhovens, H. *et al.* (1999) Aberrant splicing in the presenilin-1 intron 4 mutation causes presenile Alzheimer's disease by increased Abeta42 secretion. *Hum Mol Genet*, **8**, 1529-1540.
64 Schon, E.A. and Area-Gomez, E. (2010) Is Alzheimer's disease a disorder of mitochondria-associated membranes? *Journal of Alzheimer's disease : JAD*, **20 Suppl 2**, S281-292.
65 Laudon, H., Karlstrom, H., Mathews, P.M., Farmery, M.R., Gandy, S.E., Lundkvist, J., Lendahl, U. and Naslund, J. (2004) Functional domains in presenilin 1: the Tyr-288 residue controls gamma-secretase activity and endoproteolysis. *J Biol Chem*, **279**, 23925-23932.
66 Wolfe, M.S., Xia, W., Ostaszewski, B.L., Diehl, T.S., Kimberly, W.T. and Selkoe, D.J. (1999) Two transmembrane aspartates in presenilin-1 required for presenilin endoproteolysis and gamma-secretase activity. *Nature*, **398**, 513-517.
67 Raux, G., Gantier, R., Thomas-Anterion, C., Boulliat, J., Verpillat, P., Hannequin, D., Brice, A., Frebourg, T. and Campion, D. (2000) Dementia with prominent frontotemporal features associated with L113P presenilin 1 mutation. *Neurology*, **55**, 1577-1578.
68 Pratt, E.B., Wentzell, J.S., Maxson, J.E., Courter, L., Hazelett, D. and Christian, J.L. (2011) The cell giveth and the cell taketh away: an overview of Notch pathway

activation by endocytic trafficking of ligands and receptors. *Acta Histochem*, **113**, 248-255.
69 Cheng, H.T. and Kopan, R. (2005) The role of Notch signaling in specification of podocyte and proximal tubules within the developing mouse kidney. *Kidney Int*, **68**, 1951-1952.
70 Li, S., Zhang, X., Wang, Y., Ji, H., Du, Y. and Liu, H. (2012) DAPT protects brain against cerebral ischemia by down-regulating the expression of Notch 1 and Nuclear factor kappa B in rats. *Neurol Sci*.
71 Kitzmann, M., Bonnieu, A., Duret, C., Vernus, B., Barro, M., Laoudj-Chenivesse, D., Verdi, J.M. and Carnac, G. (2006) Inhibition of Notch signaling induces myotube hypertrophy by recruiting a subpopulation of reserve cells. *J Cell Physiol*, **208**, 538-548.
72 Shen, J., Bronson, R.T., Chen, D.F., Xia, W., Selkoe, D.J. and Tonegawa, S. (1997) Skeletal and CNS defects in Presenilin-1-deficient mice. *Cell*, **89**, 629-639.
73 Wong, P.C., Zheng, H., Chen, H., Becher, M.W., Sirinathsinghji, D.J., Trumbauer, M.E., Chen, H.Y., Price, D.L., Van der Ploeg, L.H. and Sisodia, S.S. (1997) Presenilin 1 is required for Notch1 and DII1 expression in the paraxial mesoderm. *Nature*, **387**, 288-292.
74 Einhauer, A. and Jungbauer, A. (2001) The FLAG peptide, a versatile fusion tag for the purification of recombinant proteins. *J Biochem Biophys Methods*, **49**, 455-465.
75 Kozak, M. (1987) An analysis of 5'-noncoding sequences from 699 vertebrate messenger RNAs. *Nucleic Acids Res*, **15**, 8125-8148.
76 Field, J., Nikawa, J., Broek, D., MacDonald, B., Rodgers, L., Wilson, I.A., Lerner, R.A. and Wigler, M. (1988) Purification of a RAS-responsive adenylyl cyclase complex from Saccharomyces cerevisiae by use of an epitope addition method. *Mol Cell Biol*, **8**, 2159-2165.
77 Nornes, S., Groth, C., Camp, E., Ey, P., Lardelli, M., McCarty, R. and Tamme, R. (2003) Developmental control of Presenilin1 expression, endoproteolysis, and interaction in zebrafish embryos. *Exp Cell Res*, **289**, 124-132.

Supplemental Data

Supplemental Data Figure 1

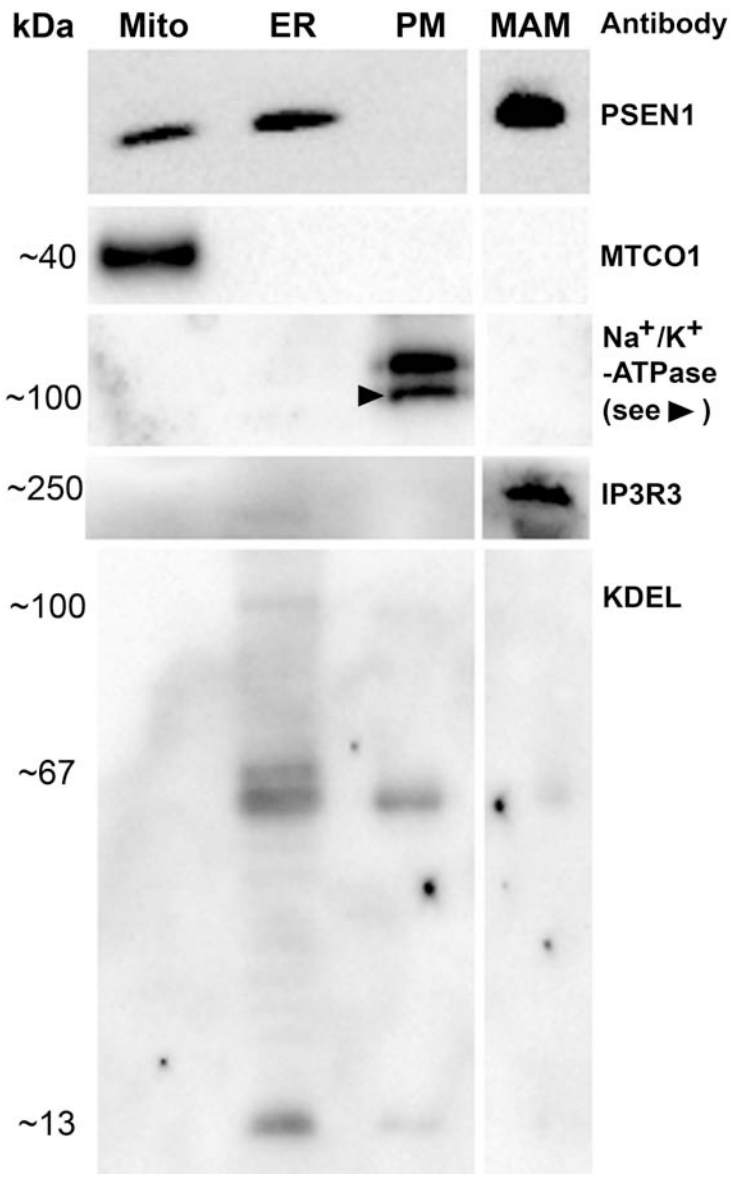

Fractionation of mouse brain cellular membranes into plasma membrane (PM), mitochondrial membranes (Mito), mitochondrial associated membranes (MAM) and non-MAM endoplasmic reticulum (ER). This was performed according to the procedure described by Area Gomez et al. 2009 *Am. J. Pathol*. 175: 1810-1816. Fractions were identified by their physical behaviour during the fractionation procedure and confirmed

by western immunoblotting using antibodies recognising proteins MTCO1 (in mitochondria, Abcam, Cambridge, UK, Cat. No. ab14705), Na+/K+-ATPase (in PM, Abcam, Cat. No. ab7671), IP3R3 (in MAM, Millipore, Temecula, USA, Cat. No. AB9076) and KDEL (predominantly in non-MAM ER, Abcam, ab12223). Secondary antibodies were donkey anti-mouse Ig, (Rockland, Gilbertsville, USA, Cat. No. 610-703-124) and donkey, anti-rabbit Ig, (Rockland, 611-703-127). Western immunoblotting used the conditions recommended by the antibody providers.

Supplemental Data Figure 2

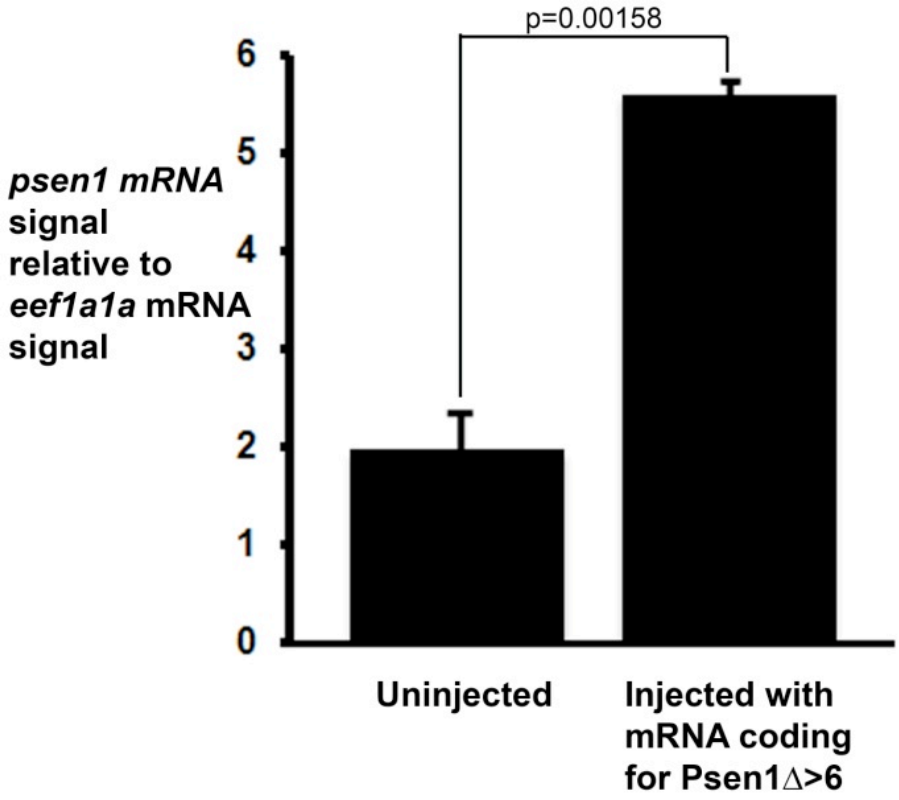

qPCR comparison of total *psen1* transcript levels (spliced endogenous mRNA plus injected synthetic mRNA encoding truncated Psen1 protein, Psen1D>6) in embryos at 24 hpf. Measurement of the *psen1* qPCR signal was relative to the signal from qPCR of *eef1a1a*. While comparisons between *psen1*- and *eef1a1a*-qPCR reactions cannot be informative in terms of relative quantities of mRNA, the ratio of these relative qPCR signals in uninjected versus injected embryos indicates less than a three-fold difference in total *psen1* mRNA levels between uninjected and injected embryos.

Supplemental Data Figure 3

Sequences showing predicted premature termination codons (PTCs) in *psen1* transcripts with altered splicing due to injection of morpholinos MoPsen15Ac and MoPsen16Ac. Exonic sequence is shown in **bold** type. Intronic sequence is *italicised*. Premature stop codons are shown in red. Details of PTCs arising from other morpholinos affecting *psen1* splicing can be found in the supplemental data accompanying Nornes et al. 2008 *Hum. Mol. Genet.* 17: 402-412.

Injection of MoPsen15Ac causes retention of intron 4 and a premature stop codon early in intron 4:

Exon 4
CTA AAT GAT GGG ATG GAC ACC AGC CGG CAC ACA AGC AGC ACC

GCG GCG CCG CCC AGC CGT AAT GAG GTG GAG CTG AAC GGG CAG

CCG CCC ACC GCT CCG CCC CCG CAG GTG GTC ACA GAC AGT GAG

GAA GAC GAG GAC GAG GAG CTC ACT CTC AAA TAT GGG GCG AAG

CAC GTC ATC ATG CTG TTC ATT CCC GTC ACG CTC TGC ATG GTG

GTG GTG GTG GCG ACC ATC AAA TCT GTC AGC TTC TAC ACA CAG
Intron 4
AAG GAC GGA CAG CAG CTG ***TGA*** *GGA GCT CCC TAA AAA*

Injection of MoPsen16Ac causes retention of intron 5 with the open reading frame continuing (but frameshifted) through exon 6 with a premature stop codon early in exon 7:

Exon 5
ATC TAC ACC CCG TTT CGT GAG GAC ACG GAG ACG GTG GGT CAG

CGA GCT CTG CAC TCC ATG CTC AAC GCC ATC ATC ATG ATC AGT

GTG ATC GTG GTC ATG ACC CTG GTG CTG GTG GTG CTC TAC AAG
Intron 5
TAC AGA TGC TAC AAG *GTT TGC TCA CAT GAT GCT GAA TAC TCA*

TCA GCT ATT CTT TTT GCA CGC ATT ACA GAT TTG TTT TTT TTT
Exon 6
*TTT GCA G***GT GAT TCA AGC CTG GCT GTT CTT CTC CAA CCT CCT**
Exon 7
CCT GCT CTT CTT TTT CTC CTT AAT TTA TTT GGG GGA AGT GTT

CAA GAC GTA TAA CGT

Supplemental Table 1: Notch signaling assays

Assays of Notch signaling by comparison of relative *neurogenin1* expression in the trunk region of 24 hpf embryos. The procedure followed in this assay is described in Nornes et al. 2008 *Hum. Mol. Genet.* 17: 402-412.

* human hPSEN1Δ>7 into which the P242LfsX11 mutation has been introduced.

Injection	Embryos counted		Change in *neurog1* expression	Chi-square value	p-value
	Same	**Changed**			
Effects of injection of mRNAs coding for truncated forms of zebrafish Psen1					
mRNA Psen1Δ>4 mRNA stop (-ve control)	133 140	49 10	lighter	23.189	0.00000922
mRNA Psen1 Δ>5 mRNA stop (-ve control)	115 90	3 3	none	0.088	ns
mRNA Psen1 Δ>6 mRNA stop (-ve control)	84 83	39 10	darker	13.26	0.000027142
mRNA Psen1 Δ>7 mRNA stop (-ve control)	115 126	61 4	darker	44.579	0 (p is very small) very significant
mRNA Psen1 Δ>8 mRNA stop (-ve control)	73 47	6 5	none	0.166	ns
mRNA Psen1NTF mRNA stop (-ve control)	92 96	42 49	none	0.19	ns
Analysis of the dependence of Psen1 Δ>4's ability to increase γ-secretase activity on the presence of endogenous Psen1 or Psen2					
mRNA Psen1 Δ>4 and Psen1 blocked (MoPsen1Tln) mRNA stop (-ve control) and Psen1 **not** blocked	12 24	24 1	darker	23.955	9.9e-7
mRNA Psen1 Δ>4 and Psen1 blocked (MoPsen1Tln) mRNA stop (-ve control) and Psen1 blocked (MoPsen1Tln)	44 41	16 11	none	0.463	ns
mRNA Psen1 Δ>4 and Psen2 blocked (MoPsen2Tln) mRNA stop (-ve control) and Psen2 **not** blocked	4 19	20 4	darker	20.437	0.00000616
mRNA Psen1 Δ>4 and Psen2 blocked (MoPsen2Tln) mRNA stop (-ve control) and Psen2 blocked (MoPsen2Tln)	14 49	42 6	lighter	46.439	0 (p is very small) very significant
Effects of injection of mRNAs coding for truncated forms of human PSEN1					
mRNA PSEN1 Δ>4 mRNA stop (-ve control)	93 138	34 14	lighter	16.17	0.00030813
mRNA PSEN1 Δ>5 mRNA stop (-ve control)	90 86	6 5	none	0.048	ns
mRNA PSEN1 Δ>6 mRNA stop (-ve control)	90 100	34 3	darker	25.039	5.60E-07
mRNA PSEN1 Δ>7 mRNA stop (-ve control)	80 79	48 4	darker	28.957	7.00E-08
mRNA PSEN1 Δ>8 mRNA stop (-ve control)	83 84	9 8	none	0.87	ns
mRNA PSEN1NTF mRNA stop (-ve control)	127 78	26 17	none	0.033	ns
mRNA PSEN1AcneInversa* mRNA stop (-ve control)	77 73	25 3	lighter	13.891	0.00019372

Supplementary Data Table 2: Assays of zebrafish Appa cleavage at 12 hpf after injection of mRNAs encoding truncations of the NTF of zebrafish Psen1

To assay γ-secretase activity we injected a mixture of mRNAs encoding AppaC86::dGFP and free GFP (that is not subject to γ-secretase cleavage). We then measured the relative amounts* of the two proteins on western immunoblots. (Greater γ-secretase activity results in a lower ratio of AppaC86::GFP to free GFP.) Development of this assay is described in detail elsewhere (Wilson & Lardelli, Journal of Alzheimer's Disease, 2013, DOI 10.3233/JAD-130332, in press).

* The intensity of each western immunoblot band, either AppaC86::dGFP or free GFP, was quantified on a Typhoon trio imaging device (Amersham Bioscience Corp., Piscataway, NJ, USA).

Variations in relative Appa cleavage due to various treatments are observed by comparing the AppaC86:dGFP bands on blots after normalisation. To normalise the data, the intensities of the free GFP standards in each replicate set were normalised to the mean of these intensities and then the AppaC86::dGFP intensity values were adjusted accordingly. Fold changes for the AppaC86::dGFP values were then calculated against the "untreated" sample and these values from the replicate sets were included in the statistical analysis.

Assay of Appa cleavage at 12 hpf after injection of mRNAs encoding truncations of the NTF of zebrafish Psen1.

	Intensity of AppaC86::dGFP	Intensity of free GFP standard	Normalised	Fold change relative to untreated AppaC86::dGFP
Replicate 1				
Psen1Δ>4	0.94	18.59	1.012582869	0.470415235
Psen1Δ>5	3.62	21.21	3.428727594	1.592882663
Psen1Δ>6	2.16	20.73	2.097336054	0.974358606
Psen1Δ>7	1.68	19.28	1.752181347	0.814010216
Psen1Δ>8	1.46	19.11	1.535049363	0.713137294
Psen1NTF	2.19	21.7	2.021018146	0.938903627
Stop	2.55	23.64	2.107677458	0.979162909
Untreated	2.62	23.74	2.152529921	1
DAPT	2.73	13.31	3.656311842	1.69861139
Mean		20.14555556		
Replicate 2				
Psen1Δ>4	1.03	17	1.122578074	0.383784994
Psen1Δ>5	4.07	14.91	4.891214681	1.672199775
Psen1Δ>6	3.86	22.2	3.132360954	1.070885992
Psen1Δ>7	3.59	21.73	3.003589911	1.026861976
Psen1Δ>8	3.44	21.37	2.944391172	1.006623217
Psen1NTF	3.49	20.4	3.168424246	1.083154792
Stop	3.31	20.48	2.990833383	1.022500797
Untreated	3.92	23.42	2.925018143	1
DAPT	3.32	6.6	5.466910951	1.869017792
Mean		18.67888889		
Replicate 3				
Psen1Δ>4	1.04	24.92	1.125382664	0.531935965
Psen1Δ>5	3.02	22.95	3.487077842	1.648241247
Psen1Δ>6	2.92	29.32	2.686486044	1.269824566
Psen1Δ>7	2.93	31.46	2.464730294	1.165007011
Psen1Δ>8	2.13	25.17	2.2852562	1.080174777
Psen1NTF	2.63	29.38	2.413865106	1.140964503
Stop	2.04	23.26	2.332215765	1.10237121
Untreated	2.36	29.96	2.11563559	1
DAPT	4.29	27.92	4.168150937	1.97016488
Mean		27.14888889		

Mean of Replicates 1,2, and 3

In order to graph and compare each individual sample, the mean of their three replicates has been calculated with the standard error of the mean.

Replicate	Mean of Fold change relative to untreated AppaC86::dGFP	Standard Error of the Mean
Psen1Δ>4	0.46	0.04359
Psen1Δ>5	1.637	0.02404
Psen1Δ>6	1.103	0.08819
Psen1Δ>7	1	0.1044
Psen1Δ>8	0.9333	0.1135
Psen1NTF	1.033	0.03528
Stop	1.053	0.05925
DAPT	1.847	0.07881

Further Statistical Analysis

Paired t-test	**p-value**
Psen1Δ>4	0.0065
Psen1Δ>5	0.0014
Psen1Δ>6	0.362
Psen1Δ>7	1
Psen1Δ>8	0.6164
Psen1NTF	0.4631
Stop	0.4774
DAPT	0.0086

One-way analysis of variance

The statistical significance of changes in relative intensity were assessed by one-way ANOVA with the Bonferroni Post Hoc test.

	Mean Diff.	**t**	**Significant?P < 0.01?**	**Summary**	**99% CI of diff**
Psen1Δ>4 vs Untreated	0.54	5.4	Yes	**	0.09013 to 0.9899
Psen1Δ>5 vs Untreated	0.6367	6.367	Yes	***	0.1868 to 1.087
Psen1Δ>6 vs Untreated	0.1033	1.033	No	ns	-0.3465 to 0.5532
Psen1Δ>7 vs Untreated	0	0	No	ns	-0.4499 to 0.4499
Psen1Δ>8 vs Untreated	-0.06667	0.6667	No	ns	-0.5165 to 0.3832
Psen1NTF vs Untreated	-0.05333	0.5333	No	ns	-0.5032 to 0.3965
Stop vs Untreated	0.03333	0.3333	No	ns	-0.4165 to 0.4832
DAPT vs Untreated	0.8467	8.467	Yes	****	0.3968 to 1.297

Assay of Appa cleavage at 12 hpf after injection of Mo's blocking endogenous expression of zebrafish Psen1 and Psen2.

	Intensity of AppaC86::dGFP	Intensity of free GFP standard	Normalised	Fold change relative to untreated AppaC86::dGFP
Replicate 1				
MoPsen15Ac	3.44	6.15	3.992027908	0.652647183
MoPsen17Ac	7.32	7.91	6.735998787	1.101252479
MoPsen18Ac	4.36	7.32	4.363306537	0.713346646
MoPsen19Ac	5.17	7.17	5.279783103	0.863179228
Untreated	6.31	7.55	6.116670711	1
DAPT	11.29	8.23	9.896088275	1.617888022
MoControl	5.68	7.05	5.893656909	0.963540002
GFP control 1		6.79		
GFP control 2		7.76		
Mean		7.325555556		
Replicate 2				
MoPsen15Ac	4.28	28.67	4.418825559	0.293430552
MoPsen17Ac	17.25	29.76	17.17496625	1.140497572
MoPsen18Ac	10.74	27.43	11.53780786	0.766164058
MoPsen19Ac	13.37	29.12	13.60062097	0.903144435
Untreated	15.59	30.64	15.05918704	1
DAPT	25.41	30.41	24.74206802	1.642988294
MoControl	15.09	30.89	14.44889568	0.959473818
GFP control 1		29.36		
GFP control 2		30.4		
Mean		29.63111111		

Replicate 3

MoPsen15Ac	8.87	11.61	9.357741702	0.460772675
MoPsen17Ac	19.79	13.13	18.42973953	0.907475399
MoPsen18Ac	17.68	11.89	18.2492394	0.898587621
MoPsen19Ac	16.8	13.37	15.31706611	0.7542082
Untreated	18.66	11.2	20.30880347	1
DAPT	36.82	12.97	34.76870941	1.712001865
MoControl	17.13	11.42	18.33686172	0.90290212
GFP control 1		12.93		
GFP control 2		12.05		
Mean		12.28555556		

Mean of Replicates 1,2, and 3

In order to graph and compare each individual sample, the mean of their three replicates has been calculated with the standard error of the mean.

Replicates	Mean of Fold change relative to untreated AppaC86::dGFP	Standard Error of the Mean
MoPsen15Ac	0.4667	0.104
MoPsen17Ac	1.05	0.07095
MoPsen18Ac	0.7933	0.05608
MoPsen19Ac	0.8367	0.04485
DAPT	1.657	0.02728
MoControl	0.94	0.02

Further Statistical Analysis

Paired t-test	p-value
MoPsen15Ac	0.036
MoPsen17Ac	0.554
MoPsen18Ac	0.0664
MoPsen19Ac	0.0985
DAPT	0.0017
MoControl	0.0955

Bonferroni's Multiple Comparison Test	**Mean Diff.**	**t**	**Significant? P < 0.05?**	**Summary**	**95% CI of diff**
MoPsen15Ac vs Untreated	-0.5333	5.639	Yes	**	-0.8870 to -0.1796
MoPsen17Ac vs Untreated	0.05	0.5287	No	ns	-0.3037 to 0.4037
MoPsen18Ac vs Untreated	-0.2067	2.185	No	ns	-0.5604 to 0.1470
MoPsen19Ac vs Untreated	-0.1633	1.727	No	ns	-0.5170 to 0.1904
DAPT vs Untreated	-0.6567	6.943	Yes	****	-1.010 to -0.3030
MoControl vs Untreated	0.06	0.6344	No	ns	-0.2937 to 0.4137

ns, not significant, i.e. p ≥ 0.01
*, p<0.05
**, p < 0.01
***, p < 0.001
****, p < 0.0001

Assay of Appa cleavage at 12 hpf after injection of mRNA expressing zfPsen1 truncations after exon 4 and Mo's blocking endogenous expression of zebrafish Psen1 and Psen2.

	Average Intensity of AppaC86::dGFP	Avergage intensity of free GFP standard	Normalised	Fold change relative to untreated AppaC86::dGFP
Psen1Δ>4	7.29	26.41	7.851749083	0.457342911
Psen1Δ>4 + MoPsen1Tln	25.11	30.57	23.39446444	1.362663574
Psen1Δ>4 + MoPsen2Tln	12.53	30.99	11.4900297	0.669262807
MoControl	17.47	28.49	17.54631487	1.022024855
Untreated	16.83	28.04	17.16818801	1
DAPT	32.08	27.19	33.67755373	1.961625403
Mean		28.615	18.52138331	

Replicate 2

Psen1Δ>4	1.73	23.94	1.789767442	0.511277687
Psen1Δ>4 + MoPsen1Tln	4.7	23.05	5.031066003	1.43721007
Psen1Δ>4 + MoPsen2Tln	1.17	24.23	1.196737465	0.341868529
MoControl	3.64	27.71	3.212340368	0.91765998
Untreated	3.44	24.36	3.500578035	1
DAPT	5.92	25.49	5.754472375	1.643863476
Mean		24.79666667	3.414160281	

Replicate 3

Psen1Δ>4	2.42	10.5	2.478841567	0.330522993
Psen1Δ>4 + MoPsen1Tln	11.23	9.79	12.2439523	1.632580238
Psen1Δ>4 + MoPsen2Tln	3.95	12.85	3.183490785	0.424479287
MoControl	8.21	10.43	8.463026173	1.128440306
Untreated	6.56	9.22	7.499755304	1
DAPT	15.19	11.78	13.75263125	1.833743995
Mean		10.76166667		

Mean of Replicates 1,2, and 3

In order to graph and compare each individual sample, the mean of their three replicates has been calculated with the standard error of the mean.

Replicates	Mean of Fold change relative to untreated AppaC86::dGFP	Standard Error of the Mean
Psen1Δ>4	0.4333	0.05364
Psen1Δ>4 + MoPsen1Tln	1.477	0.08007
Psen1Δ>4 + MoPsen2Tln	0.4767	0.09939
MoControl	1.023	0.06064
Untreated	1	0
DAPT	1.81	0.09292

Further Statistical Analysis

Paired t-test	p-value
Psen1Δ>4	0.0088
Psen1Δ>4 + MoPsen1Tln	0.0271
Psen1Δ>4 + MoPsen2Tln	0.0342
MoControl	0.7375
DAPT	0.0129

One-way analysis of variance

The statistical significance of changes in relative intensity were assessed by one-way ANOVA with the Bonferroni Post Hoc test.

Bonferroni's Multiple Comparison Test	Mean Diff.	t	Significant? P < 0.05?	Summary	95% CI of diff
Psen1Δ>4 vs Psen1Δ>4 + MoPsen1Tln	-1.043	10.19	Yes	****	-1.417 to -0.6696
Psen1Δ>4 vs Psen1Δ>4 + MoPsen2Tln	-0.04333	0.423	No	ns	-0.4171 to 0.3304
Psen1Δ>4 vs Untreated	-0.5667	5.532	Yes	**	-0.9404 to -0.1929
Psen1Δ>4 vs DAPT	-1.377	13.44	Yes	****	-1.750 to -1.003
Psen1Δ>4 vs MoControl	-0.59	5.76	Yes	**	-0.9638 to -0.2162
Psen1Δ>4 + MoPsen1Tln vs Psen1Δ>4 + MoPsen2Tln	1	9.762	Yes	****	0.6262 to 1.374
Psen1Δ>4 + MoPsen1Tln vs Untreated	0.4767	4.653	Yes	**	0.1029 to 0.8504
Psen1Δ>4 + MoPsen1Tln vs DAPT	-0.3333	3.254	No	ns	-0.7071 to 0.04044
Psen1Δ>4 + MoPsen1Tln vs MoControl	0.4533	4.426	Yes	*	0.07956 to 0.8271
Psen1Δ>4 + MoPsen2Tln vs Untreated	-0.5233	5.109	Yes	**	-0.8971 to -0.1496
Psen1Δ>4 + MoPsen2Tln vs DAPT	-1.333	13.02	Yes	****	-1.707 to -0.9596
Psen1Δ>4 + MoPsen2Tln vs MoControl	-0.5467	5.337	Yes	**	-0.9204 to -0.1729
Untreated vs DAPT	-0.81	7.908	Yes	****	-1.184 to -0.4362
Untreated vs MoControl	-0.02333	0.2278	No	ns	-0.3971 to 0.3504
DAPT vs MoControl	0.7867	7.68	Yes	****	0.4129 to 1.160

ns, not significant, i.e. p ≥ 0.01
*, p<0.05
**, p < 0.01
***, p < 0.001
****, p < 0.0001

Assay of Appa cleavage at 12 hpf after injection of mRNAs encoding truncations of the NTF of human PSEN1.

	Average Intensity of AppaC86::dGFP	Average intensity of free GFP standard	Normalised	Fold change relative to untreated AppaC86::dGFP
Replicate 1				
hPSEN1Δ>4	0.92	12.12	0.932069122	0.403240907
hPSEN1Δ>5	4.69	11.9	4.835541482	1.935204067
hPSEN1Δ>6	2.42	12.27	2.422189451	0.96937042
hPSEN1Δ>7	3.01	12.93	2.850962635	1.140967254
hPSEN1Δ>8	3.07	13.03	2.882794716	1.153706587
hPSEN1NTF	3.04	14.07	2.597188094	1.039405614
Untreated	2.3	11.22	2.498724328	1
Stop	2.37	11.33	2.553544739	1.021939359
DAPT	4.46	11.66	4.685562291	1.875181763
Mean		12.28111111		
Replicate 2				
hPSEN1Δ>4	0.76	11.4	0.847155061	0.524386531
hPSEN1Δ>5	2.98	14.01	2.7177168	1.682258835
hPSEN1Δ>6	1.3	8.6	1.731762879	1.07195621
hPSEN1Δ>7	1.79	14.72	1.533756148	0.949390617
hPSEN1Δ>8	1.22	14.69	1.048195703	0.648830107
hPSEN1NTF	1.74	14.5	1.520641988	0.94127299
Untreated	2.09	15.8	1.615516438	1
DAPT	2.77	10.37	3.309228579	2.048402914
stop	1.56	11.8	1.690437484	0.955679493
Mean		12.87666667		
Replicate 3				
hPSEN1Δ>4	0.45	7.63	0.464951429	0.443247705
hPSEN1Δ>5	2.24	8.97	1.934101084	1.843818113
hPSEN1Δ>6	0.84	6.62	0.975407574	0.929875986
hPSEN1Δ>7	1.04	7.67	1.069283401	1.019369732
hPSEN1Δ>8	1.14	8.43	1.062320146	1.012731519
hPSEN1NTF	1.27	8.21	1.21886386	1.161967842
Untreated	1.05	7.9	1.048965226	1
DAPT	1.64	6.91	1.844105308	1.7580233
Stop	1.29	8.69	1.159601577	1.105471896
Mean		7.892222222		

Mean of Replicates 1,2, and 3

In order to graph and compare each individual sample, the mean of their three replicates has been calculated with the standard error of the mean.

Replicates	Mean of Fold change relative to untreated AppaC86::dGFP	Standard Error of the Mean
hPSEN1Δ>4	0.4533	0.03528
hPSEN1Δ>5	1.82	0.07572
hPSEN1Δ>6	0.99	0.04163
hPSEN1Δ>7	1.037	0.05548
hPSEN1Δ>8	0.9367	0.1489
hPSEN1NTF	1.047	0.0636
DAPT	1.895	0.08431
Stop	1.03	0.04359

Further Statistical Analysis

Paired t-test	**p-value**
hPSEN1Δ>4	0.0041
hPSEN1Δ>5	0.0084
hPSEN1Δ>6	0.8326
hPSEN1Δ>7	0.5766
hPSEN1Δ>8	0.712
hPSEN1NTF	0.5394
Stop	0.5624
DAPT	0.0092

One-way analysis of variance

The statistical significance of changes in relative intensity were assessed by one-way ANOVA with the Bonferroni Post Hoc test.

Bonferroni's Multiple Comparison Test	Mean Diff.	t	Significant? P < 0.01?	Summary	99% CI of diff
hPSEN1Δ>4 vs Untreated	-0.5467	5.348	Yes	**	-1.007 to -0.08681
hPSEN1Δ>5 vs Untreated	0.82	8.022	Yes	****	0.3601 to 1.280
hPSEN1Δ>6 vs Untreated	-0.01	0.09783	No	ns	-0.4699 to 0.4499
hPSEN1Δ>7 vs Untreated	0.03667	0.3587	No	ns	-0.4232 to 0.4965
hPSEN1Δ>8 vs Untreated	-0.06333	0.6196	No	ns	-0.5232 to 0.3965
hPSEN1NTF vs Untreated	0.04667	0.4565	No	ns	-0.4132 to 0.5065
Stop vs Untreated	0.03	0.2935	No	ns	-0.4299 to 0.4899
DAPT vs Untreated	-0.895	8.756	Yes	****	-1.355 to -0.4351

Assay of Appa cleavage at 12 hpf after injection of mRNAs encoding the *P242LfsX11* mutation of the NTF of human Psen1.

	Average Intensity of AppaC86::dGFP	Avergage intensity of free GFP standard	Normalised	Fold change relative to untreated AppaC86::dGFP
Replicate 1				
hPSEN1-P242LfsX11	27.16	103.35	26.16567703	0.924274759
stop	29.79	105.9	27.93746239	0.986861196
Untreated	26.42	92.57	28.30941424	1
DAPT	49.16	96.98	50.50117553	1.783900405
Mean		99.7		
Replicate 2				
hPSEN1-P242LfsX11	3.4	18.81	2.843674606	0.907826966
stop	3.29	15.77	3.370392824	1.075978766
Untreated	3.36	17.26	3.132397154	1
DAPT	5.04	12.82	6.082919889	1.941937624
Mean		16.165		
Replicate 3				
hPSEN1-P242LfsX11	3.54	16	3.249737954	1.056807049
stop	3.63	15.14	3.543469146	1.152327733
Untreated	3.41	16.24	3.075053254	1
DAPT	5.02	11.77	6.044368555	1.965614269
Mean		14.7875		

Mean of Replicates 1,2, and 3

In order to graph and compare each individual sample, the mean of their three replicates has been calculated with the standard error of the mean.

Replicates	Mean of Fold change relative to untreated C86	Standard Error of the Mean
hPSEN1-P242LfsX11	0.9633	0.04842
stop	1.073	0.04631
Untreated	1	0
DAPT	1.897	0.05897

Further Statistical Analysis

Pair t-test	p-value
hPSEN1-P242LfsX11	0.5279
stop	0.2541
DAPT	0.0043

One-way analysis of variance

The statistical significance of changes in relative intensity were assessed by one-way ANOVA with the Bonferroni Post Hoc test.

Bonferroni's Multiple Comparison Test	Mean Diff.	t	Significant? P < 0.01?	Summary	99% CI of diff
hPSEN1-P242LfsX11 vs Untreated	-0.03667	0.581	No	ns	-0.3295 to 0.2562
STOP vs Untreated	0.07333	1.162	No	ns	-0.2195 to 0.3662
DAPT vs Untreated	-0.8967	14.21	Yes	****	-1.190 to -0.6038

ns, not significant, i.e. p ≥ 0.01
**, p < 0.01
***, p < 0.001
****, p < 0.0001

CHAPTER IV

Research Paper III

HMGA1 controls an ancient alternative splicing mechanism that truncates PRESENILIN proteins under hypoxia to boost γ-secretase activity and suppress the unfolded protein response.

Hani Moussavi-Nik[1], Morgan Newman[1], Lachlan Wilson[1], Esmaeil Ebrahimie[1], Simon Wells[1], Mark Van Der Hoek[7], Giuseppe Verdile[2,3], Gavin Chapman[5,6], Sharon Pursglove[5,6], Louise O'Keefe[1], Ralph Martins [2,3,4] and Michael Lardelli[1]

[1]Discipline of Genetics, School of Molecular and Biomedical Science, The University of Adelaide, SA 5005, Australia, [2]Centre of Excellence for Alzheimer's Disease Research and Care, School of Exercise, Biomedical and Health, [3]Sir James McCusker Alzheimer's Disease Sciences, Edith Cowan University, Joondalup, WA 6027, Australia, [5] Development Biology Program, Victor Chang Cardiac Research Institute, Sydney, NSW, Australia, [6]St. Vincent's Clinical School, University of New South Wales, Sydney, NSW, Australia, [7]Adelaide Microarray Centre, IMVS Main Building, Frome Road, Adelaide, SA 5000, Australia.

STATEMENT OF AUTHORSHIP

HMGA1 controls an ancient alternative splicing mechanism that truncates PRESENILIN proteins under hypoxia to boost γ-secretase activity and suppress the unfolded protein response.

Unsubmitted Manuscript.

Hani Moussavi-Nik (First Author)

- Development of PCR primers and RT- and Q- PCR analysis on:
    - Hypoxia and chemical mimicry of hypoxia treated morpholino and mRNA injected zebrafish embryos
    - Hypoxia and chemical mimicry of hypoxia treated guinea pig cells
- Bioinfomatic analysis of PS2V binding site in different species.
- qRT-PCR of UPR related genes.

Certification that the statement of contribution is accurate and permission is given for the inclusion of the paper in the thesis

Signed…… ……Date

Morgan Newman (Co-author)

- Editing of paper
- Injection of HMGA1 morpholino and mRNA.
- Development and injection of UPR assay
- Zebrafish Notch assay (Except where noted)

Certification that the statement of contribution is accurate and permission is given for the inclusion of the paper in the thesis

Signed…… ……Date

Lachlan Wilson (Candidate/Co-author)

- Performed all Appa assay experiments, statistical analysis and injections.
- Performed all HMW western blot analysis and corresponding injections.
- Performed all preliminary IP experiments, injections and preparations of IP samples.
- Performed zebrafish Notch assay on K115Efx10.

Certification that the statement of contribution is accurate and permission is given for the inclusion of the paper in the thesis

Signed

…… ……Date……

Esmaeil Ebrahimie (Co-author)

- Microarray data analysis and gene expression network construction

Certification that the statement of contribution is accurate and permission is given for the inclusion of the paper in the thesis

Signed…… …….Date

Simon Wells (Co-author)

- Preliminary work on Notch assay analysis.

Certification that the statement of contribution is accurate and permission is given for the inclusion of the paper in the thesis

Signed…… …….Date

Mark Van Der Hoek (Co-author)

- Performed microarray and preliminary analysis

Certification that the statement of contribution is accurate and permission is given for the inclusion of the paper in the thesis

Signed…… …….Date

Giuseppe Verdile (co-author)

- Human cell culture experiments on Notch and APP (preliminary and not in the paper).
- Analysis of human PS2V in human cell culture.

Certification that the statement of contribution is accurate and permission is given for the inclusion of the paper in the thesis

Signed

…… …….Date……

Gavin Chapman (co-author)

Analysis of Mouse cultured cells for PS2V.

Certification that the statement of contribution is accurate and permission is given for the inclusion of the paper in the thesis

Signed

…… ……Date……

Sharon Pursglove (co-author)

Performed mouse cell culture analysis of Notch

Certification that the statement of contribution is accurate and permission is given for the inclusion of the paper in the thesis

Signed

…… ……Date……

Louise O'Keefe (co-author)

Conducted hypoxia tests in flies for the alternative splicing of PS2V in *Drosophila*.

Certification that the statement of contribution is accurate and permission is given for the inclusion of the paper in the thesis

Signed

…… ……Date……

Ralph Martins (co-author)

Supervised development of work for Verdile..

Certification that the statement of contribution is accurate and permission is given for the inclusion of the paper in the thesis

Signed

…… …….Date……

Michael Lardelli (co-author)

Planned the research, wrote the manuscript, acted as corresponding author and supervised development of work for Newman, Wilson, Moussavi-Nik and Wells.

Certification that the statement of contribution is accurate and permission is given for the inclusion of the paper in the thesis

Signed

…… …….Date……

HMGA1 controls an ancient alternative splicing mechanism that truncates PRESENILIN proteins under hypoxia to boost γ-secretase activity and suppress the unfolded protein response.

Hani Moussavi-Nik*[1], Morgan Newman*[1], Lachlan Wilson*[1], Esmaeil Ebrahimie[2], Simon Wells[1], Mark Van Der Hoek[3], Giuseppe Verdile[4,5,6], Gavin Chapman[7], Sharon Pursglove[7], Louise O'Keefe[1], Ralph Martins[4,5], Michael Lardelli[†1].

*Joint first authors

[†] Author for correspondence

Affiliations:

1. Discipline of Genetics, School of Molecular and Biomedical Science, University of Adelaide, SA 5005, Australia

2. Technology Enhanced Learning Group, University of South Australia, SA, 5000, Australia

3. Adelaide Microarray Centre, IMVS Main Building, Frome Road, Adelaide, SA 5000, Australia

4. Centre of Excellence for Alzheimer's Disease Research and Care, School of Medical Sciences, Edith Cowan University, Joondalup, WA 6027, Australia

5. School of Psychiatry and Clinical Neurosciences, University of Western Australia, Crawley, WA, 6009, Australia.

6. School of Public Health, Curtin University, Bentley, WA 6102, Australia

7. Developmental Biology Division, Victor Chang Cardiac Research Institute, NSW 2010, Australia

Full contact details for corresponding author:

Michael Lardelli

Discipline of Genetics, School of Molecular and Biomedical Sciences, The University of Adelaide, SA 5005, Australia.

Tel. (+61 8) 83133212, Fax (+61 8) 83134362

email: michael.lardelli@adelaide.edu.au

Abstract

The *PRESENILIN* genes *PSEN1* and *PSEN2* encode two structurally related proteases essential for γ-secretase cleavage of over 70 proteins within lipid bilayers. Together, over 200 mutations causing early onset, familial Alzheimer's disease (FAD) occur in *PSEN1* and *PSEN2* but only one of these, the K115Efx10 mutation of *PSEN2*, causes truncation of the open reading frame. If translated, the truncated product would resemble a naturally occurring truncated isoform of *PSEN2* named PS2V that is induced by hypoxia and found at high levels in late onset Alzheimer's disease (AD) brains. Here we use zebrafish embryos to investigate the evolution of PS2V and its function compared to the K115Efx10 truncation. We find that zebrafish possess a PS2V-like isoform, PS1IV, produced from the fish's *PSEN1* orthologous gene rather than its *PSEN2* orthologue. We show that the molecular mechanism controlling formation of PS2V/PS1IV is conserved since the divergence of teleosts and tetrapods and was probably present in the common ancestor of the *PSEN1* and *PSEN2* genes. The structures of human PS2V and zebrafish PS1V have diverged greatly but their ability to stimulate γ-secretase activity and suppress the unfolded protein response is conserved. The K115Efx10 FAD mutation is similar to PS2V in its ability to increase Notch signalling and γ-secretase cleavage of a zebrafish orthologue of the AMYLOID BETA A4 PRECURSOR PROTEIN. This supports increased Aβ peptide production as a molecular common link between K115Efx10 FAD and sporadic late onset AD. Microarray analysis of PS1IV function reveals modulation of immune/inflammatory responses and numerous other functions.

Introduction

The *PRESENILIN* genes *PSEN1* and *PSEN2* encode two structurally related proteins that operate within γ-secretase complexes to cleave type 1 transmembrane proteins (Figure 1A, reviewed by (1)). For this reason they are essential to signalling by a wide variety of proteins such as Notch receptors, p75 and Amyloidβ Precursor Protein (AβPP). The *PRESENILIN*s also have other functions including in autophagy (2), phosphorylation of β-catenin (3) and control of chromosome segregation (4, 5). *PSEN1* is the major locus for autosomal dominant mutations causing familial Alzheimer's disease (FAD) (6) the other two known loci being *PSEN2* and *AβPP*.

At least 95% of Alzheimer's disease (AD) is sporadic. This disease shares similar histopathology with FAD including deposition of plaques of Aβ peptide that is produced from AβPP after cleavage by β-secretase and then γ-secretase (Figure 1A). However, the causes and pathological mechanism behind sporadic AD are hotly debated. One molecular change commonly observed in AD brains is an increase in alternative splicing of PSEN2 transcripts to produce a truncated isoform lacking exon 5 sequence and thus named "PS2V" (7, 8) (Figure 1 B,C). This isoform has been described as "aberrant", (9) probably because it had only been detected in human brain and not in mice or rats. However, PS2V has the remarkable property that it can increase γ-secretase activity and production of Aβ peptide from AβPP (8). Using human neuoblastoma SK-N-SH cells, Sato et al. (7) showed that PS2V formation is induced by hypoxia but not other forms of cellular stress. Under hypoxia expression of the HMGA1a protein is induced in neural

tissue and this binds to a sequence in exon 5 of PSEN2 transcripts. This interferes with spliceosome complex function at the exon 5 donor site causing exon 4 to be ligated to exon 6 and excluding exon 5 (10), (Figure 1C).

The HIGH MOBILITY GROUP AT-HOOK 1 (HMGA1) proteins are an ancient and highly conserved family primarily known for their ability to bind chromatin (reviewed by (11)). HMGA1 is expressed early in embryogenesis when embryos inhabit an hypoxic environment and many relatively undifferentiated cells exist (12). Their expression can be induced by hypoxia in adult neural tissues (13, 14) and is commonly reactivated in cancer (reviewed by (15)). Hypoxia increases Notch signalling to maintain neural stem cells in an undifferentiated state (16). This is known to involve hydroxylation of the Notch receptor protein (17, 18) and Mukherjee et al. (19) recently showed that the HIFα protein of Drosophila that controls many cellular hypoxic responses can interact directly with Notch receptor to increase its signalling in the absence of ligand. Evidence is accumulating that hypoxia (20, 21) and Notch (22) may play important roles in AD pathogenesis but how these factors might be coupled to other factors such as Aβ production is not obvious.

Over 180 mutations in PSEN1 and around 20 mutations in PSEN2 are thought to cause FAD (6, 23). All are mis-sense mutations, deletions or small insertions that preserve the C-terminal protein coding part of the open reading frame. Recently, a unique frameshift mutation, K115Efx10, was discovered in *PSEN2* and suggested to cause AD ((23), Figure

1B). If expressed this mutant allele would produce a truncated protein very similar to PS2V.

We recently showed that PS2V production is not a unique human aberration but occurs in the brains of guinea pigs and, presumably most other mammals (24). In this paper we show that PS2V can also increase Notch signalling and that the alternative splicing mechanism that produces PS2V in response to hypoxia is ancient and predates the gene duplication event that formed *PSEN1* and *PSEN2* in vertebrates. In teleosts (bony fishes) hypoxia induces expression of Hmga1a that acts on transcripts of the orthologue of *PSEN1* rather than *PSEN2* to cause an alternative splicing outcome. The novel splice product of zebrafish *psen1*, "PS1IV", nevertheless codes for a protein capable of boosting γ-secretase activity. Microarray analysis of PS1IV function demonstrates roles in modulation of a wide variety of gene products. We also use our zebrafish assay system to examine the activity of the putative truncated protein product of the K115Efx10 allele of human *PSEN2* and show that it can also boost γ-secretase activity. Our data support a unified model of sporadic AD pathogenesis where *PRESENILIN* activity plays a central role in responding to hypoxic conditions by boosting both Aβ production and Notch signalling via PS2V formation. Chronic upregulation of Aβ production in brains with ageing vasculature and insufficient oxygenation may eventually lead to oligomerisation of Aβ with pathogenic consequences.

Materials and Methods

Ethics and permits

All experimentation with animals and work with genetically modified organisms was conducted under the auspices of the University of Adelaide's Animal Ethics Committee and Institutional Biosafety Committee respectively.

Oligonucleotides

The sequences of all oligonucleotides (PCR primers and morpholino oligonucleotides) used in this study are given in Supplementary Data File 1.

Construction and cloning of cDNAs for mRNA synthesis

cDNAs encoding PRESENILIN truncations (including truncations equivalent to the NTF) were synthesised by PCR from zebrafish *psen1* and *psen2* cDNAs or human *PSEN1* and *PSEN2* cDNAs. The zebrafish Presenilin truncations are fused at their N-termini to the FLAG™ antibody tag, DYKDDDDK (25) that follows a start codon within a consensus Kozak sequence (26). The human PSEN truncations are fused at their N-termini to an HA tag (YPYDVPDYA, (27)) that follows a start codon within a consensus Kozak sequence. The cDNA encoding the putative protein product of the K115Efx10 mutation is the human hPSEN2Δ>NTF construct into which the K115Efx10 mutation has been introduced by QuikChange™ Site-Directed Mutagenesis (Stratagene Cloning

Systems, La Jolla, CA, USA). The cDNA constructs for synthesis of the negative control zebrafish and human mRNAs denoted as "stop" are full length cDNAs including N-terminal FLAG or HA tag fusions respectively but with codon 4 of the Presenilin coding sequences mutated to the stop codon TAA. All sequences were cloned into the pcGlobin2 vector (28) between the *Bam H*I and *Eco R*I restriction sites (for zebrafish cDNAs) and *Bam H*I and *Xho* I restriction sites (for human cDNAs) and their sequences confirmed by sequencing before their use for synthesis of mRNA as previously described (29).

Injection of mRNAs and morpholinos

MoHmga1aTln and MoHmga1BindBlock (Psen1) were synthesized by GeneTools LLC (Corvallis, OR, USA) and injected at 0.5mM (diluted to this concentration with MoCont as previously (29)) at the one-cell stage. hPSEN2Δ>4 and hPS2V DNA constructs including N-terminal FLAG tags DNA were synthesised by GenScript (Piscataway, NJ, USA). cDNAs encoding FLAG-tagged zPsen1Δ>3 and zPS1IV were synthesised by PCR from zebrafish *psen1* cDNA. All sequences were cloned into the pcGlobin2 vector (30) between the *Bam H*I and *Eco R*I restriction sites. Sequences were confirmed by sequencing before use for synthesis of mRNA as previously described (29). mRNAs were injected one-cell stage embryos at 100-200ng/μl (each mRNA concentration is indicated in the table of *neurogenin1*-based Notch signalling assay results (Supplementary Data File 2). As a control to show the ability of MoHmga1aTln to suppress *hmga1a* mRNA translation, the first 135 bases of the *hmga1a* coding sequence was fused in frame to EGFP in the N1-EGFP plasmid at the *EcoRI/AgeI* sites (hmga1a-135-EGFP) (BD Biosciences, NJ, USA). The plasmid was linearised with *NotI* prior to injection. 50ng/ul of the plasmid was co-injected with either 0.5 mM of MoHmga1aTln mixed with

MoCont or MoCont alone. Embryos were then observed for GFP fluorescence at ~10hpf using fluorescence microscopy (see Supplementary Data File 3).

Exposure of embryos, explants and adult fish to hypoxia and NaN_3

Danio rerio were bred and maintained at 28 °C on a 14 h light/10 h dark cycle. Embryos were collected from natural mating, grown in embryo medium (E3, (31)) and staged. For exposure of embryos with to sodium azide (NaN_3, Sigma-Aldrich CHEMIE Gmbh, Steinheim, Germany), this was performed at 100μM from 6 hpf until embryos reached developmental stages equivalent to those attained under normoxia at 48 hpf at 28.5 °C (30 embryos were used for each concentration). In the experiments for exposure of adult brain tissue to sodium azide, this was performed at a concentration of 100μM in DMEM medium after the tissue (from chicken and mouse brains) was cut into small fragments (e.g. ~1mm diameter). This was not necessary for explanted zebrafish brains. In the experiments conducted on adult zebrafish under low oxygen conditions, oxygen was depleted by bubbling nitrogen gas through the medium. Oxygen concentrations were measured using a dissolved oxygen meter (DO 6+, EUTECH instruments, Singapore). The dissolved oxygen level in the hypoxia group was measured to be 1.20±0.6 mg/l for adults; whereas the normal ambient oxygen levels were 6.6±0.45 mg/l. For exposure of adult *Drosophila melongaster* to hypoxia, healthy flies were exposed to low oxygen conditions (<1%, using AnaeroGen™, Oxoid, Basingstoke, UK) for 3 hours, and immediately frozen for later RNA extraction as below.

Appa cleavage and Notch signalling assays

Assays for γ-secretase cleavage of Appa (32) and Notch signalling (29) were performed as previously described (see Supplementary Data Files 4 and 2 respectively for raw data and statistical analysis).

RT-PCR assays for detection of splice events homologous to formation of human PS2V

Total RNA was extracted from samples mentioned above using the QIAGEN RNeasy mini kit (QIAGEN, GmbH, Hilden, Germany). 700 ng of total RNA were used to synthesize 25 µL of first-strand cDNA by reverse transcription (SuperScript III kit; Invitrogen, Camarillo, USA). For PCR amplification, 5 µL of the cDNA was used with the following primer pairs as relevant: Chicken *Psen2*: Chic Psen2: Ex.4 F: (5'-ACGGGCAGCTGATCTACACC-3') with Chic Psen2 Ex.6 R: (5'-GACCTTTCCAGTGGATGCAA-3'); Chicken *Psen1*: Chic Psen1 Ex.4 F: (5'-CTACACTCCCTTCACAGA-3'); Chic Psen1 Ex.6 R: (5'-CAGGATAAGCCATGCAGT-3'); Mouse *Psen2*: Mm Psen2 Ex.4 F: (5'-CATCGTAGTCATGACCATCTTCC-3'); MmPsen2 Ex.6 R: (5'-ACACCATGCCCACTGCC3'); Mouse *Psen1*: Mm Psen1 Ex.4 F: (5'-CTACACCCCATTCACAGA-3'); Mm Psen1 Ex.6 R: (5'-CTGCTGCAGTCGAAGGGG-3'); and *Drosophila melanogaster Psen*: Dm Psen Ex.2 F: (5'-CTGCTGTCAAATCTCCAGGCTT-3'); Dm Psen Ex.2 R: (5'-TCCGACCACTCCAAAGTTCC-3').

PCR was performed using GoTaq polymerase (Promega, Madison, USA) for 35 cycles with an annealing temperature of 56 °C for 30 s, an extension temperature of 72 °C for 1 min and a denaturation temperature of 95 °C for 40 s. The PCR products were cloned into the pGEM-T vector (Promega, Madison, USA) and sequenced.

Quantitative real-time PCR for detection of PS2V

The relative standard curve method for quantification was used to determine the expression of experimental samples compared to a basis sample. For experimental samples, target quantity was determined from the standard curve and then compared to the basis sample to determine fold changes in expression. Gene specific primers were designed for amplification of target cDNA and the cDNA from the ubiquitously expressed control gene *ef-1a*. The reaction mixture consisted of 50ng/μl of cDNA. 18 μM of forward and reverse primers and *Power* SYBR green master mix PCR solution (Applied Biosystems).

To generate the standard curve cDNA was serially diluted (100 ng, 50 ng, 25 ng, 12.5 ng). Each sample and standard curve reaction was performed in triplicate for the control gene and experimental genes. Amplification conditions were 2 min at 50 °C followed by 10 min at 95 °C and then 40–45 cycles of 15 s at 95 °C and 1 min at 60 °C. Amplification was performed on an ABI 7000 Sequence Detection System (Applied Biosystems) using 96 well plates. Cycle thresholds obtained from each triplicate were averaged and normalized against the expression of *ef-1a*, which has previously been demonstrated to be suitable for normalization for zebrafish quantitative PCR (qPCR). Each experimental sample was then compared to the basis sample to determine fold changes of expression.

The primers used for quantitative real-time PCR anaylsis of *PS1IV* mRNA levels are seen in Supplementary Data File 1. See Supplementary Data File 5 for all qPCR raw data and analysis.

Assay of the unfolded protein response (UPR)

Embryos were injected with mRNAs at the 1-cell stage. At 2hpf fertilized injected embryos were split into 2 groups. One group was left untreated and the other group was treated with 1.5μg/ml tunicamycin. At 24hpf total RNA was extracted from embryos and reversed transcribed into cDNA for qPCR analysis. qPCR was performed to determine the expression levels of unspliced *xbp-1* and spliced *xbp-1* in embryos that had been injected with mRNAs encoding either zPsen1Δ>3, zPsen2Δ>4, hPSEN2Δ>4 or the zebrafish "stop" negative control mRNA. Tunicamycin treatment causes ER stress and induces the expression of the spliced form of *xbp-1* (33). Any observed decrease in spliced *xbp-1* expression under tunicamycin treatment in the mRNA injected cDNA samples can be interpreted as these mRNAs suppressing the ER stress response. See Supplementary Data File 5 for qPCR raw data and analysis.

Microarray analysis

Embryos were collected from natural mating, grown in embryo medium (E3) and staged. Morpholinos were synthesized by Gene Tools LLC (Corvallis, OR, USA) and are listed in Supplementary Data File 1. Fertilized zebrafish eggs were injected prior to cleavage. To ensure consistency of morpholino injection, eggs were always injected with solutions

at 1 mM total concentration. Dilutions of MoHMGA1 BindBlock morpholino was carried out by mixing with standard negative control morpholino, MoCont. This ensured that phenotypic variation observed was not due to change in the total injection concentration. The maximum concentration of HMGA1 BindBlock injected was always 0.5 mM (i.e. a mixture of 0.5 mM MoCont + 0.5 mM MoHmga1BindBlock morpholino). Titration of morpholinos to find effective concentrations has been shown previously (29).

For exposure of injected embryos to sodium azide this was performed at 100μM from 6 hpf until embryos reached developmental stages equivalent to those attained under normoxia at 48 hpf at 28.5 °C (30 embryos were used for each injection batch).

Total RNA was extracted from different injection batches using the RNeasy Mini Kit according to the manufacturer's specifications. For each sample, the RNA concentration was determined with a NanoVue™ UV–vis spectrophotometer (GE Healthcare Life Sciences, Fairfield, USA). RNA integrity and quality were then estimated with an Agilent 2100 Bioanalyzer (Agilent Technologies, Palo Alto, CA), and the RNA integrity number (RIN) index was calculated for each sample. Only RNAs with a RIN number>7.0 were processed further.

To evaluate genome-wide changes in gene transcription related to the presence or absence of PS1IV under mimicry of hypoxia, we performed hybridisation anaylsis using the Zebrafish Genome Array (Affymetrix Inc. Santa Clara, CA). Briefly, mRNAs were isolated from 300ng of total RNA derived from embryos injected with

MoHMGA1BindBlock morpholino at 0.5 mM (diluted to this concentration with MoCont morpholino as previously described (29)) or with MoCont at 0.5 mM alone treated with and without sodium azide using the Eukaryotic Poly-A RNA control Kit (Affymetrix) or from uninjected embryos treated with sodium azide (see Figure 7). Subsequently, mRNAs were subjected to double-strand cDNA synthesis using the GeneChip® One Cycle cDNA Synthesis Kit (Affymetrix). The resulting double-stranded cDNAs were *in vitro* transcribed into biotin-labelled cRNAs using the IVT Labelling Kit (Affymetrix). After that, the biotin-labelled cRNAs were fragmented by heating and hybirdized with the Affymetrix Zebrafish Genome Array. Finally, the signal intensity of the chip was scanned using a GeneChip® Scanner 3000TG and analysed using the Partek Genomics Suite software (www.partek.com). Cell files were imported and intensities adjusted for GC content using Partek's own method prior to RMA background correction and quantile normalization (34-37). Mean gene probe summaries assessed for differential gene expression by ANOVA with p-value adjusted using Step-up multiple test correction. Each treatment had four biological replicates.

Statistical analysis of microarray data

Gene expression analysis was performed using the FlexArray package (McGill University, Canada). MoHmga1BindBlock-injection and MoCont-injection were assumed as treatments. Log2 ratio values were calculated as fold change by FlexArray. Those genes having a Bayesian t-test (38) with p-value ≤ 0.05 and fold change $\geq +1$ or fold change ≤ -1 were accepted as significant differentially expressed genes. Bayesian t-

test is a powerful statistical test in determining differentially expressed gene s in two different samples by decreasing Type I error rates (38).

Results

Note: The structure of the protein-coding exons in the *PRESENILIN* genes of zebrafish, human and other species is largely conserved although exon numbers vary due to differences in non-coding exons. For simplicity, below we will refer to the exons of zebrafish and other species using the identity of their cognate exons in humans.

Hypoxia-inducible alternative splicing of psen1*, not* psen2 *in zebrafish*

We recently showed that PS2V is induced in the brains of guinea pigs and probably most other mammals (except rats or mice) (24). We have also shown that hypoxia does not induce formation of a PS2V-like alternative transcript from zebrafish *psen2* (14). However, the vertebrate *PSEN1* and *PSEN2* genes are paralogues formed by an ancient gene duplication event that predates the divergence of the tetrapod and teleost lineages (39, 40). After the gene duplication event each gene underwent a degree of sub-functionalisation. To test whether hypoxia-inducible formation of "PS2V" might have been retained in the *PSEN1* gene lineage in bony fish rather than in the *PSEN2* lineage we tested for PS2V-equivalent exon loss in zebrafish *psen1* by RT-PCR amplification of cDNA spanning exons 3 to 6. We observed induction of alternative transcript formation from *psen1* using chemical mimicry of hypoxia (NaN_3 treatment) in both embryos and larvae (Figure 2A). The same alternative splicing event was detected under genuine hypoxia and in the brains of adult fish (Figure 2A). Cloning and sequencing of cDNA from the alternatively spliced transcript of *psen1* showed that it lacks exon 4 sequence

rather than the loss of exon 5 as seen in human PS2V transcripts (Figure 2B, C and Supplementary Data File 6). Therefore, we have named this alternative transcript of zebrafish *psen1* "zPS1IV".

Manabe et al (9, 10) have clearly defined the mechanism that controls loss of exon 5 sequence from human *PSEN2* transcripts to form PS2V. In humans, transcription of *HMGA1a* is induced by hypoxia and then the HMGA1a protein binds to two sites at the 3' end of exon 5 in *PSEN2* transcripts (Figure 2B,D). This appears to block funcational association of U1 snRNP with the exon 5 splice donor site causing alternative splicing of exon 4 to exon 6 ((10) Figure 2B). We have previously shown that the DNA binding region of zebrafish Hmga1a protein is highly similar to human HMGA1a but that the nucleotide sequence at the 3' end of exon 5 of zebrafish *psen2* is not highly conserved (14). This is consistent with the failure of zebrafish *psen2* to produce a PS2V equivalent. If the hypoxia-inducible alternative splicing of zebrafish *psen1* represents an ancient mechanism present in the common ancestor of the *PSEN1* and *PSEN2* genes then this might still be controlled by induction of Hmga1a. We examined the sequence of *psen1* for potential Hmga1 binding sites. Consistent with conservation of the alternative splicing mechanism, we discovered that the best match to the HMGA1a binding site consensus was at the 3' end of the *psen1* exon 5 (Figure 2D)

Since hypoxia-induced alternative splicing of *psen1* transcripts causes loss of exon 4 rather than exon 5 we tested whether binding of Hmga1a at this site still controlled the alternative splicing event. We designed a morpholino antisense oligonuclotide,

MoHmga1BindBlock, to bind over the upstream Hmga1 binding in exon 5 that, hopefully, would not interfere with the function of this exon's splice donor site (Figure 2D). Injection of this oligonucleotide into embryos followed by exposure to chemical mimicry of hypoxia (100 μM NaN_3) and RT-PCR analysis showed that MoHmga1BindBlock greatly reduced formation of PS1IV under hypoxia while the common, normoxic, splicing pattern still occurred (Figure 3A). Blockage of Hmga1 translation by injection of morpholino oligonucleotide MoHmga1aTlnBlock also greatly reduced formation of zPS1IV under chemical mimicry of hypoxia (Figure 3B). We were also able to force formation of PS1IV under normoxia by overexpression of Hmga1a in zebrafish embryos through injection of mRNA containing the Hmga1 coding sequence (Figure 3C[1],D). The evolutionary conservation of this alternative splicing system was demonstrated by the fact that forced expression of human HMGA1a in zebrafish embryos by mRNA injection also caused formation of PS1IV (Figure 3C[2]). In both these cases, the induction of PS1IV formation could be blocked by co-injection of MoHmga1aBindBlock with the Hmga1a/HMGA1a mRNA while injection of a non-translatable control mRNA was unable to induce PS1IV formation (Figure 3C[1],C[2],D). These experiments strongly support that the mechanisms controlling hypoxia-inducible alternative splicing of zebrafish *psen1* and human *PSEN2* have evolved from an ancient mechanism involving HMGA1 control of splicing in the ancestral *PRESENILIN* gene which was duplicated to form vertebrate *PSEN1* and *PSEN2*.

Predictions of hypoxia-inducible alternative splicing in other vertebrate lineages

The correlation between hypoxia-inducible alternative splicing of *PRESENILIN* gene transcripts and possession of a highly conserved HMGA1a-binding site in exon 5 can be used to predict which gene, *PSEN1* or *PSEN2*, might show this alternative splicing in any vertebrate. Alignment of the 3' region of exon 5 of *PSEN1* and *PSEN2* in various vertebrates species supports that most mammals show hypoxia-inducible alternative splicing in *PSEN2* transcripts but not those of *PSEN1* (Figure 2D). Interestingly rats and mice (both species within the subfamily *Murinae*) lack the ability to produce PS2V (24) and our tests have revealed no evidence for hypoxia-inducible splicing of *Psen1* transcripts in these species (data not shown – see Materials and Methods). *Gallus gallus* (chicken, a bird) and *Xenopus laevis* (African clawed frog, an amphibian) also do not show high conservation of the HMGA1a-binding site in exon 5 of their *PSEN1* or *PSEN2* genes (Figure 2D). We have previously shown induction of PS2V in explanted guinea pig brain tissue incubated in medium containing NaN_3 (24). As expected from our sequence analysis above, tests of mRNA extracted from chicken brains exposed to NaN_3 failed to observe exclusion of exon 4 or exon 5 from transcripts of either *PSEN1* or *PSEN2* (data not shown). Interestingly, the teleost *Fugu rubripes* (a puffer fish) does not have a well-conserved Hmga1a-binding site in exon 5 of either its *psen1* or *psen2* gene (Figure 2D) reinforcing how loss of hypoxia-controlled alternative splicing of *PRESENILIN* transcripts need not be severely detrimental to survival.

To test whether this mechanism of alternative splicing exists in the single *presenilin* gene of an insect we exposed *Drosophila melanogaster* to hypoxia before extraction of mRNA and RT-PCR. However, no such alternative splicing was observed for the *Drosophila*

melanogaster PRESENILIN orthologue *Psn* (data not shown – see Materials and Methods).

Both human PS2V and zebrafish PS1IV can boost γ-secretase activity and Notch signalling

Human PS2V consists of 124 amino acid residues (aa) and is expected to possess one transmembrane domain (Figure 2C). In contrast, deletion of zebrafish *psen1* exon 4 to form zPS1IV alters the open reading frame after exon 3 sequence to form a peptide predicted to possess only 18 aa including the 6 novel residues at its C-terminal (Figure 2C). The preservation of this mechanism of alterative splicing of the *PRESENILIN* genes for approximately 450 million years since the divergence of the teleost and tetrapod vertebrate lineages (41) suggests that these peptides serve an important function(s) in response to hypoxia despite their very different structures.

Sato et al. (8) showed that PS2V can boost γ-secretase activity and increase cleavage of the Aβ peptide from the APP protein. In a recently submitted papers, we showed that forced expression of a truncation of zebrafish Psen1 protein equivalent to human PS2V (i.e. truncated after exon 4 sequence, “Psen1Δ>4”) dominantly increases cleavage of zebrafish Appa (a paralogue of the human AβPP protein that is cleaved to produce the Aβ peptide seen in Alzheimer’s disease brains) indicating increased γ-secretase activity. Psen1Δ>4 expression also decreases *neurogenin1* gene transcript levels in the trunk region of zebrafish embryos at 24 hours of development indicating increased Notch

signalling. The equivalent truncation of human PSEN1, hPSEN1Δ>4, also possesses these activities. The apparent increase in Notch activity caused by zebrafish Psen1Δ>4 requires the presence of non-truncated endogenous Psen1 (Newman et al, submitted). We first asked whether, like Psen1Δ>4 and hPSEN1Δ>4, forced expression of human PS2V in zebrafish embryos could boost γ-secretase activity. Consistent with our expectation, injection of mRNA encoding human PS2V caused increased Appa cleavage (Figure 4A) and decreased *neurogenin1* activity (Figure 4B). This is evidence that PS2V not only increases production of Aβ in human brain but also increases signalling by NOTCH receptors. It also demonstrates that zebrafish can be used to analyse the function of human PS2V.

Human PS2V, zebrafish Psen1Δ>4 and human hPSEN1Δ>4 can all increase cleavage of Appa and Notch signalling so it remained to demonstrate this activity for a PS2V-equivalent truncation of zebrafish Psen2, i.e. Psen2Δ>4. Surprisingly, injection of an mRNA encoding this protein truncation had no measurable effect on Appa cleavage or Notch signalling (Figure 4A, B). This is consistent with our failure to detect alternative splicing of zebrafish *psen2* transcripts under hypoxia or chemical hypoxia (14).

Our previous study analysing the effects of various truncations of the zebrafish Psen1 protein found that injection into embryos of mRNA encoding Psen1 truncated after exon 3 sequence (i.e. “zPsen1Δ>3”, similar to zPS1IV but lacking its novel C-terminal aas) was very disruptive to embryo development. This precluded analysis of Appa cleavage or Notch signalling for this Psen1 truncation (Newman et al. submitted). However, in an

attempt to overcome this limitation we diluted this mRNA until injected embryos were able to develop to the 24 hpf stage (see Materials and Methods). Assessment of Appa cleavage and Notch signalling then showed that mRNA encoding this small peptide can, nevertheless, increase γ-secretase activity (Figure 5 A, B). Injection of mRNA encoding zebrafish zPS1IV (i.e. like Psen1Δ>3 but including the novel aas caused by fusion of exon3 to exon 5 sequence) also caused increased cleavage of Appa (Figure 5A). However, the observed frequency of decreased *neurogenin1* staining due to zPS1IV indicating increased Notch signalling was not sufficient to achieve statistical significance (a p value of >0.05 was obtained in our assay, Figure 5B). Differences in the ability of zPsen1Δ>3 and zPS1IV to boost Notch signalling may be due to a lesser stability of PS1IV and/or differing subcellular localisation of these two peptides due to differences in their C-terminal amino acid residues.

To examine further the conservation of structure and function between zebrafish zPS1IV and human PS2V we then examined the ability to boost Appa cleavage and Notch signalling of exon 3-derived sequences from human *PSEN2*, *PSEN1* and zebrafish *psen2*. mRNAs encoding Presenilin peptides truncated after exon 3 sequence from these three genes were unable to boost Appa cleavage or Notch signalling (Figure 5A,B). Thus, while zebrafish PS1IV and human PS2V share the conserved ability to boost γ-secretase activity, their structures have diverged sufficiently over time that exon 3 sequence from human PS2V cannot functionally substitute for zebrafish PS1IV.

Suppression of the unfolded protein response (UPR) by human PS2V and orthologous truncations is conserved

Sato et al. (8) previously showed that PS2V suppresses the unfolded protein response when its expression is forced in human HEK293T cells (a kidney-derived cell line that does not normally expressed PS2V, (13)). Induction of the UPR occurs via a change in the splicing of transcripts of the gene *XBP1* to form the isoform *XBP-1S* (42) and so quantitative PCR (qPCR) can be used to assay the relative UPR response in zebrafish embryos (42). To investigate further the conservation of function between zebrafish and human PRESENILIN truncations we examined the effects on the UPR in zebrafish embryos of forced expression of human PSEN2 truncated after exon 4 sequence (i.e. hPSEN2Δ>4, equivalent to PS2V), zebrafish Psen1 truncated after exon 3 sequence (zPsen1Δ>3, equivalent to PS1IV) and zebrafish Psen2 truncated after exon 4 sequence to resemble human PS2V (zPsen2Δ>4). Zebrafish embryos injected with a non-translatable control mRNA and then exposed to 1.5 μg/ml of the antibiotic tunicamycin at 2 hpf showed ~12-fold induction of the UPR at 24 hpg (Figure 6). In contrast, injection of mRNA coding either for hPSEN2Δ>4 or zPsen1D>3 was able to suppress UPR induction by tunicamycin to below 2-fold. Significantly, the truncation of zebrafish Psen2 to resemble human PS2V (zPsen2Δ>4) showed little ability to suppress the UPR (Figure 6) consistent with its inability to stimulate γ-secretase activity while the ability of truncations PS2V and zPsen1D>3 to suppress the UPR parallels their effects on γ-secretase activity. Thus the action on the UPR of the truncated PRESENILINs proteins

that are normally induced by hypoxia in humans and zebrafish has been conserved despite their structural divergence.

The K115Efx10 mutation of human* PSEN2 *indicates that PS2V may be a molecular common link between sporadic and familial Alzheimer's disease.

Around two hundred dominant mutations in the human PRESENILIN genes are known to cause familial Alzheimer's disease (FAD). Most of these occur in PSEN1 but a number of mutations have been described in PSEN2 (6, 23). Until recently all known FAD mutations in the PRESENILINS were mis-sense mutations or internal deletions / insertions that preserved C-terminal protein coding sequences. No FAD mutations have been found in genes encoding the other components of a γ-secretase complexes. Recently, Lee et al (2) showed that full-length (non-endoproteolysed) PSEN1 has a γ-secretase-independent function in the acidification of lysosomes required for autophagy and that FAD mutations in *PSEN1* decrease a cell's autophagy ability. Numerous studies have shown decreased autophagy in AD brains (reviewed in (43)). The function of non-endoproteolysed PSEN1 in autophagy and the recent discovery of families with mutations in other γ-secretase complex components that do not have FAD (44) strongly suggests that, contrary to some current hypotheses, decreased γ-secretase activity does not cause Alzheimer's disease. Instead, FAD-causing mutations in the *PRESENILIN* genes may promote Aβ accumulation through a failure to clear aggregate forms of this peptide.

Recently, a woman suffering early onset Alzheimer's disease was reported to be heterozygous for a nonsense mutation in PSEN2, K115Efx10 (23). This mutation is a dinucleotide deletion causing a frameshift in the *PSEN2* coding sequence only six codons prior to the end of exon 4 (Figures 1B, 4AB). If transcripts of this gene are not degraded through nonsense mediated decay then they should generate a peptide similar in structure to PS2V and might act to increase Aβ production. To test whether the putative truncated product of K115Efx10 increases γ-secretase activity we synthesised mRNA encoding it and injected this into zebrafish embryos. This increased Appa cleavage and Notch signalling (Figure 4A,B) consistent with K115Efx10 causing AD by increasing Aβ production.

Gene expression network analysis suggests roles for zebrafish PS1IV in regulating immune responses, transcription and ribosomal protein expression.

The cellular role of PS2V cannot be investigated in mice due to the apparent rapid evolution of their *Presenilin* genes and the loss of this isoform (24). However, the zebrafish is the next most genetically malleable vertebrate model and, as we have shown, it does express the PS2V-orthologous isoform, PS1IV. The morpholino MoHmga1BindBlock blocks specifically the formation of PS1IV under conditions where it would normally be induced. Therefore, we exploited MoHmga1BindBlock to investigate the effects on cellular function of loss of PS1IV under hypoxia using microarray and subsequent gene network analysis.

Zebrafish embryos were injected with Hmga1BindBlock or the negative control morpholino MoCont. They were then exposed to chemical mimicry of hypoxia from 36 hpf to 48 hpf before extraction of mRNA and analysis of gene expression on the Affymetrix Zebrafish Gene 1.0 ST Array. A number of control microarray comparisons were also made to identify genes for which expression is affected by the act of injection or by the non-specific effects of the morpholino oligonucleotides (see Figure 7). Bayesian t-tests produced lists of genes with significantly decreased or increased expression in the comparisons. The final list of genes with significantly increased or decreased expression due to decreased PS1IV formation under mimicry of hypoxia was generated after removal of genes showing significantly altered expression in the controls (see Figure 7 and Tables 1 and 2). To validate the microarray results, we conducted quantitative real time PCR (qPCR) analysis for a selection of the genes with significantly altered expression (see Supplementary Data File 5) and that appear to represent nodes in a gene network analysis to be described in detail elsewhere (Ebrahimie, Moussavi Nik, Newman & Lardelli, manuscript in preparation).

Among the genes showing increased expression under hypoxia without PS1IV (i.e. normally repressed by the formation of PS1IV) were numerous genes involved with modulation of immune responses (*HRH2*, *NLRP3*, *IL17RA*, *CD22*, *ACY1*, *IRF4*, *XCL2* etc., Table 1). However, without further analysis we are uncertain whether their combined effect would be to, overall, activate or suppress immune responses and whether these responses are restricted to any particular tissues (e.g. humoral or neural or both).

Genes involved in regulation of TOR signalling (*RICTOR*, *PKD1*) blood pressure and formation of vascular structures (e.g. *AGTR1* and *ANGPTL2*), and cell proliferation (*PIM3*, *ACY1*, *OLFM4*) also show increased expression when PS1IV is suppressed. This set of genes also included two known to be involved in neurological conditions, *GAK* (associated with Parkinsons Disease (45)) and *CAMTA1* (associated with cerebellar ataxia, nonprogressive, with mental retardation (46)).

The number of genes showing significant decreases in expression due to PS1IV (i.e. normally dependent on PS1IV for increased expression under mimicry of hypoxia) was greater in number and included genes encoding transcription factors or proteins involved in chromatin remodelling (e.g. *NKX3-2*, *SRCAP*, *GBX2*, *TCF25*, *SMARCA4*, *POU4F2*), genes involved in ER function (*CALR*), intracellular signalling (*OCRL*, *AIDA*, *PLEKHA4*, *PLCB1*, *MAPKAPK5*) and a considerable number of ribosomal proteins (see Table 2). Once again, genes involved in immune response regulation were identified (*IL1B*, *NLRP12*, *GRAMD1B*). A detailed gene network analysis from this microarray data incorporating gene ontology information will be presented elsewhere (Moussavi Nik, Newman, Ebrahimie & Lardelli, manuscript in preparation).

Discussion

PRESENILIN genes are found in the plants, fungi and animals reflecting their important roles in cell biology. However, despite considerable study (focussed mainly on their role in γ-secretase activity) their functions are relatively poorly understood. Recently our comprehension of PRESENILIN biology was radically altered by the analyses of Area-Gomez et al. (47) who discovered that PRESENILIN proteins and the γ-secretase cleavage of AβPP are concentrated in the mitochondrial associated membranes (MAM) that exist in a perinuclear region of the ER closely juxtaposed to mitochondria. MAM are responsible for regulating mitochondrial activity as well as disulphide bond formation (reviewed in (48)). Both oxidative phosphorylation by mitochondria and disulphide bond formation (oxidative protein folding) in the MAM are dependent on electron transport chains that require oxygen for efficient function and that generate substantial quantities of reactive oxygen species, especially if oxygen is limiting (49). In previous work (14, 21) we have analysed the response to low oxygen levels of the genes encoding proteins required for formation of the Aβ peptide that accumulates in the brains of people with Alzheimer's disease (7). We showed that, similar to humans, expression of these genes appears to be upregulated in zebrafish brains under hypoxia. Therefore, increased expression of Aβ under low oxygen is a selectively advantageous response that has been conserved during almost half a billion years of divergent vertebrate evolution. This supports that Aβ may be protective to neurons under stress (reviewed by (50)) and is

consistent with a number of analyses showing that Aβ can function as an antioxidant (51-55) (although Aβ complexed with metal ions appears capable of generating reactive oxygen species via the Fenton reaction (56, 57)).

In this paper we have shown further evidence for an important role of PRESENILIN genes in cellular responses to low oxygen. The PS2V splicing isoform of human *PSEN2* transcripts is generated under hypoxic conditions (7, 8) through induction of HMGA1a that binds to exon 5 sequence in transcripts (9, 10). While PS2V appears absent from mice and rats it is present in guinea pigs (and probably most other mammals) consistent with their greater conservation of numerous genes implicated in Alzheimer's disease pathology (24). We have shown that an orthologue of the PS2V isoform, PS1IV, exists in the zebrafish, a species of teleost (bony) fish. Like human PS2V, zebrafish PS1IV is produced in response to hypoxia as a result of induction of zebrafish Hmga1a protein that binds in transcribed *psen1* exon sequence cognate with exon 5 of human *PSEN2*. Unexpectedly however, this results in exclusion of exon 4 sequence rather than exon 5 sequence as in human *PSEN2* transcripts. The resultant very short PS1IV peptide appears, nevertheless, to be able to stimulate γ-secretase activity and suppress the unfolded protein response in a similar way to PS2V (7, 8) despite loss of any apparent homology between the PS2V and PS1IV sequences. Indeed, the two phenomena are probably related as shown by Sato et al. (8) who were able to increase γ-secretase by suppression of the UPR in mouse Neuro 2a cells using a dominant negative form of ER stress monitoring protein ERN1 (IRE1) (8). We recently showed that the ability of PS2V-like molecules to stimulate γ-secretase activity is reliant on the presence of full-length PRESENILIN

proteins, apparently by direct interaction with them (Newman et al. submitted). It will be interesting to test both whether the short PS1IV protein retains this dependency and whether the dominant negative form of ERN1 shows similar behaviour.

The conservation of PS2V function over nearly half a billion years is additional evidence that stimulation of Aβ production under low oxygen is selectively advantageous. The most parsimonious explanation for the conservation of this oxygen-sensitive alternative splicing event in the *PSEN2* gene of mammals and the *psen1* gene of teleosts is that the mechanism was present in the common ancestor of the *PSEN1* and *PSEN2* genes and was lost from one of the duplicate pair due to sub-functionalisation after the divergence of the teleost and tetrapod lineages. However, we found no evidence for formation of PS2V-related splicing isoforms in those large vertebrate clades the amphibians and the birds and even some mammals (mice, rats) and teleosts (*Fugu rubripes*) appear to have lost this mechanism entirely. Deeper insight into the biological roles of PS2V and the existence of any redundant mechanisms will be required to understand why this mechanism is not absolutely conserved across all vertebrate species. Our microarray analysis of the gene regulatory effects of PS1IV loss under chemical mimicry of hypoxia is the first transcriptomic interrogation of the function of this conserved splicing event and is the first step towards greater understanding of its role. It suggests involvement of PS1IV in modulating immune, vascular and proliferative responses.

Why is PS2V expressed at high levels in the brains of people with late onset, sporadic AD? Its presence is probably a marker of the high levels of oxidative stress known to

occur in brains with overt AD (58, 59) and suggests that this may be due to restricted oxygen levels. (Although the hypoxic response regulator HIF1α protein is reported to be downregulated in overt AD postmortem brains (60), HIF1α mRNA is observed to increase during normal brain aging (61)). We suggest that PS2V and Aβ may be elements of a homeostatic mechanism for regulating levels of reactive oxygen species in the brain. Aβ production may be enhanced in the MAM to buffer increased ROS when oxygen levels fluctuate below normal (possibly due to temporarily increased neuronal activity). Aβ may also have a role in activating HIF1α expression in order to reduce oxidative stress by increasing the flow of glucose through glycolysis and the hexose monophosphate shunt (62). However, in an aging brain where vascular function is deteriorating (such that both oxygen delivery and Aβ clearance is inefficient) both PS2V and Aβ may become chronically upregulated and Aβ may begin to oligomerise and aggregate. This would both reduce the levels of soluble Aβ antioxidant and possibly damage neurons and vasculature further by generating additional oxidative stress to further suppress oxidative phosphorylation. Such a model is consistent with numerous observations suggesting a role for hypoxia in development of AD (reviewed by (63)) and would also explain the close correlation between the risk factors for AD and cardiovascular disease (64, 65). Our observation that the putative truncated protein produced by the K115Efx10 FAD mutation of PSEN2 is similar to PS2V in its ability to boost γ-secretase activity suggests that this mutation may be pathogenic via chronic upregulation of Aβ production despite normal oxygen levels rather than due to decreased γ-secretase activity as previously suggested (23). We are currently attempting to engineer

a homologous mutation into the *psen1* gene of zebrafish so that its effects on the transcriptome can be compared with those of PS1IV.

Acknowledgements

We thank Kapowie Poultry Services, Kapunda, South Australia for scavenged chicken brains. This work was supported by grant 13033 from the Judith Jane Mason & Harold Stannett Williams Memorial Foundation to ML and by the Australian National Health and Medical Research Council (NHMRC, Project Grant 453622 to ML and RM and Project Grant 1003209 to GC), the Cancer Council of South Australia (research grant to ML), The Australian Research Council (ARC) Centre for the Molecular Genetics of Development (research funds to ML), the School of Molecular and Biomedical Sciences of the University of Adelaide (support of ML and MN), the late Douglas Anders (funds to ML), grants from the McCusker Alzheimer's Disease Research Foundation, the Department of Veterans Affairs, and Hollywood Private Hospital (to RM), funds from McCusker Alzheimer's Disease Research Foundation, particularly the generous support from Helen Sewell (to GV), Edith Cowan University's Strategic Research Grant (to GV) and the Australian Research Council (Discovery Project Grant DP1094119 to GC). We are indebted to Lindsay Carthew for his generous support of MN.

Figures

Figure 1

A. Presenilins act within γ-secretase complexes to cleave Type 1 transmembrane domain proteins such as Notch and AβPP within lipid bilayers. Before γ-secretase cleavage can occur the proteins must be truncated in luminal spaces or extracellularly by other proteases such as the α- or β-secretase activities that cleave AβPP. When AβPP is cleaved by β-secretase, subsequent γ-secretase cleavage produces the Amyloidβ peptide involved in Alzheimer's disease. Many γ-secretase substrates have cytosolic domains that migrate into the nucleus when released to modulate gene activity as part of transcription regulatory complexes. **B**. Diagram illustrating the multiple transmembrane domain structure of Presenilin proteins. Protein sequence derived from successive exons is illustrated by alternating thick and thin lines. The coding exons are numbered according to the human *PSEN1* and *PSEN2* genes. N- and C-termini are indicated as well as the site of the endoproteolysis event (arrowhead) that is thought to activate γ-secretase activity. "D" indicated the essential asparate residues at the catalytic site (star). The position of the K115fx10 mutation in the PSEN2 coding sequence is indicated. This is thought to be the only Alzheimer's disease mutation known that truncates a PRESENILIN coding sequence. (All other mutations are in-frame ands preserve C-terminal sequences). If translated, K115Efx10 mutant transcripts would produce a truncated protein similar the PS2V isoform of PSEN2 that is generated after an alternative splicing event that excludes exon 5 sequences (dashed) from transcripts. **C**. Hypoxia causes mitochondria to generate reactive oxygen species (ROS) that induce expression of HMGA1a in neurons. HMGA1a

binds to human *PSEN2* transcripts at the 3’ end of exon 5 and excludes splicing factors. Consequently, exon 4 is ligated to exon 6 resulting in a frameshift, early termination of the coding sequence and translation of the truncated protein isoform PS2V.

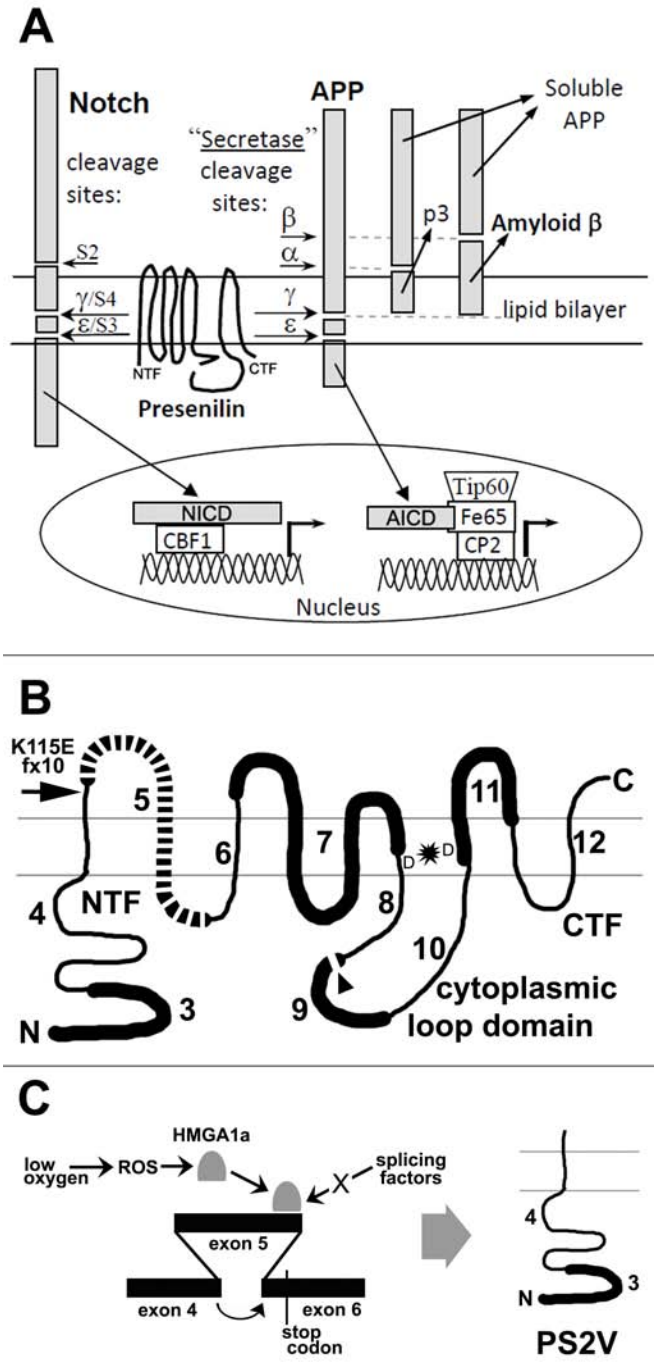
A
Notch
APP
Soluble APP
"Secretase" cleavage sites:
cleavage sites:
β
α
p3
Amyloid β
S2
γ/S4
ε/S3
γ
ε
lipid bilayer
NTF
CTF
Presenilin
Tip60
NICD
CBF1
AICD
Fe65
CP2
Nucleus
B
K115E fx10
5
6
7
D
D
11
C
12
4
NTF
8
CTF
10
cytoplasmic loop domain
N
3
9
C
HMGA1a
low oxygen
ROS
splicing factors
X
exon 5
exon 4
exon 6
stop codon
4
N
3
PS2V

Figure 2

RT-PCR amplification of sequence between exons 3 and 7 in zebrafish *psen2* transcripts does not indicate any alternative splicing induced by hypoxia (14) but this is seen for zebrafish *psen1* transcripts. **A**. NaN3 can be used to mimic hypoxia in zebrafish embryos or explanted adult brains and results in exclusion of exon 4 sequence from transcripts to generate the isoform PS1IV (filled arrowheads). This is also observed in the brains of adult fish after exposure to actual hypoxia. cDNA amplified from full-length transcript is indicated by unfilled arrowheads. B. In zebrafish, Hmga1a is induced by hypoxia (14) and binds in the 3' end of the exon 5 sequence of *psen1* transcripts but causes exclusion of exon 4 and ligation of exon 3 sequence to exon 5 resulting in a frameshift and termination of the open reading in exon 5 (see also Supplementary Data File 6). This generates the PS1IV isoform, the open reading frame of which would encode a protein only 18 aa in length (see C) compared to the 124 aa of human PS2V (see C). **C**. PS2V and putative PS1IV proteins. There is no recognisable sequence homology between these protein sequences. **D**. The apparently bipartite binding site of HMGA1a protein on exon 5 of human *PSEN2* transcripts is highly conserved in most mammals but not, apparently, rodents of the family *Muridae* including *Mus musculus and Rattus norvegicus* or in the chicken or the amphibian *Xenopus laevis*. In zebrafish the Hmga1-binding site is more highly conserved in *psen1* than *psen2* transcripts implying that splicing of the ancestral *PRESENILIN* gene was regulated by HMGA1-binding before the ancient duplication event that formed *PSEN1* and *PSEN2*. Yellow highlighting indicates the Hmga1a-binding

site in exon 5 of zebrafish *psen1* transcripts. The sequence to which morpholino MoHmga1BindBlock hybridises to inhibit the action of Hmga1 is shown. Arrowheads indicate conserved HMGA1a-binding sites.

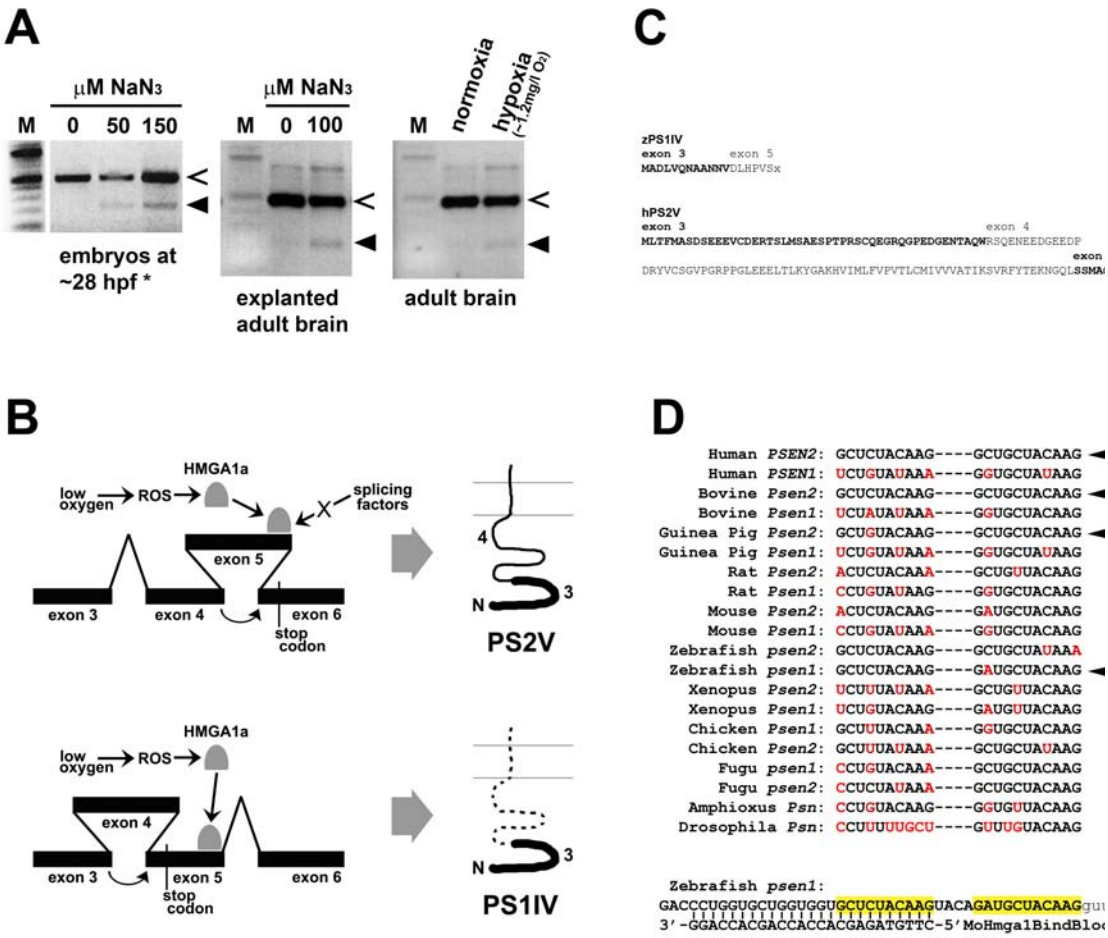
A
μM NaN3
M 0 50 150
embryos at ~28 hpf *
μM NaN3
M 0 100
explanted adult brain
M
normoxia
hypoxia (~1.2mg/l O2)
adult brain
C
zPS1IV
exon 3 exon 5
MADLVQNAANNVDLHPVSx
hPS2V
exon 3 exon 4
MLTFMASDSEEEVCDERTSLMSAESPTPRSCQEGRQGPEDGENTAQWRSQENEEDGEEDP
exon
DRYVCSGVPGRPPGLEEELTLKYGAKHVIMLFVPVTLCMIVVVATIKSVRFYTEKNGQLSSMA
B
HMGA1a
low oxygen
ROS
splicing factors
exon 3
exon 4
exon 5
exon 6
stop codon
4
N
3
PS2V
HMGA1a
low oxygen
ROS
exon 4
exon 3
exon 5
exon 6
stop codon
N
3
PS1IV
D
Human PSEN2: GCUCUACAAG----GCUGCUACAAG
Human PSEN1: UCUGUAUAAA----GGUGCUAUAAG
Bovine Psen2: GCUCUACAAG----GCUGCUACAAG
Bovine Psen1: UCUAUAUAAA----GGUGCUACAAG
Guinea Pig Psen2: GCUGUACAAG----GCUGCUACAAG
Guinea Pig Psen1: UCUGUAUAAA----GGUGCUAUAAG
Rat Psen2: ACUCUACAAA----GCUGUUACAAG
Rat Psen1: CCUGUAUAAG----GGUGCUACAAG
Mouse Psen2: ACUCUACAAG----GAUGCUACAAG
Mouse Psen1: CCUGUAUAAA----GGUGCUACAAG
Zebrafish psen2: GCUCUACAAG----GCUGCUAUAAA
Zebrafish psen1: GCUCUACAAG----GAUGCUACAAG
Xenopus Psen2: UCUUUAUAAA----GCUGUUACAAG
Xenopus Psen1: UCUGUACAAG----GAUGUUACAAG
Chicken Psen1: GCUUUACAAA----GGUGCUACAAG
Chicken Psen2: GCUUUAUAAA----GCUGCUAUAAG
Fugu psen1: CCUGUACAAA----GCUGCUACAAG
Fugu psen2: CCUCUAUAAA----GCUGCUACAAG
Amphioxus Psn: CCUGUACAAG----GGUGUUACAAG
Drosophila Psn: CCUUUUUGCU----GUUGUACAAG
Zebrafish psen1:
GACCCUGGUGCUGGUGGUGCUCUACAAGUACAGAUGCUACAAGgu
3'-GGACCACGACCACCACGAGATGTTC-5'MoHmga1BindBlo

Figure 3

A. Mimicry of hypoxia by NaN_3 exposure induces the alternative splicing event in *psen1* transcripts that generates PS1IV as revealed by RT-PCR between exons 3 and 7. Injection of an inactive, negative control morpholino MoCont has no apparent effect on PS1IV formation (filled arrowhead) but injection of MoHmga1BindBlock that binds over part of the putative Hmga1 binding site in exon 5 of *psen1* transcripts inhibits PS1IV formation. **B**. Injection into zebrafish embryos of a morpholino inhibiting translation of Hmga1a mRNA, MoHmga1aTlnB, blocks formation of PS1IV under chemical mimicry of hypoxia (filled arrowhead). **C**. Injection into zebrafish embryos of mRNA coding either for zebrafish Hmga1a protein (**C**$^{\mathbf{1}}$) or human HMGA1a protein (**C**$^{\mathbf{2}}$) can induce formation of PS1IV under normoxia (filled arrowheads). Co-injection of MoHmga1BindBlock blocks this induction. **D**. qPCR detecting specifically PS1IV formation indicates at least a 3-fold induction of PS1IV by forced expression of zebrafish Hmga1a under normoxia. All PCRs were conducted on embryos at 48 hpf. Unfilled arrowheads indicate cDNA amplified from full-length trancripts.

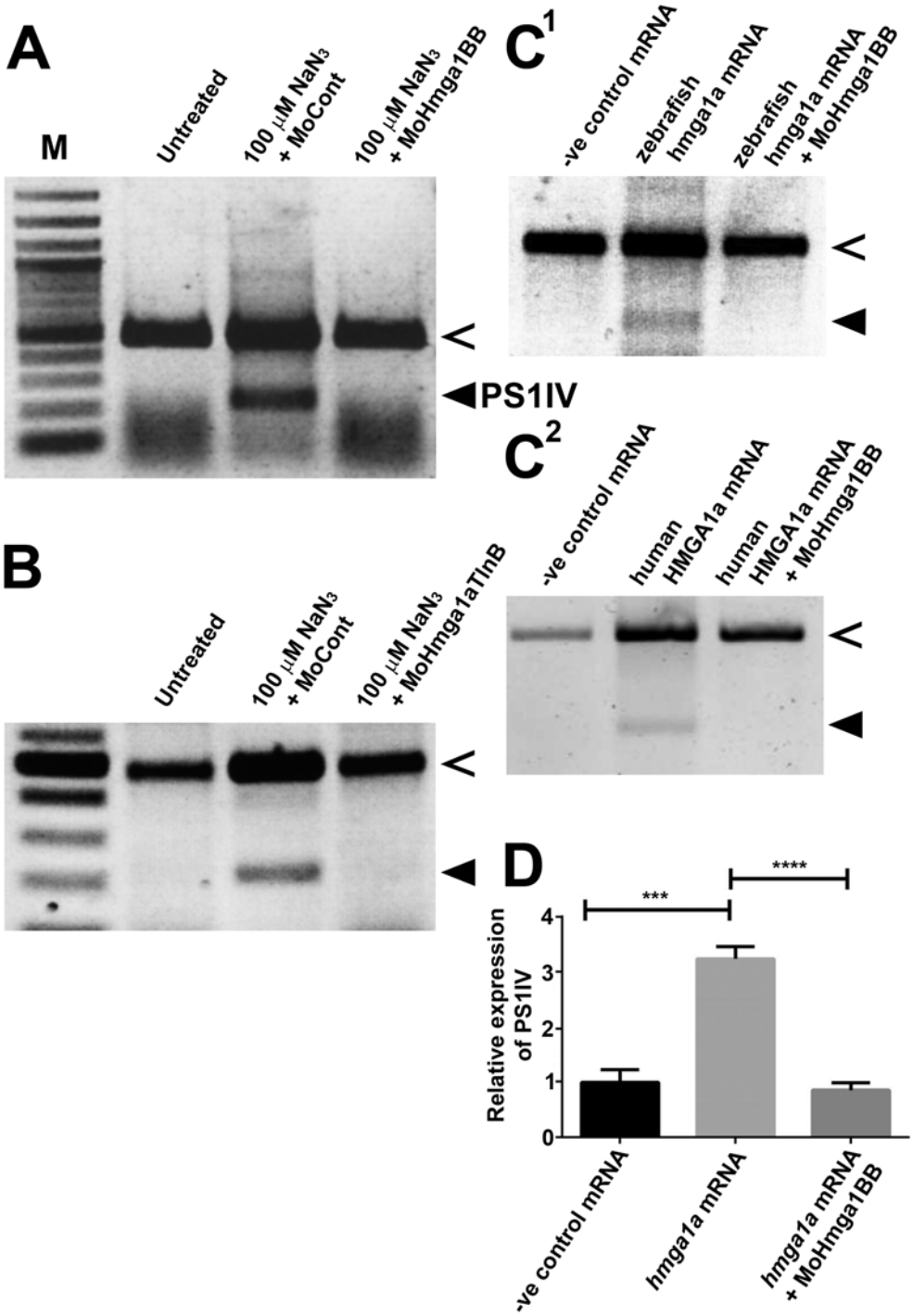
A
M
Untreated
100 μM NaN3 + MoCont
100 μM NaN3 + MoHmga1BB
PS1IV
B
Untreated
100 μM NaN3 + MoCont
100 μM NaN3 + MoHmga1aTInB
C1
-ve control mRNA
zebrafish hmga1a mRNA
zebrafish hmga1a mRNA + MoHmga1BB
C2
-ve control mRNA
human HMGA1a mRNA
human HMGA1a mRNA + MoHmga1BB
D
Relative expression of PS1IV
***
****
-ve control mRNA
hmga1a mRNA
hmga1a mRNA + MoHmga1BB

Figure 4

A. Assay for γ-secretase cleavage of an Appa-derived substrate as described in (32). Values significantly below 1.0 (horizontal line) indicate increased γ-secretase cleavage of the substrate while values significantly above 1.0 indicate decreased γ-secretase activity. **, $p<0.01$; ****, $p<0.0001$; ns, not significant ($p\geq0.01$). Error bars are standard errors of the means. DAPT indicates treatment with 100 μM of this γ-secretase inhibitor. All the truncations except the PS2V-equivalent truncation of zebrafish Psen2 can stimulate γ-secretase activity. **B**. *Neurogenin1* expression-based assay of Notch signalling as described in (29). All the truncations except the PS2V-equivalent truncation of zebrafish Psen2 can significantly stimulate Notch signalling. + indicates $p<0.000000001$; ns, not significant ($p\geq0.01$).

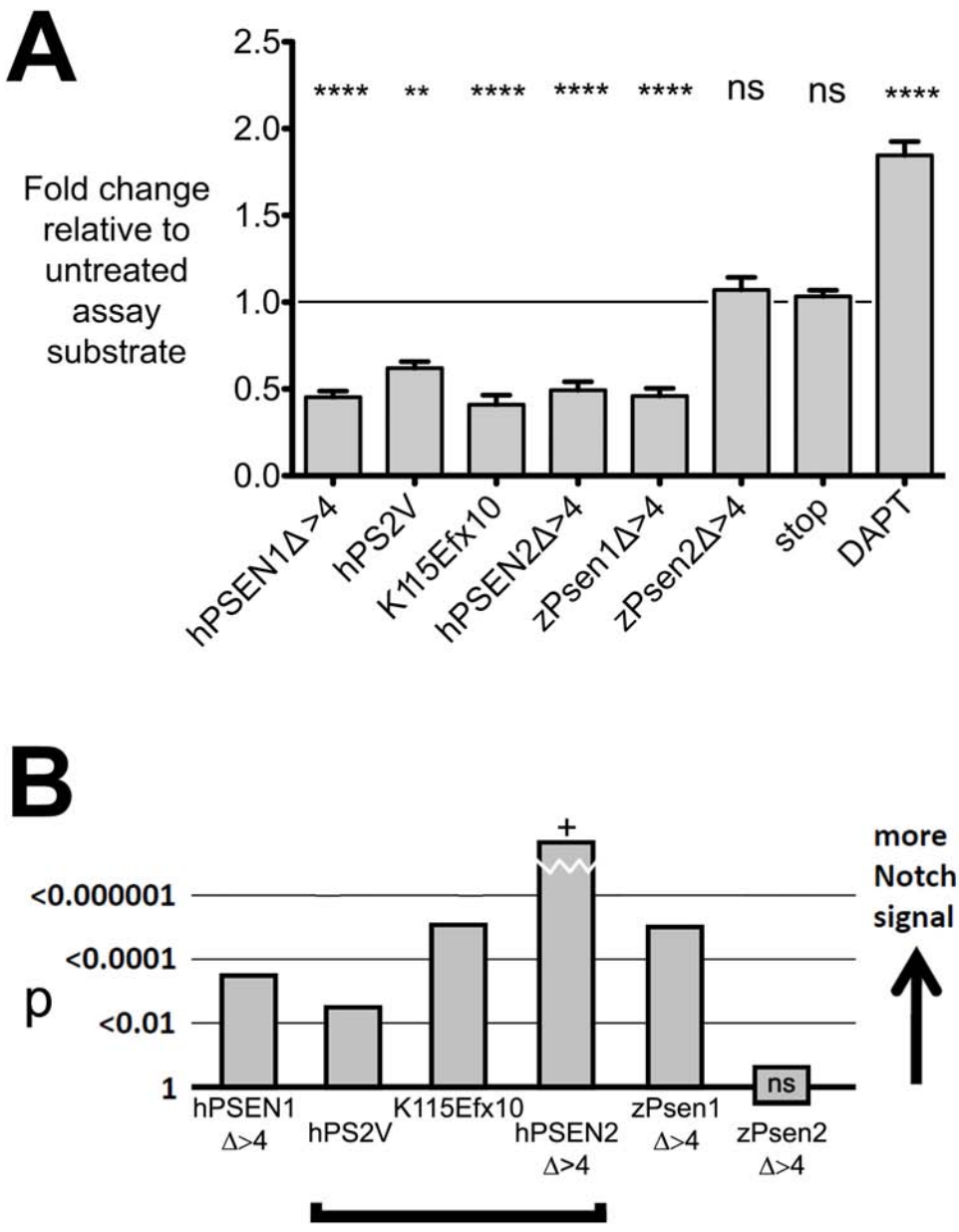
A
Fold change relative to untreated assay substrate
2.5
2.0
1.5
1.0
0.5
0.0
**** ** **** **** **** ns ns ****
hPSEN1Δ>4
hPS2V
K115Efx10
hPSEN2Δ>4
zPsen1Δ>4
zPsen2Δ>4
stop
DAPT
B
p
<0.000001
<0.0001
<0.01
1
+
more Notch signal
ns
hPSEN1 Δ>4
hPS2V
K115Efx10
hPSEN2 Δ>4
zPsen1 Δ>4
zPsen2 Δ>4

Figure 5

A. Assay for γ-secretase cleavage of an Appa-derived substrate as described in (32). Values significantly below 1.0 (horizontal line) indicate increased γ-secretase cleavage of the substrate while values significantly above 1.0 indicate decreased γ-secretase activity. Only zebrafish *psen1* exon3-derived sequences, zPS1IV and zPsen1D>3 show an ability to stimulate γ-secretase cleavage. The exon 3-derived protein sequences of zebrafish Psen2 and human PSEN1 and PSEN2 lack this activity. (Truncations of human PSEN1 and PSEN2 proteins require exon 4-derived sequences in order to stimulate γ-secretase cleavage of Appa, see Figure 4A). **, $p<0.01$; ****, $p<0.0001$; ns, not significant ($p\geq0.01$). Error bars are standard errors of the means. DAPT indicates treatment with 100 μM of this γ-secretase inhibitor. **B**. *Neurogenin1* expression-based assay of Notch signalling as described in (29). Only zebrafish *psen1* exon3-derived sequence zPsen1D>3 shows an ability to stimulate Notch signalling. ns, not significant ($p\geq0.01$).

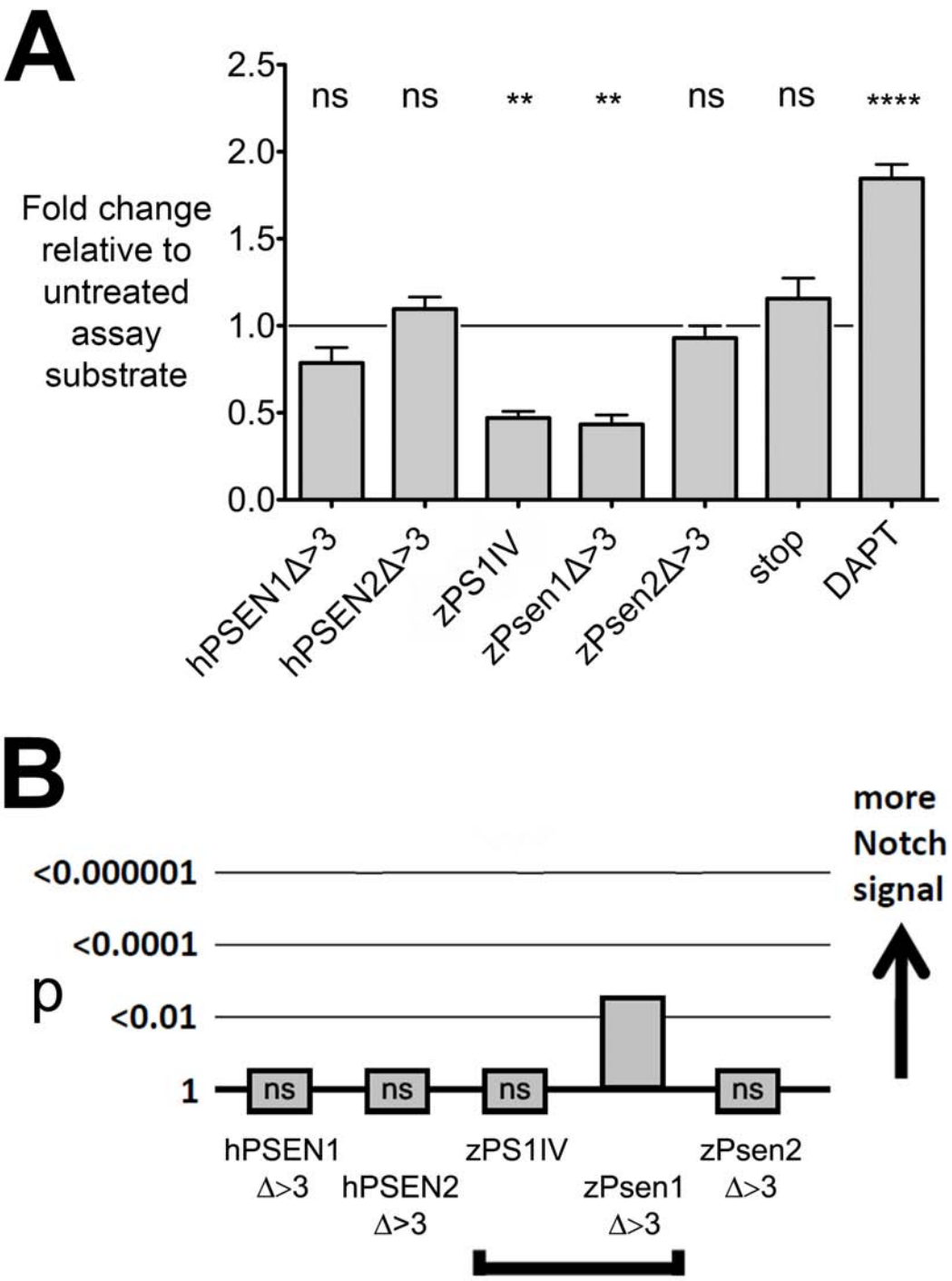
A
Fold change relative to untreated assay substrate
2.5
2.0
1.5
1.0
0.5
0.0
ns
ns
**
**
ns
ns
****
hPSEN1Δ>3
hPSEN2Δ>3
zPS1IV
zPsen1Δ>3
zPsen2Δ>3
stop
DAPT
B
p
<0.000001
<0.0001
<0.01
1
more Notch signal
ns
ns
ns
ns
hPSEN1 Δ>3
hPSEN2 Δ>3
zPS1IV
zPsen1 Δ>3
zPsen2 Δ>3

Figure 6

A qPCR-based assay for induction of the unfolded protein response (UPR) by tunicamycin (Tun) based on changes in zebrafish *xbp1* splicing (42). Injection of negative control untranslatable mRNA (Control) or mRNA encoding a truncation of human Psen2 protein equivalent to human PS2V (zPsen2D>4) is unable to prevent many fold induction of the UPR. In contrast, an equivalent truncation of human PSEN2 (hPSEN2D>4) or protein coded only by exon 3 of zebrafish *psen1* (zPsen1D>3) can both severely inhibit UPR induction (arrows). "-" indicates no exposure to tunicamycin.

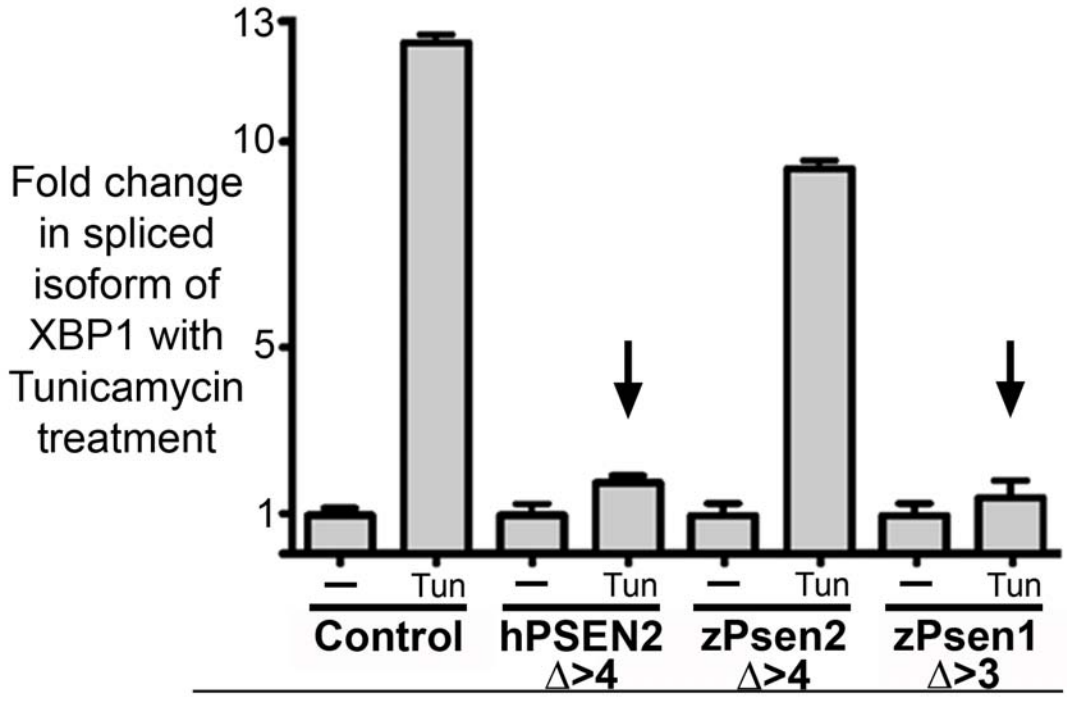

Figure 7

Microarray comparisons to detect statistically significant changes in gene expression including the control comparisons used to refine the set of genes for which expression is altered by loss of PS1V (under mimicry of hypoxia).

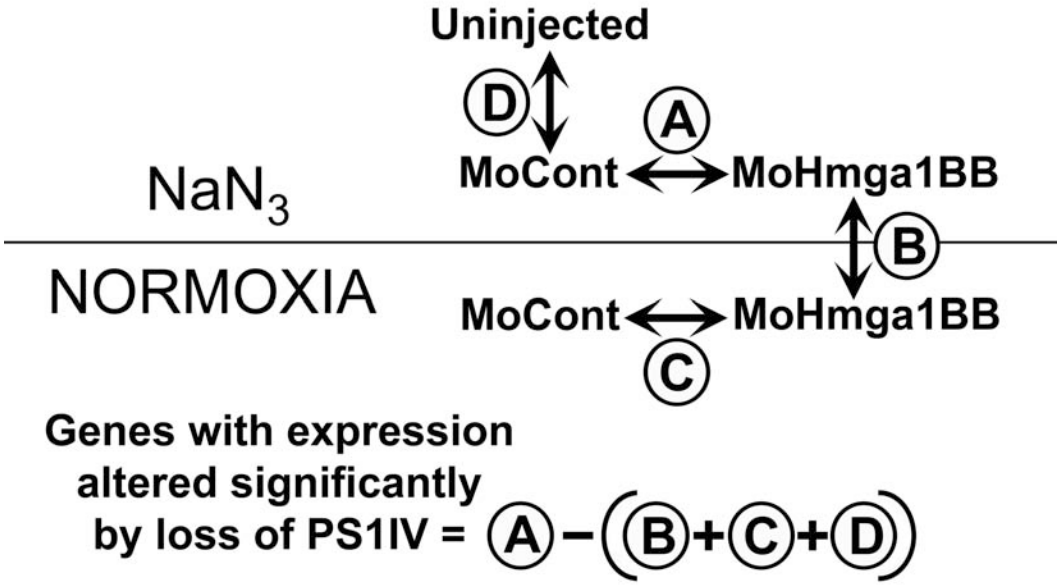

Tables

Table 1. Genes with altered transcript levels due to expression of PS1IV (p≤0.05)

Genes up-regulated by PS1IV					Genes down-regulated by PS1IV				
GENE NAME	**FOLD CHANGE***	**p-VALUE**	**qPCR ?**	**POSSIBLE ROLE**	**GENE NAME**	**FOLD CHANGE***	**p-VALUE**	**qPCR ?**	**POSSIBLE ROLE**
TUBB	-4.01	2.33E-15		Cytoskelet.	*HSPA4*	3.85	1.09E-11		Hsp70 prot8
IL1B	-2.87	0.0075	**	Immun.	*PIM3*	2.80	0.00020		Prolif.
POU4F2	-2.49	3.65E-12		Txn. factor	*CAMTA1*	2.47	2.73E-07	**	EENPCA
SRCAP	-2.45	6.66E-07		Chromatin	*ANGPTL2*	2.02	3.07E-07		Immun.
CKMT1A	-2.36	8.44E-10			*RICTOR*	1.83	8.6E-05		↑AKT
RPL9	-2.26	2.09E-06		Ribo. prot.	*PKD1*	1.77	0.00056	**	
AIDA	-2.24	1.02E-08			*HRH2*	1.72	9.85E-05		Immun.
CALR	-2.14	0.00021		UPR	*HLA-DPB1*	1.67	0.0029		
SYN2	-2.10	9.42E-07			*IRF4*	1.67	0.0017	**	Immun.
AMPD1	-2.08	0.00085			*RBM5*	1.64	0.0017		
HSDL2	-2.08	4.92E-08			*PTPRH*	1.58	0.0035		
GBX2	-2.02	1.28E-06		Brain dev.	*ECM2*	1.49	0.00069		
SSU72	-1.99	8.32E-05			*IL17RA*	1.47	0.0012		Immun.
UBAC1	-1.92	3.98E-06			*NLRP3*	1.44	0.0088		Immun.
LSMD1	-1.91	2.01E-08			*ACY1*	1.44	0.0033		Immun./Prolif.
POP7	-1.85	1.68E-06			*NOTCH2*	1.44	0.039		
TCF25	-1.83	4.22E-06			*MSL1*	1.40	0.018		
RAB3C	-1.80	5.40E-05		Prolif.	*OLFM4*	1.40	0.00083		Prolif.
RPS15A	-1.79	0.048		Ribo. prot.	*NRN1L*	1.39	0.051		
SGCG	-1.74	0.00065		Cytoskelet.	*EBP*	1.37	0.040		Cholesterol
RRM2	-1.70	0.00079			*POLR3G*	1.36	0.00065		
CETN2	-1.69	1.93E-05			*CD22*	1.34	0.020		Immun.
HSPA8	-1.67	0.016			*FOXE3*	1.31	0.0026		Txn. factor
TRIB2	-1.65	4.84E-07			*HTR3B*	1.30	0.00088		
MAPKAPK5	-1.60	7.23E-06	**	Immun.	*GAK*	1.23	0.0065		
TTC26	-1.58	0.0051			*MRC2*	1.23	0.048		
RPL7A	-1.58	1.18E-05			*AGTR1*	1.21	0.033		
SLC25A5	-1.57	0.018							
OCRL	-1.53	0.0026			**Abbreviations**				
SHISA7	-1.51	0.015			↑AKT = Involved in activation of AKT				
RGS8	-1.48	0.0069			Apoptosis = Implicated in apoptosis or its regulation				
TRIAP1	-1.46	9.17E-05		Apoptosis	Brain dev. = Regulates brain development				
SMARCA4	-1.44	0.0127	**		Cholesterol = Implicated in cholesterol regulation				
RPS20	-1.43	0.014			Chromatin = Implicated in regulation of chromatin structure				
RPL28	-1.39	0.0027		Ribo. prot.	Cytoskelet. = Implicated in cytoskeleton or its regulation				
RPL26	-1.39	0.0027		Ribo. prot.	EENPCA = Involved in Cellular Ataxia, Non-Progressive with Mental Retardation.				
PLCB1	-1.36	0.0076			Immun. = Implicated in Immunity / Inflammation				
EEF1B2	-1.34	0.019			PIP3 = Binds to PIP3				
MRPS12	-1.30	0.0060			Ribo. prot. = Ribosomal protein				
NLRP12	-1.28	0.0017		Immun.	Txn. Factor = transcription factor				
GORASP1	-1.24	0.049			UPR = Involved in unfolded protein response				
PLEKHA4	-1.14	0.017		PIP3 signal	qPCR? = Direction of change in expression confirmed by qPCR				
GRAMD1B	-1.13	0.022							
RPS19	-1.09	0.050		Ribo. prot.					
GZMM	-1.08	0.048		Immun.	*This is the fold change in the presence of MoHmga1BindBlock, Hence genes normally upregulated by PS1IV show decreased expression and vice versa.				

References

1 Smolarkiewicz, M., Skrzypczak, T. and Wojtaszek, P. (2013) The very many faces of presenilins and the gamma-secretase complex. *Protoplasma*.

2 Lee, J.H., Yu, W.H., Kumar, A., Lee, S., Mohan, P.S., Peterhoff, C.M., Wolfe, D.M., Martinez-Vicente, M., Massey, A.C., Sovak, G. *et al.* (2010) Lysosomal proteolysis and autophagy require presenilin 1 and are disrupted by Alzheimer-related PS1 mutations. *Cell*, **141**, 1146-1158.

3 Kang, D.E., Soriano, S., Xia, X., Eberhart, C.G., De Strooper, B., Zheng, H. and Koo, E.H. (2002) Presenilin couples the paired phosphorylation of beta-catenin independent of axin: implications for beta-catenin activation in tumorigenesis. *Cell*, **110**, 751-762.

4 Li, J., Xu, M., Zhou, H., Ma, J. and Potter, H. (1997) Alzheimer presenilins in the nuclear membrane, interphase kinetochores, and centrosomes suggest a role in chromosome segregation. *Cell*, **90**, 917-927.

5 Boeras, D.I., Granic, A., Padmanabhan, J., Crespo, N.C., Rojiani, A.M. and Potter, H. (2008) Alzheimer's presenilin 1 causes chromosome missegregation and aneuploidy. *Neurobiol Aging*, **29**, 319-328.

6 Cruts, M., Theuns, J. and Van Broeckhoven, C. (2012) Locus-specific mutation databases for neurodegenerative brain diseases. *Hum Mutat*, **33**, 1340-1344.

7 Sato, N., Hori, O., Yamaguchi, A., Lambert, J.C., Chartier-Harlin, M.C., Robinson, P.A., Delacourte, A., Schmidt, A.M., Furuyama, T., Imaizumi, K. *et al.* (1999) A novel presenilin-2 splice variant in human Alzheimer's disease brain tissue. *Journal of Neurochemistry*, **72**, 2498-2505.

8 Sato, N., Imaizumi, K., Manabe, T., Taniguchi, M., Hitomi, J., Katayama, T., Yoneda, T., Morihara, T., Yasuda, Y., Takagi, T. *et al.* (2001) Increased production of beta-amyloid and vulnerability to endoplasmic reticulum stress by an aberrant spliced form of presenilin 2. *Journal of Biological Chemistry*, **276**, 2108-2114.

9 Manabe, T., Katayama, T., Sato, N., Gomi, F., Hitomi, J., Yanagita, T., Kudo, T., Honda, A., Mori, Y., Matsuzaki, S. *et al.* (2003) Induced HMGA1a expression causes aberrant splicing of Presenilin-2 pre-mRNA in sporadic Alzheimer's disease. *Cell Death and Differentiation*, **10**, 698-708.

10 Manabe, T., Ohe, K., Katayama, T., Matsuzaki, S., Yanagita, T., Okuda, H., Bando, Y., Imaizumi, K., Reeves, R., Tohyama, M. *et al.* (2007) HMGA1a: sequence-specific RNA-binding factor causing sporadic Alzheimer's disease-linked exon skipping of presenilin-2 pre-mRNA. *Genes to Cells*, **12**, 1179-1191.

11 Cleynen, I. and Van de Ven, W.J. (2008) The HMGA proteins: a myriad of functions (Review). *Int J Oncol*, **32**, 289-305.

12 Zhou, X., Benson, K.F., Ashar, H.R. and Chada, K. (1995) Mutation responsible for the mouse pygmy phenotype in the developmentally regulated factor HMGI-C. *Nature*, **376**, 771-774.

13 Yanagita, T., Manabe, T., Okuda, H., Matsuzaki, S., Bando, Y., Katayama, T. and Tohyama, M. (2005) Possible involvement of the expression and phosphorylation of N-Myc in the induction of HMGA1a by hypoxia in the human neuroblastoma cell line. *Neurosci Lett*, **374**, 47-52.

14 Moussavi Nik, S.H., Newman, M. and Lardelli, M. (2011) The response of HMGA1 to changes in oxygen availability is evolutionarily conserved. *Exp Cell Res*, **317**, 1503-1512.
15 Shah, S.N. and Resar, L.M. (2012) High mobility group A1 and cancer: potential biomarker and therapeutic target. *Histol Histopathol*, **27**, 567-579.
16 Gustafsson, M.V., Zheng, X., Pereira, T., Gradin, K., Jin, S., Lundkvist, J., Ruas, J.L., Poellinger, L., Lendahl, U. and Bondesson, M. (2005) Hypoxia requires notch signaling to maintain the undifferentiated cell state. *Dev Cell*, **9**, 617-628.
17 Coleman, M.L., McDonough, M.A., Hewitson, K.S., Coles, C., Mecinovic, J., Edelmann, M., Cook, K.M., Cockman, M.E., Lancaster, D.E., Kessler, B.M. *et al.* (2007) Asparaginyl hydroxylation of the Notch ankyrin repeat domain by factor inhibiting hypoxia-inducible factor. *J Biol Chem*, **282**, 24027-24038.
18 Zheng, X., Linke, S., Dias, J.M., Zheng, X., Gradin, K., Wallis, T.P., Hamilton, B.R., Gustafsson, M., Ruas, J.L., Wilkins, S. *et al.* (2008) Interaction with factor inhibiting HIF-1 defines an additional mode of cross-coupling between the Notch and hypoxia signaling pathways. *Proc Natl Acad Sci U S A*, **105**, 3368-3373.
19 Mukherjee, T., Kim, W.S., Mandal, L. and Banerjee, U. (2011) Interaction between Notch and Hif-alpha in development and survival of Drosophila blood cells. *Science*, **332**, 1210-1213.
20 Correia, S.C., Carvalho, C., Cardoso, S., Santos, R.X., Placido, A.I., Candeias, E., Duarte, A.I. and Moreira, P.I. (2013) Defective HIF Signaling Pathway And Brain Response To Hypoxia In Neurodegenerative Diseases: Not An "Iffy" Question! *Current pharmaceutical design*.
21 Moussavi Nik, S.H., Wilson, L., Newman, M., Croft, K., Mori, T.A., Musgrave, I. and Lardelli, M. (2012) The BACE1-PSEN-AbetaPP regulatory axis has an ancient role in response to low oxygen/oxidative stress. *J Alzheimers Dis*, **28**, 515-530.
22 Ethell, D.W. (2010) An amyloid-notch hypothesis for Alzheimer's disease. *The Neuroscientist : a review journal bringing neurobiology, neurology and psychiatry*, **16**, 614-617.
23 Jayadev, S., Leverenz, J.B., Steinbart, E., Stahl, J., Klunk, W., Yu, C.E. and Bird, T.D. (2010) Alzheimer's disease phenotypes and genotypes associated with mutations in presenilin 2. *Brain*, **133**, 1143-1154.
24 Sharman, M.J., Moussavi Nik, S.H., Chen, M.M., Ong, D., Wijaya, L., Laws, S.M., Taddei, K., Newman, M., Lardelli, M., Martins, R.N. *et al.* (2013) The Guinea Pig as a Model for Sporadic Alzheimer's Disease (AD): The Impact of Cholesterol Intake on Expression of AD-Related Genes. *PLoS One*, **8**, e66235.
25 Einhauer, A. and Jungbauer, A. (2001) The FLAG peptide, a versatile fusion tag for the purification of recombinant proteins. *J Biochem Biophys Methods*, **49**, 455-465.
26 Kozak, M. (1987) An analysis of 5'-noncoding sequences from 699 vertebrate messenger RNAs. *Nucleic Acids Res*, **15**, 8125-8148.
27 Field, J., Nikawa, J., Broek, D., MacDonald, B., Rodgers, L., Wilson, I.A., Lerner, R.A. and Wigler, M. (1988) Purification of a RAS-responsive adenylyl cyclase complex from Saccharomyces cerevisiae by use of an epitope addition method. *Mol Cell Biol*, **8**, 2159-2165.

28 Ro, H., Soun, K., Kim, E.J. and Rhee, M. (2004) Novel vector systems optimized for injecting in vitro-synthesized mRNA into zebrafish embryos. *Molecules and Cells*, **17**, 373-376.
29 Nornes, S., Newman, M., Verdile, G., Wells, S., Stoick-Cooper, C.L., Tucker, B., Frederich-Sleptsova, I., Martins, R. and Lardelli, M. (2008) Interference with splicing of Presenilin transcripts has potent dominant negative effects on Presenilin activity. *Hum Mol Genet*, **17**, 402-412.
30 Ro, H., Soun, K., Kim, E.J. and Rhee, M. (2004) Novel vector systems optimized for injecting in vitro-synthesized mRNA into zebrafish embryos. *Mol Cells*, **17**, 373-376.
31 Westerfield, M. (2007) *The Zebrafish Book: A guide for the laboratory use of zebrafish (Danio rerio)*. University of Oregon Press, Eugene, OR, USA.
32 Wilson, L. and Lardelli, M. (2013) The Development of an in vivo gamma-Secretase Assay using Zebrafish Embryos. *J Alzheimers Dis*.
33 Gansner, J.M. and Gitlin, J.D. (2008) Essential role for the alpha 1 chain of type VIII collagen in zebrafish notochord formation. *Dev Dyn*, **237**, 3715-3726.
34 Wu, Z.J., Irizarry, R.A., Gentleman, R., Martinez-Murillo, F. and Spencer, F. (2004) A model-based background adjustment for oligonucleotide expression arrays. *Journal of the American Statistical Association*, **99**, 909-917.
35 Bolstad, B.M., Irizarry, R.A., Astrand, M. and Speed, T.P. (2003) A comparison of normalization methods for high density oligonucleotide array data based on variance and bias. *Bioinformatics*, **19**, 185-193.
36 Irizarry, R.A., Bolstad, B.M., Collin, F., Cope, L.M., Hobbs, B. and Speed, T.P. (2003) Summaries of Affymetrix GeneChip probe level data. *Nucleic Acids Res*, **31**, e15.
37 Irizarry, R.A., Hobbs, B., Collin, F., Beazer-Barclay, Y.D., Antonellis, K.J., Scherf, U. and Speed, T.P. (2003) Exploration, normalization, and summaries of high density oligonucleotide array probe level data. *Biostatistics*, **4**, 249-264.
38 Fox, R.J. and Dimmic, M.W. (2006) A two-sample Bayesian t-test for microarray data. *BMC bioinformatics*, **7**, 126.
39 Leimer, U., Lun, K., Romig, H., Walter, J., Grunberg, J., Brand, M. and Haass, C. (1999) Zebrafish (Danio rerio) presenilin promotes aberrant amyloid beta-peptide production and requires a critical aspartate residue for its function in amyloidogenesis. *Biochemistry*, **38**, 13602-13609.
40 Groth, C., Nornes, S., McCarty, R., Tamme, R. and Lardelli, M. (2002) Identification of a second presenilin gene in zebrafish with similarity to the human Alzheimer's disease gene presenilin2. *Dev Genes Evol*, **212**, 486-490.
41 Kumar, S. and Hedges, S.B. (1998) A molecular timescale for vertebrate evolution. *Nature*, **392**, 917-920.
42 Hu, M.C., Gong, H.Y., Lin, G.H., Hu, S.Y., Chen, M.H., Huang, S.J., Liao, C.F. and Wu, J.L. (2007) XBP-1, a key regulator of unfolded protein response, activates transcription of IGF1 and Akt phosphorylation in zebrafish embryonic cell line. *Biochem Biophys Res Commun*, **359**, 778-783.
43 Rubinsztein, D.C., DiFiglia, M., Heintz, N., Nixon, R.A., Qin, Z.H., Ravikumar, B., Stefanis, L. and Tolkovsky, A. (2005) Autophagy and its possible roles in nervous system diseases, damage and repair. *Autophagy*, **1**, 11-22.

44 Wang, B., Yang, W., Wen, W., Sun, J., Su, B., Liu, B., Ma, D., Lv, D., Wen, Y., Qu, T. *et al.* (2010) Gamma-secretase gene mutations in familial acne inversa. *Science*, **330**, 1065.
45 Tseng, W.E., Chen, C.M., Chen, Y.C., Yi, Z., Tan, E.K. and Wu, Y.R. (2013) Genetic Variations of GAK in Two Chinese Parkinson's Disease Populations: A Case-Control Study. *PLoS One*, **8**, e67506.
46 Thevenon, J., Lopez, E., Keren, B., Heron, D., Mignot, C., Altuzarra, C., Beri-Dexheimer, M., Bonnet, C., Magnin, E., Burglen, L. *et al.* (2012) Intragenic CAMTA1 rearrangements cause non-progressive congenital ataxia with or without intellectual disability. *Journal of medical genetics*, **49**, 400-408.
47 Area-Gomez, E., de Groof, A.J.C., Boldogh, I., Bird, T.D., Gibson, G.E., Koehler, C.M., Yu, W.H., Duff, K.E., Yaffe, M.P., Pon, L.A. *et al.* (2009) Presenilins Are Enriched in Endoplasmic Reticulum Membranes Associated with Mitochondria. *American Journal of Pathology*, **175**, 1810-1816.
48 Simmen, T., Lynes, E.M., Gesson, K. and Thomas, G. (2010) Oxidative protein folding in the endoplasmic reticulum: tight links to the mitochondria-associated membrane (MAM). *Biochim Biophys Acta*, **1798**, 1465-1473.
49 Bell, E.L., Klimova, T.A., Eisenbart, J., Moraes, C.T., Murphy, M.P., Budinger, G.R.S. and Chandel, N.S. (2007) The Q(o) site of the mitochondrial complex III is required for the transduction of hypoxic signaling via reactive oxygen species production. *J Cell Biol*, **177**, 1029-1036.
50 Giuffrida, M.L., Caraci, F., De Bona, P., Pappalardo, G., Nicoletti, F., Rizzarelli, E. and Copani, A. (2010) The monomer state of beta-amyloid: where the Alzheimer's disease protein meets physiology. *Reviews in the neurosciences*, **21**, 83-93.
51 Baruch-Suchodolsky, R. and Fischer, B. (2009) Abeta40, either soluble or aggregated, is a remarkably potent antioxidant in cell-free oxidative systems. *Biochemistry*, **48**, 4354-4370.
52 Nadal, R.C., Rigby, S.E. and Viles, J.H. (2008) Amyloid beta-Cu2+ complexes in both monomeric and fibrillar forms do not generate H2O2 catalytically but quench hydroxyl radicals. *Biochemistry*, **47**, 11653-11664.
53 Smith, M.A., Casadesus, G., Joseph, J.A. and Perry, G. (2002) Amyloid-beta and tau serve antioxidant functions in the aging and Alzheimer brain. *Free Radic Biol Med*, **33**, 1194-1199.
54 Kontush, A. (2001) Amyloid-beta: an antioxidant that becomes a pro-oxidant and critically contributes to Alzheimer's disease. *Free Radic Biol Med*, **31**, 1120-1131.
55 Kontush, A., Donarski, N. and Beisiegel, U. (2001) Resistance of human cerebrospinal fluid to in vitro oxidation is directly related to its amyloid-beta content. *Free radical research*, **35**, 507-517.
56 Huang, X., Atwood, C.S., Hartshorn, M.A., Multhaup, G., Goldstein, L.E., Scarpa, R.C., Cuajungco, M.P., Gray, D.N., Lim, J., Moir, R.D. *et al.* (1999) The A beta peptide of Alzheimer's disease directly produces hydrogen peroxide through metal ion reduction. *Biochemistry*, **38**, 7609-7616.
57 Rival, T., Page, R.M., Chandraratna, D.S., Sendall, T.J., Ryder, E., Liu, B., Lewis, H., Rosahl, T., Hider, R., Camargo, L.M. *et al.* (2009) Fenton chemistry and oxidative stress mediate the toxicity of the beta-amyloid peptide in a Drosophila model of Alzheimer's disease. *Eur J Neurosci*, **29**, 1335-1347.

58 Smith, C.D., Carney, J.M., Starke-Reed, P.E., Oliver, C.N., Stadtman, E.R., Floyd, R.A. and Markesbery, W.R. (1991) Excess brain protein oxidation and enzyme dysfunction in normal aging and in Alzheimer disease. *Proc Natl Acad Sci U S A*, **88**, 10540-10543.
59 Martins, R.N., Harper, C.G., Stokes, G.B. and Masters, C.L. (1986) Increased cerebral glucose-6-phosphate dehydrogenase activity in Alzheimer's disease may reflect oxidative stress. *J Neurochem*, **46**, 1042-1045.
60 Liu, Y., Liu, F., Iqbal, K., Grundke-Iqbal, I. and Gong, C.X. (2008) Decreased glucose transporters correlate to abnormal hyperphosphorylation of tau in Alzheimer disease. *FEBS Lett*, **582**, 359-364.
61 Lu, T., Pan, Y., Kao, S.Y., Li, C., Kohane, I., Chan, J. and Yankner, B.A. (2004) Gene regulation and DNA damage in the ageing human brain. *Nature*, **429**, 883-891.
62 Soucek, T., Cumming, R., Dargusch, R., Maher, P. and Schubert, D. (2003) The regulation of glucose metabolism by HIF-1 mediates a neuroprotective response to amyloid beta peptide. *Neuron*, **39**, 43-56.
63 Daulatzai, M.A. (2013) Death by a thousand cuts in Alzheimer's disease: hypoxia-the prodrome. *Neurotoxicity research*, **24**, 216-243.
64 Launer, L.J. (2002) Demonstrating the case that AD is a vascular disease: epidemiologic evidence. *Ageing research reviews*, **1**, 61-77.
65 Yarchoan, M., Xie, S.X., Kling, M.A., Toledo, J.B., Wolk, D.A., Lee, E.B., Van Deerlin, V., Lee, V.M., Trojanowski, J.Q. and Arnold, S.E. (2012) Cerebrovascular atherosclerosis correlates with Alzheimer pathology in neurodegenerative dementias. *Brain*, **135**, 3749-3756.

Supplemental Data

Supplementary Data File 1

Table 1

PCR primer and morpholino sequences

PCR primers	Sequence (5′–3′)	Amplifies with	To form
zfEx3	CGGAATTCTCACACATTATTGGCAGCATT	zfForwardtag	zPsen1Δ>3
zfEx4	GGAATTCTTACTGCTGTCCGTCCTTCTG	zfForwardtag	zPsen1Δ>4
zfPS2Ex3	GGAATTCTTA CCGTTTGCTGTCTGTGTCCTGG	zfPS2Forwardtag	zPsen2Δ>3
zfEx3++	CGGAATTCTCACGAAACGGGGTGTAGAT CCACATTATTGGCAGCATT	zfForwardtag	zPS1V
zfPS2Ex4	GGAATTCTTACCGCTGTCCGCTCTTC	zfPS2Forwardtag	zPsen2Δ>4
zfTAA	CGGGATCCACCATGGACTACAAAGACGA CGACGACAAAATGGCTGATTAAGTGCAG	zfFullLengthRev	zebrafish “stop” negative control
zfForwardtag	CGGGATCCACCATGGACTACAAAGACGA CGACGACAAAATGGCTGATTTAGTGCAG	zfEx3, zfEx4.	zPsen1Δ>3, zPsen1Δ>4,
zfFullLengthRev	GGAATTCTTATATGTAGAACTGATGGAC G	zfTAA	zebrafish “stop” negative control
zfPS2Forwardtag	CGGGATCCACCATGCAGTACAAAGACGA CGACGACAAAATGAATACCTCAGACAGT GAAGAG	zfPS2Ex3, zfPS2Ex4	zPsen2Δ>3, zPsen2Δ>4,
huEx3	CCGCTCGAGCTATAGCTGCCCATCCTTCC	huForwardtag	hPSEN1Δ>3
huEx4	CCGCTCGAGCTATAGCTGCCCATCCTTC	huForwardtag	hPSEN1Δ>4
huPS2Ex3	CCGCTCGAGCTACCACTGGGCAGTGTTC TCTC	huPS2Forwardtag	hPSEN2Δ>3
huPS2Ex4	CCGCTCGAGCTAGAGCTGTCCATTCTTCT CTG	huPS2Forwardtag	hPSEN2Δ>4

huTAA	CGGGATCCACCATGTACCCATACGATGTTCCAGATTACGCTATGACAGAGTAACCTGCACCG	huFullengthRev	human “stop” negative control
huForwardtag	CGGGATCCACCATGTACCCATACGATGTTCCAGATTACGCTATGACAGAGTTACCTGCACCG	huEx4, huEx3,	hPSEN1Δ>4, Δ>3
huFullLengthRev	CCGCTCGAGCTAGATATAAAATTGATGGAATGC	huTAA	human “stop” negative control
huPS2Forwardtag	CGGGATCCACCATGTACCCATACGATGTTCCAGATTACGCTATGCTCACATTCATGGCCTCTG	huPS2Ex3, huPS2Ex4	hPSEN2Δ>3, hPSEN2Δ>4
xbp-1 (u) sense	GCCCAGCAGTCCCCAAAT	xbp-1 (u/s) anti-sense	zebrafish full length xbp-1
xbp-1 (s) sense	CTGAGTCCGCAGCAGGTG	xbp-1 (u/s) anti-sense	zebrafish spliced xbp-1
xbp-1 (u/s) anti-sense	GGATGTCCAGAATACCAAGCAG	xbp-1 (s) sense xbp-1 (u) sense	zebrafish spliced xbp-1 zebrafish full length xbp-1
hmga1aEcoRI sense	CGGAATTCATGAGTGATTCTGGCAAGG	hmga1aAgeI antisense	zebrafish Hmga1a
hmga1aAgeI antisense	ACCGGTCTTCCTCTGGGTCTCTTCG	hmga1aEcoRI sense	zebrafish Hmga1a
QuikChange™ Site-Directed Mutagenesis primers	**Sequence (5′–3′)**	**Used with primer**	**Produces**
K115Efx10forward	GCGCTTCTACACAGAGAAGAATGGACAGCT	K115Efx10reverse	K115Efx10
K115Efx10reverse	AGCTGTCCATTCTTCTCTGTGTAGAAGCGC	K115Efx10forward	K115Efx10
Morpholinos	**Sequence (5′–3′)**	**Function**	
MoCont	CCTCTTACCTCAGTTACAATTTATA	Negative control morpholino	
MoHmga1aTln	CTGTGTCCTTGCCAGAATCACTCAT	MoHmga1a blocking morpholino	
MoHmga1aBind	CTTGTAGAGCACCACCAGCACCAGG	Psen1 Hmga1a binding site blocker morpholino	

Block(Psen1)			
zf SMARCA4 (F)	CCGCATGAAAAATCACCACTG	zf SMARCA4 (R)	Full length zebrafish SMARCA4
zf SMARCA4 (R)	GGGCAGCAGGAAGTTGAGC	zf SMARCA4 (F)	Full length zebrafish SMARCA4
zfIL1B (F)	GTCATCCAAGAGCGTGAAGTGA	zfIL1B (R)	Full length zebrafish IL1B
zfIL1B (R)	GCTCTCAGTGTGACGGCCT	zfIL1B (F)	Full length zebrafish IL1B
zf MAPKAPK5(F)	CTGGTGTGGATCAACGAGGAA	zf MAPKAPK5(R)	Full length zebrafish MAPKAPK
zf MAPKAPK5(R)	GTAACCCAGACGCTCATTCCAC	zf MAPKAPK5(F)	Full length zebrafish MAPKAPK
zfIRF4 (F)	GCCATCATCAGCGAGTCATCT	zfIRF4(R)	Full length zebrafish IRF4
zfIRF4(R)	TGCCCCTCGTCCTCCAAATAGA	zfIRF4 (F)	Full length zebrafish IRF4
zfCAMTA1(F)	TGAGAAGCCGACTTTGCCTGCTCC	zfCAMTA1(R)	Full length zebrafish CAMTA1
zfCAMTA1(R)	AGGCAAAGTCGGCTTCTCAA	zfCAMTA1(F)	Full length zebrafish CAMTA1
zf PKD1(F)	CGCAGGTTGGAGATTACAGTTTAG	zf PKD1(R)	Full length zebrafish PKD1
zf PKD1(R)	GGCAGGAAGTACACAGTGTTGTTG	zf PKD1(F)	Full length zebrafish PKD1
zfPS1Ex4.dl (F)	TGTGGATCTACACCCCGTTTC	zfPS1Ex4.dl (R)	Zebrafish psen1 IV (zPSIV)
zfPS1Ex4.dl (R)	AGCAGGAGGAGGTTGGAGAAG	zfPS1Ex4.dl (F)	Zebrafish psen1 IV (zPSIV)

Supplementary Data 2

Injection	Embryos counted		Change in *neurogenin-1* expression	Chi-square value	p-value
	Same	**Changed**			
Zebrafish (FLAG TAG mRNA)					
zPsen1Δ>3 100ng/ul Stop	87 93	67 34	lighter	8.47	0.0036
zPsen1ΔIV100ng/ul Stop	139 103	37 32	none	0.32	0.57281206 (ns)
zPsen1Δ>4 200ng/ul Stop	133 140	49 10	lighter	23.189	0.00000922
zPsen2Δ>3 100ng/ul Stop	83 90	33 32	none	0.15	0.70141891 (ns)
zPsen2Δ>4 200ng/ul Stop	93 78	61 45	none	2.69	0.60670571 (ns)
Human (HA TAG mRNA except where noted*)					
hPSEN1Δ>3 100ng/ul Stop	134 103	31 30	none	0.64	0.42298749 (ns)
hPSEN1Δ>4 200ng/ul Stop	93 138	34 14	lighter	16.17	0.00030813
hPSEN2Δ>3 200ng/ul Stop	131 147	27 35	none	0.26	ns
hPSEN2Δ>4 200ng/ul Stop	66 104	60 11	lighter	41.9	0.00000000 (p is very small)
hPSEN2Δ>4 **FLAG*** 200ng/ul Stop	81 100	28 15	lighter	5.768	0.0163
hPS2V 200ng/ul Stop	40 51	20 5	lighter	10.1	0.0014
K115Efx10 200ng/ul Stop	89 101	37 7	lighter	19.95	0.000008

Supplementary Data File 3

MoHmga1aTln Control

As a control to show the ability of MoHmga1aTln to suppress *hmga1a* mRNA translation, the first 135 bases of the *hmga1a* coding sequence was fused in frame to EGFP in the N1-EGFP plasmid at the *EcoRI/AgeI* sites (hmga1a-135-EGFP) (BD Biosciences, NJ, USA) (Primers listed in Table 1). The plasmid was linearised with *NotI* prior to injection. 50ng/ul of the plasmid was co-injected with either 0.5 mM of MoHmga1aTln mixed with MoCont or MoCont alone. Embryos were then observed for GFP fluorescence at ~10hpf using fluorescence microscopy.

Supplementary Figure.

A1,A2, injection of *hmga1a*-135-EGFP and MoCont (13 out of 30 injected embryos had fluorescent spots of GFP expression). **B1,B2,** injection of *hmga1a*-135-EGFP and MoHmga1aTln (none out of 33 injected embryos had GFP expression).

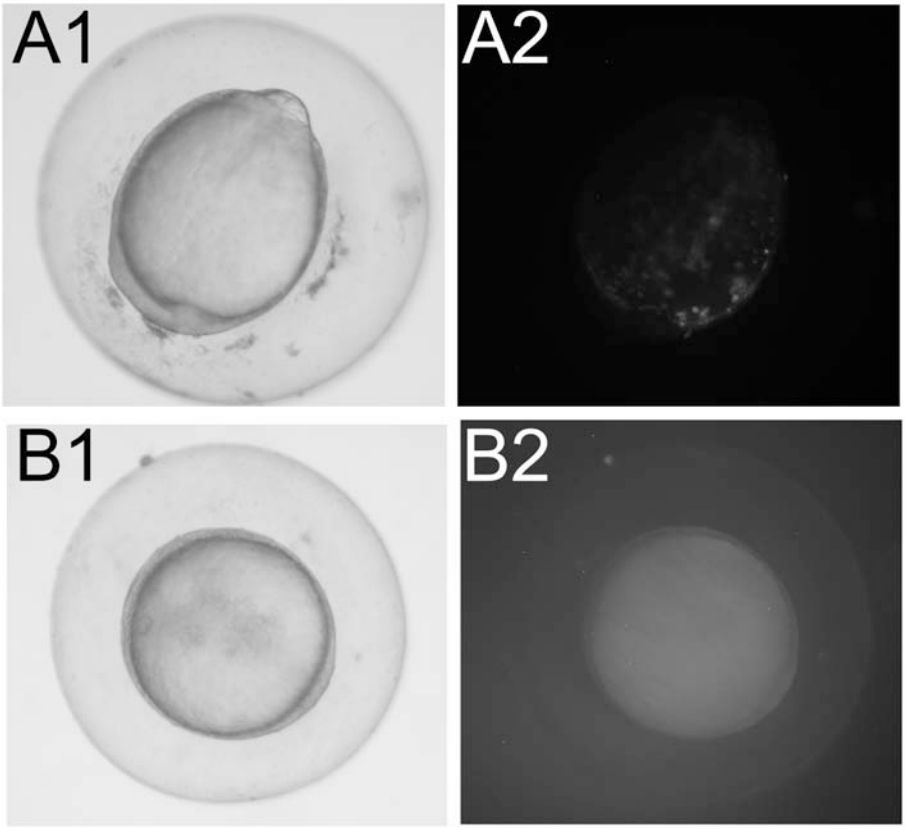

Supplementary Data Files 4: Assays of zebrafish Appa cleavage at 12 hpf after injection of mRNAs encoding truncations of the NTF of human and zebrafish PRESENILIN1 and PRESENILIN2

To assay γ-secretase activity we injected a mixture of mRNAs encoding AppaC86::dGFP and free GFP (that is not subject to γ-secretase cleavage). We then measured the relative amounts* of the two proteins on western immunoblots. (Greater γ-secretase activity results in a lower ratio of AppaC86::GFP to free GFP.) Development of this assay is described in detail elsewhere (Wilson & Lardelli, Journal of Alzheimer's Disease, 2013, DOI 10.3233/JAD-130332, in press).

* The intensity of each western immunoblot band, either AppaC86::dGFP or free GFP, was quantified on a Typhoon trio imaging device (Amersham Bioscience Corp., Piscataway, NJ, USA).

Variations in relative Appa cleavage due to various treatments are observed by comparing the AppaC86:dGFP bands on blots after normalisation. To normalise the data, the intensities of the free GFP standards in each replicate set were normalised to the mean of these intensities and then the AppaC86::dGFP intensity values were adjusted accordingly. Fold changes for the AppaC86::dGFP values were then calculated against the "untreated" sample and these values from the replicate sets were included in the statistical analysis.

Assay of Appa cleavage at 12 hpf after injection of mRNAs encoding truncations of the NTF (primarily **Δ**>4) of human and zebrafish PRESENILIN1 and 2.

	Intensity of AppaC86::dGFP	Intensity of free GFP standard	Normalised	Fold change relative to untreated AppaC86::dGFP
Replicate 1				
hPSEN1Δ>4	10.03	11.42	5.483028846	0.40053639
hPS2V	6.96	5.08	9.42040724	0.688162695
K115Efx10	13.12	11.91	6.354072398	0.464166302
hPSEN2Δ>4	9.25	9.98	6.751767534	0.493218013

zPsen1Δ>4	6.59	8.01	6.462337387	0.472075081
zPsen2Δ>4	18.77	9.53	14.77553592	1.079355952
stop	11.91	6.38	14.14986143	1.033650301
Untreated	8.93	3.67	13.68921521	1
DAPT	16.49	4.74	23.03283654	1.682553468
		7.857777778		

Replicate 2

hPSEN1Δ>4	9.56	25.21	8.519528883	0.501568637
hPS2V	9.64	22.93	9.557554491	0.562680126
K115Efx10	8.29	23.4	8.04772554	0.473792247
hPSEN2Δ>4	7.85	25.12	7.026712931	0.413682362
zPsen1Δ>4	6.83	23.9	6.480188642	0.381506939
zPsen2Δ>4	13.46	18.49	15.9734718	0.940403231
stop	14.82	20.16	16.49885642	0.971334101
Untreated	15.02	19.76	16.98576874	1
DAPT	37.58	25.65	32.76266347	1.928830186
		22.73555556		

Replicate 3

hPSEN1Δ>4	1.23	13.16	1.139945632	0.437164493
hPS2V	1.24	8.79	1.591123596	0.610189399
K115Efx10	0.68	10.28	0.789923885	0.302932583
hPSEN2Δ>4	2.16	15.87	1.524487133	0.584634588
zPsen1Δ>4	1.25	10.94	1.384786154	0.531059833
zPsen2Δ>4	3.62	14.05	3.092220007	1.185853741
stop	3.2	13.73	2.816962668	1.080293675
Untreated	2.44	11.42	2.607589706	1
DAPT	4.87	12.12	4.926484233	1.889286578
		12.26222222		

Mean of Replicates 1,2, and 3

In order to graph and compare each individual sample, the mean of their three replicates has been calculated with the standard error of the mean.

Replicate	Mean of Fold change relative to untreated AppaC86::dGFP	Standard Error of the Mean
hPSEN1Δ>4	0.4533	0.03528
hPS2V	0.62	0.03786
K115Efx10	0.41	0.05508
hPSEN2Δ>4	0.4933	0.0491
zPsen1Δ>4	0.46	0.04359
zPsen2Δ>4	1.07	0.07234
stop	1.027	0.0318
DAPT	1.833	0.07753

Further Statistical Analysis

Paired t-test	**p-value**
hPSEN1Δ>4	0.0041
hPS2V	0.0098
K115Efx10	0.0086
hPSEN2Δ>4	0.0093
zPsen1Δ>4	0.0065
zPsen2Δ>4	0.4353
stop	0.4899
DAPT	0.0085

One-way analysis of variance

The statistical significance of changes in relative intensity were assessed by one-way ANOVA with the Bonferroni Post Hoc test.

	Mean Diff.	t	Significant? p< 0.01?	Summary	99% CI of diff
hPSEN1Δ>4 vs Untreated	-0.5467	7.769	Yes	****	-0.8632 to -0.2301
hPS2V vs Untreated	0.38	5.401	Yes	**	0.06347 to 0.6965
K115Efx10 vs Untreated	0.59	8.385	Yes	****	0.2735 to 0.9065
hPSEN2Δ>4 vs Untreated	-0.5067	7.201	Yes	****	-0.8232 to -0.1901
zPsen1Δ>4 vs Untreated	-0.54	7.675	Yes	****	-0.8565 to -0.2235
zPsen2Δ>4 vs Untreated	0.07	0.9949	No	ns	-0.2465 to 0.3865
stop vs Untreated	0.02667	0.379	No	ns	-0.2899 to 0.3432
DAPT vs Untreated	-0.8333	11.84	Yes	****	-1.150 to -0.5168

Assay of Appa cleavage at 12 hpf after injection of mRNAs encoding truncations of the NTF (primarily **Δ**>3) of human and zebrafish PRESENILIN 1 and 2.

	Intensity of AppaC86::dGFP	Intensity of free GFP standard	Normalised	Fold change relative to untreated AppaC86::dGFP
Replicate 1				
hPSEN1Δ>3	3.43	33.17	3.600492766	0.613967413
hPSEN2Δ>3	7.04	40.62	5.887339923	1.003927822

zPS1IV	2.82	34.77	2.830906747	0.482735171
zPsen1Δ>3	2.76	36.02	2.671834981	0.45560975
zPsen2Δ>3	6.42	40.81	5.333906317	0.909554573
stop	6.15	34.49	6.223119897	1.061186085
Untreated	5.19	30.37	5.864305973	1
DAPT	9.23	28.99	10.79411546	1.840646703
Mean		34.905		

Replicate 2

hPSEN1Δ>3	5.87	8.47	7.796011899	0.886538176
hPSEN2Δ>3	12.78	16.03	9.309060982	1.058597402
zPS1IV	4.83	12.96	4.694463064	0.533839709
zPsen1Δ>3	10.64	19.88	4.500767476	0.51181325
zPsen2Δ>3	6.61	11.45	7.216271691	0.820611927
stop	8.93	12.51	8.998181458	1.023245152
Untreated	8.02	11.39	8.793768964	1
DAPT	12.96	8.16	17.53101834	1.993572769
Mean		12.60625		

Replicate 3

hPSEN1Δ>3	12.55	38.25	12.64120166	0.860441851
hPSEN2Δ>3	15.95	33.48	18.04051389	1.227953922
zPS1IV	7.43	46.24	5.943228653	0.404534537
zPsen1Δ>3	5.22	41.09	4.87317415	0.331699715
zPsen2Δ>3	13.49	32.47	15.61170776	1.062633686
stop	18.74	35.1	20.40826369	1.38911827
Untreated	13.97	36.54	14.69152349	1
DAPT	30.28	45.07	25.1403374	1.711213777
Mean		38.53		

Mean of Replicates 1,2, and 3

In order to graph and compare each individual sample, the mean of their three replicates has been calculated with the standard error of the mean.

Replicates	Mean of Fold change relative to untreated AppaC86::d GFP	Standard Error of the Mean
hPSEN1Δ>3	0.7867	0.08876
hPSEN2Δ>3	1.097	0.06888
zPS1IV	0.47	0.03786
zPsen1Δ>3	0.4333	0.05364
zPsen2Δ>3	0.93	0.07
stop	1.157	0.1172
DAPT	1.847	0.0809

Further Statistical Analysis

Paired t-test	p-value
hPSEN1Δ>3	0.1381
hPSEN2Δ>3	0.2956
zPS1IV	0.0051
zPsen1Δ>3	0.0088
zPsen2Δ>3	0.4226
stop	0.3132
DAPT	0.009

One-way analysis of variance

The statistical significance of changes in relative intensity were assessed by one-way ANOVA with the Bonferroni Post Hoc test.

Bonferroni's Multiple Comparison Test	**Mean Diff.**	**t**	**Significant? p< 0.01?**	**Summary**	**95% CI of diff**

hPSEN1Δ>3 vs Untreated	-0.2133	2.079	No	ns	-0.6760 to 0.2493
hPsen2Δ>3 vs Untreated	-0.09667	0.942	No	ns	-0.5593 to 0.3660
zPS1IV vs Untreated	-0.53	5.165	Yes	**	-0.9927 to -0.0673
zPsen1Δ>3 vs Untreated	-0.5667	5.522	Yes	**	-1.029 to -0.1040
zPsen2Δ>3 vs Untreated	-0.07	0.6821	No	ns	-0.5327 to 0.3927
stop vs Untreated	0.1567	1.527	No	ns	-0.3060 to 0.6193
DAPT vs Untreated	-0.8467	8.251	Yes	****	-1.309 to -0.3840

ns, not significant, i.e. $p \geq 0.01$
*, $p<0.05$
**, $p < 0.01$
***, $p < 0.001$
****, $p < 0.0001$

Nomenclature

DAPT	Treatment with dipeptide γ-secretase inhibitor N-[N-(3,5-difluorophenacetyl)-L- alanyl]-S-phenylglycine t-butyl ester (DAPT)
Stop	AppaC86::dGFP co-injected with the negative control encoding zebrafish full length cDNA including N-terminal FLAG with codon 4 of the Presenilin coding sequences mutated to the stop codon TAA.
Untreated	AppaC86::dGFP Untreated.

Supplementary Data File 5

Observed decrease in spliced *xbp-1* expression under tunicamycin treatment in the mRNA injected cDNA samples. 'FC' denotes Fold Change. P values are from 1-way ANOVA statistical analysis.

	Replicate 1	**Replicate 2**	**Replicate 3**
Control Stop (FC)	1	1	1
Control Stop + Tunicamycin (FC)	12.65	11.85	12.23
zPsen2Δ>4 (FC)	1	1	1
zPsen2Δ>4 + Tunicmycin (FC)	9.62	8.53	9.52
P value (zPsen2Δ>4 + Tunicamycin vs zPsen2Δ>4)	0.00065	0.00021	0.00078

	Replicate 1	**Replicate 2**	**Replicate 3**
Control TAA	1	1	1
Control Stop+ Tunicamycin (FC)	12.65	11.85	12.23
zPsen1Δ>3 (FC)	1	1	1
zPsen1Δ>3 + Tunicmycin (FC)	1.37	1.72	2.23
P value (zPsen2Δ>4 + Tunicamycin vs zPsen2Δ>4)	0.00042	0.0053	0.0005

	Replicate 1	**Replicate 2**	**Replicate 3**
Control Stop (FC)	1	1	1
Control Stop+ Tunicamycin (FC)	12.65	11.85	12.23
hPsen2Δ>4 (FC)	1	1	1
hPsen2Δ>4 + Tunicamycin (FC)	1.37	1.54	1.65
P value	0.0023	0.0056	0.0012

qRT-PCR validation of the microarray.

	Microarray data		RT-qPCR data	
	FC	**Significance**	**FC**	**Significance**
IL1B	-2.86	0.0075	-2.55	0.0001
MAPKAPK5	-1.60	0.0000072	-2.04	0.00001
SMARCA4	-1.44	0.012	-1.74	0.0002
CAMTA1	2.47	0.00000027	2.61	0.0002
IRF4(MUM1)	1.66	0.0016	1.60	0.003
PKD1	1.76	0.00056	1.65	0.008

qRT-PCR analysis of PS1IV.

	Replicate 1	**Replicate 2**	**Replicate3**
Control Stop	1	1	1
Hmga1 mRNA	5.166425	4.781745	6.990611
HmgBB+mRNA	2.238808	2.157222	4.934277
P value (HMGA1 mRNA vs HMGA1BB+mRNA)	**0.0006**	**0.0023**	**0.0391**

Supplementary Data File 6

The sequence of cDNA from the alternatively spliced transcript of zebrafish *psen1*.

Start codon Exon 3 Stop codon Exon 5

GTTCCGATGGCTGATTTAGTGCAGAATGCTGCCAATAATGTG|GATCTACACCCCGTTTCGTGAGGACACGGAGACG
GTGGGTCAGCGAGCTCTGCACTCCATGCTCAACGCCATCATCATGATCAGTGTGATCGTGGTCATGACCCTGGTGCT
GGTGGTGCTCTACAAGTACAGATGCTACAAG|GTGATTCAAGCCTGGCTGTTCTTCTCCAACCTCCTCCTGCTCTTC
TTTTTCTCCTTAATTTATTTGGG

Exon 6

Discussion

In chapter II of this thesis, a novel assay has been developed that allows for the *in vivo* analysis of γ-secretase activity. This is the first assay of its kind in zebrafish. This assay has the ability to be used to investigate a wide range of γ-secretase modulating events, including measuring the inhibition of AβPP cleavage by newly developed drugs and analyzing the effect that PSEN mutations have on γ-secretase processing. We have effectively used this assay to show that both Psen1 and Psen2 proteins contribute to γ-secretase cleavage of the Appa (a paralogue of human AβPP) substrate in zebrafish. This is consistent with the observations of Yonemura *et al* on the roles of human PSEN1 and PSEN2 in the cleavage of AβPP [194]. This assay was utilized in Chapter III to show that various truncations of human PSEN1 (or zebrafish Psen1) protein have starkly differential effects on Notch signalling and cleavage of Appa. Different truncations can suppress or stimulate Notch signalling but not Appa cleavage and vice versa. This is significant as an aberrant transcript resulting from the G183V PSEN mutation in Picks disease suppresses cleavage of Appa but not Notch signalling. However, in contrast, the truncated protein potentially produced by the P242LfsX11 acne inversa mutation has no effect on Appa cleavage and unexpectedly enhances Notch signalling. Wang et al [42] suggest that the FAI phenotype is due to haploinsufficiency for genes encoding components of the γ-secretase complex – i.e. a loss of function phenotype. Our result suggests that the effects of these mutations, or at least those of the P242LfsX11 mutation of PSEN1, may be more complex. This hypothesis has been explored further in chapter

IV where we investigated the evolution of PS2V and its function compared to the K115Efx10 truncation. We have found that zebrafish possess a PS2V-like isoform, PS1IV, produced from the *Danio rerio PSEN1* orthologous gene rather than its *PSEN2* orthologue. We showed that the molecular mechanism controlling formation of PS2V/PS1IV and the ability to stimulate γ-secretase activity and suppress the unfolded protein response is conserved. The K115Efx10 FAD mutation is similar to PS2V in its ability to increase Notch signalling and γ-secretase cleavage of zebrafish *Appa*. This supports an increase in Aβ peptide production as a molecular common link between K115Efx10 FAD and sporadic late onset AD.

Each chapter has its own discussion and conclusion that goes into the individual findings in detail. Those discussions will not be reiterated here. I will however, describe some concerns and address some of the issues that have been highlighted during the peer review of the papers, in particular chapter III.

A common criticism of research utilizing zebrafish is its appropriateness as a model of human AD. In disease states such as AD, genes encoding truncated PRESENILINs are found concomitantly with wild-type *PRESENILIN* genes. However, previous analyses of truncated PRESENILINs have examined their biochemical activities in backgrounds lacking full-length proteins. This is explained in greater detail on pg 85 in chapter III. However it is worth reiterating that differences between the results obtained in chapters III and IV for the activity of Presenilin truncations in AβPP cleavage and Notch signalling compared to previous work by others in cell free systems are probably because

our analysis has examined the expression of truncated PRESENILINs in the presence of endogenous gene expression. This highlights the importance of examining dominant mutations in their real, heterozygous state - in the presence of a normal allele – rather than in isolation since the activity of the dominant mutation can be dependent on the function of the normal allele.

It has been suggested (by one reviewer) that the injection of synthetic mRNA into zebrafish embryos is in many ways a less controlled experiment than transient or stable overexpression of PSEN in human cell lines. However, experiments involving genes transfected into cultured cells involve much higher levels of expression than are physiologically normal. The cells themselves can display aberrant patterns of gene expression due to the fact that they are not in their normal three-dimensional environment of cell-cell contacts and signalling. If the cells are from an immortalised line then further abnormalities of gene expression must exist. One of the great advantages of work with zebrafish embryos is the ability to, in a very controlled fashion, simultaneously force and suppress (or otherwise manipulate) the expression of multiple genes. The experiments in chapters III and IV are based on this. The internal consistency of the data supports the validity of this approach. The advantages of our approach relative to cell-free assays and cell transfection are described in the text of the manuscripts.

To further support the physiological relevance of our data we made an effort to monitor and measure non-endogenous gene expression. In chapters II-IV of this thesis, morpholino antisense oligonucleotides have been used that interfere with the splicing of the endogenous *psen* to generate truncated proteins. It has been previously shown that the

levels of interference with the endogenous transcripts are, in most cases, minor but can still cause strong dominant phenotypes [329]. Since it is the endogenous transcript that is being manipulated the levels of expression of the truncated protein must be physiologically relevant. Quantitative PCR has also been performed to compare the levels of *psen1* mRNA with and without injection of one of the deletion constructs. The results show that levels of total mRNA are ~3 fold higher in the mRNA-injected embryos. This demonstrates that injected mRNAs are at levels comparable to the endogenous mRNA.

In chapter III and IV we have used different techniques to measure AβPP cleavage and Notch signalling in zebrafish. The assay for Notch signalling relies on the measurement of *neurogenin 1* transcripts by *in situ* hybridization, which are negatively regulated by Notch signaling. In contrast, AβPP cleavage is measured after overexpression of a truncated and GFP-tagged AβPP construct by Western blotting as developed in Chapter II. It was suggested by one reviewer that to accurately compare the effects of an intervention/treatment on AβPP and Notch signalling it is absolutely critical to use assays that rely on the same methodology, e.g., measurement of proteolytic release of endogenous AICD/NICD domains by Western blotting. The reviewer citeed that this has been illustrated by the misleading marketing of so-called “NOTCH-sparing” γ-secretase inhibitors like BMS-708163. This inhibitor was initially described to offer a 200-fold window between the inhibition of NOTCH and AβPP cleavage. These results were obtained with a reporter-based transcriptional assay to measure NOTCH activity and measurement of AβPP cleavage by quantification of an AβPP proteolytic product. However, the reviewer cited recent studies using proteolytic assays for both AβPP and

NOTCH cleavage that show that this window does not exist and that this inhibitor might even be more selective for Notch [345, 346]. The reviewer suggested that the claims in chapters III and IV that some PSEN splice variants differentially affected AβPP and NOTCH cleavage are not valid and could be entirely due to the different methodologies of the assays. However these comments above are based on views founded in, and framed by, cell-free assays of γ-secretase activity. As discussed in Chapter III (pg. 84) as well as the introduction to this thesis (pg. 36), there are serious questions over the relevance of these assays for Alzheimer's disease. One should not judge the relevance of an *in vivo* assay by the standards of an *in vitro* assay for which γ-secretase activity is examined under conditions that are far from normal. While it is true that the AβPP and Notch assays utilised in this thesis have different methodological bases, it is highly unlikely that the observations of differences in the effects on AβPP cleavage and Notch signalling of different truncations are artefacts of the procedures themselves. If this were true, one would not expect that some truncations produce increases in both AβPP cleavage and Notch signalling while others produce differences. To support the validity of our assays we subsequently performed the experiments showing that the Psen1Δ>4 truncation requires the presence of endogenous Psen1 in order to stimulate both the γ-secretase cleavage of Appa and Notch signalling.

Further Directions

Development of the Appa γ-secretase assay

Chapter II describes the development of an assay for the cleavage of a modified *Appa* protein in zebrafish to monitor of γ-secretase activity. This assay is effective and forms a prototype for in vivo assays of γ-secretase cleavage of the many other substrates of this enzyme activity. However, it also has scope for improvement. As noted in Chapter II the products of γ-secretase cleavage of all of the variant *Appa* substrates (in effect derivatives of C100 fused to dGFP) proved too unstable to detect by our Western blotting procedure. This is not unexpected since AICD has very rapid turnover and a halflife that is potentially as short as 5 min [252]. Indeed, one difficulty in determining a physiological role for AICD has been its instability. Furthermore, the Appa::C86* substrate was coupled to an exceptionally destablised GFP tag. It would be ideal to have an assay where one could measure the ratio of cleaved to uncleaved substrate. This might be achieved by having a more stable form of GFP tagged to the *Appa* substrate. This form of GFP would have greater perdurance, possibly allowing visualisation of the cleavage fragment. The current assay requires the careful co-injection of equal concentrations and volumes of a standard together with the assay construct. It would be beneficial to include an expression standard that is automatically stoichiometrically co-expressed with the assay construct. This could be achieved by having a mCherry tag linked to the assay substrate via a viral 2a sequence (that causes translation of two separate peptides from one open reading frame in a mRNA). This would allow for the co-expression of mCherry with the

Appa::dGFP fusion protein in a 1:1 ratio and would make comparison of the results of multiple injections simpler and more accurate. The ability to perform *in vivo*, high throughput, simple analyses requiring only a moderate degree of technical proficiency would increase our ability to investigate PRESENILIN activity and γ-secretase cleavage events.

The development of γ-secretase assays utilizing other substrates

While the study of AβPP proteolytic cleavage is important for AD research and a well-understood mechanism for the analysis γ-secretase activity, it is not provide a complete picture of γ-secretase. The substrate specificity and regulation of γ-secretase cleavage events, as outline in the introduction of this thesis, remain poorly understood. By investigating the processing of other substrates we could garner insight into what substrate characteristics are critical for recruitment to γ-secretase processing.

The p75NTR and NRH1 transmembrane proteins share high sequence similarity in their transmembrane and intracellular (ICD) domains. However, Kanning *et al* (2003) observed that while p75NTR is a substrate of γ-secretase, NRH1 is not, despite the two proteins sharing the same sequence at the location of γ-secretase cleavage sites [347]. As yet the p75NTR and NRH1 orthologs have not both been defined in *Danio rerio*. this could be done by utilising protein database searches, BLAST analyses and genomic alignments of homologous sequences. Then, assay constructs for these proteins could be developed (in a fashion similar to development of the Appa::dGFP substrate described in

Chapter II) If assays could be developed in which p75NTR cleavage via γ-secretase could be observed and NRH1 cleavage (not mediated by γ-secretase) could be demonstrated, it would allow experiments such as amino acid residue swap or domain swap experiments to be undertaken. This might allow one to determine the essential structural substrate requirements for cleavage by γ-secretase.

The localisation of PRESENILIN truncations to the Mitochondrial Associated Membranes

The PSEN1 protein is largely localised to the MAM and PSEN2 resides exclusively in this structure [17]. In Chapters III and IV of this thesis the diverse effects that different PSEN truncations have on Notch signaling and AβPP cleavage are shown, but where do truncations of the PRESENILINs localise in order to exert their dominant effects? Does differential localisation of the truncations explain differences in their activities? Fusing GFP to the N-termini of PRESENILIN truncations could enable observation of their sub-cellular localisation by confocal microscopy. This would show whether PRESENILIN truncations with different activities are localised to different positions within cells and may help to explain why different truncations of PRESENILIN proteins can result in very different diseases. For example, the PS2V truncation seen in sporadic AD may show a different localisation to the PSEN P242LfsX11 mutation associated with familial acne inversa (FAI). Alternatively, if they show similar localisations then their different disease effects would more likely be due to differences in their protein structures and their

interactions with binding partners.

To identify the binding partners of truncated PRSENILIN proteins that integrate into higher molecular weight (HMW) complexes.

As seen in Chapter III it has been shown that truncated forms of PRESENILIN can incorporate into HMW complexes (some of which are sufficiently stable to survive SDS-PAGE). Therefore, these complexes could be analyzed in detail using 2-dimensional blue native PAGE (BN-PAGE). Western blotting to detect their N-terminal FLAG tags would identify the positions of spots containing truncated forms of Psen. The protein components of the same spots on identical gels could then be analysed by proteomic analysis such as MALDI-TOF. Anti-FLAG antibodies could also be used to immunoprecipitate complexes containing FLAG-tagged, truncated PRESENILIN followed by 2-dimensional SDS-PAGE and analysis of the protein composition of spots identified by silver staining.

The failure to detect PRESENILIN truncations in γ-secretase complexes would imply that these truncations exert their effects on Notch signalling and Appa cleavage by means other than incorporation. Psen1 truncated after exon 5 sequence appears to integrate avidly into HMW complexes but does not affect γ-secretase function. The detection of differences in the components of proteins binding to Psen1 truncated after exon 5 sequence and forms of Psen1 truncated after exon 3,4,6 and exon 7 sequences could reveal which interactions are important for modulating γ-secretase activity.

References

1. Prince, M., et al., *The global prevalence of dementia: a systematic review and metaanalysis.* Alzheimer's and dementia : the journal of the Alzheimer's Association, 2013. **9**(1): p. 63-75 e2.
2. Wimo, A., et al., *The worldwide economic impact of dementia 2010.* Alzheimer's and dementia : the journal of the Alzheimer's Association, 2013. **9**(1): p. 1-11 e3.
3. Bekris, L.M., et al., *Genetics of Alzheimer disease.* Journal of geriatric psychiatry and neurology, 2010. **23**(4): p. 213-27.
4. Campion, D., et al., *Early-onset autosomal dominant Alzheimer disease: prevalence, genetic heterogeneity, and mutation spectrum.* American journal of human genetics, 1999. **65**(3): p. 664-70.
5. Brickell, K.L., et al., *Early-onset Alzheimer disease in families with late-onset Alzheimer disease: a potential important subtype of familial Alzheimer disease.* Archives of neurology, 2006. **63**(9): p. 1307-11.
6. Hardy, J. and D. Allsop, *Amyloid deposition as the central event in the aetiology of Alzheimer's disease.* Trends in pharmacological sciences, 1991. **12**(10): p. 383-8.
7. Hardy, J. and D.J. Selkoe, *The amyloid hypothesis of Alzheimer's disease: progress and problems on the road to therapeutics.* Science, 2002. **297**(5580): p. 353-6.
8. Hardy, J.A. and G.A. Higgins, *Alzheimer's disease: the amyloid cascade hypothesis.* Science, 1992. **256**(5054): p. 184-5.
9. Selkoe, D.J., *The molecular pathology of Alzheimer's disease.* Neuron, 1991. **6**(4): p. 487-98.
10. Price, D.L. and S.S. Sisodia, *Mutant genes in familial Alzheimer's disease and transgenic models.* Annual review of neuroscience, 1998. **21**: p. 479-505.
11. Alonso Vilatela, M.E., M. Lopez-Lopez, and P. Yescas-Gomez, *Genetics of Alzheimer's disease.* Archives of medical research, 2012. **43**(8): p. 622-31.
12. Suzuki, N., et al., *An increased percentage of long amyloid beta protein secreted by familial amyloid beta protein precursor (beta APP717) mutants.* Science, 1994. **264**(5163): p. 1336-40.
13. Younkin, S.G., *Evidence that A beta 42 is the real culprit in Alzheimer's disease.* Annals of neurology, 1995. **37**(3): p. 287-8.
14. Scheuner, D., et al., *Secreted amyloid beta-protein similar to that in the senile plaques of Alzheimer's disease is increased in vivo by the presenilin 1 and 2 and APP mutations linked to familial Alzheimer's disease.* Nature medicine, 1996. **2**(8): p. 864-70.
15. Bentahir, M., et al., *Presenilin clinical mutations can affect gamma-secretase activity by different mechanisms.* Journal of neurochemistry, 2006. **96**(3): p. 732-42.

16. Walsh, D.M. and D.J. Selkoe, *A beta oligomers - a decade of discovery.* Journal of neurochemistry, 2007. **101**(5): p. 1172-84.
17. Glabe, C.C., *Amyloid accumulation and pathogensis of Alzheimer's disease: significance of monomeric, oligomeric and fibrillar Abeta.* Sub-cellular biochemistry, 2005. **38**: p. 167-77.
18. Lesne, S., et al., *A specific amyloid-beta protein assembly in the brain impairs memory.* Nature, 2006. **440**(7082): p. 352-7.
19. Shankar, G.M., et al., *Amyloid-beta protein dimers isolated directly from Alzheimer's brains impair synaptic plasticity and memory.* Nature medicine, 2008. **14**(8): p. 837-42.
20. Ethell, D.W., *An amyloid-notch hypothesis for Alzheimer's disease.* The Neuroscientist : a review journal bringing neurobiology, neurology and psychiatry, 2010. **16**(6): p. 614-7.
21. Hyman, B.T., K. Marzloff, and P.V. Arriagada, *The lack of accumulation of senile plaques or amyloid burden in Alzheimer's disease suggests a dynamic balance between amyloid deposition and resolution.* Journal of neuropathology and experimental neurology, 1993. **52**(6): p. 594-600.
22. McLean, C.A., et al., *Soluble pool of Abeta amyloid as a determinant of severity of neurodegeneration in Alzheimer's disease.* Annals of neurology, 1999. **46**(6): p. 860-6.
23. Terry, R.D., et al., *Physical basis of cognitive alterations in Alzheimer's disease: synapse loss is the major correlate of cognitive impairment.* Annals of neurology, 1991. **30**(4): p. 572-80.
24. Lesne, S., L. Kotilinek, and K.H. Ashe, *Plaque-bearing mice with reduced levels of oligomeric amyloid-beta assemblies have intact memory function.* Neuroscience, 2008. **151**(3): p. 745-9.
25. Nordberg, A., *Amyloid plaque imaging in vivo: current achievement and future prospects.* European journal of nuclear medicine and molecular imaging, 2008. **35 Suppl 1**: p. S46-50.
26. Villemagne, V.L., et al., *The ART of loss: Abeta imaging in the evaluation of Alzheimer's disease and other dementias.* Molecular neurobiology, 2008. **38**(1): p. 1-15.
27. Caughey, B. and P.T. Lansbury, *Protofibrils, pores, fibrils, and neurodegeneration: separating the responsible protein aggregates from the innocent bystanders.* Annual review of neuroscience, 2003. **26**: p. 267-98.
28. Turner, P.R., et al., *Roles of amyloid precursor protein and its fragments in regulating neural activity, plasticity and memory.* Progress in neurobiology, 2003. **70**(1): p. 1-32.
29. Beckett, C., et al., *Nuclear signalling by membrane protein intracellular domains: the AICD enigma.* Cellular signalling, 2012. **24**(2): p. 402-9.
30. Gerald, Z. and W. Ockert, *Alzheimer's disease market: hope deferred.* Nature reviews. Drug discovery, 2013. **12**(1): p. 19-20.
31. Assal, F. and M. van der Meulen, *Pharmacological interventions in primary care: hopes and illusions.* Frontiers of neurology and neuroscience, 2009. **24**: p. 54-65.
32. Supnet, C. and I. Bezprozvanny, *Presenilins function in ER calcium leak and Alzheimer's disease pathogenesis.* Cell Calcium, 2011. **50**(3): p. 303-9.

33. Matsubara-Tsutsui, M., et al., *Molecular evidence of presenilin 1 mutation in familial early onset dementia.* American journal of medical genetics, 2002. **114**(3): p. 292-8.
34. Marjaux, E., D. Hartmann, and B. De Strooper, *Presenilins in memory, Alzheimer's disease, and therapy.* Neuron, 2004. **42**(2): p. 189-92.
35. Korovaitseva, G.I., et al., *Presenilin polymorphisms in Alzheimer's disease.* Lancet, 1997. **350**(9082): p. 959.
36. Newman, M., I.F. Musgrave, and M. Lardelli, *Alzheimer disease: amyloidogenesis, the presenilins and animal models.* Biochimica et biophysica acta, 2007. **1772**(3): p. 285-97.
37. Wolfe, M.S., *Processive proteolysis by gamma-secretase and the mechanism of Alzheimer's disease.* Biological chemistry, 2012. **393**(9): p. 899-905.
38. Sjogren, M. and C. Andersen, *Frontotemporal dementia--a brief review.* Mechanisms of ageing and development, 2006. **127**(2): p. 180-7.
39. Li, D., et al., *Mutations of presenilin genes in dilated cardiomyopathy and heart failure.* American journal of human genetics, 2006. **79**(6): p. 1030-9.
40. Gianni, D., et al., *Protein aggregates and novel presenilin gene variants in idiopathic dilated cardiomyopathy.* Circulation, 2010. **121**(10): p. 1216-26.
41. Li, A., et al., *Changes in the expression of the Alzheimer's disease-associated presenilin gene in drosophila heart leads to cardiac dysfunction.* Current Alzheimer research, 2011. **8**(3): p. 313-22.
42. Wang, B., et al., *Gamma-secretase gene mutations in familial acne inversa.* Science, 2010. **330**(6007): p. 1065.
43. Pink, A.E., et al., *Mutations in the gamma-secretase genes NCSTN, PSENEN, and PSEN1 underlie rare forms of hidradenitis suppurativa (acne inversa).* The Journal of investigative dermatology, 2012. **132**(10): p. 2459-61.
44. Cowburn, R.F., et al., *Presenilin-mediated signal transduction.* Physiology & behavior, 2007. **92**(1-2): p. 93-7.
45. McCarthy, J.V., *Involvement of presenilins in cell-survival signalling pathways.* Biochemical Society transactions, 2005. **33**(Pt 4): p. 568-72.
46. Annaert, W. and B. De Strooper, *Presenilins: molecular switches between proteolysis and signal transduction.* Trends in neurosciences, 1999. **22**(10): p. 439-43.
47. Koo, E.H. and R. Kopan, *Potential role of presenilin-regulated signaling pathways in sporadic neurodegeneration.* Nature medicine, 2004. **10 Suppl**: p. S26-33.
48. Raurell, I., et al., *Presenilin-1 interacts with plakoglobin and enhances plakoglobin-Tcf-4 association. Implications for the regulation of beta-catenin/Tcf-4-dependent transcription.* The Journal of biological chemistry, 2006. **281**(3): p. 1401-11.
49. Baki, L., et al., *PS1 activates PI3K thus inhibiting GSK-3 activity and tau overphosphorylation: effects of FAD mutations.* The EMBO journal, 2004. **23**(13): p. 2586-96.
50. Dewachter, I., et al., *Modulation of synaptic plasticity and Tau phosphorylation by wild-type and mutant presenilin1.* Neurobiology of aging, 2008. **29**(5): p. 639-52.

51. Feng, R., et al., *Forebrain degeneration and ventricle enlargement caused by double knockout of Alzheimer's presenilin-1 and presenilin-2.* Proceedings of the National Academy of Sciences of the United States of America, 2004. **101**(21): p. 8162-7.
52. Saura, C.A., et al., *Loss of presenilin function causes impairments of memory and synaptic plasticity followed by age-dependent neurodegeneration.* Neuron, 2004. **42**(1): p. 23-36.
53. Zhu, M., et al., *Increased oxidative stress and astrogliosis responses in conditional double-knockout mice of Alzheimer-like presenilin-1 and presenilin-2.* Free radical biology and medicine, 2008. **45**(10): p. 1493-9.
54. Takahashi, N., et al., *Two novel spliced presenilin 2 transcripts in human lymphocyte with oxidant stress and brain.* Molecular and cellular biochemistry, 2003. **252**(1-2): p. 279-83.
55. LaFerla, F.M., *Calcium dyshomeostasis and intracellular signalling in Alzheimer's disease.* Nature reviews. Neuroscience, 2002. **3**(11): p. 862-72.
56. Mattson, M.P., *ER calcium and Alzheimer's disease: in a state of flux.* Science signaling, 2010. **3**(114): p. pe10.
57. Cook, D.G., et al., *Presenilin 1 deficiency alters the activity of voltage-gated Ca2+ channels in cultured cortical neurons.* Journal of neurophysiology, 2005. **94**(6): p. 4421-9.
58. Leissring, M.A., et al., *Capacitative calcium entry deficits and elevated luminal calcium content in mutant presenilin-1 knockin mice.* The Journal of cell biology, 2000. **149**(4): p. 793-8.
59. Yoo, A.S., et al., *Presenilin-mediated modulation of capacitative calcium entry.* Neuron, 2000. **27**(3): p. 561-72.
60. Green, K.N., et al., *SERCA pump activity is physiologically regulated by presenilin and regulates amyloid beta production.* The Journal of cell biology, 2008. **181**(7): p. 1107-16.
61. Cheung, K.H., et al., *Mechanism of Ca2+ disruption in Alzheimer's disease by presenilin regulation of InsP3 receptor channel gating.* Neuron, 2008. **58**(6): p. 871-83.
62. Stutzmann, G.E., et al., *Enhanced ryanodine receptor recruitment contributes to Ca2+ disruptions in young, adult, and aged Alzheimer's disease mice.* The Journal of neuroscience : the official journal of the Society for Neuroscience, 2006. **26**(19): p. 5180-9.
63. Cheung, K.H., et al., *Gain-of-function enhancement of IP3 receptor modal gating by familial Alzheimer's disease-linked presenilin mutants in human cells and mouse neurons.* Science signaling, 2010. **3**(114): p. ra22.
64. Zatti, G., et al., *Presenilin mutations linked to familial Alzheimer's disease reduce endoplasmic reticulum and Golgi apparatus calcium levels.* Cell Calcium, 2006. **39**(6): p. 539-50.
65. Nelson, O., et al., *Familial Alzheimer disease-linked mutations specifically disrupt Ca2+ leak function of presenilin 1.* The Journal of clinical investigation, 2007. **117**(5): p. 1230-9.
66. Shen, J. and R.J. Kelleher, 3rd, *The presenilin hypothesis of Alzheimer's disease: evidence for a loss-of-function pathogenic mechanism.* Proceedings of the

National Academy of Sciences of the United States of America, 2007. **104**(2): p. 403-9.
67. Michno, K., et al., *Intracellular calcium deficits in Drosophila cholinergic neurons expressing wild type or FAD-mutant presenilin.* PLoS One, 2009. **4**(9): p. e6904.
68. Herms, J., et al., *Capacitive calcium entry is directly attenuated by mutant presenilin-1, independent of the expression of the amyloid precursor protein.* The Journal of biological chemistry, 2003. **278**(4): p. 2484-9.
69. Lee, J.H., et al., *Lysosomal proteolysis and autophagy require presenilin 1 and are disrupted by Alzheimer-related PS1 mutations.* Cell, 2010. **141**(7): p. 1146-58.
70. Williamson, W.R. and P.R. Hiesinger, *On the role of v-ATPase V0a1-dependent degradation in Alzheimer disease.* Communicative & integrative biology, 2010. **3**(6): p. 604-7.
71. Neely, K.M., K.N. Green, and F.M. LaFerla, *Presenilin is necessary for efficient proteolysis through the autophagy-lysosome system in a gamma-secretase-independent manner.* The Journal of neuroscience : the official journal of the Society for Neuroscience, 2011. **31**(8): p. 2781-91.
72. Neely, K.M. and K.N. Green, *Presenilins mediate efficient proteolysis via the autophagosome-lysosome system.* Autophagy, 2011. **7**(6): p. 664-5.
73. Sherrington, R., et al., *Cloning of a gene bearing missense mutations in early-onset familial Alzheimer's disease.* Nature, 1995. **375**(6534): p. 754-60.
74. Rogaev, E.I., et al., *Familial Alzheimer's disease in kindreds with missense mutations in a gene on chromosome 1 related to the Alzheimer's disease type 3 gene.* Nature, 1995. **376**(6543): p. 775-8.
75. Lee, M.K., et al., *Expression of presenilin 1 and 2 (PS1 and PS2) in human and murine tissues.* The Journal of neuroscience : the official journal of the Society for Neuroscience, 1996. **16**(23): p. 7513-25.
76. Benkovic, S.A., et al., *Regional and cellular localization of presenilin-2 RNA in rat and human brain.* Experimental neurology, 1997. **145**(2 Pt 1): p. 555-64.
77. Berezovska, O., et al., *Developmental regulation of presenilin mRNA expression parallels notch expression.* Journal of neuropathology and experimental neurology, 1997. **56**(1): p. 40-4.
78. Berezovska, O., M.Q. Xia, and B.T. Hyman, *Notch is expressed in adult brain, is coexpressed with presenilin-1, and is altered in Alzheimer disease.* Journal of neuropathology and experimental neurology, 1998. **57**(8): p. 738-45.
79. Lah, J.J., et al., *Light and electron microscopic localization of presenilin-1 in primate brain.* The Journal of neuroscience : the official journal of the Society for Neuroscience, 1997. **17**(6): p. 1971-80.
80. Moussaoui, S., et al., *Immunohistochemical analysis of presenilin-1 expression in the mouse brain.* FEBS letters, 1996. **383**(3): p. 219-22.
81. Blanchard, V., et al., *Immunohistochemical analysis of presenilin 2 expression in the mouse brain: distribution pattern and co-localization with presenilin 1 protein.* Brain research, 1997. **758**(1-2): p. 209-17.

82. Kumar, A. and M.K. Thakur, *Presenilin 1 and 2 are expressed differentially in the cerebral cortex of mice during development.* Neurochemistry international, 2012. **61**(5): p. 778-82.
83. Culvenor, J.G., et al., *Presenilin 2 expression in neuronal cells: induction during differentiation of embryonic carcinoma cells.* Experimental cell research, 2000. **255**(2): p. 192-206.
84. Thakur, M.K. and S. Ghosh, *Age and sex dependent alteration in presenilin expression in mouse cerebral cortex.* Cellular and molecular neurobiology, 2007. **27**(8): p. 1059-67.
85. Annaert, W.G., et al., *Presenilin 1 controls gamma-secretase processing of amyloid precursor protein in pre-golgi compartments of hippocampal neurons.* The Journal of cell biology, 1999. **147**(2): p. 277-94.
86. Siman, R. and J. Velji, *Localization of presenilin-nicastrin complexes and gamma-secretase activity to the trans-Golgi network.* Journal of neurochemistry, 2003. **84**(5): p. 1143-53.
87. Kimura, N., et al., *Age-related changes in the localization of presenilin-1 in cynomolgus monkey brain.* Brain research, 2001. **922**(1): p. 30-41.
88. Vetrivel, K.S., et al., *Association of gamma-secretase with lipid rafts in post-Golgi and endosome membranes.* The Journal of biological chemistry, 2004. **279**(43): p. 44945-54.
89. Pasternak, S.H., et al., *Presenilin-1, nicastrin, amyloid precursor protein, and gamma-secretase activity are co-localized in the lysosomal membrane.* The Journal of biological chemistry, 2003. **278**(29): p. 26687-94.
90. Ankarcrona, M. and K. Hultenby, *Presenilin-1 is located in rat mitochondria.* Biochemical and biophysical research communications, 2002. **295**(3): p. 766-70.
91. Li, J., et al., *Alzheimer presenilins in the nuclear membrane, interphase kinetochores, and centrosomes suggest a role in chromosome segregation.* Cell, 1997. **90**(5): p. 917-27.
92. Area-Gomez, E., et al., *Presenilins are enriched in endoplasmic reticulum membranes associated with mitochondria.* The American journal of pathology, 2009. **175**(5): p. 1810-6.
93. Laudon, H., et al., *A nine-transmembrane domain topology for presenilin 1.* The Journal of biological chemistry, 2005. **280**(42): p. 35352-60.
94. Spasic, D., et al., *Presenilin-1 maintains a nine-transmembrane topology throughout the secretory pathway.* The Journal of biological chemistry, 2006. **281**(36): p. 26569-77.
95. Wolfe, M.S., et al., *Two transmembrane aspartates in presenilin-1 required for presenilin endoproteolysis and gamma-secretase activity.* Nature, 1999. **398**(6727): p. 513-7.
96. Fukumori, A., et al., *Three-amino acid spacing of presenilin endoproteolysis suggests a general stepwise cleavage of gamma-secretase-mediated intramembrane proteolysis.* The Journal of neuroscience : the official journal of the Society for Neuroscience, 2010. **30**(23): p. 7853-62.
97. De Strooper, B., T. Iwatsubo, and M.S. Wolfe, *Presenilins and gamma-Secretase: Structure, Function, and Role in Alzheimer Disease.* Cold Spring Harbor perspectives in medicine, 2012. **2**(1): p. a006304.

98. Sobhanifar, S., et al., *Structural investigation of the C-terminal catalytic fragment of presenilin 1.* Proceedings of the National Academy of Sciences of the United States of America, 2010. **107**(21): p. 9644-9.
99. Kim, T.W., et al., *Endoproteolytic cleavage and proteasomal degradation of presenilin 2 in transfected cells.* The Journal of biological chemistry, 1997. **272**(17): p. 11006-10.
100. Ratovitski, T., et al., *Endoproteolytic processing and stabilization of wild-type and mutant presenilin.* The Journal of biological chemistry, 1997. **272**(39): p. 24536-41.
101. Brunkan, A.L. and A.M. Goate, *Presenilin function and gamma-secretase activity.* Journal of neurochemistry, 2005. **93**(4): p. 769-92.
102. Sato, N., et al., *A novel presenilin-2 splice variant in human Alzheimer's disease brain tissue.* Journal of Neurochemistry, 1999. **72**(6): p. 2498-505.
103. Sato, N., et al., *Increased production of beta-amyloid and vulnerability to endoplasmic reticulum stress by an aberrant spliced form of presenilin 2.* The Journal of Biological Chemistry, 2001. **276**(3): p. 2108-14.
104. Manabe, T., et al., *Induced HMGA1a expression causes aberrant splicing of Presenilin-2 pre-mRNA in sporadic Alzheimer's disease.* Cell Death Differ, 2003. **10**(6): p. 698-708.
105. Ohe, K. and A. Mayeda, *HMGA1a trapping of U1 snRNP at an authentic 5' splice site induces aberrant exon skipping in sporadic Alzheimer's disease.* Molecular Cell Biology, 2010. **30**(9): p. 2220-8.
106. Manabe, T., et al., *HMGA1a: sequence-specific RNA-binding factor causing sporadic Alzheimer's disease-linked exon skipping of presenilin-2 pre-mRNA.* Genes to Cells, 2007. **12**(10): p. 1179-91.
107. Smith, M.J., et al., *Expression of truncated presenilin 2 splice variant in Alzheimer's disease, bipolar disorder, and schizophrenia brain cortex.* Brain Research Molecular Brain Research, 2004. **127**(1-2): p. 128-35.
108. Katayama, T., et al., *Induction of neuronal death by ER stress in Alzheimer's disease.* The Journal of Chemical Neuroanatomy, 2004. **28**(1-2): p. 67-78.
109. Nishikawa, A., et al., *Novel function of PS2V: change in conformation of tau proteins.* Biochem Biophys Res Commun, 2004. **318**(2): p. 435-8.
110. Parks, A.L. and D. Curtis, *Presenilin diversifies its portfolio.* Trends in genetics : TIG, 2007. **23**(3): p. 140-50.
111. Huppert, S.S., et al., *Analysis of Notch function in presomitic mesoderm suggests a gamma-secretase-independent role for presenilins in somite differentiation.* Developmental cell, 2005. **8**(5): p. 677-88.
112. Thinakaran, G. and A.T. Parent, *Identification of the role of presenilins beyond Alzheimer's disease.* Pharmacological research : the official journal of the Italian Pharmacological Society, 2004. **50**(4): p. 411-8.
113. Hass, M.R., et al., *Presenilin: RIP and beyond.* Seminars in Cellular and Developmental Biology, 2009. **20**(2): p. 201-10.
114. Leissring, M.A., I. Parker, and F.M. LaFerla, *Presenilin-2 mutations modulate amplitude and kinetics of inositol 1, 4,5-trisphosphate-mediated calcium signals.* The Journal of biological chemistry, 1999. **274**(46): p. 32535-8.

115. Tu, H., et al., *Presenilins form ER Ca2+ leak channels, a function disrupted by familial Alzheimer's disease-linked mutations.* Cell, 2006. **126**(5): p. 981-93.
116. Chan, S.L., et al., *Presenilin-1 mutations increase levels of ryanodine receptors and calcium release in PC12 cells and cortical neurons.* The Journal of biological chemistry, 2000. **275**(24): p. 18195-200.
117. Leissring, M.A., et al., *Alzheimer's presenilin-1 mutation potentiates inositol 1,4,5-trisphosphate-mediated calcium signaling in Xenopus oocytes.* Journal of neurochemistry, 1999. **72**(3): p. 1061-8.
118. Zhang, Z., et al., *Destabilization of beta-catenin by mutations in presenilin-1 potentiates neuronal apoptosis.* Nature, 1998. **395**(6703): p. 698-702.
119. Kang, D.E., et al., *Presenilin couples the paired phosphorylation of beta-catenin independent of axin: implications for beta-catenin activation in tumorigenesis.* Cell, 2002. **110**(6): p. 751-62.
120. De Strooper, B. and W. Annaert, *Where Notch and Wnt signaling meet. The presenilin hub.* The Journal of cell biology, 2001. **152**(4): p. F17-20.
121. Marambaud, P., et al., *A presenilin-1/gamma-secretase cleavage releases the E-cadherin intracellular domain and regulates disassembly of adherens junctions.* The EMBO journal, 2002. **21**(8): p. 1948-56.
122. Serban, G., et al., *Cadherins mediate both the association between PS1 and beta-catenin and the effects of PS1 on beta-catenin stability.* The Journal of biological chemistry, 2005. **280**(43): p. 36007-12.
123. McCarthy, J.V., C. Twomey, and P. Wujek, *Presenilin-dependent regulated intramembrane proteolysis and gamma-secretase activity.* Cellular and molecular life sciences : CMLS, 2009. **66**(9): p. 1534-55.
124. Haapasalo, A. and D.M. Kovacs, *The many substrates of presenilin/gamma-secretase.* Journal of Alzheimer's disease : JAD, 2011. **25**(1): p. 3-28.
125. Hemming, M.L., et al., *Proteomic profiling of gamma-secretase substrates and mapping of substrate requirements.* PLoS biology, 2008. **6**(10): p. e257.
126. Sato, T., et al., *Active gamma-secretase complexes contain only one of each component.* The Journal of biological chemistry, 2007. **282**(47): p. 33985-93.
127. Edbauer, D., et al., *Reconstitution of gamma-secretase activity.* Nature cell biology, 2003. **5**(5): p. 486-8.
128. De Strooper, B., *Aph-1, Pen-2, and Nicastrin with Presenilin generate an active gamma-Secretase complex.* Neuron, 2003. **38**(1): p. 9-12.
129. *The structure of the presenilin 1 (S182) gene and identification of six novel mutations in early onset AD families. Alzheimer's Disease Collaborative Group.* Nature genetics, 1995. **11**(2): p. 219-22.
130. Gu, Y., et al., *APH-1 interacts with mature and immature forms of presenilins and nicastrin and may play a role in maturation of presenilin.nicastrin complexes.* The Journal of biological chemistry, 2003. **278**(9): p. 7374-80.
131. Shirotani, K., et al., *Identification of distinct gamma-secretase complexes with different APH-1 variants.* The Journal of biological chemistry, 2004. **279**(40): p. 41340-5.
132. Serneels, L., et al., *Differential contribution of the three Aph1 genes to gamma-secretase activity in vivo.* Proceedings of the National Academy of Sciences of the United States of America, 2005. **102**(5): p. 1719-24.

133. Serneels, L., et al., *gamma-Secretase heterogeneity in the Aph1 subunit: relevance for Alzheimer's disease.* Science, 2009. **324**(5927): p. 639-42.
134. Fortna, R.R., et al., *Membrane topology and nicastrin-enhanced endoproteolysis of APH-1, a component of the gamma-secretase complex.* The Journal of biological chemistry, 2004. **279**(5): p. 3685-93.
135. Hebert, S.S., et al., *Coordinated and widespread expression of gamma-secretase in vivo: evidence for size and molecular heterogeneity.* Neurobiology of disease, 2004. **17**(2): p. 260-72.
136. Ma, G., et al., *APH-1a is the principal mammalian APH-1 isoform present in gamma-secretase complexes during embryonic development.* The Journal of neuroscience : the official journal of the Society for Neuroscience, 2005. **25**(1): p. 192-8.
137. Dejaegere, T., et al., *Deficiency of Aph1B/C-gamma-secretase disturbs Nrg1 cleavage and sensorimotor gating that can be reversed with antipsychotic treatment.* Proceedings of the National Academy of Sciences of the United States of America, 2008. **105**(28): p. 9775-80.
138. Kleiger, G., et al., *GXXXG and AXXXA: common alpha-helical interaction motifs in proteins, particularly in extremophiles.* Biochemistry, 2002. **41**(19): p. 5990-7.
139. Lee, S.F., et al., *A conserved GXXXG motif in APH-1 is critical for assembly and activity of the gamma-secretase complex.* The Journal of biological chemistry, 2004. **279**(6): p. 4144-52.
140. Pardossi-Piquard, R., et al., *APH1 polar transmembrane residues regulate the assembly and activity of presenilin complexes.* The Journal of biological chemistry, 2009. **284**(24): p. 16298-307.
141. Chen, A.C., et al., *Aph-1 associates directly with full-length and C-terminal fragments of gamma-secretase substrates.* The Journal of biological chemistry, 2010. **285**(15): p. 11378-91.
142. Yu, G., et al., *Nicastrin modulates presenilin-mediated notch/glp-1 signal transduction and betaAPP processing.* Nature, 2000. **407**(6800): p. 48-54.
143. Shah, S., et al., *Nicastrin functions as a gamma-secretase-substrate receptor.* Cell, 2005. **122**(3): p. 435-47.
144. Fagan, R., et al., *Nicastrin, a presenilin-interacting protein, contains an aminopeptidase/transferrin receptor superfamily domain.* Trends in biochemical sciences, 2001. **26**(4): p. 213-4.
145. Chen, F., et al., *Nicastrin binds to membrane-tethered Notch.* Nature cell biology, 2001. **3**(8): p. 751-4.
146. Morais, V.A., et al., *Cellular localization of Nicastrin affects amyloid beta species production.* FEBS letters, 2008. **582**(3): p. 427-33.
147. Dries, D.R., et al., *Glu-333 of nicastrin directly participates in gamma-secretase activity.* The Journal of biological chemistry, 2009. **284**(43): p. 29714-24.
148. Chavez-Gutierrez, L., et al., *Glu(332) in the Nicastrin ectodomain is essential for gamma-secretase complex maturation but not for its activity.* J Biol Chem, 2008. **283**(29): p. 20096-105.
149. Futai, E., S. Yagishita, and S. Ishiura, *Nicastrin is dispensable for gamma-secretase protease activity in the presence of specific presenilin mutations.* The Journal of biological chemistry, 2009. **284**(19): p. 13013-22.

150. Zhao, G., et al., *Gamma-secretase composed of PS1/Pen2/Aph1a can cleave notch and amyloid precursor protein in the absence of nicastrin.* The Journal of neuroscience : the official journal of the Society for Neuroscience, 2010. **30**(5): p. 1648-56.
151. Hayashi, I., et al., *Neutralization of the gamma-secretase activity by monoclonal antibody against extracellular domain of nicastrin.* Oncogene, 2012. **31**(6): p. 787-98.
152. Pamren, A., et al., *Mutations in nicastrin protein differentially affect amyloid beta-peptide production and Notch protein processing.* The Journal of biological chemistry, 2011. **286**(36): p. 31153-8.
153. Crystal, A.S., et al., *Membrane topology of gamma-secretase component PEN-2.* The Journal of biological chemistry, 2003. **278**(22): p. 20117-23.
154. Steiner, H., et al., *PEN-2 is an integral component of the gamma-secretase complex required for coordinated expression of presenilin and nicastrin.* The Journal of biological chemistry, 2002. **277**(42): p. 39062-5.
155. Prokop, S., et al., *Requirement of PEN-2 for stabilization of the presenilin N-/C-terminal fragment heterodimer within the gamma-secretase complex.* The Journal of biological chemistry, 2004. **279**(22): p. 23255-61.
156. Chiang, P.M., et al., *Specific domains in anterior pharynx-defective 1 determine its intramembrane interactions with nicastrin and presenilin.* Neurobiology of aging, 2012. **33**(2): p. 277-85.
157. Shirotani, K., et al., *Immature nicastrin stabilizes APH-1 independent of PEN-2 and presenilin: identification of nicastrin mutants that selectively interact with APH-1*. Journal of neurochemistry, 2004. **89**(6): p. 1520-7.
158. Arawaka, S., et al., *The levels of mature glycosylated nicastrin are regulated and correlate with gamma-secretase processing of amyloid beta-precursor protein.* Journal of neurochemistry, 2002. **83**(5): p. 1065-71.
159. Yang, D.S., et al., *Mature glycosylation and trafficking of nicastrin modulate its binding to presenilins.* The Journal of biological chemistry, 2002. **277**(31): p. 28135-42.
160. Kaether, C., et al., *Endoplasmic reticulum retention of the gamma-secretase complex component Pen2 by Rer1*. EMBO reports, 2007. **8**(8): p. 743-8.
161. Spasic, D., et al., *Rer1p competes with APH-1 for binding to nicastrin and regulates gamma-secretase complex assembly in the early secretory pathway.* The Journal of cell biology, 2007. **176**(5): p. 629-40.
162. Kaether, C., et al., *The presenilin C-terminus is required for ER-retention, nicastrin-binding and gamma-secretase activity*. The EMBO journal, 2004. **23**(24): p. 4738-48.
163. Capell, A., et al., *Gamma-secretase complex assembly within the early secretory pathway.* The Journal of biological chemistry, 2005. **280**(8): p. 6471-8.
164. Kim, S.H. and S.S. Sisodia, *Evidence that the "NF" motif in transmembrane domain 4 of presenilin 1 is critical for binding with PEN-2.* The Journal of biological chemistry, 2005. **280**(51): p. 41953-66.
165. Prokop, S., C. Haass, and H. Steiner, *Length and overall sequence of the PEN-2 C-terminal domain determines its function in the stabilization of presenilin fragments.* Journal of neurochemistry, 2005. **94**(1): p. 57-62.

166. Kim, S.H. and S.S. Sisodia, *A sequence within the first transmembrane domain of PEN-2 is critical for PEN-2-mediated endoproteolysis of presenilin 1.* The Journal of biological chemistry, 2005. **280**(3): p. 1992-2001.
167. Tolia, A., L. Chavez-Gutierrez, and B. De Strooper, *Contribution of presenilin transmembrane domains 6 and 7 to a water-containing cavity in the gamma-secretase complex.* The Journal of biological chemistry, 2006. **281**(37): p. 27633-42.
168. Zhou, S., et al., *Regulation of gamma-secretase activity in Alzheimer's disease.* Biochemistry, 2007. **46**(10): p. 2553-63.
169. Zhou, S., et al., *CD147 is a regulatory subunit of the gamma-secretase complex in Alzheimer's disease amyloid beta-peptide production.* Proceedings of the National Academy of Sciences U S A, 2005. **102**(21): p. 7499-504.
170. Takashima, A., et al., *Presenilin 1 associates with glycogen synthase kinase-3beta and its substrate tau.* Proceedings of the National Academy of Sciences U S A, 1998. **95**(16): p. 9637-41.
171. Kirschenbaum, F., et al., *Glycogen synthase kinase-3beta regulates presenilin 1 C-terminal fragment levels.* Journal of Biological Chemistry, 2001. **276**(33): p. 30701-7.
172. Klein, J., *Functions and pathophysiological roles of phospholipase D in the brain.* Journal of Neurochemistry, 2005. **94**(6): p. 1473-87.
173. Cai, D., et al., *Presenilin-1 regulates intracellular trafficking and cell surface delivery of beta-amyloid precursor protein.* Journal of Biological Chemistry, 2003. **278**(5): p. 3446-54.
174. Dolcini, V., et al., *TMP21 regulates Abeta production but does not affect caspase-3, p53, and neprilysin.* Biochemical and Biophysical Research Communications, 2008. **371**(1): p. 69-74.
175. Liao, Y.F., et al., *Tumor necrosis factor-alpha, interleukin-1beta, and interferon-gamma stimulate gamma-secretase-mediated cleavage of amyloid precursor protein through a JNK-dependent MAPK pathway.* Journal of Biological Chemistry, 2004. **279**(47): p. 49523-32.
176. Blasko, I., et al., *TNFalpha plus IFNgamma induce the production of Alzheimer beta-amyloid peptides and decrease the secretion of APPs.* Faseb Journal, 1999. **13**(1): p. 63-8.
177. Blasko, I., et al., *Costimulatory effects of interferon-gamma and interleukin-1beta or tumor necrosis factor alpha on the synthesis of Abeta1-40 and Abeta1-42 by human astrocytes.* Neurobiology of Disease, 2000. **7**(6 Pt B): p. 682-9.
178. Gianni, D., et al., *Platelet-derived growth factor induces the beta-gamma-secretase-mediated cleavage of Alzheimer's amyloid precursor protein through a Src-Rac-dependent pathway.* The Journal of biological chemistry, 2003. **278**(11): p. 9290-7.
179. Shirotani, K., et al., *Gamma-secretase activity is associated with a conformational change of nicastrin.* The Journal of biological chemistry, 2003. **278**(19): p. 16474-7.
180. Sato, C., et al., *Structure of the catalytic pore of gamma-secretase probed by the accessibility of substituted cysteines.* The Journal of neuroscience : the official journal of the Society for Neuroscience, 2006. **26**(46): p. 12081-8.

181. Herreman, A., et al., *Total inactivation of gamma-secretase activity in presenilin-deficient embryonic stem cells.* Nature cell biology, 2000. **2**(7): p. 461-2.
182. Herreman, A., et al., *Presenilin 2 deficiency causes a mild pulmonary phenotype and no changes in amyloid precursor protein processing but enhances the embryonic lethal phenotype of presenilin 1 deficiency.* Proceedings of the National Academy of Sciences of the United States of America, 1999. **96**(21): p. 11872-7.
183. Zhang, Z., et al., *Presenilins are required for gamma-secretase cleavage of beta-APP and transmembrane cleavage of Notch-1.* Nature cell biology, 2000. **2**(7): p. 463-5.
184. Donoviel, D.B., et al., *Mice lacking both presenilin genes exhibit early embryonic patterning defects.* Genes & development, 1999. **13**(21): p. 2801-10.
185. Li, Y.M., et al., *Photoactivated gamma-secretase inhibitors directed to the active site covalently label presenilin 1.* Nature, 2000. **405**(6787): p. 689-94.
186. Jayadev, S., et al., *Alzheimer's disease phenotypes and genotypes associated with mutations in presenilin 2.* Brain : a journal of neurology, 2010. **133**(Pt 4): p. 1143-54.
187. Zhao, B., et al., *Identification of gamma-secretase inhibitor potency determinants on presenilin.* The Journal of biological chemistry, 2008. **283**(5): p. 2927-38.
188. Lee, J., et al., *Identification of presenilin 1-selective gamma-secretase inhibitors with reconstituted gamma-secretase complexes.* Biochemistry, 2011. **50**(22): p. 4973-80.
189. Shen, J., et al., *Skeletal and CNS defects in Presenilin-1-deficient mice.* Cell, 1997. **89**(4): p. 629-39.
190. Wong, P.C., et al., *Presenilin 1 is required for Notch1 and DII1 expression in the paraxial mesoderm.* Nature, 1997. **387**(6630): p. 288-92.
191. De Strooper, B., et al., *Deficiency of presenilin-1 inhibits the normal cleavage of amyloid precursor protein.* Nature, 1998. **391**(6665): p. 387-90.
192. Franberg, J., et al., *Minor contribution of presenilin 2 for gamma-secretase activity in mouse embryonic fibroblasts and adult mouse brain.* Biochemical and biophysical research communications, 2011. **404**(1): p. 564-8.
193. Lai, M.T., et al., *Presenilin-1 and presenilin-2 exhibit distinct yet overlapping gamma-secretase activities.* The Journal of biological chemistry, 2003. **278**(25): p. 22475-81.
194. Yonemura, Y., et al., *Comparison of presenilin 1 and presenilin 2 gamma-secretase activities using a yeast reconstitution system.* The Journal of biological chemistry, 2011. **286**(52): p. 44569-75.
195. Jayadev, S., et al., *Presenilin 2 is the predominant gamma-secretase in microglia and modulates cytokine release.* PLoS One, 2010. **5**(12): p. e15743.
196. Cam, J.A., et al., *The low density lipoprotein receptor-related protein 1B retains beta-amyloid precursor protein at the cell surface and reduces amyloid-beta peptide production.* The Journal of biological chemistry, 2004. **279**(28): p. 29639-46.
197. Kim, D.Y., et al., *BACE1 regulates voltage-gated sodium channels and neuronal activity.* Nature cell biology, 2007. **9**(7): p. 755-64.

198. Huovila, A.P., et al., *Shedding light on ADAM metalloproteinases.* Trends in biochemical sciences, 2005. **30**(7): p. 413-22.
199. Schlondorff, J., J.D. Becherer, and C.P. Blobel, *Intracellular maturation and localization of the tumour necrosis factor alpha convertase (TACE).* The Biochemical journal, 2000. **347 Pt 1**: p. 131-8.
200. Jolly-Tornetta, C. and B.A. Wolf, *Protein kinase C regulation of intracellular and cell surface amyloid precursor protein (APP) cleavage in CHO695 cells.* Biochemistry, 2000. **39**(49): p. 15282-90.
201. Skovronsky, D.M., et al., *Protein kinase C-dependent alpha-secretase competes with beta-secretase for cleavage of amyloid-beta precursor protein in the trans-golgi network.* The Journal of biological chemistry, 2000. **275**(4): p. 2568-75.
202. Daugherty, B.L. and S.A. Green, *Endosomal sorting of amyloid precursor protein-P-selectin chimeras influences secretase processing.* Traffic, 2001. **2**(12): p. 908-16.
203. Kinoshita, A., et al., *Demonstration by FRET of BACE interaction with the amyloid precursor protein at the cell surface and in early endosomes.* Journal of cell science, 2003. **116**(Pt 16): p. 3339-46.
204. Stephens, D.J. and B.M. Austen, *Metabolites of the beta-amyloid precursor protein generated by beta-secretase localise to the trans-Golgi network and late endosome in 293 cells.* Journal of neuroscience research, 1996. **46**(2): p. 211-25.
205. Walter, J., et al., *Phosphorylation regulates intracellular trafficking of beta-secretase.* The Journal of biological chemistry, 2001. **276**(18): p. 14634-41.
206. Chyung, J.H. and D.J. Selkoe, *Inhibition of receptor-mediated endocytosis demonstrates generation of amyloid beta-protein at the cell surface.* The Journal of biological chemistry, 2003. **278**(51): p. 51035-43.
207. Kim, S.H., et al., *Evidence that assembly of an active gamma-secretase complex occurs in the early compartments of the secretory pathway.* The Journal of biological chemistry, 2004. **279**(47): p. 48615-9.
208. Hansson, C.A., et al., *Nicastrin, presenilin, APH-1, and PEN-2 form active gamma-secretase complexes in mitochondria.* The Journal of biological chemistry, 2004. **279**(49): p. 51654-60.
209. Jutras, I., et al., *Gamma-secretase is a functional component of phagosomes.* The Journal of biological chemistry, 2005. **280**(43): p. 36310-7.
210. Fukumori, A., et al., *Presenilin-dependent gamma-secretase on plasma membrane and endosomes is functionally distinct.* Biochemistry, 2006. **45**(15): p. 4907-14.
211. Chyung, J.H., D.M. Raper, and D.J. Selkoe, *Gamma-secretase exists on the plasma membrane as an intact complex that accepts substrates and effects intramembrane cleavage.* The Journal of biological chemistry, 2005. **280**(6): p. 4383-92.
212. Kaether, C., et al., *Amyloid precursor protein and Notch intracellular domains are generated after transport of their precursors to the cell surface.* Traffic, 2006. **7**(4): p. 408-15.
213. Vaccari, T., et al., *Endosomal entry regulates Notch receptor activation in Drosophila melanogaster.* The Journal of cell biology, 2008. **180**(4): p. 755-62.

214. Gupta-Rossi, N., et al., *Monoubiquitination and endocytosis direct gamma-secretase cleavage of activated Notch receptor.* The Journal of cell biology, 2004. **166**(1): p. 73-83.
215. Vassar, R., et al., *Beta-secretase cleavage of Alzheimer's amyloid precursor protein by the transmembrane aspartic protease BACE.* Science, 1999. **286**(5440): p. 735-41.
216. Zhang, M., et al., *Presenilin/gamma-secretase activity regulates protein clearance from the endocytic recycling compartment.* FASEB journal : official publication of the Federation of American Societies for Experimental Biology, 2006. **20**(8): p. 1176-8.
217. Schon, E.A. and E. Area-Gomez, *Is Alzheimer's disease a disorder of mitochondria-associated membranes?* Journal of Alzheimer's disease : JAD, 2010. **20 Suppl 2**: p. S281-92.
218. Beel, A.J. and C.R. Sanders, *Substrate specificity of gamma-secretase and other intramembrane proteases.* Cellular and molecular life sciences : CMLS, 2008. **65**(9): p. 1311-34.
219. Struhl, G. and A. Adachi, *Requirements for presenilin-dependent cleavage of notch and other transmembrane proteins.* Molecular cell, 2000. **6**(3): p. 625-36.
220. Kopan, R. and M.X. Ilagan, *Gamma-secretase: proteasome of the membrane?* Nature reviews. Molecular cell biology, 2004. **5**(6): p. 499-504.
221. Bossy-Wetzel, E., R. Schwarzenbacher, and S.A. Lipton, *Molecular pathways to neurodegeneration.* Nature medicine, 2004. **10 Suppl**: p. S2-9.
222. Querfurth, H.W. and F.M. LaFerla, *Alzheimer's disease.* The New England journal of medicine, 2010. **362**(4): p. 329-44.
223. Weihofen, A. and B. Martoglio, *Intramembrane-cleaving proteases: controlled liberation of proteins and bioactive peptides.* Trends in cell biology, 2003. **13**(2): p. 71-8.
224. Takami, M. and S. Funamoto, *gamma-Secretase-Dependent Proteolysis of Transmembrane Domain of Amyloid Precursor Protein: Successive Tri- and Tetrapeptide Release in Amyloid beta-Protein Production.* International journal of Alzheimer's disease, 2012. **2012**: p. 591392.
225. Yu, C., et al., *Characterization of a presenilin-mediated amyloid precursor protein carboxyl-terminal fragment gamma. Evidence for distinct mechanisms involved in gamma -secretase processing of the APP and Notch1 transmembrane domains.* The Journal of biological chemistry, 2001. **276**(47): p. 43756-60.
226. Gu, Y., et al., *Distinct intramembrane cleavage of the beta-amyloid precursor protein family resembling gamma-secretase-like cleavage of Notch.* The Journal of biological chemistry, 2001. **276**(38): p. 35235-8.
227. Sato, T., et al., *A helix-to-coil transition at the epsilon-cut site in the transmembrane dimer of the amyloid precursor protein is required for proteolysis.* Proceedings of the National Academy of Sciences of the United States of America, 2009. **106**(5): p. 1421-6.
228. Pester, O., et al., *The backbone dynamics of the amyloid precursor protein transmembrane helix provides a rationale for the sequential cleavage mechanism of gamma-secretase.* Journal of the American Chemical Society, 2013. **135**(4): p. 1317-29.

229. Tomita, T. and T. Iwatsubo, *Structural biology of presenilins and signal Peptide peptidases.* The Journal of biological chemistry, 2013. **288**(21): p. 14673-80.
230. Qi-Takahara, Y., et al., *Longer forms of amyloid beta protein: implications for the mechanism of intramembrane cleavage by gamma-secretase.* The Journal of neuroscience : the official journal of the Society for Neuroscience, 2005. **25**(2): p. 436-45.
231. Takami, M., et al., *gamma-Secretase: successive tripeptide and tetrapeptide release from the transmembrane domain of beta-carboxyl terminal fragment.* The Journal of neuroscience : the official journal of the Society for Neuroscience, 2009. **29**(41): p. 13042-52.
232. Kornilova, A.Y., C. Das, and M.S. Wolfe, *Differential effects of inhibitors on the gamma-secretase complex. Mechanistic implications.* The Journal of biological chemistry, 2003. **278**(19): p. 16470-3.
233. Beher, D., et al., *Selected non-steroidal anti-inflammatory drugs and their derivatives target gamma-secretase at a novel site. Evidence for an allosteric mechanism.* The Journal of biological chemistry, 2004. **279**(42): p. 43419-26.
234. Tian, G., et al., *The mechanism of gamma-secretase: multiple inhibitor binding sites for transition state analogs and small molecule inhibitors.* The Journal of biological chemistry, 2003. **278**(31): p. 28968-75.
235. Hoke, D.E., et al., *In vitro gamma-secretase cleavage of the Alzheimer's amyloid precursor protein correlates to a subset of presenilin complexes and is inhibited by zinc.* Febs Journal, 2005. **272**(21): p. 5544-57.
236. Takasugi, N., et al., *The role of presenilin cofactors in the gamma-secretase complex.* Nature, 2003. **422**(6930): p. 438-41.
237. Kimberly, W.T., et al., *Gamma-secretase is a membrane protein complex comprised of presenilin, nicastrin, Aph-1, and Pen-2.* Proceedings of the National Academy of Sciences of the United States of America, 2003. **100**(11): p. 6382-7.
238. Fraering, P.C., et al., *Purification and characterization of the human gamma-secretase complex.* Biochemistry, 2004. **43**(30): p. 9774-89.
239. Scheuner, D., et al., *Secreted amyloid beta-protein similar to that in the senile plaques of Alzheimer's disease is increased in vivo by the presenilin 1 and 2 and APP mutations linked to familial Alzheimer's disease.* Nature Medicine, 1996. **2**(8): p. 864-70.
240. Gravina, S.A., et al., *Amyloid beta protein (A beta) in Alzheimer's disease brain. Biochemical and immunocytochemical analysis with antibodies specific for forms ending at A beta 40 or A beta 42(43).* The Journal of biological chemistry, 1995. **270**(13): p. 7013-6.
241. Elliott, P.R., et al., *Inhibitory conformation of the reactive loop of alpha 1-antitrypsin.* Nature Structural and Molecular Biology, 1996. **3**(8): p. 676-81.
242. Poduslo, J.F., et al., *Permeability and residual plasma volume of human, Dutch variant, and rat amyloid beta-protein 1-40 at the blood-brain barrier.* Neurobiology of Disease, 1997. **4**(1): p. 27-34.
243. Sernee, M.F., et al., *Selecting cells with different Alzheimer's disease gamma-secretase activity using FACS. Differential effect on presenilin exon 9 gamma- and epsilon-cleavage.* European Journal of Biochemistry, 2003. **270**(3): p. 495-506.

244. Bouwman, F.H., et al., *Usefulness of longitudinal measurements of beta-amyloid1-42 in cerebrospinal fluid of patients with various cognitive and neurologic disorders.* Clinical Chemistry, 2006. **52**(8): p. 1604-6.
245. Karlstrom, H., et al., *A sensitive and quantitative assay for measuring cleavage of presenilin substrates.* The Journal of biological chemistry, 2002. **277**(9): p. 6763-6.
246. Kakuda, N., et al., *Equimolar production of amyloid beta-protein and amyloid precursor protein intracellular domain from beta-carboxyl-terminal fragment by gamma-secretase.* The Journal of biological chemistry, 2006. **281**(21): p. 14776-86.
247. Wiley, J.C., et al., *Familial Alzheimer's disease mutations inhibit gamma-secretase-mediated liberation of beta-amyloid precursor protein carboxy-terminal fragment.* Journal of Neurochemistry, 2005. **94**(5): p. 1189-201.
248. Zhang, L., et al., *Biochemical characterization of the gamma-secretase activity that produces beta-amyloid peptides.* Biochemistry, 2001. **40**(16): p. 5049-55.
249. Deroo, B.J. and T.K. Archer, *Proteasome inhibitors reduce luciferase and beta-galactosidase activity in tissue culture cells.* The Journal of biological chemistry, 2002. **277**(23): p. 20120-3.
250. Florean, C., et al., *High content analysis of gamma-secretase activity reveals variable dominance of presenilin mutations linked to familial Alzheimer's disease.* Biochimica Biophysica Acta, 2008. **1783**(8): p. 1551-60.
251. Edbauer, D., et al., *Insulin-degrading enzyme rapidly removes the beta-amyloid precursor protein intracellular domain (AICD).* The Journal of biological chemistry, 2002. **277**(16): p. 13389-93.
252. Cupers, P., et al., *The amyloid precursor protein (APP)-cytoplasmic fragment generated by gamma-secretase is rapidly degraded but distributes partially in a nuclear fraction of neurones in culture.* Journal of neurochemistry, 2001. **78**(5): p. 1168-78.
253. Edbauer, D., et al., *Insulin-degrading enzyme rapidly removes the beta-amyloid precursor protein intracellular domain (AICD).* The Journal of biological chemistry, 2002. **277**(16): p. 13389-93.
254. Venugopal, C., M.A. Pappolla, and K. Sambamurti, *Insulysin cleaves the APP cytoplasmic fragment at multiple sites.* Neurochemical research, 2007. **32**(12): p. 2225-34.
255. Farris, W., et al., *Insulin-degrading enzyme regulates the levels of insulin, amyloid beta-protein, and the beta-amyloid precursor protein intracellular domain in vivo.* Proceedings of the National Academy of Sciences of the United States of America, 2003. **100**(7): p. 4162-7.
256. Nunan, J., et al., *The C-terminal fragment of the Alzheimer's disease amyloid protein precursor is degraded by a proteasome-dependent mechanism distinct from gamma-secretase.* European journal of biochemistry / FEBS, 2001. **268**(20): p. 5329-36.
257. Buoso, E., et al., *beta-Amyloid precursor protein metabolism: focus on the functions and degradation of its intracellular domain.* Pharmacological research : the official journal of the Italian Pharmacological Society, 2010. **62**(4): p. 308-17.

258. McGowan, E., et al., *Amyloid phenotype characterization of transgenic mice overexpressing both mutant amyloid precursor protein and mutant presenilin 1 transgenes.* Neurobiology of Disease, 1999. **6**(4): p. 231-44.
259. Grilli, M., et al., *Alzheimer's disease linking neurodegeneration with neurodevelopment.* Functional Neurology, 2003. **18**(3): p. 145-8.
260. McLendon, C., et al., *Cell-free assays for gamma-secretase activity.* FASEB Journal, 2000. **14**(15): p. 2383-6.
261. Li, Y.M., et al., *Presenilin 1 is linked with gamma-secretase activity in the detergent solubilized state.* Proceedings of the National Academy of Sciences of the United States of America, 2000. **97**(11): p. 6138-43.
262. Pinnix, I., et al., *A novel gamma -secretase assay based on detection of the putative C-terminal fragment-gamma of amyloid beta protein precursor.* The Journal of biological chemistry, 2001. **276**(1): p. 481-7.
263. Franberg, J., et al., *Rat brain gamma-secretase activity is highly influenced by detergents.* Biochemistry, 2007. **46**(25): p. 7647-54.
264. Womack, M.D., D.A. Kendall, and R.C. MacDonald, *Detergent effects on enzyme activity and solubilization of lipid bilayer membranes.* Biochimica Biophysica Acta, 1983. **733**(2): p. 210-5.
265. Wahrle, S., et al., *Cholesterol-dependent gamma-secretase activity in buoyant cholesterol-rich membrane microdomains.* Neurobiology of Disease, 2002. **9**(1): p. 11-23.
266. Sawamura, N., et al., *Modulation of amyloid precursor protein cleavage by cellular sphingolipids.* The Journal of biological chemistry, 2004. **279**(12): p. 11984-91.
267. Vetrivel, K.S., et al., *Spatial segregation of gamma-secretase and substrates in distinct membrane domains.* The Journal of biological chemistry, 2005. **280**(27): p. 25892-900.
268. Banerjee, P., et al., *Differential solubilization of lipids along with membrane proteins by different classes of detergents.* Chemistry and Physics of Lipids, 1995. **77**(1): p. 65-78.
269. Grimm, M.O., et al., *Independent inhibition of Alzheimer disease beta- and gamma-secretase cleavage by lowered cholesterol levels.* The Journal of biological chemistry, 2008. **283**(17): p. 11302-11.
270. Yagishita, S., et al., *Abeta46 is processed to Abeta40 and Abeta43, but not to Abeta42, in the low density membrane domains.* The Journal of biological chemistry, 2008. **283**(2): p. 733-8.
271. Zhao, G., et al., *The same gamma-secretase accounts for the multiple intramembrane cleavages of APP.* Journal of Neurochemistry, 2007. **100**(5): p. 1234-46.
272. Area-Gomez, E., et al., *Presenilins are enriched in endoplasmic reticulum membranes associated with mitochondria.* American Journal of Pathology, 2009. **175**(5): p. 1810-6.
273. Schon, E.A. and E. Area-Gomez, *Is Alzheimer's disease a disorder of mitochondria-associated membranes?* Journal of Alzheimers Disease, 2010. **20 Suppl 2**: p. S281-92.

274. Winkler, E., et al., *Generation of Alzheimer disease-associated amyloid beta42/43 peptide by gamma-secretase can be inhibited directly by modulation of membrane thickness.* The Journal of Biological Chemistry, 2012. **287**(25): p. 21326-34.
275. Area-Gomez, E., et al., *Upregulated function of mitochondria-associated ER membranes in Alzheimer disease.* EMBO Journal, 2012. **31**(21): p. 4106-23.
276. van Tijn, P., et al., *Presenilin mouse and zebrafish models for dementia: Focus on neurogenesis.* Progress in Neurobiology, 2011. **93**(2): p. 149-64.
277. Sarasa, M. and P. Pesini, *Natural non-trasgenic animal models for research in Alzheimer's disease.* Current Alzheimer Research, 2009. **6**(2): p. 171-8.
278. Donoviel, D.B., et al., *Mice lacking both presenilin genes exhibit early embryonic patterning defects.* Genes and Development, 1999. **13**(21): p. 2801-10.
279. Yamada, K. and T. Nabeshima, *Animal models of Alzheimer's disease and evaluation of anti-dementia drugs.* Pharmacology and Therapeutics, 2000. **88**(2): p. 93-113.
280. Games, D., et al., *Alzheimer-type neuropathology in transgenic mice overexpressing V717F beta-amyloid precursor protein.* Nature, 1995. **373**(6514): p. 523-7.
281. Hsiao, K., et al., *Correlative memory deficits, Abeta elevation, and amyloid plaques in transgenic mice.* Science, 1996. **274**(5284): p. 99-102.
282. Newman, M., I.F. Musgrave, and M. Lardelli, *Alzheimer disease: amyloidogenesis, the presenilins and animal models.* Biochimica et Biophysica Acta, 2007. **1772**(3): p. 285-97.
283. Sturchler-Pierrat, C., et al., *Two amyloid precursor protein transgenic mouse models with Alzheimer disease-like pathology.* Proceedings of the National Academy of Sciences of the United States of America, 1997. **94**(24): p. 13287-92.
284. Calhoun, M.E., et al., *Neuron loss in APP transgenic mice.* Nature, 1998. **395**(6704): p. 755-6.
285. Calhoun, M.E., et al., *Neuronal overexpression of mutant amyloid precursor protein results in prominent deposition of cerebrovascular amyloid.* Proceedings of the National Academy of Sciences of the United States of America, 1999. **96**(24): p. 14088-93.
286. Duff, K., et al., *Increased amyloid-beta42(43) in brains of mice expressing mutant presenilin 1.* Nature, 1996. **383**(6602): p. 710-3.
287. Borchelt, D.R., et al., *Accelerated amyloid deposition in the brains of transgenic mice coexpressing mutant presenilin 1 and amyloid precursor proteins.* Neuron, 1997. **19**(4): p. 939-45.
288. Holcomb, L., et al., *Accelerated Alzheimer-type phenotype in transgenic mice carrying both mutant amyloid precursor protein and presenilin 1 transgenes.* Nature Medicine, 1998. **4**(1): p. 97-100.
289. Irizarry, M.C., et al., *Abeta deposition is associated with neuropil changes, but not with overt neuronal loss in the human amyloid precursor protein V717F (PDAPP) transgenic mouse.* Journal of Neuroscience, 1997. **17**(18): p. 7053-9.
290. Takeuchi, A., et al., *Age-related amyloid beta deposition in transgenic mice overexpressing both Alzheimer mutant presenilin 1 and amyloid beta precursor protein Swedish mutant is not associated with global neuronal loss.* American Journal of Pathology, 2000. **157**(1): p. 331-9.

291. West, M.J., et al., *Differences in the pattern of hippocampal neuronal loss in normal ageing and Alzheimer's disease.* Lancet, 1994. **344**(8925): p. 769-72.
292. Gomez-Isla, T., et al., *Profound loss of layer II entorhinal cortex neurons occurs in very mild Alzheimer's disease.* Journal of Neuroscience, 1996. **16**(14): p. 4491-500.
293. Irizarry, M.C., et al., *APPSw transgenic mice develop age-related A beta deposits and neuropil abnormalities, but no neuronal loss in CA1.* Journal of Neuropathology and Experimental Neurology, 1997. **56**(9): p. 965-73.
294. Braak, H. and E. Braak, *Neuropathological stageing of Alzheimer-related changes.* Acta Neuropathologica, 1991. **82**(4): p. 239-59.
295. Link, C.D., *C. elegans models of age-associated neurodegenerative diseases: lessons from transgenic worm models of Alzheimer's disease.* Experimental Gerontology, 2006. **41**(10): p. 1007-13.
296. Daigle, I. and C. Li, *apl-1, a Caenorhabditis elegans gene encoding a protein related to the human beta-amyloid protein precursor.* Proceedings of the National Academy of Sciences of the United States of America, 1993. **90**(24): p. 12045-9.
297. Hornsten, A., et al., *APL-1, a Caenorhabditis elegans protein related to the human beta-amyloid precursor protein, is essential for viability.* Proceedings of the National Academy of Sciences of the United States of America, 2007. **104**(6): p. 1971-6.
298. Levitan, D., et al., *Assessment of normal and mutant human presenilin function in Caenorhabditis elegans.* Proceedings of the National Academy of Sciences of the United States of America, 1996. **93**(25): p. 14940-4.
299. Li, X. and I. Greenwald, *HOP-1, a Caenorhabditis elegans presenilin, appears to be functionally redundant with SEL-12 presenilin and to facilitate LIN-12 and GLP-1 signaling.* Proceedings of the National Academy of Sciences of the United States of America, 1997. **94**(22): p. 12204-9.
300. Arduengo, P.M., et al., *The presenilin protein family member SPE-4 localizes to an ER/Golgi derived organelle and is required for proper cytoplasmic partitioning during Caenorhabditis elegans spermatogenesis.* Journal of Cell Science, 1998. **111 (Pt 24)**: p. 3645-54.
301. Link, C.D., *Expression of human beta-amyloid peptide in transgenic Caenorhabditis elegans.* Proceedings of the National Academy of Sciences of the United States of America, 1995. **92**(20): p. 9368-72.
302. Link, C.D., et al., *Visualization of fibrillar amyloid deposits in living, transgenic Caenorhabditis elegans animals using the sensitive amyloid dye, X-34.* Neurobiology of Aging, 2001. **22**(2): p. 217-26.
303. Wu, Y. and Y. Luo, *Transgenic C. elegans as a model in Alzheimer's research.* Current Alzheimer Research, 2005. **2**(1): p. 37-45.
304. Link, C.D., et al., *Gene expression analysis in a transgenic Caenorhabditis elegans Alzheimer's disease model.* Neurobiol Aging, 2003. **24**(3): p. 397-413.
305. Fonte, V., et al., *Interaction of intracellular beta amyloid peptide with chaperone proteins.* Proceedings of the National Academy of Sciences of the United States of America, 2002. **99**(14): p. 9439-44.
306. Sonnhammer, E.L. and R. Durbin, *Analysis of protein domain families in Caenorhabditis elegans.* Genomics, 1997. **46**(2): p. 200-16.

307. Butterfield, D.A., et al., *Elevated oxidative stress in models of normal brain aging and Alzheimer's disease.* Life Sciences, 1999. **65**(18-19): p. 1883-92.
308. Yatin, S.M., et al., *In vitro and in vivo oxidative stress associated with Alzheimer's amyloid beta-peptide (1-42).* Neurobiology of Aging, 1999. **20**(3): p. 325-30; discussion 339-42.
309. Yang, A.J., et al., *Intracellular A beta 1-42 aggregates stimulate the accumulation of stable, insoluble amyloidogenic fragments of the amyloid precursor protein in transfected cells.* The Journal of biological chemistry, 1995. **270**(24): p. 14786-92.
310. Drake, J., C.D. Link, and D.A. Butterfield, *Oxidative stress precedes fibrillar deposition of Alzheimer's disease amyloid beta-peptide (1-42) in a transgenic Caenorhabditis elegans model.* Neurobiology of Aging, 2003. **24**(3): p. 415-20.
311. Niimura, M., et al., *Aph-1 contributes to the stabilization and trafficking of the gamma-secretase complex through mechanisms involving intermolecular and intramolecular interactions.* The Journal of biological chemistry, 2005. **280**(13): p. 12967-75.
312. Guo, M., et al., *A reporter for amyloid precursor protein gamma-secretase activity in Drosophila.* Human Molecular Genetics, 2003. **12**(20): p. 2669-78.
313. Luo, L.Q., L.E. Martin-Morris, and K. White, *Identification, secretion, and neural expression of APPL, a Drosophila protein similar to human amyloid protein precursor.* The Journal of neuroscience : the official journal of the Society for Neuroscience, 1990. **10**(12): p. 3849-61.
314. Torroja, L., et al., *Neuronal overexpression of APPL, the Drosophila homologue of the amyloid precursor protein (APP), disrupts axonal transport.* Current Biology, 1999. **9**(9): p. 489-92.
315. Luo, L., T. Tully, and K. White, *Human amyloid precursor protein ameliorates behavioral deficit of flies deleted for Appl gene.* Neuron, 1992. **9**(4): p. 595-605.
316. Gunawardena, S. and L.S. Goldstein, *Disruption of axonal transport and neuronal viability by amyloid precursor protein mutations in Drosophila.* Neuron, 2001. **32**(3): p. 389-401.
317. Stokin, G.B., et al., *Axonopathy and transport deficits early in the pathogenesis of Alzheimer's disease.* Science, 2005. **307**(5713): p. 1282-8.
318. Summerton, J. and D. Weller, *Morpholino antisense oligomers: design, preparation, and properties.* Antisense Nucleic Acid Drug Development, 1997. **7**(3): p. 187-95.
319. Nasevicius, A. and S.C. Ekker, *Effective targeted gene 'knockdown' in zebrafish.* Nature Genetics, 2000. **26**(2): p. 216-20.
320. Musa, A., H. Lehrach, and V.A. Russo, *Distinct expression patterns of two zebrafish homologues of the human APP gene during embryonic development.* Development genes and evolution, 2001. **211**(11): p. 563-7.
321. Joshi, P., et al., *Amyloid precursor protein is required for convergent-extension movements during Zebrafish development.* Developmental biology, 2009. **335**(1): p. 1-11.
322. Sarasa, M., et al., *Alzheimer beta-amyloid precursor proteins display specific patterns of expression during embryogenesis.* Mech Dev, 2000. **94**(1-2): p. 233-6.

323. Song, P. and S.W. Pimplikar, *Knockdown of amyloid precursor protein in zebrafish causes defects in motor axon outgrowth.* PLoS One, 2012. **7**(4): p. e34209.
324. Groth, C., et al., *Identification of a second presenilin gene in zebrafish with similarity to the human Alzheimer's disease gene presenilin2.* Development genes and evolution, 2002. **212**(10): p. 486-90.
325. Leimer, U., et al., *Zebrafish (Danio rerio) presenilin promotes aberrant amyloid beta-peptide production and requires a critical aspartate residue for its function in amyloidogenesis.* Biochemistry, 1999. **38**(41): p. 13602-9.
326. Nornes, S., et al., *Developmental control of Presenilin1 expression, endoproteolysis, and interaction in zebrafish embryos.* Experimental Cell Research, 2003. **289**(1): p. 124-32.
327. Nornes, S., et al., *Developmental control of Presenilin1 expression, endoproteolysis, and interaction in zebrafish embryos.* Experimental cell research, 2003. **289**(1): p. 124-32.
328. Campbell, W.A., et al., *Zebrafish lacking Alzheimer presenilin enhancer 2 (Pen-2) demonstrate excessive p53-dependent apoptosis and neuronal loss.* Journal of neurochemistry, 2006. **96**(5): p. 1423-40.
329. Nornes, S., et al., *Interference with splicing of Presenilin transcripts has potent dominant negative effects on Presenilin activity.* Human molecular genetics, 2008. **17**(3): p. 402-12.
330. Kwok, J.B., et al., *Presenilin-1 mutation L271V results in altered exon 8 splicing and Alzheimer's disease with non-cored plaques and no neuritic dystrophy.* The Journal of biological chemistry, 2003. **278**(9): p. 6748-54.
331. Perez-Tur, J., et al., *A mutation in Alzheimer's disease destroying a splice acceptor site in the presenilin-1 gene.* Neuroreport, 1995. **7**(1): p. 297-301.
332. Prihar, G., et al., *Structure and alternative splicing of the presenilin-2 gene.* Neuroreport, 1996. **7**(10): p. 1680-4.
333. van Tijn, P., et al., *Presenilin mouse and zebrafish models for dementia: focus on neurogenesis.* Progress in neurobiology, 2011. **93**(2): p. 149-64.
334. Nornes, S., et al., *Independent and cooperative action of Psen2 with Psen1 in zebrafish embryos.* Experimental cell research, 2009. **315**(16): p. 2791-801.
335. Francis, R., et al., *aph-1 and pen-2 are required for Notch pathway signaling, gamma-secretase cleavage of betaAPP, and presenilin protein accumulation.* Developmental cell, 2002. **3**(1): p. 85-97.
336. Campbell, W.A., et al., *Zebrafish lacking Alzheimer presenilin enhancer 2 (Pen-2) demonstrate excessive p53-dependent apoptosis and neuronal loss.* The Journal of Neurochemistry, 2006. **96**(5): p. 1423-40.
337. Strausberg, R.L., et al., *Generation and initial analysis of more than 15,000 full-length human and mouse cDNA sequences.* Proceedings of the National Academy of Sciences of the United States of America, 2002. **99**(26): p. 16899-903.
338. Dovey, H.F., et al., *Functional gamma-secretase inhibitors reduce beta-amyloid peptide levels in brain.* The Journal of Neurochemistry, 2001. **76**(1): p. 173-81.
339. Geling, A., et al., *A gamma-secretase inhibitor blocks Notch signaling in vivo and causes a severe neurogenic phenotype in zebrafish.* EMBO Reports, 2002. **3**(7): p. 688-94.

340. Nornes, S., et al., *Interference with splicing of Presenilin transcripts has potent dominant negative effects on Presenilin activity.* Human Molecular Genetics, 2008. **17**(3): p. 402-12.
341. Groth, C., et al., *Identification of a second presenilin gene in zebrafish with similarity to the human Alzheimer's disease gene presenilin2.* Development Genes and Evolution, 2002. **212**(10): p. 486-90.
342. Nornes, S., et al., *Developmental control of Presenilin1 expression, endoproteolysis, and interaction in zebrafish embryos.* Experimental Cell Research, 2003. **289**(1): p. 124-32.
343. Newman, M., et al., *Altering presenilin gene activity in zebrafish embryos causes changes in expression of genes with potential involvement in Alzheimer's disease pathogenesis.* The Journal of Alzheimers Disease, 2009. **16**(1): p. 133-47.
344. Suzuki, Y., et al., *An alternative spliced mouse presenilin-2 mRNA encodes a novel gamma-secretase inhibitor.* FEBS Letters, 2009. **583**(9): p. 1403-8.
345. Crump, C.J., et al., *BMS-708,163 targets presenilin and lacks notch-sparing activity.* Biochemistry, 2012. **51**(37): p. 7209-11.
346. Chavez-Gutierrez, L., et al., *The mechanism of gamma-Secretase dysfunction in familial Alzheimer disease.* The EMBO journal, 2012. **31**(10): p. 2261-74.
347. Kanning, K.C., et al., *Proteolytic processing of the p75 neurotrophin receptor and two homologs generates C-terminal fragments with signaling capability.* The Journal of neuroscience : the official journal of the Society for Neuroscience, 2003. **23**(13): p. 5425-36.

APPENDIX I

Research Paper IV

A zebrafish melanophore model of amyloid beta toxicity.

Morgan Newman[1], Lachlan Wilson[1], Giuseppe Verdile[2,3,4], Esther Camp[1]

Ralph Martins [2,3,4] and Michael Lardelli[1]

[1]Discipline of Genetics, School of Molecular and Biomedical Science, The University of Adelaide, SA 5005, Australia, [2]Centre of Excellence for Alzheimer's Disease Research and Care, School of Exercise, Biomedical and Health, [3]SirJames McCusker Alzheimer's Disease Sciences, Edith Cowan University, Joondalup, WA 6027, Australia, [4]Neurosciences, University of Western Australia, Crawley, WA 6009, Australia, Department of Pharmacology, Howard.

Zebrafish, 2010, Vol7, No2 155-9.

ZEBRAFISH
Volume 7, Number 2, 2010

DOI: 10.1089/zeb.2009.0628

A Zebrafish Melanophore Model of Amyloidβ Toxicity

Morgan Newman,[1] Lachlan Wilson,[1] Esther Camp,[1,*] Giuseppe Verdile,[2–4] Ralph Martins,[2–4] and Michael Lardelli[1]

Abstract

Reliable animal models are required to facilitate the understanding of neurodegenerative pathways in Alzheimer's disease. Animal models can also be employed to search for disease-modifying drugs. The embryos and larvae of zebrafish are particularly advantageous for this purpose. For Alzheimer's disease, drugs that can ameliorate amyloidβ (Aβ) toxicity have therapeutic and/or prophylactic potential. We attempted to generate a zebrafish model of Aβ toxicity that would be viable and fertile but have a highly visible pigmentation phenotype in larvae. The larvae could then be arrayed in microtiter plates to screen compound libraries for drugs acting to reduce Aβ toxicity. We used the promoter of the zebrafish *mitfa* (*nacre*) gene to drive expression of the pathological 42 amino acid species of human Aβ, Aβ_{42}, specifically in the highly visible melanophores (melanocytes) of transgenic zebrafish. However, the transgenic fish only showed an aberrant pigment phenotype in adults at the advanced age of 16 months. Nevertheless, our results show that alteration of zebrafish pigment pattern may be useful for analysis of toxic peptide action.

Introduction

There is considerable evidence supporting the idea that Alzheimer's disease is caused primarily by the accumulation of amyloidβ (Aβ) peptides in the brain. The Aβ_{42} isoform is more hydrophobic than shorter forms. Consequently, it is less soluble and more prone to aggregation to form oligomers and, ultimately, amyloid plaques. Oligomerization and accumulation of Aβ_{42} is thought to result in neuronal cytotoxicity that induces neuropathological events leading to neurodegeneration.[1] The exact mechanism by which Aβ peptide accumulation induces neurotoxicity is unclear.

Reliable animal models are required to facilitate study of the neurodegenerative pathways in Alzheimer's disease (AD). They aid in elucidation of the molecular, cellular, and pathological changes that trigger the onset of cognitive decline. Further, models are needed that can facilitate testing for compounds that affect various points of the pathogenic cascade in the hope of finding disease-modifying drugs.

Most transgenic models of Aβ action have been generated in mice.[2,3] However, the utility of these mice in screening drug libraries for compounds that may combat Aβ toxicity is limited. Two invertebrate models better suited to drug screening exist. In 1995, Link[4] generated a model of Aβ molecular pathology in *Caenorhabditis elegans* by engineering these animals to express human Aβ_{42} specifically in muscle cells. These nematodes produced muscle-specific Aβ deposits that were immunoreactive with anti-Aβ antibodies. The transgenic larvae displayed progressive muscle paralysis and vacuoles that were attributed to Aβ toxicity. A *Drosophila* model of Aβ_{42} toxicity was developed by Crowther and colleagues[5] in 2005. They expressed the Arctic mutant form of human Aβ in the central nervous system (CNS) and retina of transgenic flies. This resulted in intracellular accumulation of Aβ associated with progressive locomotor deficits and premature death.

The zebrafish is an advantageous model organism for studies of developmental gene function and disease processes in the nervous system. As vertebrates, they possess a brain structure similar to that found in mammals. However, their use in drug screening is facilitated by their ready availability in large numbers, their small size as embryos and newly hatched larvae, and their development outside the mother in an aqueous medium. Transgenic zebrafish can be generated through use of efficient vectors such as the Sleeping Beauty transposase system.[6] We employed this system to generate transgenic zebrafish possessing human Aβ_{42} under the

[1]Discipline of Genetics, School of Molecular and Biomedical Science, The University of Adelaide, Adelaide, Australia.
[2]Centre of Excellence for Alzheimer's Disease Research and Care, School of Exercise, Biomedical, and Health Sciences, Edith Cowan University, Joondalup, Australia.
[3]Sir James McCusker Alzheimer's Disease Research Unit, Hollywood Private Hospital, Nedlands, Australia.
[4]School of Psychiatry and Clinical Neurosciences, University of Western Australia, Crawley, Australia.
*Present address: School of Biological Sciences and Cell and Developmental Biology, University of East Anglia, Norwich, Norfolk, United Kingdom.

control of the *mitfa* promoter that drives expression specifically in their highly visible melanophores.[7] We aimed to produce zebrafish in which Aβ_{42} toxicity caused aberrant pigmentation patterns on embryos or larvae without affecting their viability or fertility. These animals could then be used to screen for drugs that suppress the transgenic phenotype. Such drugs would be candidate suppressors of Aβ_{42} toxicity.

Materials and Methods

Transgene construction and transgenesis

Linearized pT2-*mitfa*-Aβ-EGFP DNA (see Results section) was coinjected into embryos at the one-cell stage with transposase mRNA generated from the pSBRNAX plasmid.[6] The transposase recognizes inverted repeats flanking the insert in pT2 and excises the insert for integration into the genome. Adult fish were raised from injected embryos and were then outbred individually to wild-type fish. Progeny from each mating were pooled, and genomic DNA was purified from each pool for testing by polymerase chain reaction (PCR) for the presence of the pT2-*mitfa*-Aβ-EGFP transgene (Fig. 1A and see PCR1 below). An improved PCR test with less nonspecific amplification (Fig. 1A and see PCR2 below) was developed to test for the transgene in tail-clips from individual aged adult fish.

Nucleic acid purification/preparation

Genomic DNA preparation from zebrafish tail-clips was performed essentially as described by Rehbein and Bogerd,[8] with adult fish anesthetized in 168 μg/mL tricaine solution before tail-clipping. Proteases were removed by phenol/chloroform extraction and then ethanol precipitation. RNA was extracted from adult zebrafish skin using the Qiagen RNeasy Mini kit (Qiagen, Hilden, Germany). RNA samples were precipitated with lithium chloride (Ambion, Austen, TX) and re-dissolved in water before treatment with RQ1Dnase to remove any traces of contaminating DNA. These were then reverse transcribed into cDNA as previously described in Newman *et al.*[9]

Polymerase chain reactions

PCR1: 30 cycles of 94°C 30 s at 94°C, 1 min at 58°C, and 1 min at 72°C using primer pair 1: 5′CCATGGTGTGGGCCGA3′ and 5′TCACGCTATGACAACCACCG3′.

PCR2: 30 cycles of 30 s at 94°C, 1 min at 60°C, and 1 min at 72°C using primer pair 2: 5′GGCCCATCAGACAACAAAGT3′ and 5′TTCGCTCACGCTATGACAAC3′.

Nested PCR for detection of expression of *mitfa*: The initial PCR used primers 5′GGTTCATGGATGCAGGACTT3′ and 5′GCTGGAAGAAGCTACAACGG3′ with 30 cycles of 20 s at 98°C, 20 s at 63°C, and 30 s at 72°C (25 μL total volume). Two microliters of the initial PCR was then placed into a second, nested PCR using the primers 5′CACGATTCCAGTTTCAGCAA3′ and 5′AATACGGAGCAGGAGATGTC3′ with 30 cycles of 20 s at 98°C, 20 s at 65°C, and 30 s at 72°C (25 μL total volume).

Whole-mount in situ *hybridization*

Embryos were fixed in 4% formaldehyde in the embryo medium before manual de-chorionation. Whole-mount *in situ* transcript hybridization (WISH) was then performed essentially as described by Jowett[10] using a digoxigenin-labeled antisense EGFP RNA probe.

Results

To construct a transgene for expression of human Aβ_{42} peptide specifically in zebrafish melanophores, we fused an optimized secretory signal peptide sequence ("HMM+38," see Barash *et al.*[11]) to DNA coding for human Aβ_{42} followed by a stop codon. This coding sequence was then inserted into a derivative of the Sleeping Beauty vector pT2[6] containing a ~1 kb fragment of the zebrafish *mitfa* promoter (GenBank accession AF211890, and see Dorsky *et al.*[12]). The insertion of the HMM+38::Aβ_{42} fusion into the pT2 derivative was performed such that it separated the vector's EGFP coding sequences from the *mitfa* promoter. The resultant transgene was named pT2-*mitfa*-Aβ-EGFP (Fig. 1A). Transcripts from the *mitfa* promoter of pT2-*mitfa*-Aβ-EGFP should include the vector's EGFP coding sequences, but these would not be translated.

To generate transgenic fish, linearized pT2-*mitfa*-Aβ-EGFP DNA was coinjected into embryos with transposase mRNA at the one-cell stage.[6] At 24 hpf a subset of the injected embryos was fixed for WISH against EGFP coding sequence. This should detect transcripts from the transgene that include the nontranslated EGFP coding sequence. As expected, this revealed cells expressing the transgene in positions consistent with migrating melanophores (e.g., see Fig. 1B). Extended staining was required to reveal these cells (32 h at 4°C and 8 h at room temperature), implying that the cloned *mitfa* promoter is not highly active and/or that the transcripts are relatively unstable.

Ten adult fish were raised from injected embryos and were then outbred individually to wild-type fish. Progeny from each mating were pooled before extraction of genomic DNA to test for the presence of the transgene (see PCR1 in Materials and Methods section). This revealed that two of the original injected adult fish were transmitting the transgene to their progeny. Out-crossed progeny from these fish were then grown to adulthood. Transgenic individuals were detected from among the progeny using a PCR (PCR1) on genomic DNA purified from the fish after tail-clipping. Ultimately, two independent lines of transgenic fish, line 1 and line 2, were established.

We could not discern any abnormalities in embryos and larvae from lines 1 or 2, when visible pigmentation developed after 24 h of development. Therefore, these transgenic lines were not useful for screening of compound libraries to find drugs that ameliorate Aβ toxicity. However, by 16 months of age some adult fish in both lines began to show loss of stripes of melanin pigmentation but retention of normal reflective pigment (in iridophores) and yellow pigmentation (in xanthophores). In many cases, small foci of melanin pigmentation could be observed, especially in the fins of the stripeless fish (Fig. 1D lower panel). We do not know whether this represents cells with abnormal melanosome distribution or cells dying in a manner consistent with a progressive, age-dependent phenomenon (or both).

The populations of each transgenic line of fish were the outbred progeny of single individuals heterozygous for the transgene, so one would expect approximately half the fish in these populations to possess the transgene (unless multiple

transgene inserts were present in a line). At 16 months the line 1 population had 7 of 30 fish and the line 2 population had 3 of 22 fish that lacked normal dark stripes. At 19 months line 1 had 10 of 30 fish and line 2 had 6 of 22 fish that lacked normal dark stripes. The final observations were made at 24 months, where 11 of 30 fish (33%) of the line 1 population and 6 of 22 fish (27%) of the line 2 population lacked normal dark stripes. In contrast, the progeny of a nontransgenic sibling of the founders of transgenic lines 1 and 2 all showed normal pigmentation at 24 months of age (21 fish observed).

The late onset of the apparent pigment loss phenotype of the *mitfa*-Aβ-EGFP transgene implies that the transgene is active in melanophores (or their precursors) in adult skin. (However, it is possible that early transgene expression might predispose aged melanophores to premature loss, e.g., by sensitizing these cells to accumulated stress.) Since it has not yet been demonstrated formally that the endogenous *mitfa* promoter is active in the skin of adult wild-type zebrafish, we performed a nested reverse transcription (RT)-PCR test[13] to detect *mitfa* transcripts. No amplified product was evident after agarose gel electrophoresis of the reaction products. However, when 2 μL of the initial PCR was then placed into a second, nested PCR a signal indicating the presence of *mitfa* cDNA was evident (Fig. 1C). Hence, *mitfa* is transcribed in adult zebrafish skin.

A similar nested RT-PCR was used to detect expression of the *mitfa*-Aβ-EGFP transgene in the skin of affected transgenic fish. Total cellular RNA was extracted from the excised dorsal skin of individual transgenic fish from line 1. However, despite performing RT-PCR with three separate sets of initial and nested PCR primer pairs, we were unable to detect the presence of transgene transcripts (data not shown). This may be due to a combination of factors (see Discussion section).

To support that the age-dependent stripe loss was due to the presence of the transgene, we tested the transgenic status of eight stripeless fish and eight fish with stripes in the line 1 population as well as three fish from a wild-type population. An improved PCR test with less nonspecific amplification, PCR2, was performed on DNA samples prepared from the clipped tails of these fish. All stripeless fish and six of eight striped fish were shown to be transgenic (Fig. 1E, F). As expected, the PCR test was negative for the wild-type fish (data not shown). Thus, presumed expression of Aβ_{42} in the melanophores of zebrafish results in noticeable loss of melanin pigmentation by 16 months. If this represents melanophore

FIG. 1. (**A**) The pT2-*mitfa*-Aβ-EGFP transgene. The transposon construct in the Sleeping Beauty vector. The binding positions of the primer sets used for polymerase chain reaction (PCR) tests are indicated above the transgene. Arrows at the end of the transgene are the inserted repeats recognized by the transposase mRNA. (**B**) Whole-mount *in situ* transcript hybridization for transcripts containing EGFP coding sequences in a 24 hpf embryo. A lateral view (slightly oblique, sagittal optical section) at the midregion of the yolk extension (ye). Dorsal is to the top. Arrowheads indicate putative immature melanophores lacking pigmentation. The upper indicated cell was observed to lie near the level of the horizontal myoseptum in the region between the notochord (nc) and the myotome (my), consistent with the medial pathway of melanocyte migration in zebrafish (Jesuthasan, 1996). The indicated cells appeared somewhat dendritic. (**C**) Nested reverse transcription (RT)-PCR to detect *mitfa* transcription in the skin of wild-type adult zebrafish. Lane 1 is the PCR product from wild-type skin; lane 2 is the negative (no RNA/cDNA) control. M indicates the DNA marker ("2-Log DNA Ladder"). (**D**) Adult zebrafish at 16 months. Upper panel: a representative normal adult zebrafish. Lower panel: a transgenic fish that had specific loss of melanophores. (**1**) and (**2**) are enlarged images of corresponding areas of the caudal fin (see boxes). (**E, F**) PCR on genomic DNA from zebrafish tail clips to detect the presence of the transgene. Eight striped fish (**E**, lanes 1–8) and eight stripeless fish (**F**, lanes 1–8) from an outcross of line 1 were tail clipped, and genomic DNA was tested for the presence of the transgene. '+' indicates detection of transgene and '−' indicates no detection. (**F**) Lane 9 is blank, lane 10 is a negative control (no DNA) reaction, and lane 11 is from a reaction containing pT2-*mitfa*-Aβ-EGFP plasmid DNA as a template as a positive control. M indicates the DNA marker, which is "2-Log DNA Ladder" supplied by New England BioLabs (Ipswich, MA). Color images available online at www.liebertonline.com/zeb.

loss, it may occur by their premature death and/or failure to maintain a precursor cell population (if these also express *mitfa*). Unfortunately, by the time the pigmentation phenotype was observed at 16 months, these fish were no longer fertile, thus precluding propagation of the transgenic lines for further observation.

Discussion

Three types of pigment cells differentiate from the neural crest during zebrafish embryo development: the starkly visible black melanophores, the less obvious yellow xanthophores, and the silvery reflective iridophores.[14] Zebrafish *nacre* mutants lack all melanophores and have marginally reduced xanthophores and increased iridophore numbers.[7] The zebrafish *mitfa/nacre* gene is a duplicate of an ancestral ortholog of the human *MITF* gene.[7] *MITF* is a key regulator of the melanocyte/melanophore lineage and is involved in the differentiation, growth, and survival of pigment cells.[15] Importantly, *Mitf* is expressed in adult mouse hair follicles[16] and *MITF* is expressed in adult human skin since melanocytes are distributed throughout the epidermis.[15] This study provides RT-PCR evidence for expression of endogenous *mitfa* in adult zebrafish skin. We presume that this occurs primarily or exclusively in melanophores since, in humans, the *TYROSINASE* gene (required for melanin pigment formation in melanocytes) is activated by binding of the MITF transcription factor.[17] This idea is supported by the apparent late manifestation of the toxic effect of Aβ_{42} expression in zebrafish; that is, aberrant pigmentation was not observed until 16 months of age (although the possibility exists that expression of Aβ_{42} from the *mitfa* promoter in melanophores or melanophore precursors may predispose melanophores or their precursors for cell death at a later time point).

Transcripts from the *mitfa*-Aβ-EGFP transgene could be detected in injected embryos at 24 hpf (Fig. 1B). The positions of the cells expressing the transgene were consistent with what we know of melanophore differentiation and migration,[18] supporting that the transgene is active in these cells, at least at this early time point. Our failure to detect transcripts of the transgene by RT-PCR in the skin of affected adults may be due to one or a combination of factors. For example, the transgene may be transcribed at relatively low levels compared to the endogenous *mitfa* gene due to possible lack of enhancer elements in the cloned *mitfa* promoter. (Indeed, detection of the transgene by WISH in the as yet pigmentless melanophores of the 24 hpf embryo required an extended staining reaction.) Also, the insertion sites of the transgene in lines 1 and 2 may have been suboptimal for promoter activity, and/or the transgene transcript may be relatively unstable. These factors, combined with the small proportion of all adult skin cells that melanophores represent and the ongoing toxic effects of the transgene on the melanophores in these aged fish, may have reduced the concentration of transgene mRNA to levels below which our RT-PCR could not amplify it. Nevertheless, we think that it is highly improbable that the observed pigment loss phenotypes are artefactual since only fish possessing the transgene were affected and the presence of the transgene specifically affected melanophores rather than the other two pigment cell types (xanthophores and iridophores) in which *mitfa* is not expressed. (Note, *mitfa* expression has been observed in some cells that may be xanthophore precursors,[19] but xanthophores do not require *mitfa* activity to differentiate.[7]) Unfortunately, the age and infertility of the transgenic fish prevented us from propagating them for future analysis and limited the number of individuals we had available to study. We note that in the only previously published work to have used the *mitfa* promoter in germline transgenics, Patton *et al.*[20] only reported expression of their oncogenic transgene within tumor tissue and not in embryos (see Fig. 3C of Patton *et al.*[20]), and detection of the action of the transgene in adult fish was by observation of changes in pigmentation pattern alone.

Melanocyte stem cells (MSC) exist in humans and mice, as evident through the mammalian hair follicle cycle.[21] Age-associated graying is a result of loss of MSCs from the hair follicle.[22] The existence of MSCs in zebrafish adults has been proposed since melanophores can be observed throughout the regenerating caudal fin 4 days after its amputation.[23] Thus, the delayed phenotype observed in the transgenic fish expressing human Aβ_{42} could be due to the presence of MSCs during development and in adults producing new melanophores as the transgenic ones die. It is possible that, as the fish age, the ability of MSCs to generate melanophores and new MSCs declines, such that the toxicity of human Aβ_{42} eventually reduces MSC and melanophore numbers. Therefore, the age-related loss of melanophores due to human Aβ_{42} toxicity may be similar to age-associated graying in humans, which is due to loss of MSCs.

The *mitfa* promoter has previously been used to analyze the function of the human *BRAF* gene activity in melanoma formation using zebrafish,[20] but we believe that our study is the first example of using this promoter to examine the function of a protein not commonly associated with melanophore biology. Future work will examine the effects of increased Aβ toxicity and whether this can overcome melanophore regeneration to produce an early phenotype more amenable to screening of libraries of chemical compounds.

Acknowledgments

This work was carried out under the auspices of the Animal Ethics Committee of The University of Adelaide. Research was supported by funds from the School of Molecular and Biomedical Research of the University of Adelaide and by National Health and Medical Research Council (NHMRC) Project Grant 453622 awarded to Michael Lardelli and Ralph Martins. Ralph Martins is supported by grants from the McCusker Foundation for Alzheimer's Disease Research. Giuseppe Verdile is supported by the National Health and Medical Research Council and is generously supported by Grants Mr. Warren Milner (Milner English College—Perth, Western Australia) and Ms. Helen Sewell through the McCusker Foundation for Alzheimer's Disease Research.

Disclosure Statement

No competing financial interests exist.

References

1. Kirkitadze MD, Kowalska A. Molecular mechanisms initiating amyloid beta-fibril formation in Alzheimer's disease. Acta Biochim Pol 2005;52:417–423.

2. Woodruff-Pak DS. Animal models of Alzheimer's disease: therapeutic implications. J Alzheimers Dis 2008;15:507–521.
3. Morrissette DA, Parachikova A, Green KN, Laferla FM. Relevance of transgenic mouse models to human Alzheimer disease. J Biol Chem 2009;284:6033–6037.
4. Link CD. Expression of human beta-amyloid peptide in transgenic *Caenorhabditis elegans*. Proc Natl Acad Sci U S A 1995;92:9368–9372.
5. Crowther DC, Kinghorn KJ, Miranda E, Page R, Curry JA, Duthie FA, *et al*. Intraneuronal Abeta, non-amyloid aggregates and neurodegeneration in a *Drosophila* model of Alzheimer's disease. Neuroscience 2005;132:123–135.
6. Davidson AE, Balciunas D, Mohn D, Shaffer J, Hermanson S, Sivasubbu S, *et al*. Efficient gene delivery and gene expression in zebrafish using the Sleeping Beauty transposon. Dev Biol 2003;263:191–202.
7. Lister JA, Robertson CP, Lepage T, Johnson SL, Raible DW. nacre encodes a zebrafish microphthalmia-related protein that regulates neural-crest-derived pigment cell fate. Development 1999;126:3757–3767.
8. Rehbein H, Bogerd J. Identification of genetically modified zebrafish (*Danio rerio*) by protein- and DNA-analysis. J Consumer Prot Food Safety 2007;2:122–125.
9. Newman M, Tucker B, Nornes S, Ward A, Lardelli M. Altering presenilin gene activity in zebrafish embryos causes changes in expression of genes with potential involvement in Alzheimer's disease pathogenesis. J Alzheimers Dis 2009;16:133–147.
10. Jowett T. Tissue *In Situ* Hybridization. New York: John Wiley and Sons, 1997.
11. Barash S, Wang W, Shi Y. Human secretory signal peptide description by hidden Markov model and generation of a strong artificial signal peptide for secreted protein expression. Biochem Biophys Res Commun 2002;294:835–842.
12. Dorsky RI, Raible DW, Moon RT. Direct regulation of nacre, a zebrafish MITF homolog required for pigment cell formation, by the Wnt pathway. Genes Dev 2000;14:158–162.
13. Porter-Jordan K, Rosenberg EI, Keiser JF, Gross JD, Ross AM, Nasim S, Garrett CT. Nested polymerase chain reaction assay for the detection of cytomegalovirus overcomes false positives caused by contamination with fragmented DNA. J Med Virol 1990;30:85–91.
14. Lister JA. Development of pigment cells in the zebrafish embryo. Microsc Res Tech 2002;58:435–441.
15. Tachibana M. MITF: a stream flowing for pigment cells. Pigment Cell Res 2000;13:230–240.
16. Nakayama A, Nguyen MT, Chen CC, Opdecamp K, Hodgkinson CA, Arnheiter H. Mutations in microphthalmia, the mouse homolog of the human deafness gene MITF, affect neuroepithelial and neural crest-derived melanocytes differently. Mech Dev 1998;70:155–166.
17. Yasumoto K, Yokoyama K, Takahashi K, Tomita Y, Shibahara S. Functional analysis of microphthalmia-associated transcription factor in pigment cell-specific transcription of the human tyrosinase family genes. J Biol Chem 1997;272:503–509.
18. Camp E, Lardelli M. Tyrosinase gene expression in zebrafish embryos. Dev Genes Evol 2001;211:150–153.
19. Parichy DM, Ransom DG, Paw B, Zon LI, Johnson SL. An orthologue of the kit-related gene fms is required for development of neural crest-derived xanthophores and a subpopulation of adult melanocytes in the zebrafish, *Danio rerio*. Development 2000;127:3031–3044.
20. Patton EE, Widlund HR, Kutok JL, Kopani KR, Amatruda JF, Murphey RD, *et al*. BRAF mutations are sufficient to promote nevi formation and cooperate with p53 in the genesis of melanoma. Curr Biol 2005;15:249–254.
21. Oshima H, Rochat A, Kedzia C, Kobayashi K, Barrandon Y. Morphogenesis and renewal of hair follicles from adult multipotent stem cells. Cell 2001;104:233–245.
22. Nishimura EK, Granter SR, Fisher DE. Mechanisms of hair graying: incomplete melanocyte stem cell maintenance in the niche. Science 2005;307:720–724.
23. Rawls JF, Johnson SL. Zebrafish kit mutation reveals primary and secondary regulation of melanocyte development during fin stripe regeneration. Development 2000;127:3715–3724.

Address correspondence to:
Morgan Newman, Ph.D.
Discipline of Genetics
School of Molecular and Biomedical Science
The University of Adelaide
Adelaide 5005
Australia

E-mail: morgan.newman@adelaide.edu.au

APPENDIX II

Research Paper V

The BACE1-PSEN-AβPP regulatory axis has an ancient role in response to low oxygen/oxidative stress.

Seyyed Hani Moussavi Nik[1], Lachlan Wilson[1], Morgan Newman[1], Kevin Croft[2], Trevor A Mori[2], Ian Musgrave[3] and Michael Lardelli[1]

[1]Discipline of Genetics, School of Molecular and Biomedical Sciences, The University of Adelaide, SA, Australia [2]School of Medicine and Pharmacology, University of Western Australia, Level 4, Medical Research Foundation Building Rear, Perth, WA, Australia [3]Discipline of Pharmacology, School of Medical Sciences, The University of Adelaide, SA, Australia.

Journal of Alzheimer's Disease, 2012;28(3):515-30.

Journal of Alzheimer's Disease 28 (2012) 515–530
DOI 10.3233/JAD-2011-110533
IOS Press

The *BACE1-PSEN-AβPP* Regulatory Axis has an Ancient Role in Response to Low Oxygen/Oxidative Stress

Seyyed Hani Moussavi Nik[a,*], Lachlan Wilson[a], Morgan Newman[a], Kevin Croft[b], Trevor A. Mori[b], Ian Musgrave[c] and Michael Lardelli[a]

[a]*Discipline of Genetics, School of Molecular and Biomedical Sciences, The University of Adelaide, SA, Australia*
[b]*School of Medicine and Pharmacology, University of Western Australia, Level 4, Medical Research Foundation Building Rear, Perth, WA, Australia*
[c]*Discipline of Pharmacology, School of Medical Sciences, The University of Adelaide, SA, Australia*

Accepted 20 September 2011

Abstract. Oxygen homeostasis is essential for the development and normal physiology of an organism. Hypoxia causes the mitochondrial electron transport chain to generate higher levels of reactive oxygen species resulting in oxidative stress. Hypoxia can be a direct consequence of hypoperfusion, a common vascular component among Alzheimer's disease (AD) risk factors, and may play an important role in AD pathogenesis. Beta-site amyloid-β A4 precursor protein-cleaving enzyme 1 (BACE1) is responsible, with γ-secretase, for cleavage of the amyloid-β protein precursor (AβPP) to produce amyloid-β (Aβ) peptide. A recent study observed that oxidative stress increases BACE1 expression via a regulatory pathway dependent on γ-secretase cleavage of AβPP and this increases Aβ peptide production. Zebrafish embryos represent normal cells in which complex and subtle manipulations of gene activity can be performed to facilitate analysis of genes involved in human disease. Here we identify and describe the expression of *bace1*, the zebrafish ortholog of human *BACE1*. We observe that the zebrafish AD-related genes *bace1*, *psen1*, *psen2*, *appa*, and *appb* all show increased mRNA levels under hypoxia. A dominant negative form of *psen1* putatively blocking γ-secretase activity blocks *bace1* upregulation under hypoxia. Hypoxia increases *catalase* gene mRNA indicating increased oxidative stress but we did not observe increased levels of F2-isoprostanes that indicate peroxidation of arachidonic acid, possibly due to relatively low levels of arachidonic acid in zebrafish. Our results demonstrate that upregulation of *PSEN1* & *2, AβPP* and the γ-secretase-dependent upregulation of *BACE1* is an ancient, conserved, and thus selectively advantageous response to hypoxia/oxidative stress.

Keywords: Alzheimer's disease, amyloid-β protein precursor, BACE1, hypoxia, oxidative stress, presenilins, γ-secretase, zebrafish

Supplementary data available online: http://www.j-alz.com/issues/28/vol28-3.html#supplementarydata02

INTRODUCTION

The human brain consumes approximately 20% of the body's energy budget [1]. Thus, supply of oxygen to brain tissue is critical for maintaining energy production and neural function. Disruption of energy metabolism and especially mitochondrial function may be fundamental to many neurodegenerative diseases

*Correspondence to: Seyyed Hani Moussavi Nik, Discipline of Genetics, School of Molecular and Biomedical Sciences, The University of Adelaide, SA 5005, Australia. Tel.: +61 8 8303 4863; Fax: +61 8 8303 4362; E-mail: seyyed.moussavinik@adelaide.edu.au.

ISSN 1387-2877/12/$27.50

including Alzheimer's disease (AD) [2, 3]. Correct functioning of neural vasculature is critical for supply of oxygen to the brain, and there are many disparate lines of evidence indicating a vascular component in development of AD. For example, the risk factors for AD and cardiovascular disease are almost identical [4, 5] and intervention to improve cardiovascular health is the only known effective intervention to prevent AD [6]. Polymorphisms in genes associated with vascular function appear to raise the risk of developing AD [7], and changes in cortical blood flow have been observed in AD patients [8]. Several studies have shown that cerebrovascular disease such as stroke increases the risk of dementia (particularly AD) by 2-fold among elderly patients [9–11]. Neural hypoxia can be a direct consequence of hypoperfusion, a common vascular component among the AD risk factors [12]. Hypoxia causes the mitochondrial electron transport chain (ETC) to emit increased amounts of reactive oxygen species (ROS) at the Qo site of complex III [13], which is consistent with increased oxidative stress as one of the earliest markers of AD pathology. Many of the arguments supporting an important vascular component for AD are summarized by Stone [14].

Oxygen homeostasis is essential for the development and physiology of an organism. Hypoxia inducible factor 1 (HIF-1) is the principal factor in regulating oxygen homeostasis [15]. HIF-1 is a member of the basic helix-loop-helix transcription factor family which specifically binds to 5′-RCGTG-3′ hypoxia-responsive elements (HRE) in a gene's promoter region [16]. HIF-1 consists of two subunits: The α subunit (HIF-1α), the expression of which is regulated by oxygen, and the β subunit (HIF-1β, Arnt), which is ubiquitously expressed [16]. The stability of HIF-1α protein is regulated through its oxygen-dependent degradation domain [17]. It is degraded through the ubiquitition-proteasome pathway under normoxic conditions [17, 18]. When oxygen is in short supply, HIF-1 binds to HREs in promoter regions, thereby activating a wide range of genes involved in angiogenesis, erythropoiesis, cell death, and energy metabolism (reviewed in Sharp et al. [19]). Levels of HIF-1α transcripts are increased in the human frontal cortex as it ages [20] but HIF-1 expression appears to be suppressed in the brains of people with diagnosed AD [21]. This suggests that increased HIF-1 expression may be a protective, compensatory response to inefficient oxygen delivery by aging vasculature, and it illustrates the fact that AD is not a normal progression of aging but, rather, a pathological state.

There is also a large body of evidence suggesting that accumulation and deposition of amyloid-β peptide (Aβ) contributes to the development of AD neuropathology. Aβ is generated by sequential cleavages of amyloid-β protein precursor (AβPP), by β-and γ-secretases dependent primarily on the activity of the *BACE1* and *PSEN1* genes respectively (reviewed in [22, 23]). Sun and colleagues [24] showed that hypoxic conditions can increase Aβ production while Soueck et al. [25] showed that HIF-1 can be upregulated by Aβ suggesting regulatory relationships between HIF-1 and Aβ.

Two homologous β-site AβPP cleaving enzymes, BACE1 and BACE2, have been identified [26]. Both enzymes are capable of carrying out β-cleavage of AβPP *in vitro* and in cell culture [27]. BACE1 is a member of the pepsin-like family of aspartyl proteases. It is a type I transmembrane protein, which contains the characteristic dual active site motif (D-T/S-G-T/S) of an aspartic protease. *BACE1* has a tissue specific expression pattern and it is highly expressed in the pancreas and brain. *BACE2* is expressed at very low levels in brain and is mostly expressed in peripheral tissues (reviewed in [28, 29]). The majority of BACE1 is located in the Golgi and endosomal compartments [30]. BACE1 undergoes a series of complex posttranslational modifications during its maturation. ProBACE1 is cleaved by FURIN or other members of the convertase family to remove the 24 amino acid N-terminal region of the propeptide within the trans-Golgi network (TGN) [31]. Mature BACE1 has four N-glycosylation sites (Asn153, −172, −223 and −354) that are necessary for stability and that facilitate the interaction of β-secretase with AβPP resulting in increased cleavage of AβPP [32]. Phosphorylation of the cytoplasmic domain of BACE1 is necessary for correct maturation and its intracellular trafficking through the TGN and endosomal system [33]. *BACE1* gene expression is tightly controlled at both transcriptional and translational levels [30, 31]. Interestingly, Tamagno and coworkers [34] showed that oxidative stress boosts expression of *BACE1, PSEN1*, γ-secretase activity and, consequently Aβ production but that *BACE1* cannot be upregulated without PSEN/γ-secretase activity.

In recent studies it has been reported that hypoxia can alter AβPP processing by increasing BACE1 as well as γ-secretase expression and activity, resulting in Aβ overproduction [35, 36]. It also has been shown that overexpression of HIF-1α in neuronal cells increases *BACE1* mRNA and protein levels, whereas down-regulation of HIF-1α reduces the levels of *BACE1*

[36]. The orthology between human *HIF-1* and *-2* and zebrafish *hif-1* and *hif-2* has been established. Hypoxic conditions increase zebrafish *hif-1*and *hif-2* transcripts and protein levels [37].

In this study we report the identification by phylogenetic and conserved synteny analysis of the zebrafish orthologue of human *BACE1*, zebrafish *bace1*. We show that zebrafish *bace1* is expressed in a manner similar to that seen in mammals including its induction by low oxygen levels during embryogenesis and in adult brain. We also report that hypoxia or chemical blockage of the mitochondrial ETC coordinately increases mRNA levels of the zebrafish orthologues/paralogues of human *BACE1, PSEN1, PSEN2*, and *AβPP* and that the upregulation of zebrafish *bace1* activity is dependent on γ-secretase activity. Thus, the coordinate regulation of these genes in response to hypoxia/oxidative stress is conserved between zebrafish and mammals.

MATERIALS AND METHODS

Ethics

This work was conducted under the auspices of The Animal Ethics Committee of The University of Adelaide and in accordance with EC Directive 86/609/EEC for animal experiments and the Uniform Requirements for Manuscripts Submitted to Biomedical Journals.

Zebrafish husbandry and experimental procedures

Danio rerio were bred and maintained at 28°C on a 14 h light/10 h dark cycle. Embryos were collected from natural mating, grown in embryo medium (E3) [38] and staged. In the experiments conducted under low oxygen conditions, oxygen was depleted by bubbling nitrogen gas through the medium. Oxygen concentrations were measured using a dissolved oxygen meter (DO 6+, EUTECH instruments, Singapore). The dissolved oxygen level in the hypoxia group was set at 0.67 ± 0.06 mg/l for the embryos and 1.15 ± 0.6 mg/l for adults; whereas the normal ambient oxygen levels were 6.6 ± 0.45 mg/l. Embryos were exposed to hypoxia from 6 h post fertilization (hpf) until they reached a developmental stage equivalent to that of embryos under normal oxygen at 24 hpf or 48 hpf at 28.5°C. Adults were exposed to hypoxia for 3 h before immediate sacrifice and, if necessary, storage of brain tissue at –70°C before analysis. For exposure of embryos with intact chorions to sodium azide (NaN_3, Sigma-Aldrich CHEMIE Gmbh, Steinhiem, Germany), this was performed at different concentrations from 6 hpf until embryos reached developmental stages equivalent to those attained under normoxia at 24 hpf or 48 hpf at 28.5°C (30 embryos were used for each concentration).

Phylogenetic and synteny analyses

The conserved regions of BACE1-related protein sequences were aligned using ClustalW with a gap opening penalty of 10.0 and gap extension penalty of 3.0 for the pairwise alignment stage and a gap opening penalty of 10.0 and gap extension penalty of 5.0 for the multiple alignment stage [39]. MrBayes was used to generate a phylogenetic tree. The program was run under the JC69 (Juke-Cantor) model, with estimated proportion, estimated gamma distribution parameter, and optimized tree topology [40]. Tree reliability was estimated by the Maximum Likelihood Test Method, using the GTR model as support [41].

For synteny analysis, the following loci were investigated: In humans, region 117.07–117.48 M of chromosome 11; in mouse, region 45.4–45.75 M of chromosome 9; in bovine, region 26.41–27.05 M of chromosome 15; in zebrafish, region 0.05–9.5 M of chromosome 15. The genes contained in the above regions were compared using the Sanger Ensembl (http://www.ensembl.org/Danio_rerio/Info/Index) and NCBI Entrez Gene databases (http://www.ncbi.nlm.nih.gov/gene) to identify homologues.

RT-PCR assay and cloning of bace1 *mRNA expression*

Total RNA was extracted from whole embryos at different stages of development and from various adult zebrafish tissues using the QAIGEN RNeasy mini kit (QAIGEN, GmbH, Hiden, Germany). Equal concentrations of total RNA from adult tissues and embryos were used to synthesise first-strand cDNA by reverse transcription (Superscript III kit; Invitrogen, Camarillo, USA). For PCR amplification, 5 μL of cDNA was used with the primers: Bace1 F. (5′-CGCTCACTCTCCTCCTCCTACA-3′) and Bace1 R. (5′-CGCCATTACTGTCCCCGT-3′). PCR was performed using *Taq* polymerase for 35 cycles with an annealing temperature of 58°C for 30 s, extension temperature of 72°C for 1 min and denaturation temperature of 95°C for 40 s. The PCR products were cloned into the pGEM-T vector (Promega Corp., Madison, WI, USA) and sequenced.

Table 1
Gene-specific primers used for qPCR

Zebrafish gene	Forward primer	Reverse primer	Product size (bp)
psen1	5′-CTCTGCACTCCATGCTCAACG-3′	5′-CAGCCAGGCTTGAATCACCTT-3′	113
psen2	5′-GCGGCTCATCTATACCCCATT-3′	5′-CTTGTAGAGCAGCACCAGGATG-3′	133
appa	5′-GGTGGAGGTGCCGTCAGA-3′	5′-CGCTCTGGATGTTGATGTGC-3′	110
appb	5′-TAATGCTGACGACTTTGTCCCTC-3′	5′-TGCCCTCTTTGGTGCTGATC-3′	98
bace1	5′-TTACATAGAGATGGCGGTGGG-3′	5′-GAGGAGAGTGAGCGGTGGTAATA-3′	115
cat	5′-TAAAGGAGCAGGAGCGTTTGGCTA-3′	5′-TTCACTGCGAAACCACGAGGATCT-3′	120
ef-1α	5′-CCAACTTCAACGCTCAGGTCA-3′	5′-CAAACTTGCAGGCGATGTGA-3′	100
β-*actin*	5′-TTCTGGTCGGTACTGGTATTGTG-3′	5′-ATCTTCATCAGGTAGTCTGTCAGGTT-3′	110

Whole-mount in situ *hybridization (WISH)*

bace1 cDNA was amplified by PCR from wild type untreated zebrafish cDNA from adult brain tissues. PCR primers were designed to amplify a target region of 700 bp. The primers were: Bace1.F: (5′-ATCC GCCGAGAGTGGTACTAT-3′) and Bace1.R: (5′-CC ATCACACACAGCGGCA-3′). A 25 μL PCR reaction included 1 mM of each cDNA gene-specific primer, 10 mM dNTPs, and 2 U of Dynazyme DNA polymerase (Finnzymes Oy, Espoo, Finland). PCR was performed for 35 cycles with temperature at 94°C for 30 s, at 58°C for 1 min, and at 72°C for 1 min. The PCR product was purified from a 1-2% agarose/Tris–Acetate–EDTA gel prior to cloning into the pGEMT vector system (Promega Corp., Madison, WI, USA). A Digoxigenin 11-uridine 5-triphosphate (DIG) antisense labeled RNA probe was then generated using SP6 or T7 RNA polymerase from a cDNA amplified clone using M13 primers. Embryos were fixed in 4% formaldehyde in embryo medium before manual dechorionation. WISH was then performed as previously described [42, 43].

Quantitative real-time RT-PCR (qPCR)

The relative standard curve method for quantification was used to determine the expression of experimental samples compared to a basis sample. For experimental samples, target quantity was determined from the standard curve and then compared to the basis sample to determine fold changes in expression. Gene specific primers were designed for amplification of target cDNA (Table 1) and the cDNA from the ubiquitously expressed control gene *ef-1a*. The reaction mixture consisted of 50 ng/μl of cDNA, 18 μM of forward and reverse primers and Power SYBR green master mix PCR solution (Applied Biosystems, Foster City, USA).

To generate the standard curve cDNA was serially diluted (100 ng, 50 ng, 25 ng, 12.5 ng). Each sample and standard curve reaction was performed in triplicate for the *ef-1α* gene and experimental genes. Amplification conditions were 2 min at 50°C followed by 10 min at 95°C and then 40–45 cycles of 15 s at 95°C and 1 min at 60°C. Amplification was performed on an ABI 7000 Sequence Detection System (Applied Biosystems, Foster city, USA) using 96 well plates. Cycle thresholds obtained from each triplicate were averaged and normalized against the expression of *ef-1a*, which has previously been demonstrated to be suitable for normalization for zebrafish qPCR in experiments involving hypoxia [44]. Each experimental sample was then compared to the basis sample to determine fold changes of expression. Each experiment was conducted three times and triplicate PCRs were performed for each sample. The statistical significance of differences between experimental samples and normoxic controls was calculated using a two-tailed *T*-test. Note that, to check the suitability of *ef-1a* as a standard against which to measure changes in the expression of other genes under hypoxia/chemical hypoxia, we also performed qPCR to assay another common qPCR standard, β-actin, under our experimental conditions using *ef-1a* as a standard. No significant changes in β-actin mRNA levels were observed thus supporting that changes in AD-related genes described in this paper are real and not due to changes in *ef-1a* expression (See Supplementary Figure 1. available online: (http://www.j-alz.com/issues/28/vol28-3.html#supplementarydata02).

Injection of embryos

Morpholinos were synthesized by Gene Tools LLC (Corvallis, OR, USA) and are: Mo7Ac; (5′-ACGTCTTGAACACTTCCCTGGAGGG-3′) and MoCont; (5′-CCTCTTACCTCAGTTACAATTTATA-3′). Fertilized zebrafish eggs were injected prior to cleavage. To ensure consistency of morpholino injection, eggs were always injected with solutions at 1 mM total concentration. Dilution of Mo7Ac morpholino

was carried out by mixing with standard negative control morpholino, MoCon as previously described [45]. The concentration of Mo7Ac injected was 0.5 mM (i.e., a mixture containing 0.5 mM MoCont and 0.5 mM Mo7Ac morpholino).

Lipid peroxidation assay

Adult zebrafish were exposed to hypoxic conditions and brain tissue was then immediately removed and frozen at −70°C until measurement of F2-isoprostanes, a biomarker for lipid peroxidation, by stable isotope dilution gas chromatography mass spectrometry as previously described [46].

RESULTS

Identification of the zebrafish bace1 *gene by a phylogenetic approach*

The *BACE1* gene is a member of the pepsin-like family of aspartyl proteases, which are capable of carrying out β-site cleavage of AβPP *in vitro* and in cell culture (reviewed in [26]). This gene has been putatively recognized in mammals (e.g., human, mouse, and bovine), chickens, and frogs. To identify genes with possible homology to *BACE1* in zebrafish, NCBI and Ensembl Genome databases were searched using tBLASTn with the human BACE1 protein sequence as a probe.

We found one candidate previously identified as *zgc: 77409* in the NCBI genome database and located on chromosome 15 (NM_205704.1). The tBLASTn E-value for alignment between human BACE1 and this candidate was 0.0001 and was far smaller than for any other alignments indicating it as a homologue of human *BACE1*. The amino acid residue identity between human BACE1 and the candidate is 76%. To examine the phylogenetic relationship between the candidate and human *BACE1*, a Bayesian analysis was performed comparing the zebrafish gene with protein sequences of the BACE1 orthologues of human, mouse, bovine, and chicken, as well as the most closely related *BACE* gene family, the *BACE2* genes of all these species (see Supplementary Table 1 for a list of the sequence database entries used in this analysis). The gene identified putatively as zebrafish *bace1* clusters with other vertebrate *BACE1* genes while a putative zebrafish *bace2* orthologue clusters with other vertebrate *BACE2* genes (Fig. 1A).

To validate further the identified candidate gene as the zebrafish orthologue of human *BACE1*, we analyzed different motifs of human BACE1 protein and the zebrafish protein. Human BACE1 protein possesses a catalytic site with two active site domains located at amino acid (aa) residues 92–95 (DTGS) and 289–292 (DSGT) and a single transmembrane domain located near the C-terminus, which regulates BACE1 transport and promotes interaction with substrates [47]. The cytoplasmic domain is involved in BACE1 cellular trafficking and compartmentalization [48]. As seen in Fig. 1C, the active catalytic site of human BACE1 and the zebrafish candidate protein show a high level of conservation. Also in the cytoplasmic domain, the endosome targeting motif (DXXLL) at aa residues 496–500 [49] and the ubiquitination site at aa residue 501 of human BACE1 [50] are conserved in the zebrafish candidate protein. The results support that the gene identified as *bace1* is the zebrafish orthologue of human *BACE1* (Fig. 1A, C).

Analysis of synteny conservation supports the conclusion of the phylogenetic analysis

To support the putative orthology between the candidate gene and human *BACE1,* neighboring genes on each side of the zebrafish candidate gene were investigated using the NCBI Entrez Gene database. This led to identification of four zebrafish genes, *dscml1, tagln, Loc 100002762*, and *pcsk7* that are apparent orthologues of human genes and syntenic with, and downstream and upstream of, human *BACE1* on chromosome 11. The human orthology relationships of the zebrafish genes *tagln* and *pcsk7* have been established previously [51, 52]. tBLASTn searches confirmed that these neighboring genes of human *BACE1* share highest sequence identity with their nominal orthologues in zebrafish and not other homologous genes elsewhere in the genome (data not shown). The locations of orthologues of these syntenic genes in the mouse, bovine and frog genomes were also identified (Fig. 1B). Comparisons of closely linked genes in the human, zebrafish, mouse and bovine genomes identified significant conservation of synteny at this locus. Therefore, analysis of synteny conservation supports the proposed orthology between zebrafish *bace1* and human *BACE1*.

Expression of zebrafish bace1

Human *BACE1* has a tissue specific expression pattern. It is expressed at its highest levels in the pancreas and also at relatively high levels in the brain [53]. The spatial and temporal expression of zebrafish *bace1* was determined during early development and in adult

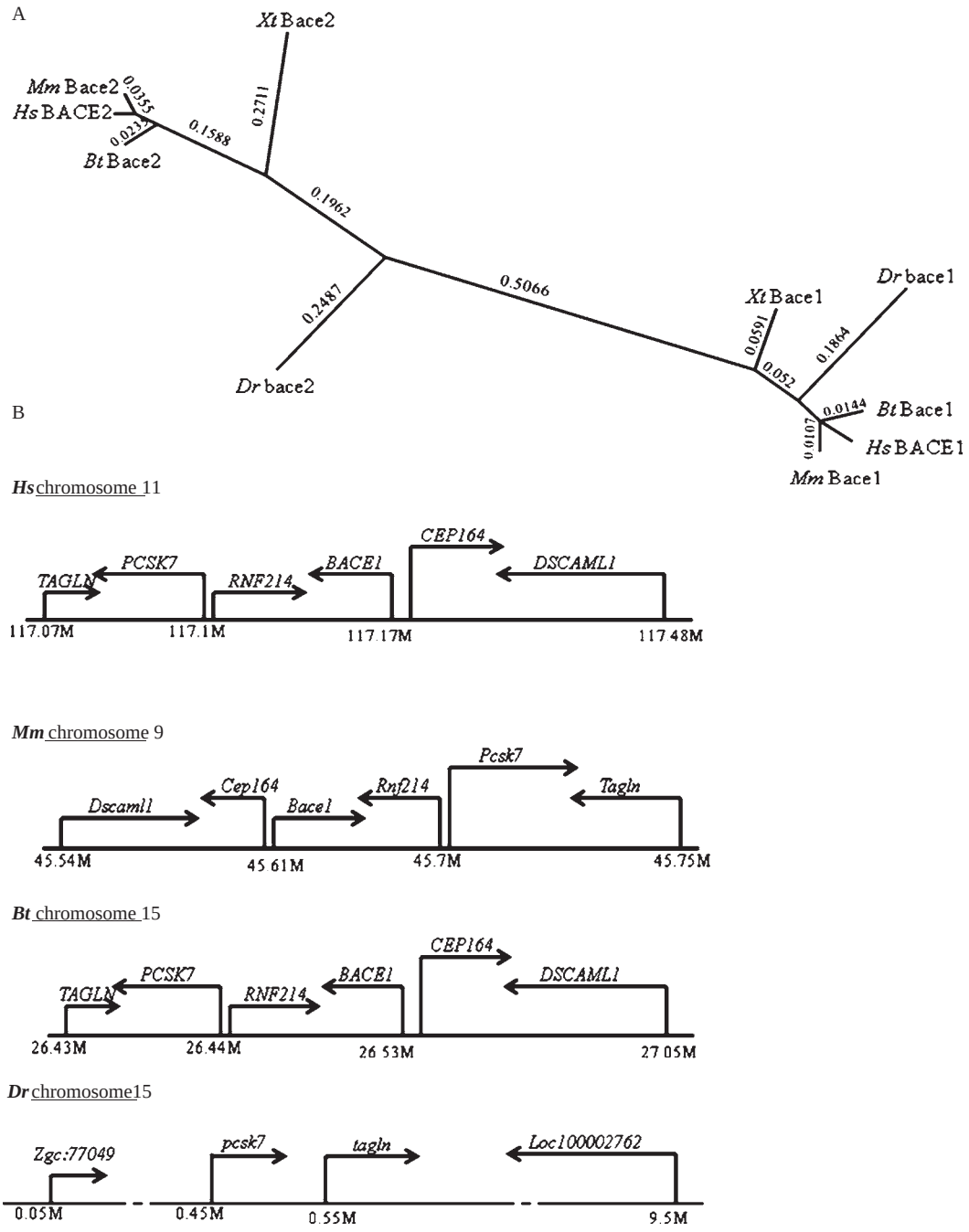

Fig. 1. A) Phylogenetic tree of Bace1 protein family generated using MrBayes. Numbers represent the aLRT branch-support values. B) Schematic showing genes syntenic with the proposed zebrafish *bace1* orthologue and the human *(Hs),* mouse *(Mm),* and bovine (*Bt*) *BACE1* genes. The chromosomal positions of these genes are shown on the numbered horizontal baselines. Numbers on the baselines indicate gene positions on the chromosomes (*M* = megabases). Arrows indicate the direction of gene transcription. C) Amino acid residue sequence alignment of the zebrafish Bace1 candidate and human BACE1 performed using ClustalW with default parameters. Dark shading indicates complete residue identity across all species. (Yellow Box: Active sites. Green box: Lipid raft sorting motif. Red box: Endosome targeting motif. Blue box: Ubiquitination motif).

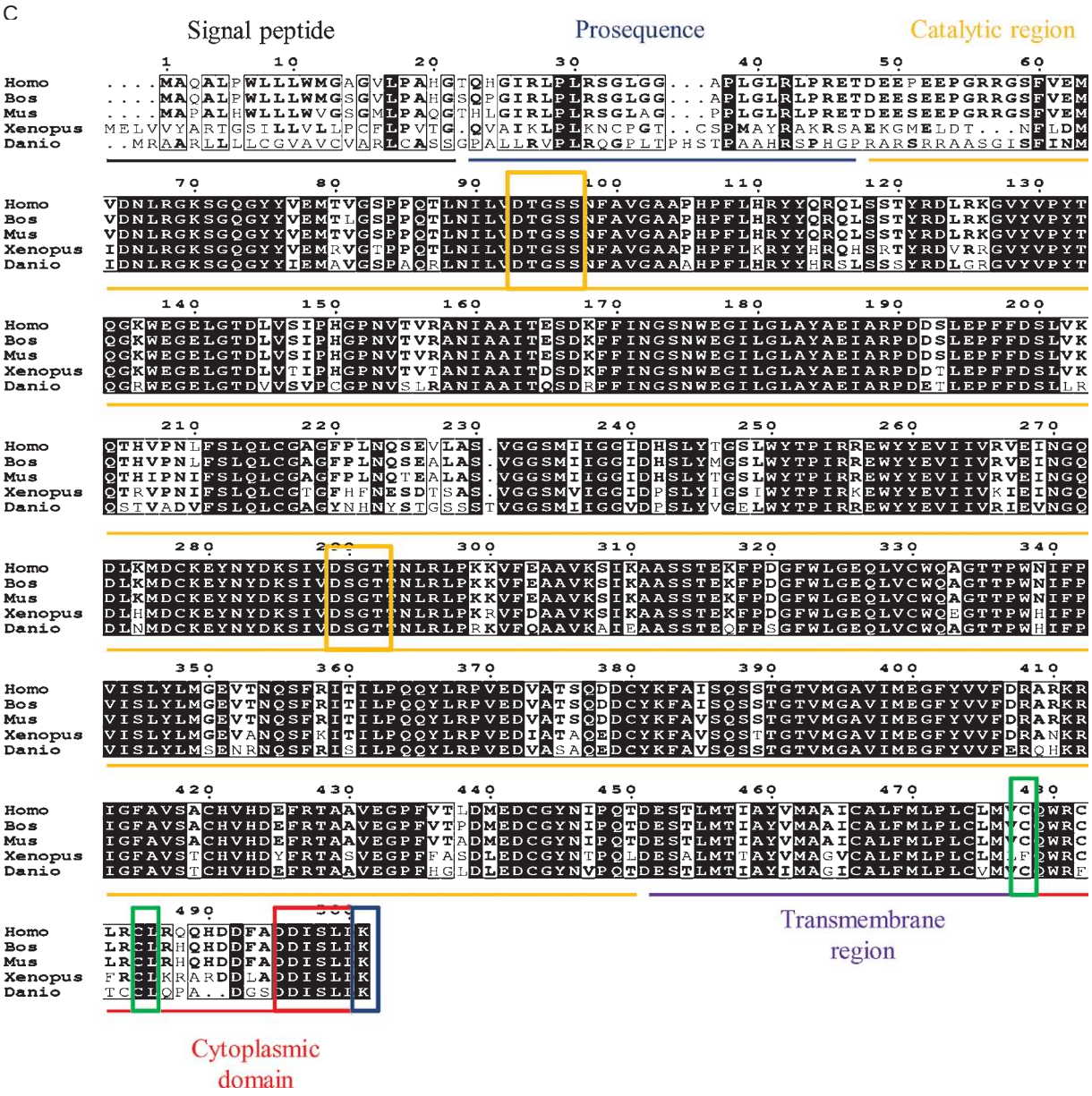

Fig. 1. (*Continued*)

tissue. Zebrafish *bace1* transcripts are easily detectable by reverse transcriptase PCR (RT-PCR) from 48 hpf and become restricted to adult brain tissue (Fig. 2A). However, *bace1* was undetectable by whole mount *in situ* transcript hybridization even after extended staining of 48hpf embryos. Indeed, the ZFIN database contains no record of any expression pattern for the *bace1*/zgc: 77409 locus in the survey by Thisse et al. [54]. To look for alternative splicing of *bace1,* we analyzed zebrafish ESTs, but no splice variant for *bace1* was detected (data not shown).

Hypoxia and ETC inhibition induce bace1 expression after embryogenesis

Recently it was shown that, under hypoxic conditions [24] or oxidative stress [34] human *BACE1* gene expression is induced resulting in increased

β-secretase activity [24, 34]. In SK-N-BE neuroblastoma cells [55] and N2 mouse neuroblastoma cells expressing human AβPP [36], overexpression of HIF-1α increases the levels of *BACE1* transcript and protein whereas, down regulation of HIF-1α reduces the levels of *BACE1*.

To test how *bace1* and other zebrafish genes related to those genes involved in AD respond to hypoxia/oxidative stress, we first needed to demonstrate that hypoxia produces oxidative stress in fish. Initially, we examined lipid peroxidation in the brains of adult fish exposed to hypoxia for 3 h by examining the level of F2-isoprostanes [46, 56]. However, we found that F2-isoprostane levels were generally low in fish brain compared to the brains of mammals and no observable difference was measured for brains under hypoxia relative to normoxia (Fig. 3A). F2-isoprostanes are derived from peroxidation of arachidonic acid. The levels of arachidonic acid in fish brain tissue are very low (∼1% of total fatty acids) [57]

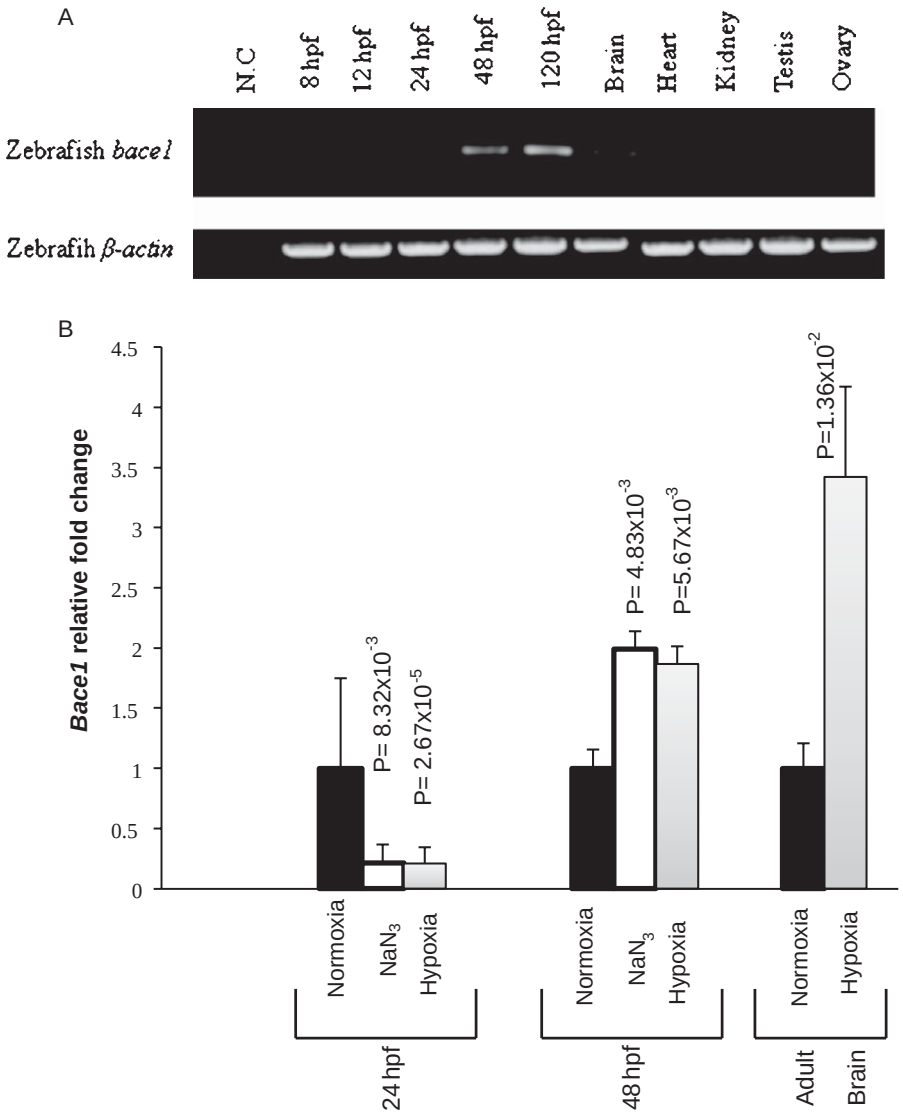

Fig. 2. A) RT-PCR of *bace1* at different developmental stages. B) Quantitative RT-PCR analysis of *bace1* expression under normoxia relative to that under hypoxia or mitochondrial ETC-inhibition by sodium azide. Expression of *ef-1a* was used as a standard. Each experiment was conducted three times and triplicate PCRs were performed for each sample. Representative experiments are shown. Fold changes in gene expression are shown relative to normoxia. Statistical significance values are for comparisons to normoxia, (two-tailed *T*-tests). Error bars show the standard errors of the means.

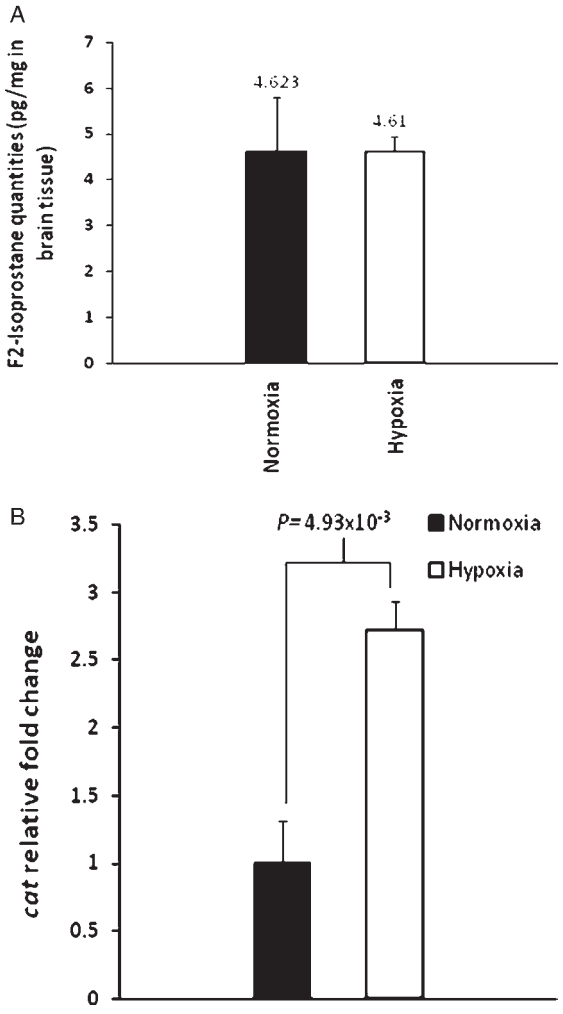

Fig. 3. A) Assessment of lipid peroxidation in zebrafish brain tissue under hypoxic conditions by measurement of F2-isoprostanes. B) qPCR analysis of *cat* expression under normoxia relative to that under hypoxia or mitochondrial ETC-inhibition by sodium azide. Representative experiments are shown. Fold changes in gene expression are shown relative to normoxia. Significance values are for comparisons to normoxia (two-tailed *T*-tests). Error bars show the standard errors of the means

compared to the levels in human brain (∼11% of total fatty acids) [58], which contributes to the low levels of F_2-isoprostanes observed and may mean that F2-isoprostanes are not a suitable biomarker for oxidative stress in fish.

Increased expression of the gene encoding Catalase, *cat*, has previously been used as a marker of oxidative stress in zebrafish [59, 60]. We analyzed *cat* mRNA levels in our hypoxic and normoxic brain samples by qPCR. Under hypoxia, *cat* mRNA levels are increased 2.8 fold which supports that hypoxia produces increased oxidative stress in fish (Fig. 3B).

To test whether hypoxia increases levels of *bace1* in zebrafish as observed for its human orthologue, comparisons of relative levels of *bace1* mRNA under normoxia and hypoxia were performed by qPCR. This showed that embryos exposed to hypoxia, when they reached a developmental stage equivalent to 24 h of development under normoxia, had decreased levels of *bace1* relative to normoxic controls (Fig. 2B). However, in hypoxic zebrafish at a developmental stage equivalent to the normoxic 48 hpf hatching stage of development (that marks the end of embryogenesis) and in brain tissue from adults exposed to hypoxia, relatively increased levels of *bace1* were observed (Fig. 2A, B). The different responses of genes to hypoxia at 24 hpf and 48 hpf are entirely consistent with the expression of other hypoxia-inducible genes in zebrafish [61, 62]. Since hypoxia raises ROS production and oxidative stress by inhibiting the mitochondrial ETC, we also tested whether chemical inhibition of the ETC using sodium azide could produce similar gene regulatory effects. We found that ETC inhibition using sodium azide caused similar responses to those seen for hypoxia at both 24 and 48 hpf (Fig. 2B). These data support that zebrafish *bace1* is induced by hypoxia/oxidative stress in a manner similar to its human orthologue by 48 hpf of development.

Hypoxic conditions and ETC inhibition also induce expression of psen1, psen2, appa, and appb

Recently studies in rat and human cardiac cell models showed that *PSEN2* mRNA levels were increased during exposure to hypoxic conditions. This increase of *PSEN2* mRNA levels was the result of regulation of *PSEN2* transcription by HIF-1 [63, 64]. To test whether hypoxia increases levels of *psen2* mRNA in zebrafish as seen for its human othologue, relative levels of *psen2* mRNA under normoxia and hypoxia were measured by qPCR. We observed that *psen2* mRNA levels are increased under hypoxic conditions in embryos at a developmental stage equivalent to that attained by embryos under normoxia at 48 hpf and in brain tissue from adults exposed to hypoxia (Fig. 3A). We also tested whether hypoxic conditions elevate transcript levels of the *psen2* homologue *psen1*, since *PSEN1* levels are increased in human neuroblastoma cells under conditions of oxidative stress [34]. The results demonstrated that *psen1* mRNA levels are increased in embryos under hypoxia at a developmental stage equivalent to that attained after 48 hpf under normoxia and in brain tissue from adults exposed to hypoxia (Fig. 3B). This is consistent with recent

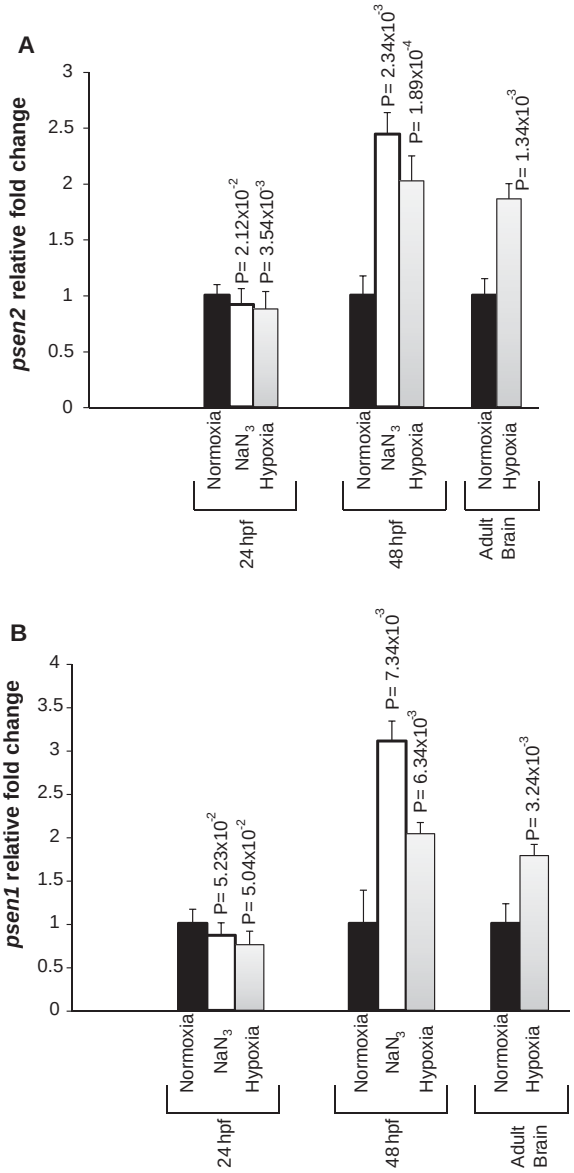

Fig. 4. qPCR analysis of *psen2* and *psen1* expression under normoxia relative to that under hypoxia or mitochondrial ETC-inhibition by sodium azide. Representative experiments are shown. Fold changes in gene expression are shown relative to normoxia. Significance values are for comparisons to normoxia (two-tailed *T*-tests). Error bars show the standard errors of the means.

observations from mammalian animal models exposed to hypoxia/oxidative stress conditions [65].

Recent reports showed that AβPP levels are induced under hypoxic conditions [36, 66]. This induction of AβPP leads to increased β- and γ-secretase cleavage and increased Aβ production (reviewed in [67]). Zebrafish possess two paralogues of the human *AβPP* gene, *appa*, and *appb* [68]. To test whether hypoxic conditions increase zebrafish *appa* and *appb* expression as for the human *AβPP* gene, we used qPCR to measure the relative levels of *appa* and *appb* mRNA under normoxia and hypoxia. Our results showed that, in hypoxic embryos equivalent to the normoxic 48hpf developmental stage and in brain tissue from adults exposed to hypoxia, both *appa* and *appb* transcript levels are increased (Fig. 4).

Expression of the genes *psen1, psen2, appa,* and *appb* also paralleled that seen for *bace1* at 24 hpf by not showing an increase under either hypoxia or chemical inhibition of the mitochondrial ETC. In contrast,

at the developmental stage of 48 hpf, both hypoxia and chemical inhibition of the mitochondrial ETC showed increased expression of all these genes. These genes were also all upregulated under hypoxia in adult zebrafish brain. If under hypoxic conditions *bace1, psen1, psen2*, *appa,* and *appb* are all upregulated, then we can presume that Aβ production would also be upregulated although this is not yet possible to test in zebrafish due to the lack of a suitable assay.

Inhibition of γ-secretase activity prevents bace1 upregulation under ETC-inhibition

Interestingly, recent studies have demonstrated that oxidative stress [34] and hypoxia [24, 69] can regulate both β-secretase and γ-secretase activities. Indeed, increased BACE1 expression is dependent on the presence of both AβPP and γ-secretase activity [34]. To test whether γ-secretase activity mediates the upregulation of *bace1* transcript levels under hypoxia/oxidative stress in zebrafish embryos, we sought to block γ-secretase simultaneously with ETC inhibition. The large volumes of support medium required in hypoxia experiments made chemical inhibition of γ-secretase in embryos or adults under hypoxia impractical, and we found that sodium azide for ETC inhibition appears to react chemically with the γ-secretase inhibitor DAPT. Therefore, we injected embryos with a morpholino antisense oligonucleotide ("Mo7Ac") that gives partial interference with *psen1* splicing and putatively generates truncated, dominant negative Psen1 protein species that dominantly interfere with the γ-secretase activity of both Psen1 and Psen2 [45]. When Mo7Ac-injected embryos are subjected to ETC-inhibition with sodium azide, *bace1* transcript levels do not increase. However, embryos injected with a negative control morpholino ("MoCont") do show increased *bace1* transcript levels in the presence of sodium azide (for zebrafish at the developmental equivalent of 48 hpf) (Fig. 5). Thus, γ-secretase activity appears to be required for upregulation of *bace1* under hypoxia which is consistent with the results seen in mammalian and human cell models.

DISCUSSION

The human *BACE1* gene has been extensively studied in relation to AD. To gain better insight into the function and dysfunction of *BACE1*, various animal models have been used. The zebrafish model system has been demonstrated to be a highly manipulable vertebrate model for genetic studies due to a combination of features including easy embryo accessibility, large embryo size, rapid embryonic development, short generation time, and a well-characterized genome.

In this study we sought to test whether zebrafish might be a suitable model in which to examine the responses of AD-related genes to hypoxia/oxidative stress. First we confirmed the identity of a potential *BACE1* orthologue in zebrafish, *bace1,* using phylogenetic and conserved synteny analysis. Alignment between human BACE1 and zebrafish Bace1 putative proteins shows high conservation, and there is a high level of conservation of gene synteny between human chromosome 11 and zebrafish chromosome 15 in this region.

BACE1 is primarily responsible for the β-secretase cleavage of AβPP. BACE1/β-secretase is an aspartic protease highly expressed in neuronal cells (reviewed in [26]). BACE1-knockout mice initially show normal development, behavior, and physiology [29], but several studies have shown that loss of BACE1 results in a variety of behavioral and physiological deficits, e.g., memory loss [70], emotional deficits [71], and myelination deficits in peripheral nerves [72]. Remarkably, hypoxia elevates BACE1 expression and activity, which results in increased Aβ production, as shown *in vitro* and in transgenic mouse models of AD [24]. One proposed mechanism for upregulation of BACE1 expression under hypoxia is that this occurs via activation of HIF-1, a transcription factor that regulates oxygen homeostasis. HIF-1 has been shown to bind to the *BACE1* promoter to regulate activity of the *BACE1* gene [36, 55].

Kajimura et al. showed that hypoxia significantly increases Hif-1α and HIF-1β mRNA expression during zebrafish embryogenesis [37]. Our results indicate that exposing zebrafish embryos to hypoxia or chemical inhibition of the mitochondrial ETC leads to a reduction of *bace1* transcript levels by a developmental stage equivalent to 24 hpf under normoxia. However, at a developmental stage equivalent to 48 hpf (when embryos begin to hatch) or in adult brain, low oxygen increases *bace1* expression. This is consistent with the results seen in mammalian models and cells under hypoxic conditions. We have previously shown that the regulation of the zebrafish gene *hmga1* under hypoxia is dramatically different at the 24 hpf developmental stage compared to what is seen at the 48 hpf developmental stage (when hatching can occur) and our observations in this study are consistent with that. We have also previously analyzed apoptosis in, and the survival of, zebrafish embryos under ETC-inhibition resembling hypoxia [62]. An increase in cell death

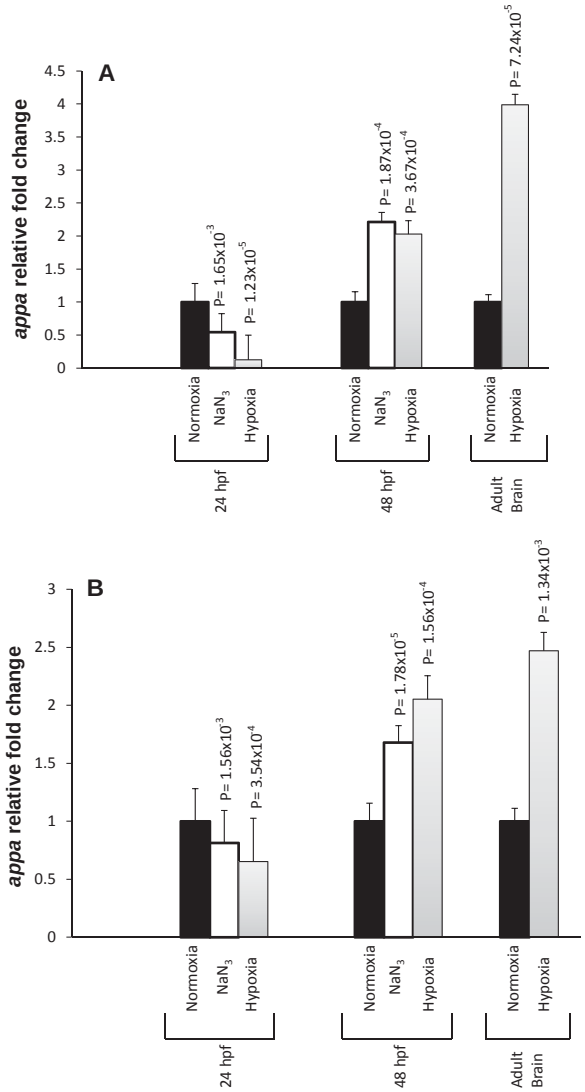

Fig. 5. qPCR analysis of *appa* and *appb* expression under normoxia relative to that under hypoxia or mitochondrial ETC-inhibition by sodium azide. Fold changes in gene expression are shown relative to normoxia. Significance values are for comparisons to normoxia (two-tailed *T*-tests). Error bars show the standard errors of the means.

was observed in the tail tip, rostral brain, and hatching glands of 48 hpf embryos after 24 h of exposure to 900 μM sodium azide. However, this cell death did not prevent resumption of development after normoxia was restored [62], and this does not support that a presumed increase in Aβ formation under hypoxia in zebrafish is toxic. Indeed, our previous work on transgenic expression of the 42 aa form of human Aβ in zebrafish melanophores is not consistent with a potent toxicity for this peptide [73].

Psen1 and Psen2 influence multiple molecular pathways, with well documented roles as components of γ-secretase complexes [65]. Recent reports showed that hypoxia induces PSEN1, PSEN2, and AβPP expression in brain tissue resulting in increased γ-secretase activity and cleavage of AβPP thereby increasing levels of Aβ species [63, 65–67]. Our data showed that exposure of zebrafish embryos to hypoxia or ETC-inhibition led to reduced transcript levels of *psen1*, *psen2*, *appa,* and *appb* by a developmental stage equivalent to 24 hpf under normoxia. However, at a developmental stage equivalent to 48 hpf or in adult brain, low oxygen levels increased *psen1*, *psen2, appa,* and *appb* expression. ETC-blockage produced

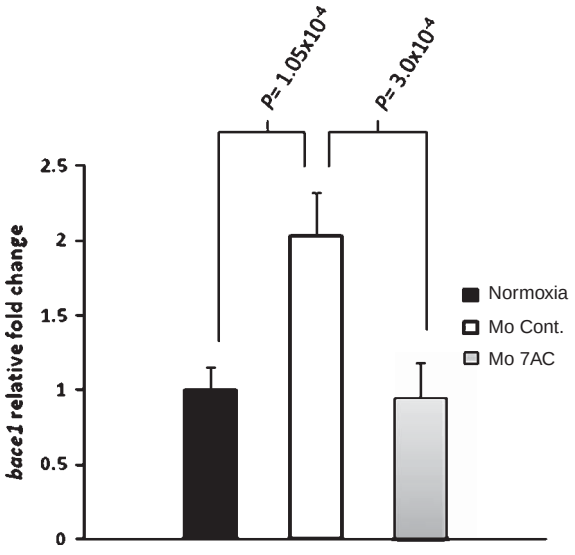

Fig. 6. Inhibition of γ-secretase activity inhibits upregulation of *bace1* mRNA levels. In mitochondrial ETC-inhibited embryos at a developmental stage equivalent to 48 hpf, γ-secretase activity was inhibited by the presence of morpholino Mo7Ac that acts on *psen1* transcript splicing to create a dominant negative effect. This prevented the increase of *bace1* mRNA levels. Embryos containing a negative control morpholino. (MOCont) still showed *bace1* upregulation under ETC-inhibition. Brackets indicate the comparisons for which significance values are given (two-tailed *T*-tests). Error bars show the standard errors of the means.

identical effects to hypoxia at developmental stages equivalent to both 24 and 48 hpf.

In a recent article, Herrup (2010) proposes that AD begins with an initiating insult/injury that triggers a chronic, stressful inflammatory process and that eventually causes a "change of state" of brain cell physiology leading to degeneration and death [74]. He envisages an "amyloid deposition cycle" where Aβ oligomerization results in microglial activation and other inflammatory responses which drive further accumulation of Aβ. If we consider the brain's vasculature and its role in supplying oxygen to neural cells, another form of amyloid deposition cycle can easily be conceived centered around hypoxia, oxidative stress, and progressive damage to brain microvasculature (below).

The work in this study shows that the coordinated upregulation of BACE1, PSEN1 & 2, and AβPP (and, therefore, presumably Aβ synthesis) in response to low oxygen/oxidative stress has been conserved in vertebrates during more than 400 million years since the mammalian and teleost fish lineages diverged. Presumably therefore, this response is selectively advantageous and is a protective response to oxygen stress. The idea that Aβ production might be a protective response to hypoxia/oxidative stress is supported by a number of papers pointing out an antioxidant role for Aβ [75–77], and there is evidence for a neuroprotective role for the $A\beta_{40}$ peptide [78, 79]. A human brain with damaged/aged vasculature would be expected to show insufficient oxygenation of neural tissues and increased oxidative stress. Under these conditions we would expect to see upregulation of the above genes and protective Aβ production. However, if the oxygen deficiency is chronic and clearance of the raised Aβ levels is deficient due to vascular damage, Aβ may form substrates that actually promote ROS formation (reviewed in [80]) and inflammatory responses might also be initiated. Cells of the vasculature, particularly endothelial cells, appear to be especially sensitive to ROS/oxidative stress (reviewed in [81]), and increased damage to the brain's vasculature will only enhance hypoxia/oxidative stress resulting in a positive feedback loop. Eventually, the positive feedback loop of low oxygen/oxidative stress leading to vascular and neural damage that further exacerbates hypoxia/oxidative stress might result in a pathological change-of-state leading to greatly accelerated neurodegeneration and frank AD where the earlier regulatory relationships (e.g., between HIF-1α and Aβ production [20]) are obscured.

To conclude, our examination of *bace1* and other genes in zebrafish has shown that the gene regulatory axis consisting of *BACE1, PSEN1* & *2,* and *AβPP* responds strongly to hypoxia/oxidative stress and that this regulatory response is highly evolutionarily conserved. The regulatory responses of these genes to hypoxia/oxidative stress may represent a core element in the development of AD. The zebrafish has proven itself to be a very versatile system for analyzing the relationships between the gene/proteins of AD and future work should focus on the responses of these genes to changes in oxygen availability.

ACKNOWLEDGMENTS

This work was supported by funds from the Cancer Council of South Australia (Research Project Grants S 24/04 and 627124) and the Discipline of Genetics at the School of Molecular and Biomedical Sciences of The University of Adelaide and by generous donations from Mr Leslie Darling and Dr Mojgan Vatani. The sources of funding listed above played no role in the study design; in the collection, analysis and interpretation of data; in the writing of the report; or in the decision to submit the paper for publication.

Authors' disclosures available online (http://www.j-alz.com/disclosures/view.php?id=1013).

REFERENCES

[1] Herculano-Houzel S (2011) Scaling of brain metabolism with a fixed energy budget per neuron: Implications for neuronal activity, plasticity and evolution. *PLoS One* **6**, e17514.

[2] Beal MF (1995) Aging, energy, and oxidative stress in neurodegenerative diseases. *Ann Neurol* **38**, 357-366.

[3] Bowling AC, Beal MF (1995) Bioenergetic and oxidative stress in neurodegenerative diseases. *Life Sci* **56**, 1151-1171.

[4] Schwartz E, Wicinski B, Schmeidler J, Haroutunian V, Hof PR (2010) Cardiovascular risk factors affect hippocampal microvasculature in early AD. *Transl Neurosci* **1**, 292-299.

[5] Nation DA, Hong S, Jak AJ, Delano-Wood L, Mills PJ, Bondi MW, Dimsdale JE (2011) Stress, exercise, and Alzheimer's disease: A neurovascular pathway. *Med Hypotheses* **76**, 847-854.

[6] Qiu C, Xu W, Fratiglioni L (2010) Vascular and psychosocial factors in Alzheimer's disease: Epidemiological evidence toward intervention. *J Alzheimers Dis* **20**, 689-697.

[7] Yuan Q, Zuo X, Jia J (2009) Association between promoter polymorphisms of vascular endothelial growth factor gene and sporadic Alzheimer's disease among Northern Chinese Han. *Neurosci Lett* **457**, 133-136.

[8] van Beek AH, Lagro J, Olde-Rikkert MG, Zhang R, Claassen JA (2011) Oscillations in cerebral blood flow and cortical oxygenation in Alzheimer's disease. *Neurobiol Aging*. doi:10.1016/j.neurobiolaging.2010.11.016.

[9] Ukraintseva S, Sloan F, Arbeev K, Yashin A (2006) Increasing rates of dementia at time of declining mortality from stroke. *Stroke* **37**, 1155-1159.

[10] Kalaria RN (2000) The role of cerebral ischemia in Alzheimer's disease. *Neurobiol Aging* **21**, 321-330.

[11] White L, Petrovitch H, Hardman J, Nelson J, Davis DG, Ross GW, Masaki K, Launer L, Markesbery WR (2002) Cerebrovascular pathology and dementia in autopsied Honolulu-Asia Aging Study participants. *Ann N Y Acad Sci* **977**, 9-23.

[12] Atkinson L, Boyle JP, Pearson HA, Peers C (2006) Chronic hypoxia inhibits Na+/Ca2+ exchanger expression in cortical astrocytes. *Neuroreport* **17**, 649-652.

[13] Bell EL, Klimova TA, Eisenbart J, Moraes CT, Murphy MP, Budinger GR, Chandel NS (2007) The Qo site of the mitochondrial complex III is required for the transduction of hypoxic signaling via reactive oxygen species production. *J Cell Biol* **177**, 1029-1036.

[14] Stone J (2008) What initiates the formation of senile plaques? The origin of Alzheimer-like dementias in capillary haemorrhages. *Med Hypotheses* **71**, 347-359.

[15] Huang LE, Willmore WG, Gu J, Goldberg MA, Bunn HF (1999) Inhibition of hypoxia-inducible factor 1 activation by carbon monoxide and nitric oxide. Implications for oxygen sensing and signaling. *J Biol Chem* **274**, 9038-9044.

[16] Wang GL, Jiang BH, Rue EA, Semenza GL (1995) Hypoxia-inducible factor 1 is a basic-helix-loop-helix-PAS heterodimer regulated by cellular O2 tension. *Proc Natl Acad Sci U S A* **92**, 5510-5514.

[17] Ivan M, Kondo K, Yang H, Kim W, Valiando J, Ohh M, Salic A, Asara JM, Lane WS, Kaelin WG Jr (2001) HIFalpha targeted for VHL-mediated destruction by proline hydroxylation: Implications for O2 sensing. *Science* **292**, 464-468.

[18] Jaakkola P, Mole DR, Tian YM, Wilson MI, Gielbert J, Gaskell SJ, Kriegsheim A, Hebestreit HF, Mukherji M, Schofield CJ, Maxwell PH, Pugh CW, Ratcliffe PJ (2001) Targeting of HIF-alpha to the von Hippel-Lindau ubiquitylation complex by O2-regulated prolyl hydroxylation. *Science* **292**, 468-472.

[19] Sharp FR, Bernaudin M (2004) HIF1 and oxygen sensing in the brain. *Nat Rev Neurosci* **5**, 437-448.

[20] Lu T, Pan Y, Kao SY, Li C, Kohane I, Chan J, Yankner BA (2004) Gene regulation and DNA damage in the ageing human brain. *Nature* **429**, 883-891.

[21] Liu Y, Liu F, Iqbal K, Grundke-Iqbal I, Gong CX (2008) Decreased glucose transporters correlate to abnormal hyperphosphorylation of tau in Alzheimer disease. *FEBS Lett* **582**, 359-364.

[22] Maltsev AV, Bystryak S, Galzitskaya OV (2011) The role of beta-amyloid peptide in neurodegenerative diseases. *Ageing Res Rev* **10**, 440-452.

[23] Verdile G, Fuller S, Atwood CS, Laws SM, Gandy SE, Martins RN (2004) The role of beta amyloid in Alzheimer's disease: Still a cause of everything or the only one who got caught? *Pharmacol Res* **50**, 397-409.

[24] Sun X, He G, Qing H, Zhou W, Dobie F, Cai F, Staufenbiel M, Huang LE, Song W (2006) Hypoxia facilitates Alzheimer's disease pathogenesis by up-regulating BACE1 gene expression. *Proc Natl Acad Sci U S A* **103**, 18727-18732.

[25] Soucek T, Cumming R, Dargusch R, Maher P, Schubert D (2003) The regulation of glucose metabolism by HIF-1 mediates a neuroprotective response to amyloid beta peptide. *Neuron* **39**, 43-56.

[26] Vassar R, Bennett BD, Babu-Khan S, Kahn S, Mendiaz EA, Denis P, Teplow DB, Ross S, Amarante P, Loeloff R, Luo Y, Fisher S, Fuller J, Edenson S, Lile J, Jarosinski MA, Biere AL, Curran E, Burgess T, Louis JC, Collins F, Treanor J, Rogers G, Citron M (1999) Beta-secretase cleavage of Alzheimer's amyloid precursor protein by the transmembrane aspartic protease BACE. *Science* **286**, 735-741.

[27] Hussain I, Powell DJ, Howlett DR, Chapman GA, Gilmour L, Murdock PR, Tew DG, Meek TD, Chapman C, Schneider K, Ratcliffe SJ, Tattersall D, Testa TT, Southan C, Ryan DM, Simmons DL, Walsh FS, Dingwall C, Christie G (2000) ASP1 (BACE2) cleaves the amyloid precursor protein at the beta-secretase site. *Mol Cell Neurosci* **16**, 609-619.

[28] Zacchetti D, Chieregatti E, Bettegazzi B, Mihailovich M, Sousa VL, Grohovaz F, Meldolesi J (2007) BACE1 expression and activity: Relevance in Alzheimer's disease. *Neurodegener Dis* **4**, 117-126.

[29] Vassar R (2002) Beta-secretase (BACE) as a drug target for Alzheimer's disease. *Adv Drug Deliv Rev* **54**, 1589-1602.

[30] Christensen MA, Zhou W, Qing H, Lehman A, Philipsen S, Song W (2004) Transcriptional regulation of BACE1, the beta-amyloid precursor protein beta-secretase, by Sp1. *Mol Cell Biol* **24**, 865-874.

[31] Benjannet S, Elagoz A, Wickham L, Mamarbachi M, Munzer JS, Basak A, Lazure C, Cromlish JA, Sisodia S, Checler F, Chretien M, Seidah NG (2001) Post-translational processing of beta-secretase (beta-amyloid-converting enzyme) and its ectodomain shedding. The pro- and transmembrane/cytosolic domains affect its cellular activity and amyloid-beta production. *J Biol Chem* **276**, 10879-10887.

[32] Capell A, Steiner H, Willem M, Kaiser H, Meyer C, Walter J, Lammich S, Multhaup G, Haass C (2000) Maturation and propeptide cleavage of beta-secretase. *J Biol Chem* **275**, 30849-30854.

[33] Walter J, Fluhrer R, Hartung B, Willem M, Kaether C, Capell A, Lammich S, Multhaup G, Haass C (2001) Phosphorylation regulates intracellular trafficking of beta-secretase. *J Biol Chem* **276**, 14634-14641.

[34] Tamagno E, Guglielmotto M, Aragno M, Borghi R, Autelli R, Giliberto L, Muraca G, Danni O, Zhu X, Smith MA, Perry G, Jo DG, Mattson MP, Tabaton M (2008) Oxidative stress activates a positive feedback between the gamma- and beta-secretase cleavages of the beta-amyloid precursor protein. *J Neurochem* **104**, 683-695.

[35] Wang R, Zhang YW, Zhang X, Liu R, Hong S, Xia K, Xia J, Zhang Z, Xu H (2006) Transcriptional regulation of APH-1A and increased gamma-secretase cleavage of APP and Notch by HIF-1 and hypoxia. *FASEB J* **20**, 1275-1277.

[36] Zhang X, Zhou K, Wang R, Cui J, Lipton SA, Liao FF, Xu H, Zhang YW (2007) Hypoxia-inducible factor 1alpha (HIF-1alpha)-mediated hypoxia increases BACE1 expression and beta-amyloid generation. *J Biol Chem* **282**, 10873-10880.

[37] Kajimura S, Aida K, Duan C (2006) Understanding hypoxia-induced gene expression in early development: *in vitro* and in vivo analysis of hypoxia-inducible factor 1-regulated zebra fish insulin-like growth factor binding protein 1 gene expression. *Mol Cell Biol* **26**, 1142-1155.

[38] Westerfield M The zebrafish book. A guide for the laboratory use of zebrafish (Danio rerio), 5th ed, University of Oregon Press, Eugene.

[39] Corpet F (1988) Multiple sequence alignment with hierarchical clustering. *Nucleic Acids Res* **16**, 10881-10890.

[40] Huelsenbeck JP, Ronquist F (2001) MRBAYES: Bayesian inference of phylogenetic trees. *Bioinformatics* **17**, 754-755.

[41] Guindon S, Gascuel O (2003) A simple, fast, and accurate algorithm to estimate large phylogenies by maximum likelihood. *Syst Biol* **52**, 696-704.

[42] Nornes S, Newman M, Wells S, Verdile G, Martins RN, Lardelli M (2009) Independent and cooperative action of Psen2 with Psen1 in zebrafish embryos. *Exp Cell Res* **315**, 2791-2801.

[43] Newman M, Tucker B, Nornes S, Ward A, Lardelli M (2009) Altering presenilin gene activity in zebrafish embryos causes changes in expression of genes with potential involvement in Alzheimer's disease pathogenesis. *J Alzheimers Dis* **16**, 133-147.

[44] van der Meer DL, van den Thillart GE, Witte F, de Bakker MA, Besser J, Richardson MK, Spaink HP, Leito JT, Bagowski CP (2005) Gene expression profiling of the long-term adaptive response to hypoxia in the gills of adult zebrafish. *Am J Physiol Regul Integr Comp Physiol* **289**, R1512-R1519.

[45] Nornes S, Newman M, Verdile G, Wells S, Stoick-Cooper CL, Tucker B, Frederich-Sleptsova I, Martins R, Lardelli M (2008) Interference with splicing of Presenilin transcripts has potent dominant negative effects on Presenilin activity. *Hum Mol Genet* **17**, 402-412.

[46] Mori TA, Croft KD, Puddey IB, Beilin LJ (1999) An improved method for the measurement of urinary and plasma F2-isoprostanes using gas chromatography-mass spectrometry. *Anal Biochem* **268**, 117-125.

[47] Hong L, Koelsch G, Lin X, Wu S, Terzyan S, Ghosh AK, Zhang XC, Tang J (2000) Structure of the protease domain of memapsin 2 (beta-secretase) complexed with inhibitor. *Science* **290**, 150-153.

[48] Walter J (2006) Control of amyloid-beta-peptide generation by subcellular trafficking of the beta-amyloid precursor protein and beta-secretase. *Neurodegener Dis* **3**, 247-254.

[49] He X, Feng L, Chang WP, Tang J (2005) GGA protein mediate the recycling pathway of memapsin 2. *J Biol Chem* **280**, 11696-11703.

[50] Kang EL, Cameron AN, Piazza F, Walker KR, Tesco G (2010) Ubiquitin regulates GGA3-mediated degradation of BACE1. *J Biol Chem* **285**, 24108-24119.

[51] Woods IG, Wilson C, Friedlander B, Chang P, Reyes DK, Nix R, Kelly PD, Chu F, Postlethwait JH, Talbot WS (2005) The zebrafish gene map defines ancestral vertebrate chromosomes. *Genome Res* **15**, 1307-1314.

[52] Georgijevic S, Subramanian Y, Rollins EL, Starovic-Subota O, Tang AC, Childs SJ (2007) Spatiotemporal expression of smooth muscle markers in developing zebrafish gut. *Dev Dyn* **236**, 1623-1632.

[53] Willem M, Lammich S, Haass C (2009) Function, regulation and therapeutic properties of beta-secretase (BACE1). *Semin Cell Dev Biol* **20**, 175-182.

[54] Thisse C, Thisse B (2005) High throughput expression analysis of ZF-models consortium clones, ZFIN Direct Data Submission (http://zfin.org).

[55] Guglielmotto M, Aragno M, Autelli R, Giliberto L, Novo E, Colombatto S, Danni O, Parola M, Smith MA, Perry G, Tamagno E, Tabaton M (2009) The up-regulation of BACE1 mediated by hypoxia and ischemic injury: Role of oxidative stress and HIF1alpha. *J Neurochem* **108**, 1045-1056.

[56] Liu W, Morrow JD, Yin H (2009) Quantification of F2-isoprostanes as a reliable index of oxidative stress *in vivo* using gas chromatography-mass spectrometry (GC-MS) method. *Free Radic Biol Med* **47**, 1101-1107.

[57] Tocher DR, Agaba M, Hastings N, Bell JG, Dick JR, Teale AJ (2002) Nutritional regulation of hepatocyte fatty acid desaturation and polyunsaturated fatty acid composition in zebrafish (Danio rerio) and tilapia (Oreochromis niloticus. *Fish Physiol Biochem* **24**, 309-320.

[58] Makrides M, Neumann MA, Byard RW, Simmer K, Gibson RA (1994) Fatty acid composition of brain, retina, and erythrocytes in breast- and formula-fed infants. *Am J Clin Nutr* **60**, 189-194.

[59] Tseng YC, Chen RD, Lucassen M, Schmidt MM, Dringen R, Abele D, Hwang PP (2011) Exploring uncoupling proteins and antioxidant mechanisms under acute cold exposure in brains of fish. *PLoS One* **6**, e18180.

[60] Jin Y, Zheng S, Pu Y, Shu L, Sun L, Liu W, Fu Z (2011) Cypermethrin has the potential to induce hepatic oxidative stress, DNA damage and apoptosis in adult zebrafish (Danio rerio). *Chemosphere* **82**, 398-404.

[61] Padilla PA, Roth MB (2001) Oxygen deprivation causes suspended animation in the zebrafish embryo. *Proc Natl Acad Sci U S A* **98**, 7331-7335.

[62] Moussavi Nik SH, Newman M, Lardelli M (2011) The response of HMGA1 to changes in oxygen availability is evolutionarily conserved. *Exp Cell Res* **317**, 1503-1512.

[63] Lukiw WJ, Gordon WC, Rogaev EI, Thompson H, Bazan NG (2001) Presenilin-2 (PS2) expression up-regulation in a model of retinopathy of prematurity and pathoangiogenesis. *Neuroreport* **12**, 53-57.

[64] Mohuczy D, Qian K, Phillips MI (2002) Presenilins in the heart: Presenilin-2 expression is increased by low glucose and by hypoxia in cardiac cells. *Regul Pept* **110**, 1-7.

[65] De Gasperi R, Sosa MA, Dracheva S, Elder GA (2010) Presenilin-1 regulates induction of hypoxia inducible factor-1alpha: Altered activation by a mutation associated with familial Alzheimer's disease. *Mol Neurodegener* **5**, 38.

[66] Pluta R (2005) Pathological opening of the blood-brain barrier to horseradish peroxidase and amyloid precursor protein following ischemia-reperfusion brain injury. *Chemotherapy* **51**, 223-226.
[67] Zhang X, Le W (2010) Pathological role of hypoxia in Alzheimer's disease. *Exp Neurol* **223**, 299-303.
[68] Musa A, Lehrach H, Russo VA (2001) Distinct expression patterns of two zebrafish homologues of the human APP gene during embryonic development. *Dev Genes Evol* **211**, 563-567.
[69] Guglielmotto M, Tamagno E, Danni O (2009) Oxidative stress and hypoixa contribute to Alzheimer's disease pathogenesis: Two sides of the same coin. *Scientific World Journal* **9**, 781-791.
[70] Ma H, Lesne S, Kotilinek L, Steidl-Nichols JV, Sherman M, Younkin L, Younkin S, Forster C, Sergeant N, Delacourte A, Vassar R, Citron M, Kofuji P, Boland LM, Ashe KH (2007) Involvement of beta-site APP cleaving enzyme 1 (BACE1) in amyloid precursor protein-mediated enhancement of memory and activity-dependent synaptic plasticity. *Proc Natl Acad Sci U S A* **104**, 8167-8172.
[71] Laird FM, Cai H, Savonenko AV, Farah MH, He K, Melnikova T, Wen H, Chiang HC, Xu G, Koliatsos VE, Borchelt DR, Price DL, Lee HK, Wong PC (2005) BACE1, a major determinant of selective vulnerability of the brain to amyloid-beta amyloidogenesis, is essential for cognitive, emotional, and synaptic functions. *J Neurosci* **25**, 11693-11709.
[72] Hu X, Hicks CW, He W, Wong P, Macklin WB, Trapp BD, Yan R (2006) Bace1 modulates myelination in the central and peripheral nervous system. *Nat Neurosci* **9**, 1520-1525.
[73] Newman M, Wilson L, Camp E, Verdile G, Martins R, Lardelli M (2010) A zebrafish melanophore model of amyloid beta toxicity. *Zebrafish* **7**, 155-159.
[74] Herrup K (2010) Reimagining Alzheimer's disease–an age-based hypothesis. *J Neurosci* **30**, 16755-16762.
[75] Kontush A (2001) Amyloid-beta: An antioxidant that becomes a pro-oxidant and critically contributes to Alzheimer's disease. *Free Radic Biol Med* **31**, 1120-1131.
[76] Nadal RC, Rigby SE, Viles JH (2008) Amyloid beta-Cu2+ complexes in both monomeric and fibrillar forms do not generate H2O2 catalytically but quench hydroxyl radicals. *Biochemistry* **47**, 11653-11664.
[77] Baruch-Suchodolsky R, Fischer B (2009) Abeta40, either soluble or aggregated, is a remarkably potent antioxidant in cell-free oxidative systems. *Biochemistry* **48**, 4354-4370.
[78] Shearer J, Szalai VA (2008) The amyloid-beta peptide of Alzheimer's disease binds Cu(I) in a linear bis-his coordination environment: Insight into a possible neuroprotective mechanism for the amyloid-beta peptide. *J Am Chem Soc* **130**, 17826-17835.
[79] Giuffrida ML, Caraci F, Pignataro B, Cataldo S, De Bona P, Bruno V, Molinaro G, Pappalardo G, Messina A, Palmigiano A, Garozzo D, Nicoletti F, Rizzarelli E, Copani A (2009) Beta-amyloid monomers are neuroprotective. *J Neurosci* **29**, 10582-10587.
[80] Wang X, Su B, Perry G, Smith MA, Zhu X (2007) Insights into amyloid-beta-induced mitochondrial dysfunction in Alzheimer disease. *Free Radic Biol Med* **43**, 1569-1573.
[81] Rojas A, Figueroa H, Re L, Morales MA (2006) Oxidative stress at the vascular wall. Mechanistic and pharmacological aspects. *Arch Med Res* **37**, 436-448.